

**Myxobacteria-derived Outer Membrane Vesicles as a Drug Delivery System to  
Treat Bacterial Infections**

Dissertation

zur Erlangung des Grades

des Doktors der Naturwissenschaften

der Naturwissenschaftlich-Technischen Fakultät

der Universität des Saarlandes

von

Adriely Góes Conceição

Saarbrücken

2021

Die vorliegende Arbeit wurde von Juni 2017 bis Oktober 2021 unter der Leitung Herrn Prof. Dr. Gregor Fuhrmann in der Fachrichtung Pharmazie der Universität des Saarlandes und am Helmholtz-Institut für Pharmazeutische Forschung Saarland angefertigt.

**Tag des Kolloquiums:** 28. Januar 2022

**Dekan:** Prof. Dr. Jörn Eric Walter

**Berichterstatter:** Prof. Dr. Gregor Fuhrmann  
Prof. Dr. Alexandra K. Kiemer

**Akad. Mitglied:** Dr. -Ing. Michael Kohlstedt

**Vorsitz:** Prof. Dr. Claus-Michael Lehr

“Simplicity is the final achievement. After one has played a vast quantity of notes and more notes, it is simplicity that emerges as the crowning reward of art.”

*Frédéric Chopin*

“When you realize there is something you don't understand, then you're generally on the right path to understanding all kinds of things.”

*Jostein Gaarder, The Solitaire Mystery*

## TABLE OF CONTENTS

<b>I. SUMMARY .....</b>	<b>V</b>
<b>II. ZUSAMMENFASSUNG.....</b>	<b>VI</b>
<b>III. GRAPHICAL ABSTRACT.....</b>	<b>VII</b>
<b>IV. ABBREVIATIONS .....</b>	<b>VIII</b>
<b>1 INTRODUCTION .....</b>	<b>9</b>
1.1 RESISTANT INFECTIONS AND THEIR MAIN MECHANISMS.....	9
1.2 NANOMEDICINE AND DRUG DELIVERY .....	12
1.3 MYXOBACTERIA AND THEIR OUTER MEMBRANE VESICLES .....	17
<b>2 AIMS OF THIS THESIS.....</b>	<b>21</b>
<b>3 MAJOR OUTCOMES OF THE THESIS .....</b>	<b>22</b>
3.1 OMV ISOLATION AND CHARACTERIZATION.....	23
3.2 THE EFFECTS OF MYXOBACTERIAL OMVs ON MAMMALIAN CELLS.....	25
3.3 THE EFFECTS OF MYXOBACTERIAL OMVs ON PLANKTONIC BACTERIA .....	27
3.4 THE EFFECTS OF MYXOBACTERIAL OMVs AGAINST INTRACELLULAR INFECTIONS AND BIOFILM FORMATION.....	28
<b>4 CONCLUSIONS AND OUTLOOK.....</b>	<b>34</b>
<b>5 REFERENCES .....</b>	<b>35</b>
<b>6 SCIENTIFIC OUTPUT .....</b>	<b>51</b>
6.1 PAPER 1: "BIOGENIC AND BIOMIMETIC CARRIERS AS VERSATILE TRANSPORTERS TO TREAT INFECTIONS" .....	51
6.2 PAPER 2: "BIOCOMPATIBLE BACTERIA-DERIVED VESICLES SHOW INHERENT ANTIMICROBIAL ACTIVITY".....	64
6.3 PAPER 3: "MYXOBACTERIA-DERIVED OUTER MEMBRANE VESICLES: POTENTIAL APPLICABILITY AGAINST INTRACELLULAR INFECTIONS" .....	89
6.4 PAPER 4: "INTERACTION OF MYXOBACTERIA-DERIVED OUTER MEMBRANE VESICLES WITH BIOFILMS: ANTIADHESIVE AND ANTIBACTERIAL EFFECTS" .....	115
<b>7 LIST OF SCIENTIFIC PUBLICATIONS .....</b>	<b>128</b>
<b>8 ACKNOWLEDGMENTS.....</b>	<b>129</b>

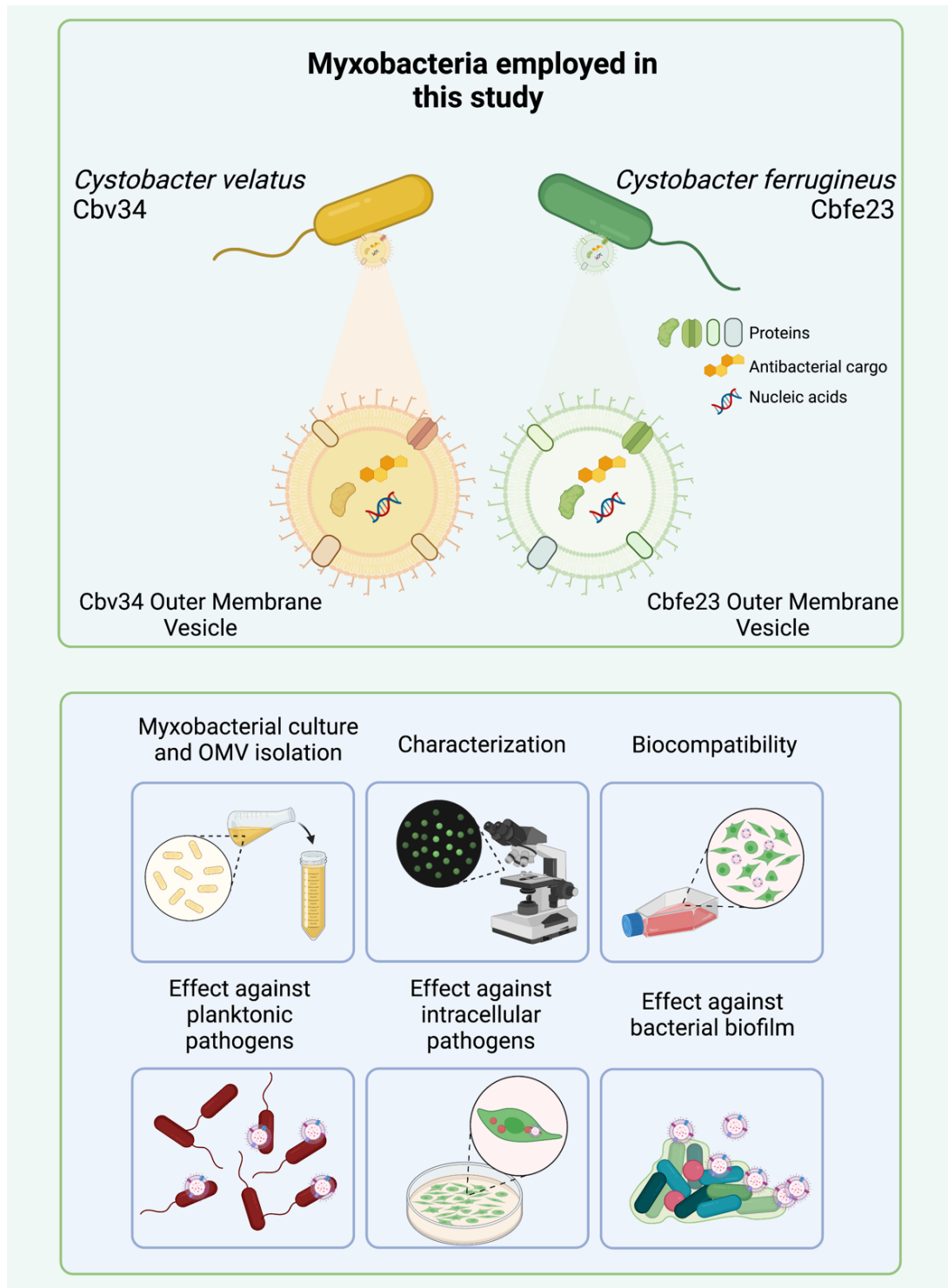
## I. Summary

Bacterial infections represent a serious risk to public health globally. The World Health Organization (WHO) estimated that infections of the lower respiratory tract were the fourth leading cause of death worldwide in 2019, killing 2.6 million people. One of the main causes of such numbers is the development of antibiotic resistance by bacteria, a process facilitated by the misuse of antibiotic compounds in humans and in animals. The employment of nanomedicine can be explored for the development of new nanocarriers that can be used for the treatment of those infections, such as extracellular vesicles (EVs) and, more specifically, outer membrane vesicles (OMVs) derived from myxobacteria, which are natural producers of antibacterial compounds. In this thesis, OMVs were isolated from the strains *Cystobacter velatus* Cbv34 and *Cystobacter ferrugineus* Cbfe23 and were characterized. The OMVs' effects on mammalian cells were promising, eliciting no negative impact in biocompatibility, and not significantly stimulating the release of pro-inflammatory cytokines. The OMVs were also successfully internalized by mammalian cells, thus able to decrease the proliferation rate of intracellular *Staphylococcus aureus*. Moreover, the myxobacterial OMVs were able to detach biofilm from surfaces and prevent their growth in a model subjected to fluid flow. The findings of this study demonstrate the substantial potential of the use of myxobacterial OMVs for the treatment of bacterial infections.

## II. Zusammenfassung

Bakterielle Infektionen sind eine globale Bedrohung der öffentlichen Gesundheit. Mit 2,6 Mio. Toten im Jahr 2019 hat die Weltgesundheitsorganisation Infektionen der unteren Atemwege mit als die vierthäufigste Todesursache eingeschätzt. Eine der Hauptursachen ist die von Bakterien entwickelte Antibiotikaresistenz, ein Prozess, der durch den Fehlgebrauch von Antibiotika bei Menschen und Tier vorangetrieben wird. Mit Hilfe der Nanomedizin können neue Trägersysteme entwickelt und für die Behandlung von Infektionen verwendet werden. Solche Partikel sind beispielsweise extrazelluläre Vesikel (EVs) oder genauer äußere Membranvesikel (OMVs) von Myxobakterien, welche als natürliche Produzenten antibiotischer Substanzen gelten. In dieser Arbeit wurden OMVs von den Stämmen *Cystobacter velatus* Cbv34 und *Cystobacter ferrugineus* Cbfe23 isoliert und charakterisiert. Die Wirkung von OMVs auf tierische Zellen war vielversprechend, da sie keinen negativen Einfluss auf die Biokompatibilität und keine signifikante Ausschüttung von proinflammatorischen Zytokinen bewirkt haben. Zudem wurden OMV erfolgreich von tierischen Zellen aufgenommen und waren daher fähig, die Proliferation von *Staphylococcus aureus* zu bremsen. Außerdem waren myxobakterielle OMV in einem Durchflussmodell in der Lage, Biofilm von Oberflächen zu lösen und deren Wachstum zu unterbinden. Die Erkenntnisse dieser Studie unterstreichen das Potential der Verwendung von myxobakteriellen OMVs zur Behandlung bakterieller Infektionen.

### III. Graphical abstract



Outer membrane vesicles (OMVs) were isolated from the myxobacterial strains *Cystobacter velatus* Cbv34 and *Cystobacter ferrugineus* Cbfe23, and their effects on mammalian cells and bacteria were studied. The OMVs elicited low toxic effects against mammalian cells and presented antimicrobial effects, becoming promising nanocarriers to treat bacterial infections. Image created with Biorender.com.

#### IV. Abbreviations

Cbfe-OMVs	Outer membrane vesicles derived from the <i>Cystobacter ferrugineus</i> Cbfe23 myxobacterium
Cbv-OMVs	Outer membrane vesicles derived from the <i>Cystobacter velatus</i> Cbv34 myxobacterium
CFU	Colony forming unity
CLSM	Confocal laser scanning microscopy
Cryo-TEM	Cryogenic transmission electron microscopy
EVs	Extracellular vesicles
LC MS	Liquid Chromatography coupled Mass Spectrometry
LPs	Liposomes
NPs	Nanoparticles
NTA	Nanoparticle tracking analysis
OD	Optical density
OMVs	Outer membrane vesicles
PBMCs	Peripheral blood mononuclear cells
PBS	Phosphate buffered saline
SEC	Size exclusion chromatography
SEM	Scanning electron microscopy
UC	Ultracentrifugation

# 1 INTRODUCTION

## 1.1 Resistant infections and their main mechanisms

Infections caused by resistant bacteria are one of the world's major public health menaces. According to estimates, 2.38 million people die every year from infections of the lower respiratory tract.<sup>1,2</sup> The number of casualties by lower respiratory tract infections such as pneumonia mainly include children younger than 5 years and adults older than 70 years, especially in lower-income countries.<sup>1,2</sup> This alarming trend is due to an increase in the amount of pathogens that are resistant to the available antibiotic treatments, which is a result of multiple factors, including the irresponsible use of antibiotic drugs, waste management, contamination of water and the use of antibiotics in farm animals.<sup>3–5</sup> There are not nearly as many new compounds being discovered today as during the “golden era” of antibiotic discovery (from the 1940s to the 1980s), when important compounds such as tetracyclines, methicillin and vancomycin made their way successfully to the hospitals and pharmacy shelves.<sup>6</sup> A new antibiotic compound has not been released in the market since daptomycin and linezolid in the 1980s.<sup>7</sup>

Bacteria can develop antibiotic resistance in several ways, such as the development of efflux pumps, their ability to modify or degrade antibiotic molecules, increase their membrane impermeability and modify the drug target (Fig. 1).<sup>8,9</sup> Bacteria can also avoid antibiotic treatment by their ability to become intracellular in mammalian cells. This is a well acknowledged mechanism of resistance that microbes like *Mycobacterium tuberculosis* and *Mycobacterium abscessus* can perform, but bacteria that were thought to be solely extracellular (e.g. *Staphylococcus aureus*) can also use this feature to become resistant.<sup>10–12</sup>

*Staphylococcus aureus* is a Gram-positive pathogen responsible for infections occurring in several parts of the body of humans and animals (e.g. lung<sup>13–17</sup>, skin<sup>18,19</sup> and ear<sup>20–22</sup>) and it has the ability to become intracellular in professional phagocytes (e.g., macrophages) and nonprofessional phagocytes (e.g., epithelial cells) by adhering to the cell surface, invading the cell in a “zipper-like” pattern and escaping

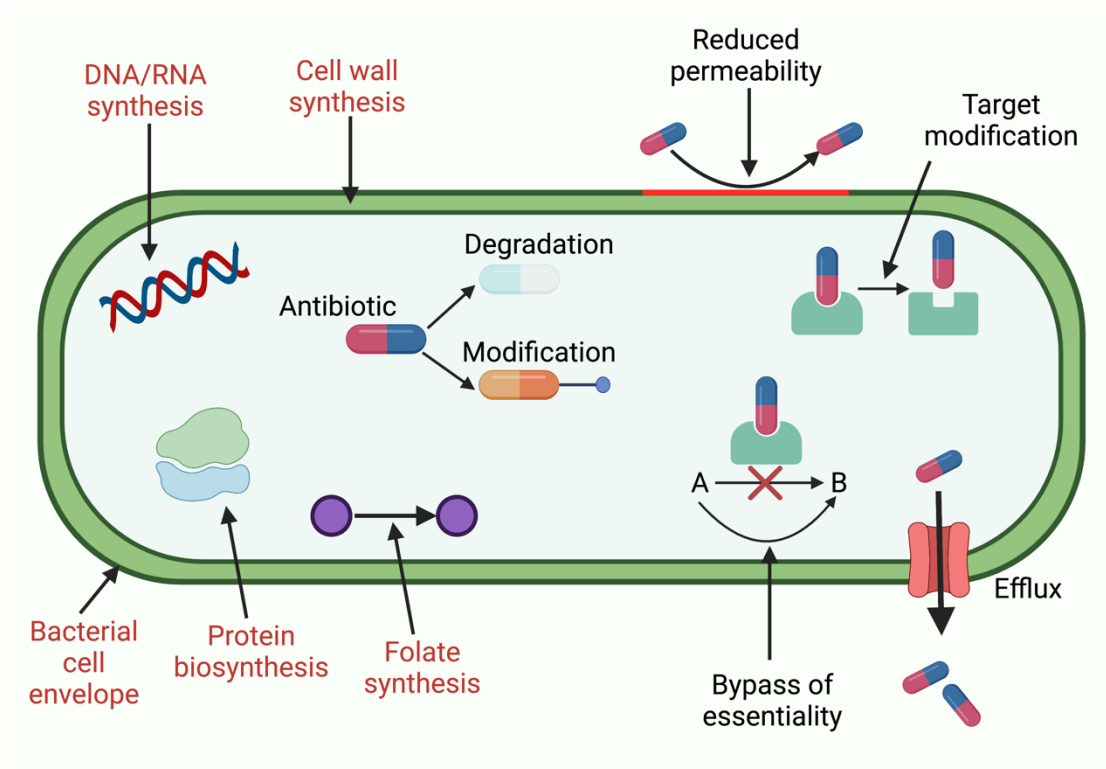


Figure 1 Scheme of antibiotic targets (in red) and bacterial mechanisms of resistance (in black) (as reviewed by Lakemeyer et al., 2018; Roponnen et al., 2021). Created with BioRender.com.

the endosomal pathway, becoming resistant in the cytosol.<sup>10,12,23</sup> This mechanism helps the bacteria to escape host cell defenses and treatment with drugs that have poor permeation through the mammalian cellular membrane, such as beta-lactams and aminoglycosides, due to their high hydrophilicity.<sup>24,25</sup> Macrolides and fluoroquinolones, on the other hand, present good diffusion through the cellular membrane, but have a short retention time inside the cell.<sup>24,25</sup> Other examples of microorganisms that become intracellular and can cause infectious diseases are: *Mycobacterium tuberculosis*, which infects macrophages and hepatocytes;<sup>26,27</sup> *Salmonella spp.*, which is internalized by macrophages and enterocytes;<sup>28,29</sup> and *Pseudomonas aeruginosa*, which becomes intracellular in macrophages and epithelial cells.<sup>30,31</sup> The current treatment of infections caused by intracellular pathogens, such as *M. tuberculosis*, is lengthy and involves the combination of different antimicrobials, which includes the use of isoniazid, rifampicin, ethambutol and pyrazinamide for two months, and then four months of rifampicin and isoniazid.<sup>32–34</sup> The length of the treatment and the use of several drugs can make it difficult to obtain patient compliance to the treatment and successful eradication of the infection.<sup>35,36</sup>

Another very important mechanism of bacterial resistance to antimicrobial treatment is the formation of bacterial biofilm. Biofilms are the main form bacteria can be found in the environment.<sup>37–39</sup> Their formation occurs when single bacteria attach to each other, become adherent to a surface, grow and form an extracellular matrix composed of polymeric substances.<sup>40–42</sup> Their formation confers bacteria the ability to become resistant to antibiotics and disinfectants, which is due to the low penetration of antimicrobial compounds, the expression of biofilm-specific genes, sparse growth and other factors.<sup>42–46</sup> They can cause several types of tissue infection (Fig. 2), such as endocarditis, osteomyelitis, otitis media, vaginosis, as well as device-related infections, such as eye infection from use of contact lenses and tissue infection due to breast implants and tissue fillers.<sup>47</sup> Biofilm formation on medical devices is also one of the main causes of infection in the hospital environment.<sup>48</sup>

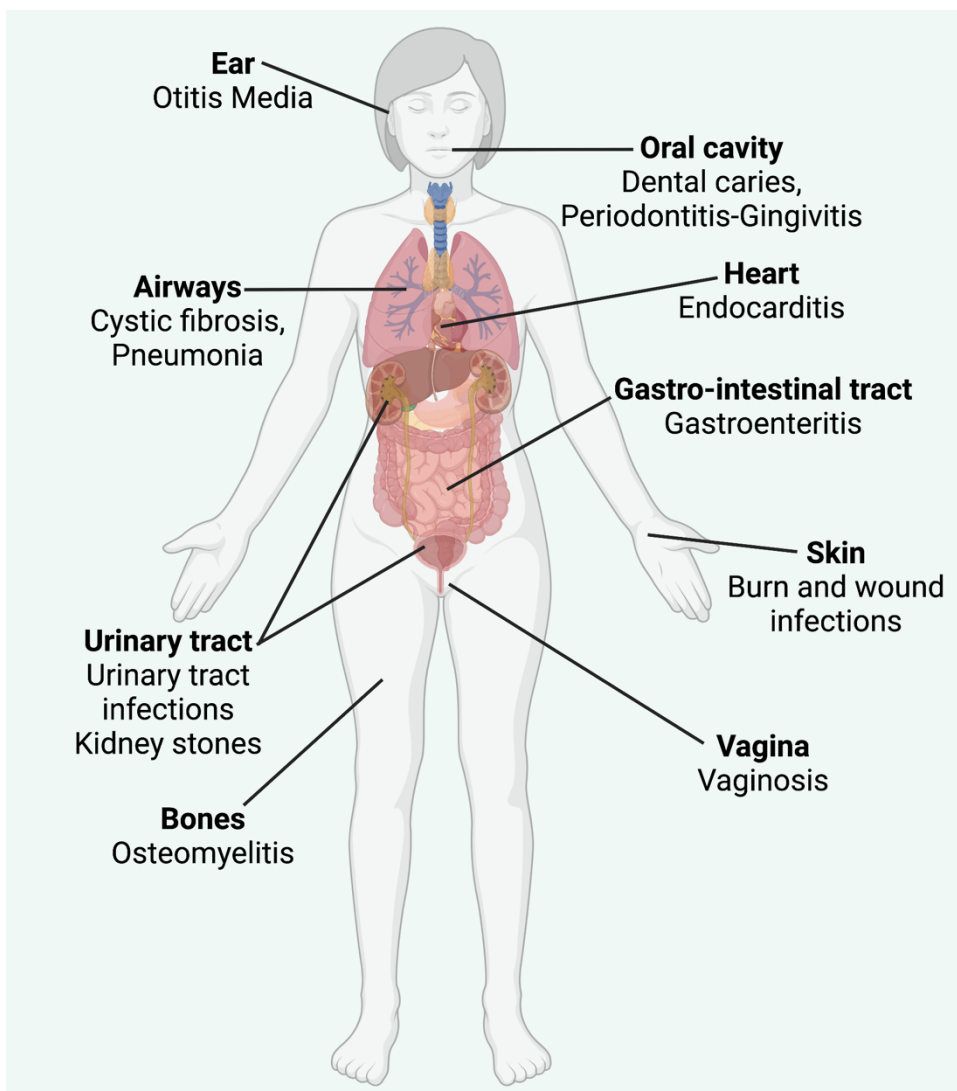


Figure 2 Main tissue biofilm-related infections in the human body (as reviewed by Birk et al., 2021; Lebeaux et al., 2013). Created with BioRender.com.

Biofilm antimicrobial resistance can develop in different ways. For example, the extracellular matrix and the extracellular DNA present in the biofilm can bind to the antibiotics and cause their inactivation by enzymes present in them.<sup>46,49-51</sup> Many antibiotics have a target on processes that depend on the metabolism of the bacteria, such as replication and cell wall synthesis. However, it has been shown that the bacteria on the outer part of the biofilm have a higher metabolic activity than the bacteria enclosed in the inner part, which compromises the antibacterial effect of the drugs and complete eradication of the biofilm.<sup>46,49,52,53</sup> For example, beta-lactams have their diffusion through the biofilm partially impaired<sup>54</sup> and have their activity impaired due to low metabolism and low growth rate of mature biofilms.<sup>55</sup> The same effect can be observed when aminoglycosides are used.<sup>56</sup>

The general anti-infective therapy of biofilm-related infections relies massively on local delivery, in order to have a high drug concentration at the site of infection and to avoid side effects caused by systemic administration, such as hepatotoxicity<sup>57</sup> and severe allergy,<sup>58</sup> and the combination of different antibiotics.<sup>46</sup> As an example of a long term and local delivered antimicrobial treatment, lung infections in patients with cystic fibrosis are treated with continuous use of inhaled colistin and tobramycin and aztreonam, ciprofloxacin and levofloxacin in on/off cycles of 28 days.<sup>46,59-64</sup> Long therapy regimes like this are one of the main causes of non-compliance to the therapy, as patients tend to stop treatment once their condition improves, some fearing that long-term use of medication could have adverse effects.<sup>65-67</sup>

## 1.2 Nanomedicine and drug delivery

Nanomedicine, according to Mast and colleagues, is “the medical intervention where nanotechnology is applied to treat or diagnose diseases.”<sup>68,69</sup> Nanotechnology is the manipulation or engineering of materials in the nanoscale range (1-1000 nm) for their properties and effects.<sup>69</sup> Among the materials manipulated by nanotechnology are nanoparticles, which can be made from organic materials, such as polymers poly lactic-co-glycolic acid (PLGA) or inorganic materials, such as iron or gold (Fig. 3).<sup>68,70-</sup>

Drug delivery systems are any type of formulation that can control the rate, the time and the location of their drug cargo.<sup>68</sup> Since nanoparticles can present one or more of these features, they are included in this classification. They have been widely explored for their advantages in targeted delivery, such as the possibilities for surface modification, overcoming low water solubility and reducing toxicity of compounds.<sup>73–75</sup>

However, the clinical translation of such synthetic carriers faces two major challenges: 1) cellular toxicity of the nanoparticles due to their materials, and 2) low retention in the body caused by clearance by the reticuloendothelial system or by mononuclear phagocytes.<sup>76,77</sup> An alternative to overcome this is the PEGylation of the nanoparticles, which seems to improve their circulation time, but seems to impair the interaction between the drug and the targeted cells.<sup>78,79</sup> Other reports claim that PEGylation does not contribute to a higher circulation time.<sup>80,81</sup> As a result, their approval by regulatory agencies to be available in the market is low.<sup>82,83</sup> However, many nanoformulations have successfully reached the market with many of them being liposomal formulations and lipid-based nanopharmaceuticals, for their excellent ability to subdue side effects caused by conventional drugs.<sup>84</sup> One of the most well

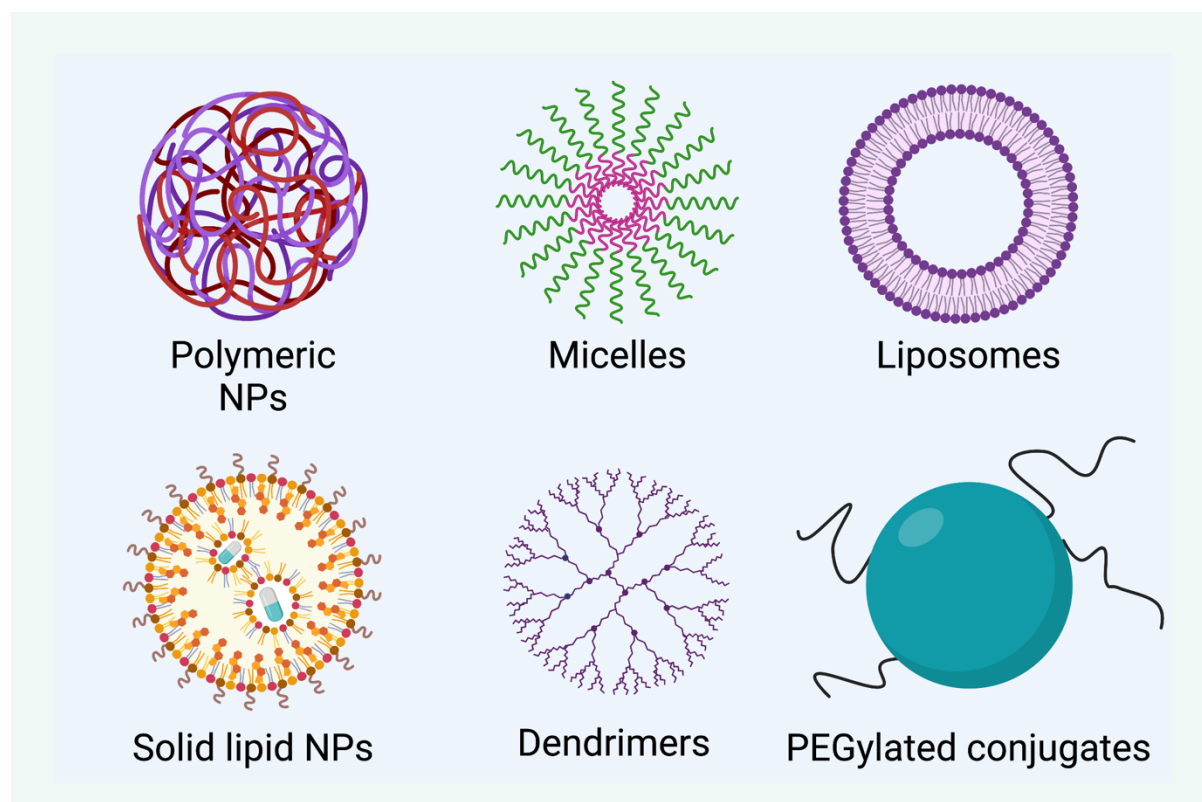


Figure 3 Examples of particles used as drug delivery systems in nanomedicine (as reviewed by Mirza and Siddiqui, 2014; Vujačić Nikezić et al., 2020; Loira-Pastoriza et al., 2014). Created with BioRender.com.

known examples is PEGylated liposomal doxorubicin (Doxil®), used in the treatment of Karposi's sarcoma<sup>85</sup> and ovarian cancer,<sup>86</sup> which was approved by FDA in 1995.<sup>87</sup>

Nanocarriers that have a biological component can be classified into three categories: 1) biogenic, 2) biomimetic or bioinspired, and 3) bioengineered (Fig. 4).<sup>88</sup> Nanocarriers which are not submitted to modification processes are defined as biogenic (e.g. extracellular vesicles derived from *Lactobacillus sp.* which are able to reduce the intestinal inflammatory response).<sup>89</sup> Carriers that imitate biological processes and features by synthetic means are classified as biomimetic or bioinspired (e.g. aspherical polymeric nanocarriers that imitate rod-shaped bacteria in order to be taken up by mammalian cells).<sup>90</sup> Bioengineered nanocarriers combine natural and artificial components by the application of bioengineering methods (e.g. extracellular vesicles loaded with drugs<sup>91</sup> and polymeric nanoparticles functionalized with bacterial proteins).<sup>92</sup>

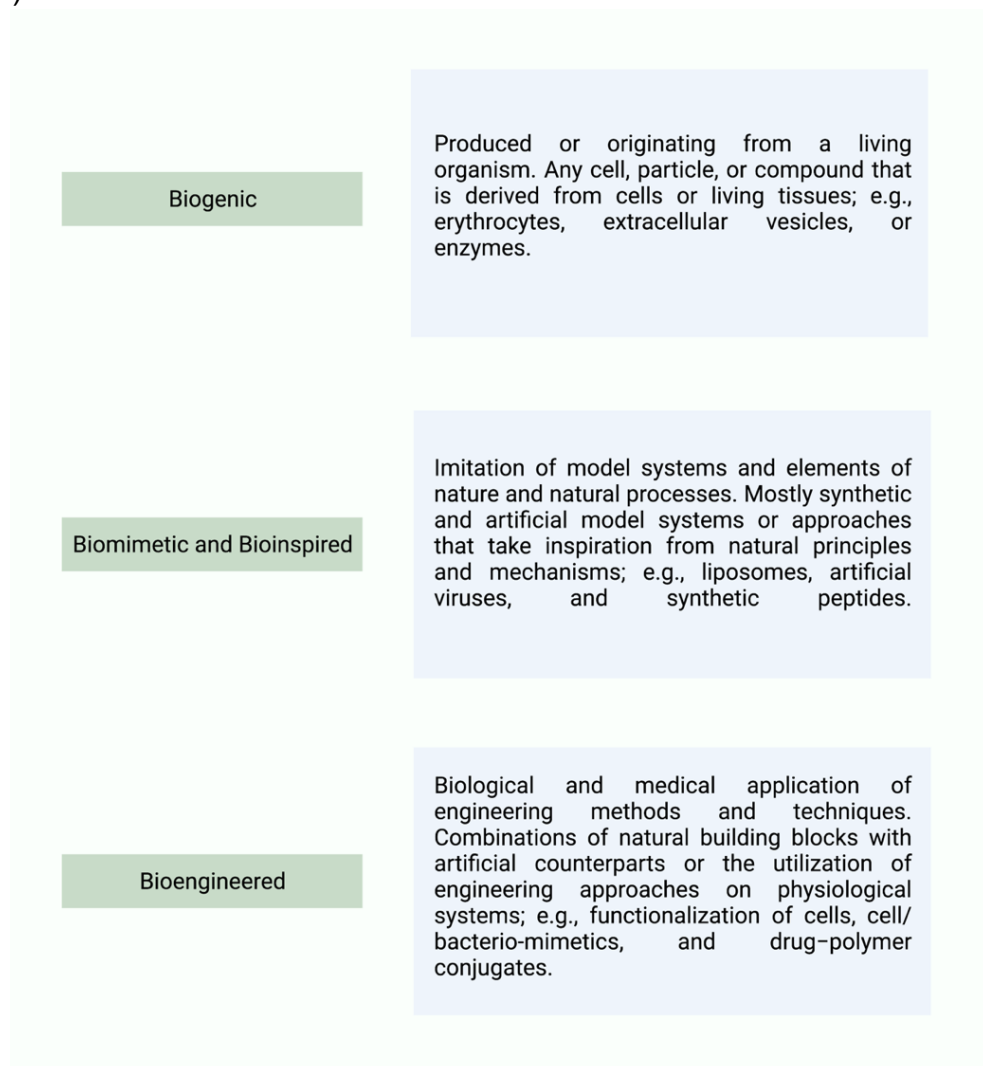


Figure 4 Definitions of biocarriers (Goes & Fuhrmann, 2018).

In the present work, attention is focused on extracellular vesicles (EVs), an example of biogenic nanocarriers. EVs is the general term used to describe lipid-bound particles that are shed by all types of organisms as a way to communicate between their own species.<sup>93–96</sup> They are classified according to their biogenesis, size and cargo. The EVs derived from mammalian cells are classified into two groups: microvesicles, derived from the plasma membrane and with a size range of 50-500 nm, but up to 1  $\mu\text{m}$ , which include microvesicles, bebbing vesicles, shedding vesicles, oncosomes, migrasomes, neurospheres and apoptotic bodies; and exosomes, derived from the endosome and with a size range of 50-150 nm, which includes prostasomes, tolerosomes, dexosomes, nanovesicles, exosome-like vesicles and others (Fig. 5).<sup>94</sup>

Over the last few years, extracellular vesicles have been studied and explored for their possible use in the drug delivery field<sup>77,97–99</sup> and diagnostics as a biomarker.<sup>100–103</sup> Their main advantage over synthetic nanocarriers is their inherent biocompatibility *in vivo*.<sup>104–108</sup> EVs can be isolated from bodily fluids (e.g. blood<sup>109</sup>, urine<sup>110</sup>, breast milk<sup>111</sup>), fruit juice (e.g. strawberry<sup>112</sup>) and bacterial cultures<sup>93,113</sup> through several methods, which should be selected considering the initial volume of fluid and resulting EV yield, among other factors. Isolation methods include ultracentrifugation (UC), density gradient UC, size exclusion chromatography (SEC) and ultrafiltration. Commercial kits aimed to isolated EVs mainly as a tool for diagnostics are also available (e.g. ME-kit, a peptide affinity precipitation kit).<sup>114,115</sup> All the mentioned methods have their advantages and drawbacks. For example, UC is a versatile method that results in a medium EV yield, but can be time consuming and the resulting pellet is low in purity.<sup>108</sup> On the other hand, SEC is a reproducible method that maintains the integrity and activity of the EVs, but runs can take up to several hours, depending on the sample, and the resulting volume of EV suspension is low.<sup>108</sup> In order to have a high yield of EVs with a high purity, a combination of isolation and purification methods may be applied.

In the context of cancer treatment, infectious and other diseases, extracellular vesicles derived from mammalian cells have to normally undergo bioengineering processes for drug loading, in order to carry antibiotics and deliver them to the desired

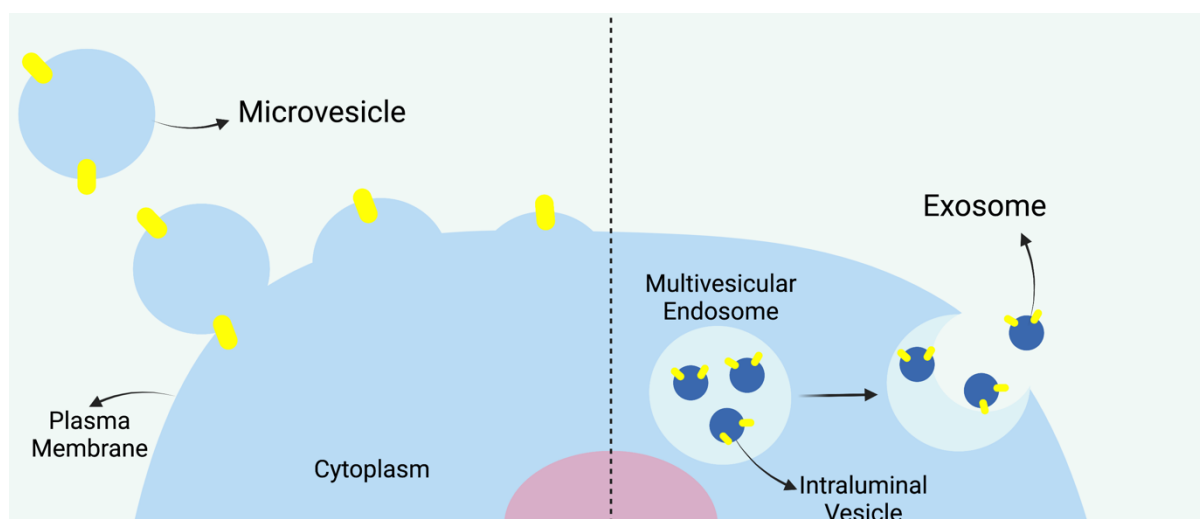


Figure 5 Scheme of the biogenesis of microvesicles and exosomes from mammalian cells. Created with BioRender.com.

site.<sup>91,116</sup> The loading of the desired molecule can happen by different methods. Hydrophobic compounds can be loaded into extracellular vesicles by co-incubation, due to the lipidic composition of their membranes, and this can be achieved by a simple protocol.<sup>117</sup> As an example, the anti-inflammatory and antioxidant compound curcumin has been loaded into EL-4-derived EVs by incubation at 22 °C for 5 min.<sup>118</sup> The anticancer drugs doxorubicin and paclitaxel have also been successfully loaded into EVs by incubation at 37 °C for 2 h.<sup>119,120</sup> Linezolid was also reported to be loaded into RAW 264.7-derived EVs at 37 °C for 1 h to treat intracellular methicillin-resistant *Staphylococcus aureus*.<sup>91</sup> Physical methods of drug loading include sonication, electroporation and extrusion, which can be used to load hydrophilic molecules, such as nucleic acids, into the EVs.<sup>117</sup> For example, miRNA-155 has been successfully loaded into B cell-derived EVs through electroporation, using high voltages, ranging between 0.14 kV to 0.2 kV, and a total EV protein concentration of 500 mg/mL to 1000 mg/mL.<sup>121</sup> Even though sonication is a less-reported method of physical cargo loading, it can be more efficient than electroporation in some cases.<sup>117</sup> For instance, paclitaxel and doxorubicin were reported to be successfully incorporated into EVs by sonication, which was followed by an incubation time of 60 min at a temperature of 37 °C to allow for the recovery of the EV membrane.<sup>122</sup> This method, however, must be applied with care, because disintegration of the EV membrane can occur.<sup>117</sup>

### 1.3 Myxobacteria and their outer membrane vesicles

Myxobacteria are a group of microbes which is part of the proteobacteria, a major phylum of Gram-negative microorganisms. They were first described by Roland Thaxter in 1892, being previously considered unusual fungi.<sup>123</sup> Their prefix “myxo” is due to a defining and specific characteristic of the myxobacteria: the production of mucus or slime.<sup>124</sup> They are mostly soil-living microorganisms<sup>125,126</sup> and they have engines that allow them to move by gliding.<sup>127</sup> When no nutrients are available, they form multicellular, species-specific, macroscopic fruiting bodies in order to survive.<sup>128,129</sup> When nutritional resources are available or in the presence of other bacteria, they aggregate and form swarms, releasing compounds that assist them in this digestion process.<sup>124,128</sup> During this process, the myxobacterial cells form mobile waves and, when they collide, they form mounds that become fruiting bodies and restart their predatory cycle (Fig. 6).<sup>130</sup>

Among the compounds produced by myxobacteria when they prey on other microorganisms and form swarms are natural antibiotics, which make them an

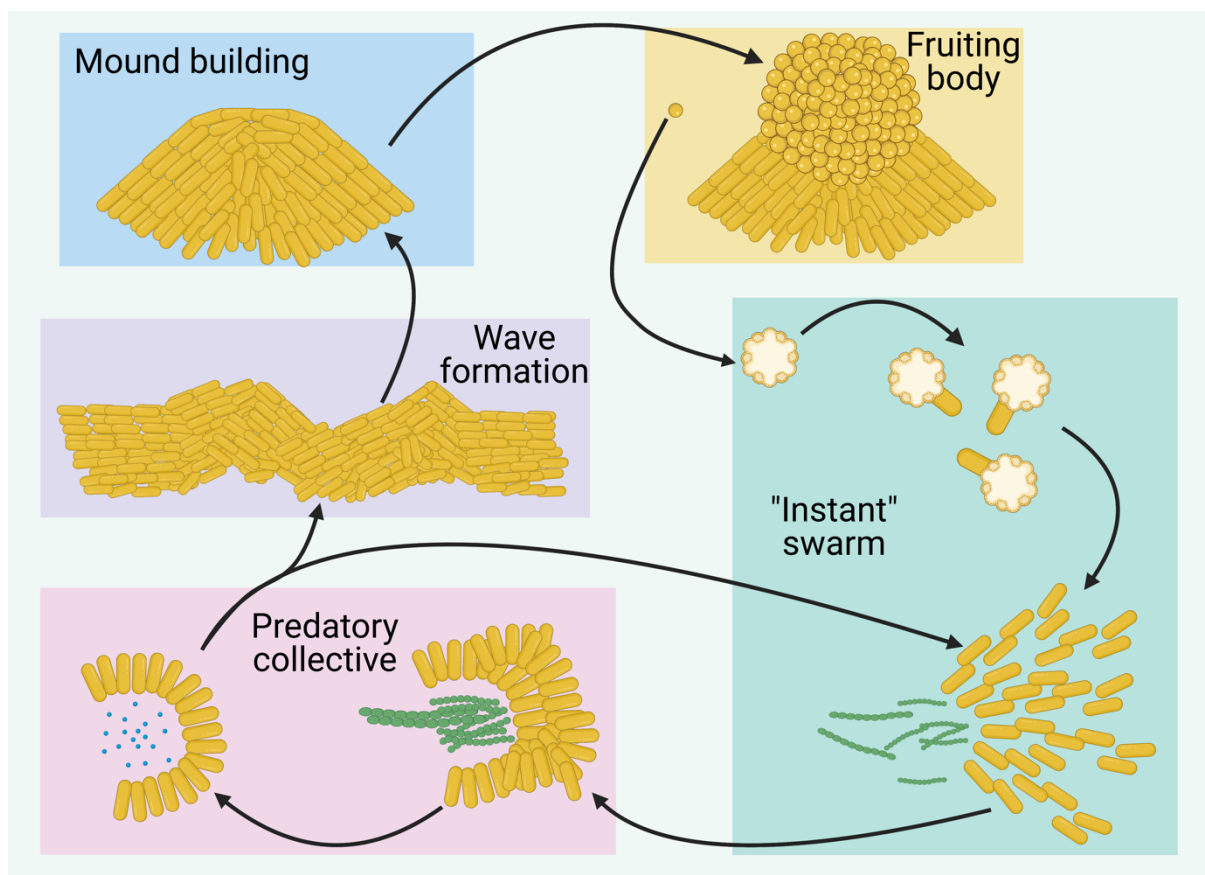


Figure 6 Scheme of *Myxococcus xanthus*' predatory cycle, a model myxobacterium. (Kaiser et al., 2010; Munoz-Dorado et al., 2016.) Created with BioRender.com.

attractive subject of study.<sup>131–135</sup> One species which has been extensively studied is *Myxococcus xanthus*. Like all myxobacteria, this species lives in the soil and preys on other bacteria<sup>136–138</sup> and is able to shed outer membrane vesicles (OMVs), which are a type of extracellular vesicle specifically shed by Gram-negative microorganisms.<sup>113,139</sup> Evans and collaborators proposed that OMVs might play a role in this predatory behavior, by packing the unknown antimicrobial compounds produced by *M. xanthus* into them and being released during the predation process.<sup>140</sup> Later, several antibiotic compounds were identified in *M. xanthus* OMVs, including Cittllin A, Mylalamids A, B and C and Myxoviresxin A, elucidating their previously described antibacterial activity against *Escherichia coli*.<sup>141</sup>

The evidence of myxobacterial OMVs maintaining the antibacterial characteristics of their “mother-cell” makes them an attractive potential drug delivery system to treat infections. Their potential as a vaccine has already been vastly explored.<sup>142–144</sup> Like EVs from mammalian cells, OMVs are spherical, phospholipid-bound nanoparticles. However, they present an inner leaflet, derived from the outer membrane of Gram-negative bacteria, and an outer leaflet of lipopolysaccharide (LPS).<sup>113,145–147</sup> OMVs can be formed by two mechanisms: 1) outer membrane bebbing, which can be triggered by iron deficiency in their environment, signaling molecules, compounds which are hydrophobic and the presence of antibiotics; and 2) explosive cells lysis, which is triggered by agents that damage nucleic acids, enzymes and antibiotics (Fig. 7).<sup>139,148,149</sup> By outer membrane bebbing, traditional OMVs are formed, consisting of a single membrane and surface proteins of their “mother-cell”.<sup>139</sup> Through explosive cell lysis, outer inner membrane vesicles (OIMV) are formed, consisting of peptidoglycan between two membranes<sup>139,150</sup> and explosive outer membrane vesicles (EOMV) are also formed (Fig. 8).<sup>139,148</sup> OMVs formed through explosive cells lysis are able to carry diverse molecules, proteins and nucleic acids derived from their “mother-cell”.<sup>148,151,152</sup> The OMV biogenesis in *M. xanthus* has been reported to happen anywhere along the outer membrane by the detachment of a single OMV or through chain-like structures that remain attached to the myxobacterial cell.<sup>141,153,154</sup>

Other species of myxobacteria also present a predatory behavior, the production of natural antibacterial compounds and are also able to produce OMVs. That is the case for *Cystobacter velatus* Cbv34 and *Cystobacter ferrugineus* Cbfe23.

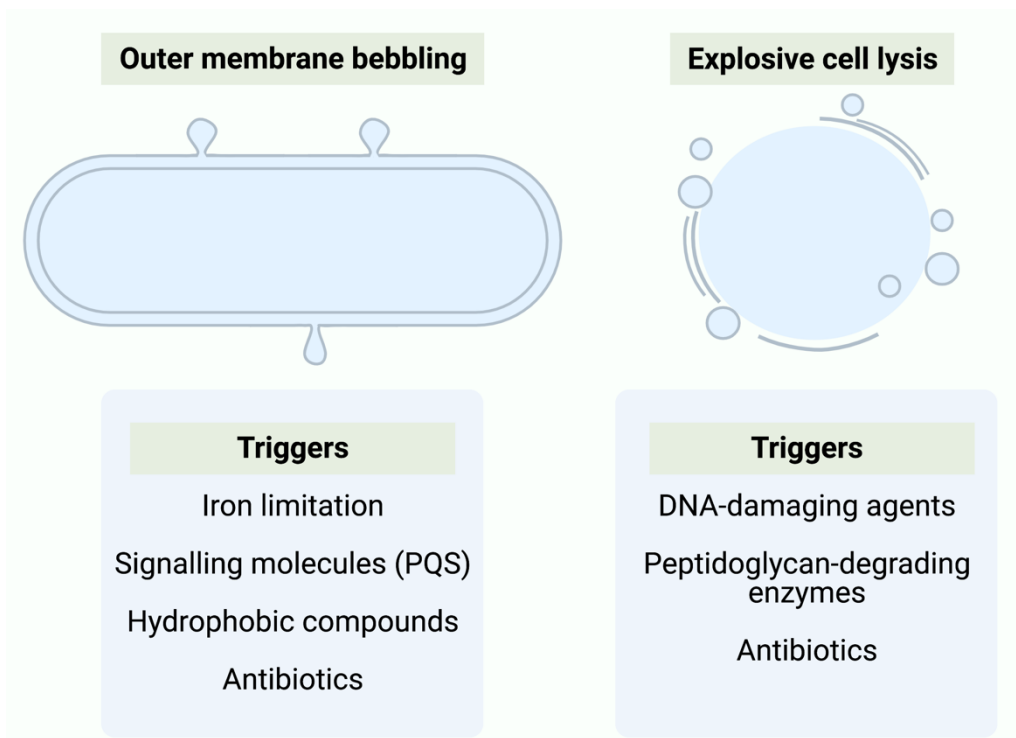


Figure 7 Mechanisms and triggers of outer membrane vesicle formation (as reviewed by Toyofuku et al., 2019). Created with BioRender.

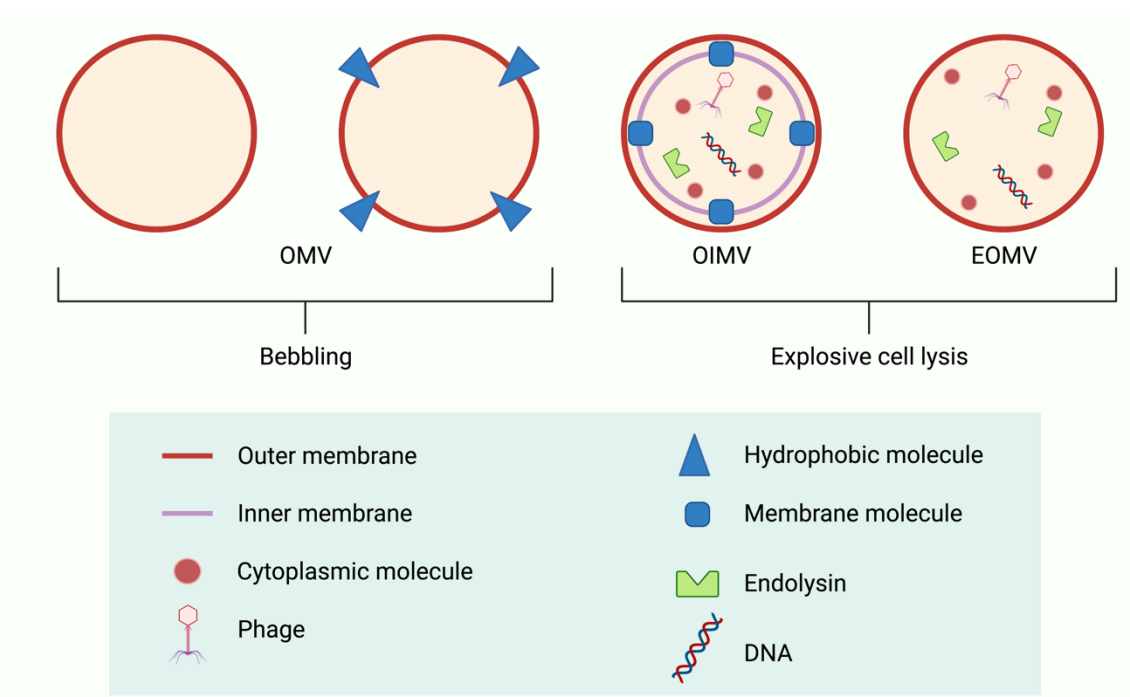


Figure 8 Types of outer membrane vesicles and their content. OMV: outer membrane vesicle; OIMV: outer inner membrane vesicle; EOMV: explosive outer membrane vesicle (as reviewed by Toyofuku et al., 2019). Created with BioRender.

*C. velatus* Cbv34 and *C. ferrugineus* Cbfe23 are myxobacterial species of the order Myxococcales, the suborder Cystobacterineae, the family Cystobacteraceae and the genus Cystobacter.<sup>155</sup> *C. velatus* Cbv34 was isolated from the soil in Rajasthan, India, in April 1995.<sup>156</sup> Crude extracts of *C. velatus* Cbv34 were able to inhibit the proliferation of several Gram-negative and Gram-positive microbes.<sup>157</sup> Upon liquid chromatography-high resolution mass spectrometry (LC-HRMS), three types of cystobactamids were identified: 919-1, 919-2 and 507.<sup>157</sup> Cystobactamids are peptides of broad-spectrum antibacterial activity. They are topoisomerase inhibitors, their main target being the bacterial gyrase.<sup>134,157</sup> The yield of cystobactamid obtained from *C. velatus* Cbv34 cultures was very low, necessitating chemical synthesis or the employment of advanced bioengineering and biotechnological processes for further development of the compound.<sup>134,157</sup> Recently, the expression of cystobactamids in a heterologous host to increase the yield of the compound produced has been described.<sup>158</sup> *C. ferrugineus* Cbfe23 was isolated from the soil in China in 1982.<sup>159,160</sup> Upon cultivation and extraction, cystodienoic acid was identified as a product of *C. ferrugineus* Cbfe23, which did not show any significant antibiotic effect, but exhibited a cytotoxic effect against the human colon cancer cell line HCT-116.<sup>160</sup>

As both myxobacteria strains are Gram-negative microorganisms and produce compounds which are active against pathogens and/or mammalian cells, their OMVs are an interesting subject of study, since they can maintain the characteristics of their “mother-cells” and potentially carry such antibiotic compounds and be applied as a biogenic drug delivery system. Therefore, in my thesis, we focus on the potential use of myxobacterial OMVs against infections caused by planktonic bacteria, intracellular bacteria, and bacterial biofilms.

## 2 AIMS OF THIS THESIS

The main goal of my research was to determine the potential of OMVs derived from the myxobacterial strains *Cystobacter velatus* Cbv34 (Cbv-OMVs) and *Cystobacter ferrugineus* Cbfe23 (Cbfe-OMVs) in treating intracellular infections and bacterial biofilm formation.

To achieve this goal, this thesis was aimed to successfully isolate, purify and characterize the OMVs. Subsequently, their effect on mammalian cells was studied through viability and toxicity assays, their influence on the release of pro-inflammatory cytokines and their interaction with bacterial and mammalian cells. Their effects on the viability of planktonic bacterial cultures were also studied, where different concentrations of OMV suspensions were used to treat planktonic bacteria of different species.

Finally, the antibacterial effect of the OMVs in an infected monoculture model of mammalian cells with *S. aureus*, treated with different concentrations of OMV suspensions was studied. Their effects against different biofilm models were also studied. Biofilms were grown on surfaces and in a microfluidic device under a constant flow. Then, they were treated with different concentrations of OMV suspensions to evaluate their ability to disrupt and prevent the formation of mature biofilms.

In summary, the main steps to achieve the aims of this research are listed below:

- (1) Myxobacterial culture, isolation and characterization of Cbv and Cbfe-OMVs.
- (2) The effect of myxobacteria-derived OMVs on mammalian cells.
- (3) The antibacterial effect of myxobacteria-derived OMVs against planktonic bacteria.
- (4) The antibacterial effect of myxobacteria-derived OMVs against intracellular infections.
- (5) The effects of myxobacteria-derived OMVs on biofilms.

### 3 MAJOR OUTCOMES OF THE THESIS

In this chapter, the main findings of three peer-reviewed, original papers are summarized and their main results presented. Results presented in different publications were combined to facilitate comprehension.

This chapter refers to the following publications:

Schulz, E., **Goes, A.**, Garcia, R., Panter, F., Koch, M., Müller, R., Fuhrmann, K., & Fuhrmann, G. (2018). Biocompatible bacteria-derived vesicles show inherent antimicrobial activity. *Journal of Controlled Release*, 290(September), 46–55. <https://doi.org/10.1016/j.jconrel.2018.09.030>

**Goes, A.**, Lapuhs, P., Kuhn, T., Schulz, E., Richter, R., Panter, F., Dahlem, C., Koch, M., Garcia, R., Kiemer, A. K., Müller, R., & Fuhrmann, G. (2020). Myxobacteria-Derived Outer Membrane Vesicles: Potential Applicability Against Intracellular Infections. *Cells*, 9(1), 194. <https://doi.org/10.3390/cells9010194>

**Goes, A.**, Vidakovic, L., Drescher, K., & Fuhrmann, G. (2021). Interaction of myxobacteria-derived outer membrane vesicles with biofilms: antiadhesive and antibacterial effects. *Nanoscale*. <https://doi.org/10.1039/D1NR02583J>

### 3.1 OMV isolation and characterization

*C. velatus* Cbv34 and *C. ferrugineus* Cbfe23 were activated by adding 500  $\mu$ L of a cryo stock to 100 mL conical flasks containing 20 mL of M-medium (*w/v*, 1.0% phytone, 1.0% maltose, 0.1% CaCl<sub>2</sub>, 0.1% MgSO<sub>4</sub>, 50 mM HEPES, pH adjusted to 7.2 with KOH) at 30 °C and 180 rpm<sup>157</sup> until the cultures were turbid, which takes three to five days. Then, the cultures were upscaled using 300 mL conical flasks by diluting the initial culture in 80 mL M-medium. Occasionally, cultures were upscaled to volumes up to 500 mL. The cultures were incubated until the stationary growth phase was reached, when they were split. OMVs were successfully isolated from *C. velatus* Cbv34 and *C. ferrugineus* Cbfe23 liquid cultures, which were at least 4 passages old, through ultracentrifugation alone or combined with size exclusion chromatography (SEC) (Fig. 9).

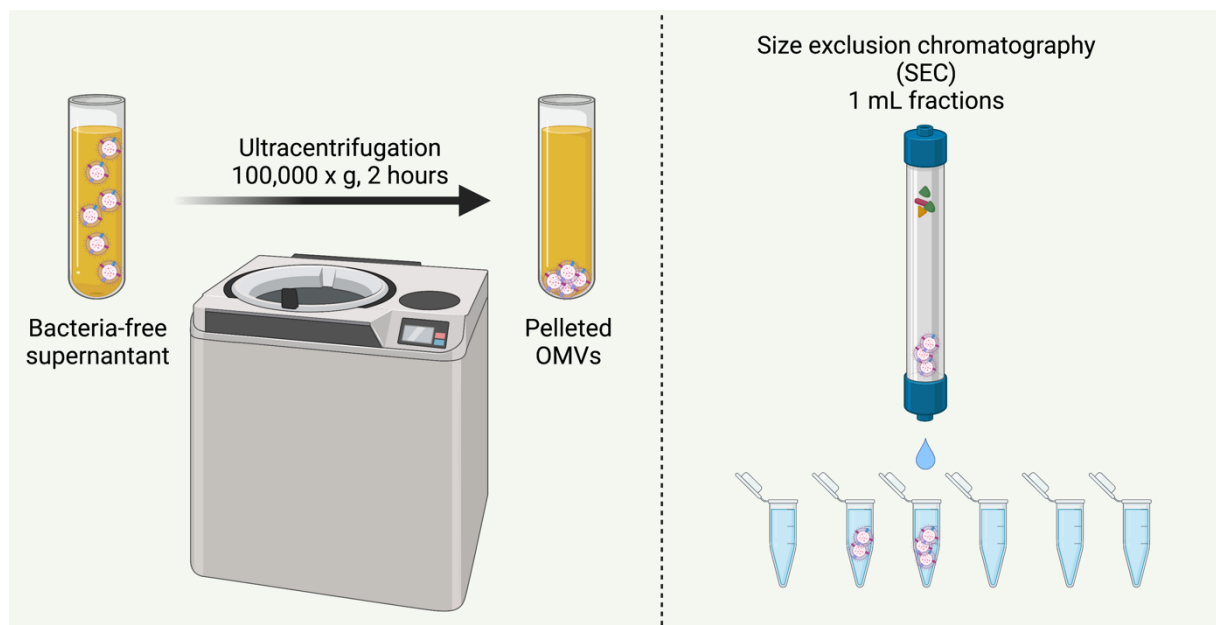


Figure 9 Scheme summarizing the OMV isolation methods used. First, the myxobacterial culture is submitted to differential centrifugation. Then, the resulting pellet is resuspended in buffer and submitted to size exclusion chromatography (SEC) for purification. Created with BioRender.com.

The main fractions of purified OMVs presented a size of  $180 \pm 18$  nm and  $126 \pm 13$  nm and a zeta potential of  $-4.7 \pm 0.6$  mV and  $-5.3 \pm 0.7$  mV for Cbv-OMVs and Cbfe-OMVs, respectively. Crude OMV pellets (without SEC purification) of Cbv34 presented OMVs with a size of  $121.1 \pm 9.6$  nm, while Cbfe23-OMVs had a size of  $101.6 \pm 2.5$  nm. Through cryogenic electron microscopy (Cryo-TEM), the OMVs revealed a spherical shape and were electron-dense with a well-formed membrane (Fig. 10).

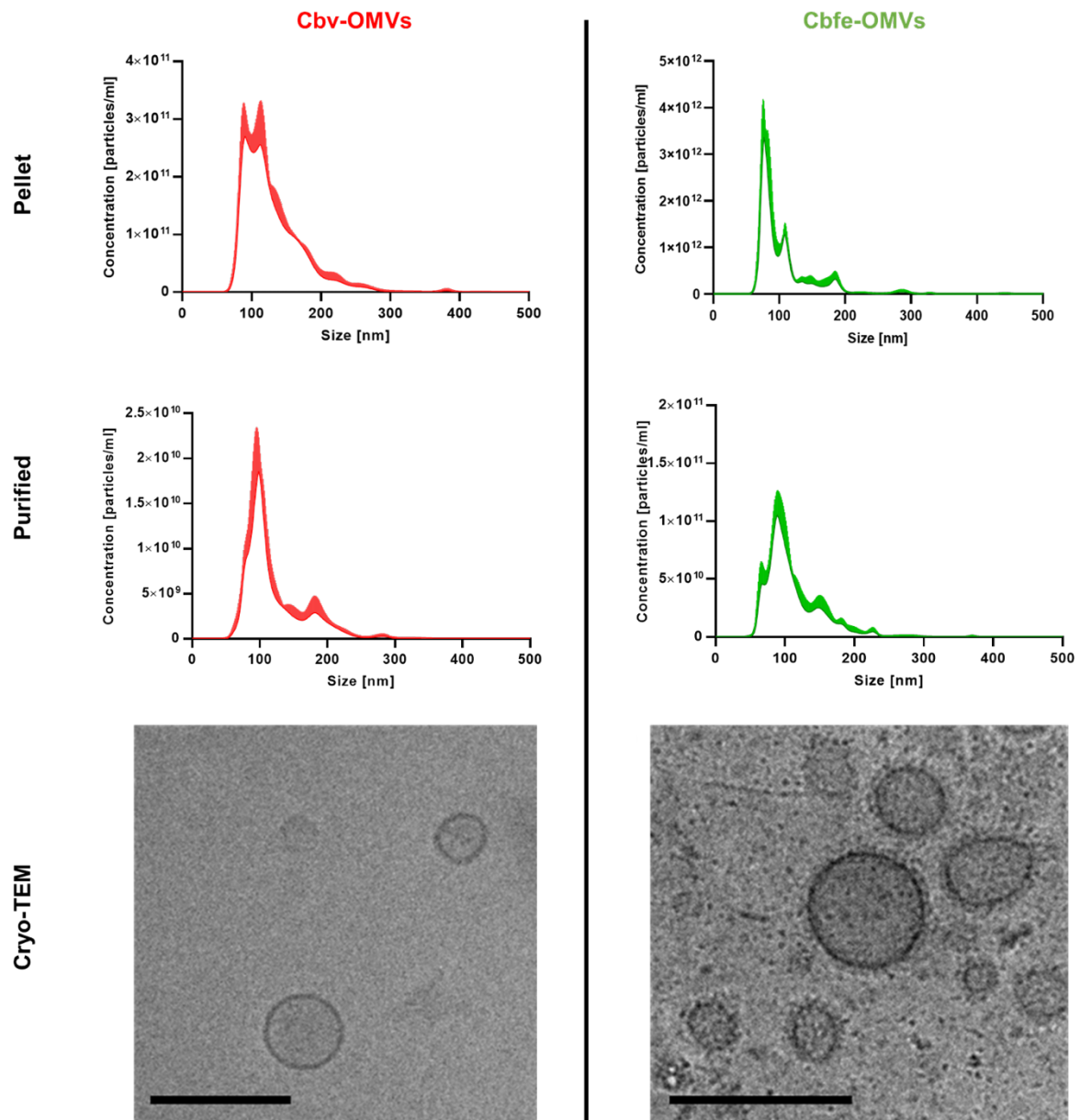


Figure 10 Representative graphs of OMV particle distribution in pellets and purified fractions, and morphology assessed by cryogenic transmission electron microscopy (Cryo-TEM). Scale bars: 200  $\mu$ m. Data from Goes, et al. 2020.

### 3.2 The effects of myxobacterial OMVs on mammalian cells

The Cbv and Cbfe-23 were tested on mammalian cell lines in order to assess possible toxicity. Through LDH assay, no significant cytotoxic effects were observed after A549 (adenocarcinomic human alveolar basal epithelial cells), RAW 264.7 (murine macrophage-like cells) and dTHP-1 cells (differentiated human monocytic cells) were treated for 24 h. However, when the viability was assessed with PrestoBlue assay, a decrease in the cells' viability was observed when they were treated with Cbfe23-OMVs in the highest concentration  $1.25 \times 10^6$  particles/cell with A549 and RAW

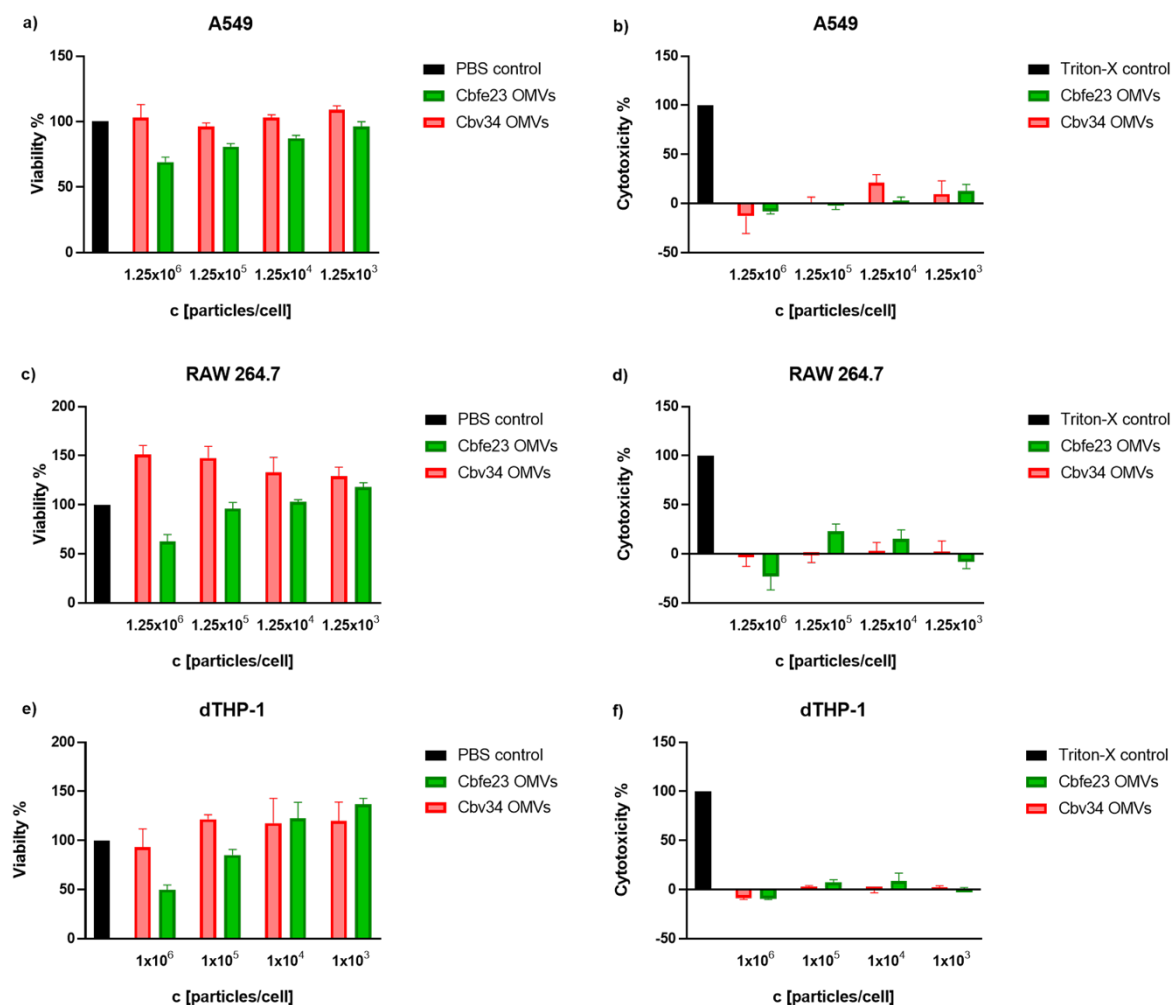


Figure 11 Cell viability and cytotoxicity assays of Cbv and Cbfe23-OMVs with different cell lines. Cbv34-OMVs do not affect the viability of cells and even stimulates the proliferation of RAW 264.7 cells when used in the highest concentration (c). Cbfe23-OMVs has a negative impact on cell viability when used in the highest concentration. Neither OMVs presented a cytotoxic effect against the cell lines tested.

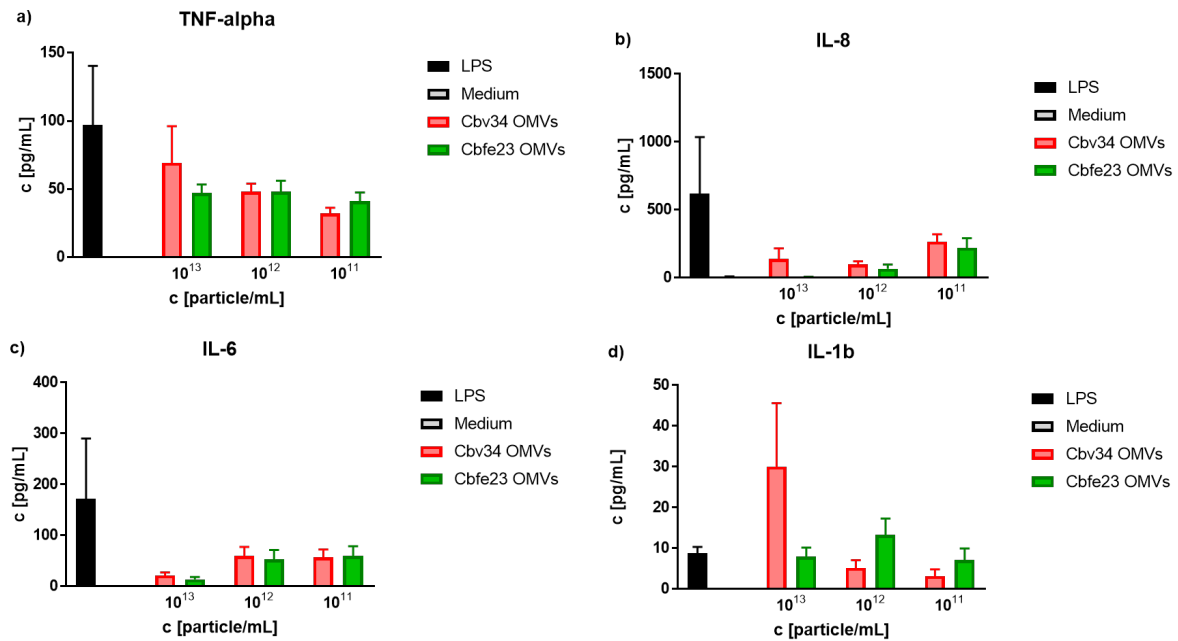


Figure 12 Pro-inflammatory cytokine release by peripheral blood mononuclear cells (PBMCs) upon treatment with Cbv34 and Cbfe23-OMVs. Data from Goes, et al. 2020.

264.7 and  $1 \times 10^6$  particles/cell with dTHP-1 cells. This effect was seen especially on dTHP-1 cells, where the viability decreased approximately 50% (Fig. 11). Upon analysis with a cytometric bead array assay, it was possible to verify that OMV treatment did not exert a significant release of the pro-inflammatory cytokines TNF-alpha, IL-8, IL-6 and IL-1b (Fig. 12), which perform an essential role in host defense by regulating the functions of the immune system.<sup>161</sup> These results display a possible safe therapeutic window for the use of Cbfe-OMVs and that Cbv-OMVs appear not to impact cell viability even in very high concentrations. Additionally, they do not exert cytotoxic effects on mammalian cells.

### 3.3 The effects of myxobacterial OMVs on planktonic bacteria

Purified fractions of Cbv and Cbfe-OMVs were incubated with *Escherichia coli* DH5-alpha and *Staphylococcus aureus* Newman in order to assess their potential antibacterial activity. The OMVs inhibited the growth of *E. coli* DH5-alpha, greatly decreasing their viability (Fig. 13 a and b). This effect persisted even after four weeks of OMV storage at 4 °C (Fig. 13 d). The vesicles were also able to decrease the viability of planktonic *S. aureus* Newman, proving they are effective against Gram-negative and Gram-positive microbes. This effect is due to their cystobactamid<sup>157,162</sup> cargo, which was confirmed by LC-MS analysis (see subchapters 6.2 and 6.3). Since the OMVs are isolated from the stationary growth phase, most of them are possibly formed through explosive cell lysis and this biogenesis mechanism allows the resulting vesicles to have diverse cargos, such as proteins, DNA and other molecules that can also contribute to their antibacterial activity.<sup>139,163</sup>

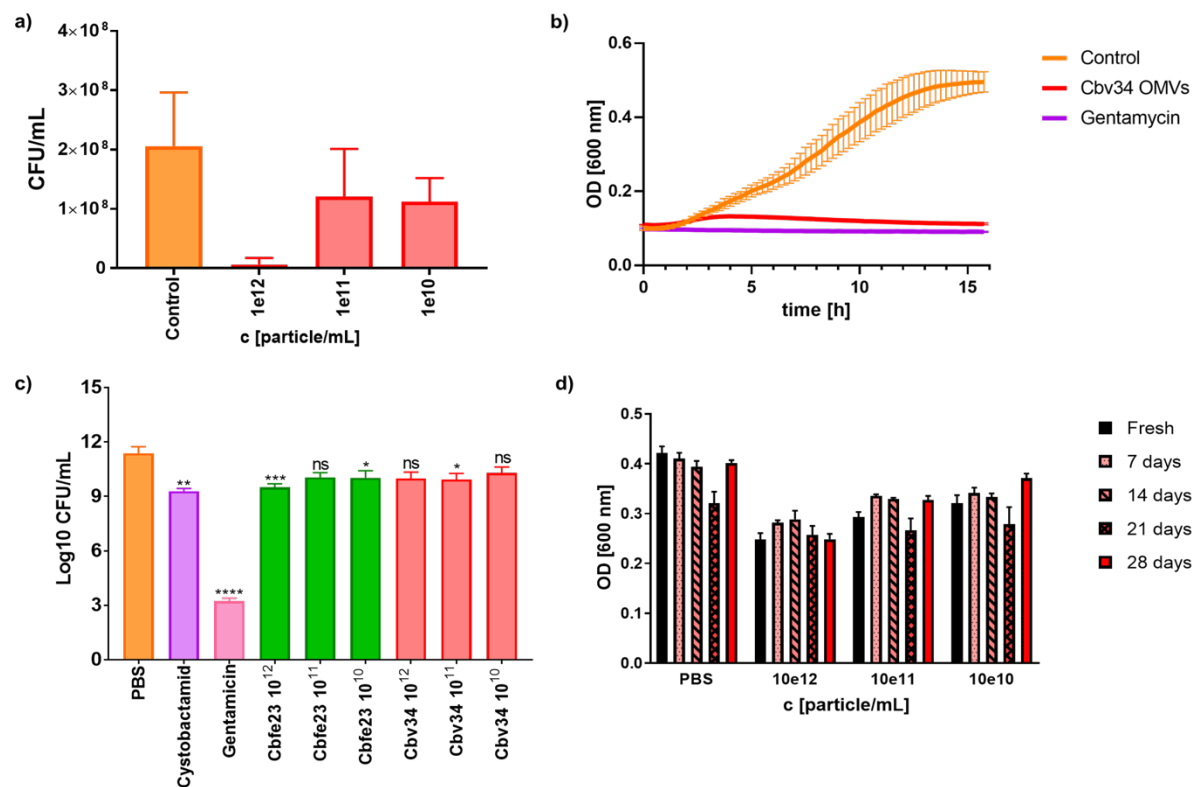


Figure 13 Antibacterial activity of Cbv34 and Cbfe23-OMVs against *E. coli* (a, b and d) and *S. aureus* (c).

### 3.4 The effects of myxobacterial OMVs against intracellular infections and biofilm formation

One of the ways in which bacteria escape treatment with antimicrobial therapy is by becoming intracellular.<sup>10,164,165</sup> Therefore, the ability of OMVs to fight intracellular infections was tested. A549 cells were infected with *S. aureus* Newman and then treated with gentamicin to kill the extracellular bacteria.<sup>91,166</sup> Then, the cells were treated with the myxobacterial OMVs for 24 h. The number of viable bacteria after treatment was assessed by colony forming unit (CFU) inoculation and counting (Fig. 14). After the treatment, free gentamicin, free, cystobactamid and the DMSO (dimethyl sulfoxide) control (solvent used with cystobactamid, which is not soluble in water) had a comparable effect on the *S. aureus* growth. When compared to the untreated control PBS, free cystobactamid had a significant antibacterial effect (Fig. 15).

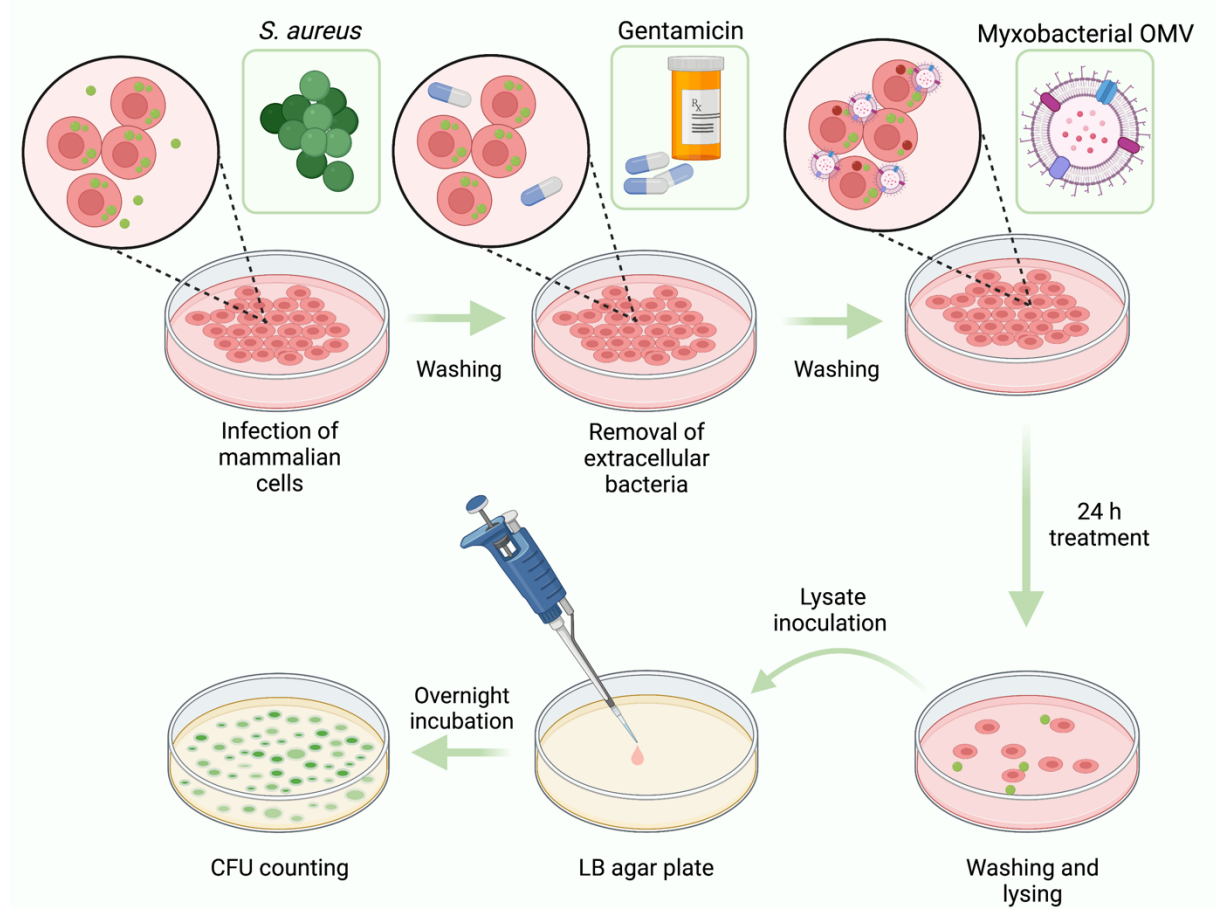


Figure 14 Scheme of the intracellular infection assay. Created with BioRender.com.

The highest concentration did not present a significant antibacterial effect when compared to the untreated control. This might be due to their negative impact on the viability of mammalian cells when used in high concentrations, as seen in subchapter 3.2. Yet, when the second highest concentration ( $10^8$  particles/mL) was used, a significant antibacterial effect was recorded. Cbv34-OMVs had a highly significant antibacterial effect when the highest concentration ( $10^{11}$  particles/mL) was used, as expected. When the bacterial suspensions dilutions with the highest antibacterial effects were compared to the amount of bacteria internalized by A549 cells at the beginning of treatment (time zero), there was no statistical significance, highlighting the OMV ability to slow down the proliferation of cells, and indicating a bacteriostatic effect.<sup>167</sup>

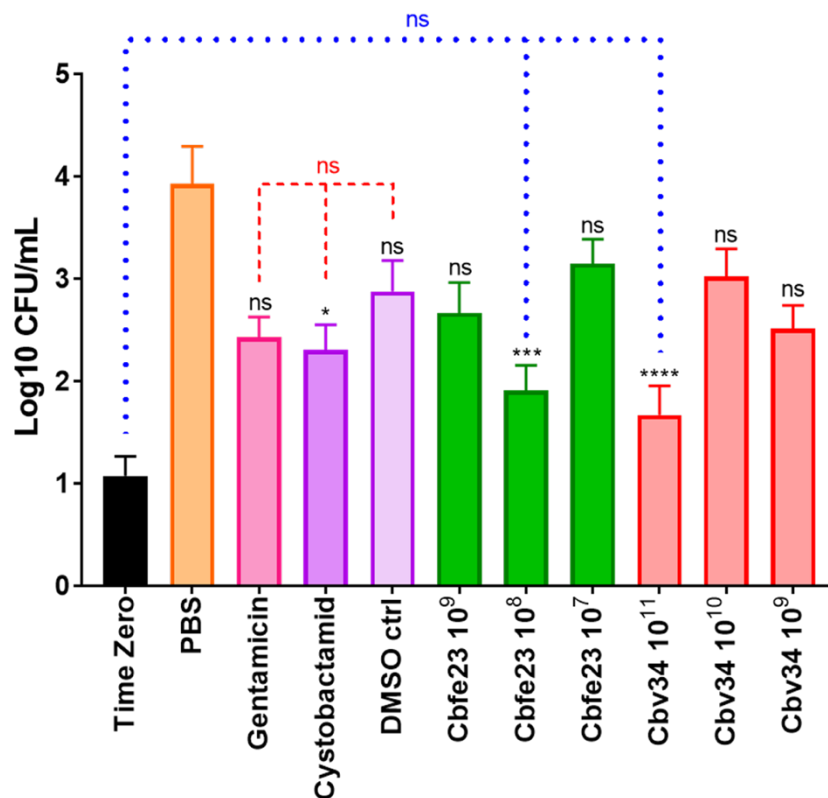


Figure 15 Antimicrobial activity of Cbv34 and Cbfe23-OMVs against intracellular *S. aureus* in A549 cells. Data from Goes, et al. 2020.

Another important way bacteria become resistant to antimicrobial treatment is by forming biofilm, as discussed in subchapter 1.1.<sup>43,45,168,169</sup> In order to test the effects of the myxobacteria on biofilms, *E. coli* TG1, a strain able to produce thick, mature biofilms,<sup>170</sup> was inoculated on glass coverslips inserted on 24-well plates and incubated at 37 °C and 5% CO<sub>2</sub> for 72 h (Fig. 16). Then, unattached bacteria were removed, and the wells were washed before being treated with different concentrations of myxobacterial OMV dilutions and the controls LB medium, PBS and cystobactamid for 24 h. Afterwards, the bacteria attached to the glass coverslips were dehydrated and prepared for scanning electron microscopy (SEM) to assess biofilm formation and attachment (Fig. 17 a). The glass coverslips treated with LB medium and PBS presented biofilm covering the entire coverslip surface, as expected. Cystobactamid did not inhibit bacterial attachment to the coverslip surface. However, the coverslips treated with the highest concentrations of Cbfe and Cbv-OMVs did not present bacterial cells adherent to their surfaces.

This result shows the myxobacterial OMVs' potential ability to detach biofilm from other surfaces and materials. In addition, the presence of viable bacterial cells was studied through fluorescence microscopy and fluorescence intensity assessment with a plate reader, by staining the biofilm with the bacterial cell viability kit LIVE/DEAD BacLight. No biofilm formation was detected after the treatment (Fig. 17 b) and the fluorescence intensity of viable cells was significantly lower when treated with both OMVs when compared to the control PBS (Fig. 18 a). The vitality of the bacterial biofilm was assessed through staining with the BacLight RedxSensor kit and flow cytometry (Fig. 18 b). The vitality of the bacterial biofilm cells significantly decreased upon treatment with the highest concentrations of Cbv and Cbfe-OMVs, when compared to both controls LB medium and PBS.

To investigate the effects of the myxobacterial OMVs on biofilms grown and maintained under flow conditions, a scenario significant in the cases of bacterial endocarditis and urinary tract infections, the pathogen *Staphylococcus epidermidis* was inoculated into a microfluidic flow chamber and then treated with the OMV suspensions and the controls TSB medium and unloaded bacteriomimetic liposomes (Fig. 19). After 8 h, the samples treated with TSB medium and the liposomes presented biofilm formation, which showed that the presence of particles such as the liposomes are not able to prevent biofilm formation under flow conditions. However,

samples treated with the myxobacterial OMV suspensions completely inhibited biofilm formation. These results evince myxobacterial OMVs' potential to treat and prevent infections caused by bacterial biofilms.

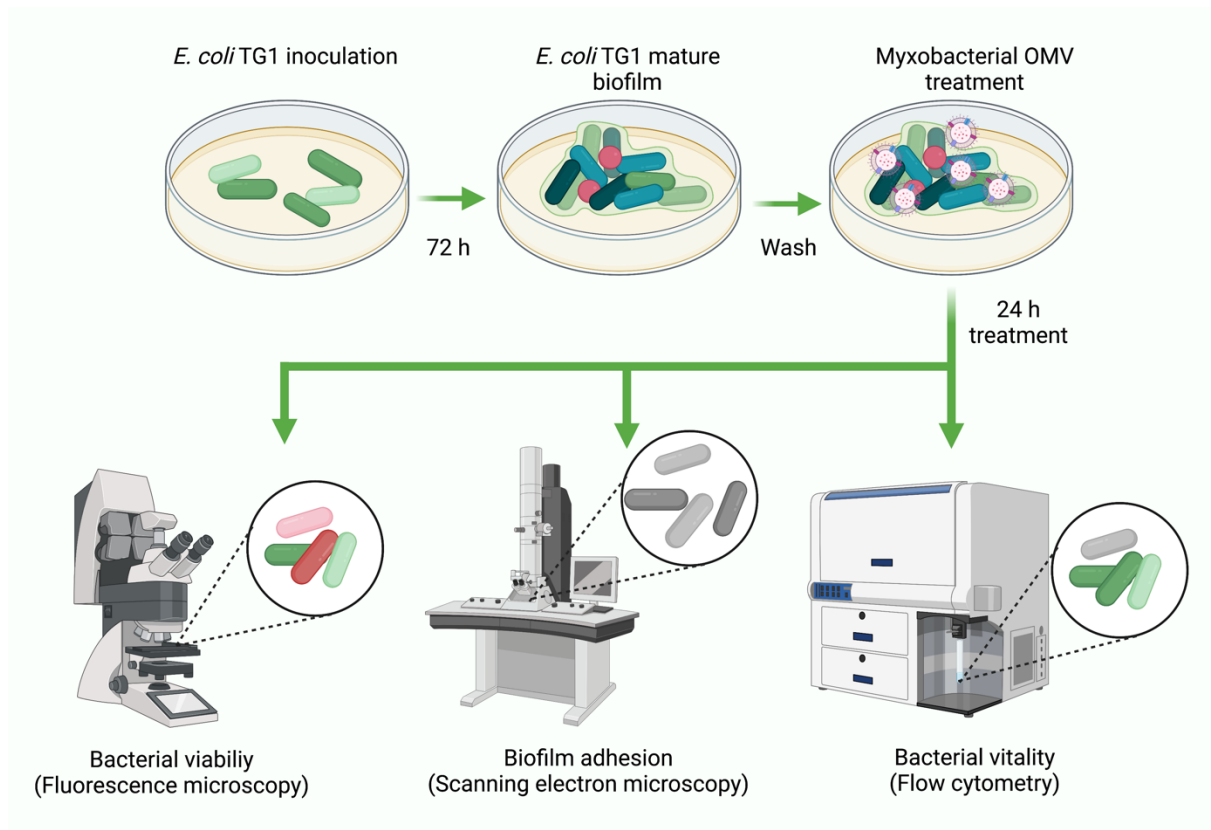


Figure 16 Scheme of the preformed biofilm assay. Created with BioRender.com.

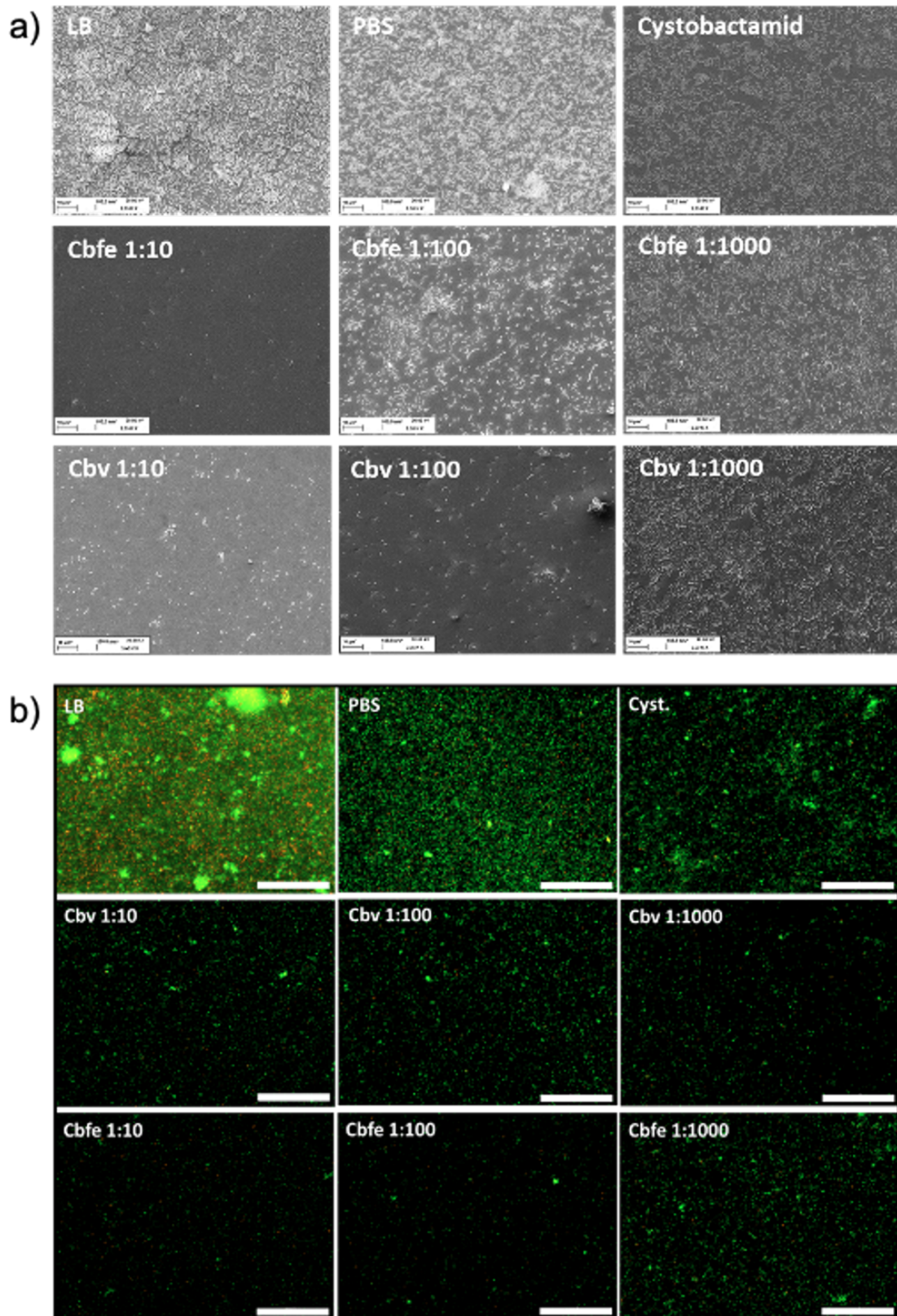


Figure 17 Effect of Cbv and Cbfe23-OMVs on preformed *E. coli* TG1 biofilms grown for 72 h and then treated for 24 h with controls and OMV dilutions. a) Scanning electron microscopy of biofilm grown on glass coverslips; b) Fluorescence microscopy of biofilms stained with Syto9 and propidium iodide (PI). Data from Goes, et al. 2021.

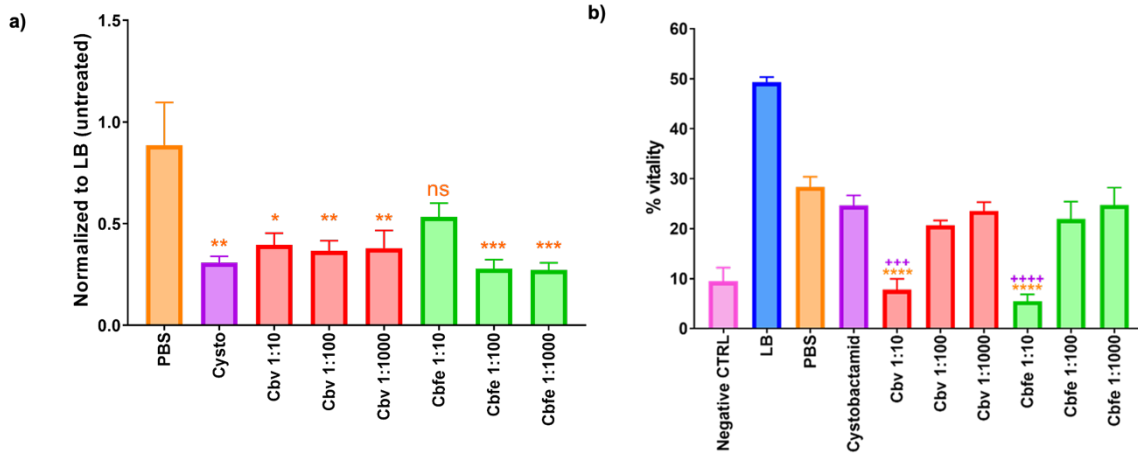


Figure 18 Effects of Cbv and Cbfe23-OMVs on preformed *E. coli* TG1 biofilms. a) Fluorescence intensity of Syto9 (viable bacteria) upon treatment with controls and OMV dilutions; b) Vitality of *E. coli* TG1 after treatment with controls and OMV dilutions Data from Goes et al., 2021.

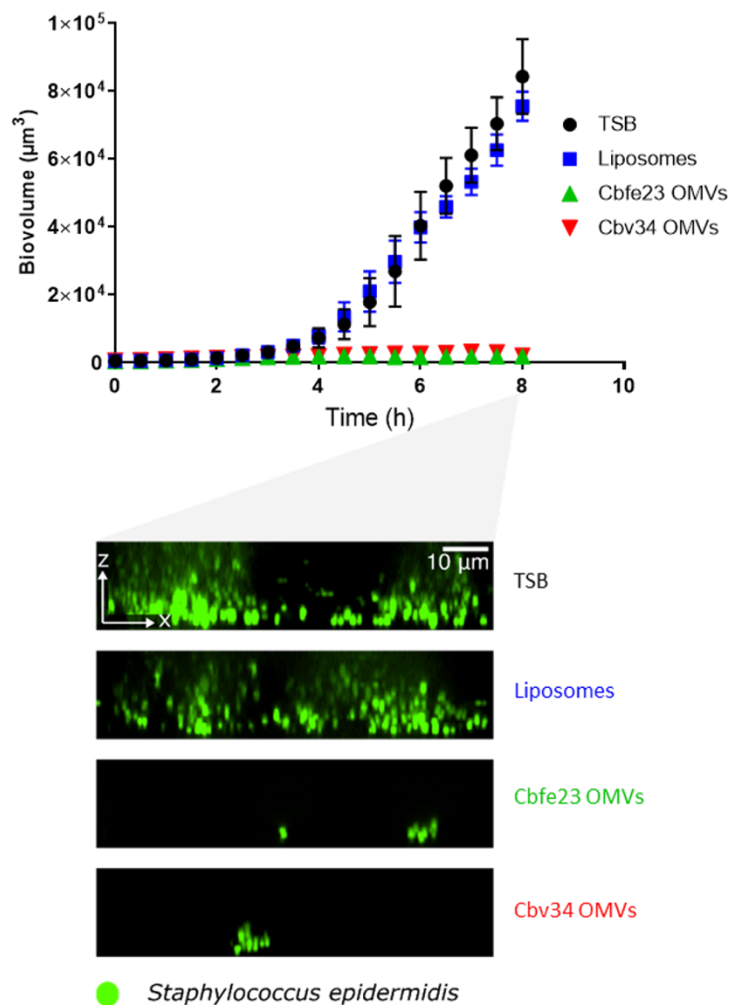


Figure 19 Effect of myxobacterial OMVs on a *S. epidermidis* biofilm grown and maintained under fluid flow conditions. Myxobacterial OMVs are able to prevent biofilm formation. Data from Goes et al., 2021.

## 4 CONCLUSIONS AND OUTLOOK

This work creates the foundation for the employment of inherently antibiotic-loaded outer membrane vesicles isolated from the myxobacterial species *Cystobacter velatus* Cbv34 and *Cystobacter ferrugineus* Cbfe23, natural producers of the potent antibiotic cystobactamid, as a novel drug carrier system for the treatment of infections caused by bacteria.

Promising results were obtained regarding their effects on mammalian cells, planktonic bacteria and infection models of intracellular infection and biofilm formation. This highlights their advantage over synthetic carriers, which normally need further functionalization and loading methods in order to have a targeted delivery, increased circulation time and therapeutic effect. The myxobacterial vesicles were able to be internalized by mammalian cells, a feature that enabled them to treat intracellular infection caused by *S. aureus in vitro*. The OMVs also showed an unprecedented antibiofilm activity, being able to detach preformed biofilm from glass surfaces, a model for biofilm grown on the surface of medical devices, and preventing their growth in a microfluidic device submitted to constant fluid flow, a model which mimics *in vivo* infections (e.g. bacterial endocarditis and urinary tract infections).

Considering the positive results obtained in this work, the antibacterial activity of Cbv and Cbfe-OMVs could be explored against other intracellular pathogens, such as *Mycobacterium abscessus*, an important pathogen responsible for persistent lung disease in patients with cystic fibrosis<sup>171–174</sup> and *Mycobacterium tuberculosis*.<sup>165,175</sup> The myxobacterial OMVs' ability to detach mature *E. coli* biofilms from glass surfaces also warrants the study of their effects on biofilms grown in other materials, such as metal alloys and zirconia, which are used in oral implants, and other rough surfaces.<sup>176,177</sup> Their effect on other important biofilm forming pathogens, including *Pseudomonas aeruginosa*,<sup>178</sup> *Helicobacter pylori*<sup>179</sup> and *Clostridium difficile*<sup>180,181</sup> would be beneficial to demonstrate myxobacterial OMVs' ability to overcome infections which are difficult to treat.

## 5 REFERENCES

1. Troeger, C. *et al.* Estimates of the global, regional, and national morbidity, mortality, and aetiologies of lower respiratory infections in 195 countries, 1990–2016: a systematic analysis for the Global Burden of Disease Study 2016. *Lancet Infect. Dis.* **18**, 1191–1210 (2018).
2. Naghavi, M. *et al.* Global, regional, and national age-sex specific mortality for 264 causes of death, 1980–2016: A systematic analysis for the Global Burden of Disease Study 2016. *Lancet* **390**, 1151–1210 (2017).
3. Machowska, A. & Lundborg, C. S. Drivers of irrational use of antibiotics in Europe. *Int. J. Environ. Res. Public Health* **16**, (2019).
4. Walsh, T. R. A one-health approach to antimicrobial resistance. *Nat. Microbiol.* **3**, 854–855 (2018).
5. Walsh, T. R. & Toleman, M. A. The new medical challenge: why NDM-1? Why Indian? *Expert Rev. Anti. Infect. Ther.* **9**, 137–141 (2011).
6. Mohr, K. I. History of antibiotics research. in *Current Topics in Microbiology and Immunology* vol. 398 237–272 (2016).
7. Durand, G. A., Raoult, D. & Dubourg, G. Antibiotic discovery: history, methods and perspectives. *Int. J. Antimicrob. Agents* **53**, 371–382 (2019).
8. Lakemeyer, M., Zhao, W., Mandl, F. A., Hammann, P. & Sieber, S. A. Thinking Outside the Box—Novel Antibacterials To Tackle the Resistance Crisis. *Angew. Chemie - Int. Ed.* **57**, 14440–14475 (2018).
9. Ropponen, H. K., Richter, R., Hirsch, A. K. H. & Lehr, C. M. Mastering the Gram-negative bacterial barrier – Chemical approaches to increase bacterial bioavailability of antibiotics. *Adv. Drug Deliv. Rev.* **172**, 339–360 (2021).
10. Garzoni, C. & Kelley, W. L. *Staphylococcus aureus*: new evidence for intracellular persistence. *Trends Microbiol.* **17**, 59–65 (2009).
11. Watkins, K. E. & Unnikrishnan, M. *Evasion of host defenses by intracellular Staphylococcus aureus*. *Advances in Applied Microbiology* vol. 112 (Elsevier

- Inc., 2020).
12. Flannagan, R. S., Heit, B. & Heinrichs, D. E. Intracellular replication of *Staphylococcus aureus* in mature phagolysosomes in macrophages precedes host cell death, and bacterial escape and dissemination. *Cell. Microbiol.* **18**, 514–535 (2016).
  13. Wolter, D. J. *et al.* *Staphylococcus aureus* small-colony variants are independently associated with worse lung disease in children with cystic fibrosis. *Clin. Infect. Dis.* **57**, 384–391 (2013).
  14. Cullen, L. & McClean, S. Bacterial adaptation during chronic respiratory infections. *Pathogens* **4**, 66–89 (2015).
  15. Mitchell, G., Grondin, G., Bilodeau, G., Cantin, A. M. & Malouin, F. Infection of polarized airway epithelial cells by normal and small-colony variant strains of *Staphylococcus aureus* is increased in cells with abnormal cystic fibrosis transmembrane conductance regulator function and is influenced by NF- $\kappa$ B. *Infect. Immun.* **79**, 3541–3551 (2011).
  16. Ulrich, M. *et al.* Localization of *Staphylococcus aureus* in Infected Airways of Patients with Cystic Fibrosis and in a Cell Culture Model of *S. aureus* Adherence. *Am. J. Respir. Cell Mol. Biol.* **19**, 83–91 (1998).
  17. Flora, M. *et al.* *Staphylococcus Aureus* in chronic airway diseases: An overview. *Respir. Med.* **155**, 66–71 (2019).
  18. Mistry, R. D. Skin and Soft Tissue Infections. *Pediatr. Clin. North Am.* **60**, 1063–1082 (2013).
  19. Livingstone, V. & Stringer, L. J. The Treatment of *Staphylococcus Aureus* Infected Sore Nipples: A Randomized Comparative Study. *J. Hum. Lact.* **15**, 241–246 (1999).
  20. Schaefer, P. & Baugh, R. F. Acute otitis externa: an update. *Am. Fam. Physician* **86**, 1055–61 (2012).
  21. Mittal, R. *et al.* Current concepts in the pathogenesis and treatment of chronic suppurative otitis media. *J. Med. Microbiol.* **64**, 1103–1116 (2015).

22. MacNeil, S. D., Westerberg, B. D. & Romney, M. G. Toward the development of evidence-based guidelines for the management of methicillin-resistant *Staphylococcus aureus* otitis. *J. Otolaryngol. Head Neck Surg.* **38**, 483–94 (2009).
23. Fraunholz, M. & Sinha, B. Intracellular staphylococcus aureus: Live-in and let die. *Front. Cell. Infect. Microbiol.* **2**, 1–10 (2012).
24. Abed, N. & Couvreur, P. Nanocarriers for antibiotics: A promising solution to treat intracellular bacterial infections. *Int. J. Antimicrob. Agents* **43**, 485–496 (2014).
25. Tulkens, P. M. Intracellular distribution and activity of antibiotics. *Eur. J. Clin. Microbiol. Infect. Dis.* **10**, 100–106 (1991).
26. Barrios-Payán, J. *et al.* Extrapulmonary Locations of *Mycobacterium tuberculosis* DNA During Latent Infection. *J. Infect. Dis.* **206**, 1194–1205 (2012).
27. Maartens, G. & Wilkinson, R. J. Tuberculosis. *Lancet* **370**, 2030–2043 (2007).
28. Santos, R. L. & Bäumlér, A. J. Cell tropism of *Salmonella enterica*. *Int. J. Med. Microbiol.* **294**, 225–233 (2004).
29. Bäumlér, A. J., Kusters, J. G., Stojiljkovic, I. & Heffron, F. *Salmonella typhimurium* loci involved in survival within macrophages. *Infect. Immun.* **62**, 1623–1630 (1994).
30. Porto, P. Del *et al.* Dysfunctional CFTR Alters the Bactericidal Activity of Human Macrophages against *Pseudomonas aeruginosa*. *PLoS One* **6**, e19970 (2011).
31. Schmiedl, A., Kerber-Momot, T., Munder, A., Pabst, R. & Tschernig, T. Bacterial distribution in lung parenchyma early after pulmonary infection with *Pseudomonas aeruginosa*. *Cell Tissue Res.* **342**, 67–73 (2010).
32. Suárez, I. *et al.* The Diagnosis and Treatment of Tuberculosis. *Dtsch. Aerzteblatt Online* **116**, 729–735 (2019).
33. Woodhead, M. *et al.* Guidelines for the management of adult lower respiratory tract infections--summary. *Clin. Microbiol. Infect.* **17 Suppl 6**, 1–24 (2011).
34. Nahid, P. *et al.* Official American Thoracic Society/Centers for Disease Control

- and Prevention/Infectious Diseases Society of America Clinical Practice Guidelines: Treatment of Drug-Susceptible Tuberculosis. *Clin. Infect. Dis.* **63**, e147–e195 (2016).
35. Lehane, E. & McCarthy, G. Medication non-adherence-exploring the conceptual mire. *Int. J. Nurs. Pract.* **15**, 25–31 (2009).
  36. Gould, E. & Mitty, E. Medication Adherence is a Partnership, Medication Compliance is Not. *Geriatr. Nurs. (Minneap)*. **31**, 290–298 (2010).
  37. Hall-Stoodley, L., Costerton, J. W. & Stoodley, P. Bacterial biofilms: from the Natural environment to infectious diseases. *Nat. Rev. Microbiol.* **2**, 95–108 (2004).
  38. Siqueira, V. M. & Lima, N. Biofilm Formation by Filamentous Fungi Recovered from a Water System. *J. Mycol.* **2013**, 1–9 (2013).
  39. Flemming, H.-C. & Wuertz, S. Bacteria and archaea on Earth and their abundance in biofilms. *Nat. Rev. Microbiol.* **17**, 247–260 (2019).
  40. de Beer, D., Stoodley, P., Roe, F. & Lewandowski, Z. Effects of biofilm structures on oxygen distribution and mass transport. *Biotechnol. Bioeng.* **43**, 1131–1138 (1994).
  41. Lawrence, J. R., Korber, D. R., Hoyle, B. D., Costerton, J. W. & Caldwell, D. E. Optical sectioning of microbial biofilms. *J. Bacteriol.* **173**, 6558–6567 (1991).
  42. Høiby, N., Bjarnsholt, T., Givskov, M., Molin, S. & Ciofu, O. Antibiotic resistance of bacterial biofilms. *Int. J. Antimicrob. Agents* **35**, 322–332 (2010).
  43. Bridier, A., Briandet, R., Thomas, V. & Dubois-Brissonnet, F. Resistance of bacterial biofilms to disinfectants: a review. *Biofouling* **27**, 1017–1032 (2011).
  44. Römling, U. & Balsalobre, C. Biofilm infections, their resilience to therapy and innovative treatment strategies. *J. Intern. Med.* **272**, 541–561 (2012).
  45. Uruén, C., Chopo-Escuin, G., Tommassen, J., Mainar-Jaime, R. C. & Arenas, J. Biofilms as promoters of bacterial antibiotic resistance and tolerance. *Antibiotics* **10**, 1–36 (2021).
  46. Ciofu, O., Rojo-Molinero, E., Macià, M. D. & Oliver, A. Antibiotic treatment of

- biofilm infections. *Apmis* **125**, 304–319 (2017).
47. Lebeaux, D., Chauhan, A., Rendueles, O. & Beloin, C. From in vitro to in vivo models of bacterial biofilm-related infections. *Pathogens* **2**, 288–356 (2013).
  48. Arciola, C. R., Campoccia, D. & Montanaro, L. Implant infections: adhesion, biofilm formation and immune evasion. *Nat. Rev. Microbiol.* **16**, 397–409 (2018).
  49. Walters, M. C., Roe, F., Bugnicourt, A., Franklin, M. J. & Stewart, P. S. Contributions of Antibiotic Penetration, Oxygen Limitation, and Low Metabolic Activity to Tolerance of *Pseudomonas aeruginosa* Biofilms to Ciprofloxacin and Tobramycin. *Antimicrob. Agents Chemother.* **47**, 317–323 (2003).
  50. Chiang, W.-C. *et al.* Extracellular DNA Shields against Aminoglycosides in *Pseudomonas aeruginosa* Biofilms. *Antimicrob. Agents Chemother.* **57**, 2352–2361 (2013).
  51. Mulcahy, H., Charron-Mazenod, L. & Lewenza, S. Extracellular DNA Chelates Cations and Induces Antibiotic Resistance in *Pseudomonas aeruginosa* Biofilms. *PLoS Pathog.* **4**, e1000213 (2008).
  52. Bagge, N. *et al.* Dynamics and Spatial Distribution of  $\beta$ -Lactamase Expression in *Pseudomonas aeruginosa* Biofilms. *Antimicrob. Agents Chemother.* **48**, 1168–1174 (2004).
  53. Werner, E. *et al.* Stratified Growth in *Pseudomonas aeruginosa* Biofilms. *Appl. Environ. Microbiol.* **70**, 6188–6196 (2004).
  54. Stewart, P. S. Theoretical aspects of antibiotic diffusion into microbial biofilms. *Antimicrob. Agents Chemother.* **40**, 2517–2522 (1996).
  55. Tanaka, G. *et al.* Effect of the Growth Rate of *Pseudomonas aeruginosa* Biofilms on the Susceptibility to Antimicrobial Agents:  $\beta$ -Lactams and Fluoroquinolones. *Chemotherapy* **45**, 28–36 (1999).
  56. Kim, J., Hahn, J.-S., Franklin, M. J., Stewart, P. S. & Yoon, J. Tolerance of dormant and active cells in *Pseudomonas aeruginosa* PA01 biofilm to antimicrobial agents. *J. Antimicrob. Chemother.* **63**, 129–135 (2009).
  57. Alshammari, T. M. *et al.* Risk of hepatotoxicity associated with fluoroquinolones:

- A national case-control safety study. *Am. J. Heal. Pharm.* **71**, 37–43 (2014).
58. Torres, M. J. *et al.* Diagnosis of immediate allergic reactions to beta-lactam antibiotics. *Allergy Eur. J. Allergy Clin. Immunol.* **58**, 961–972 (2003).
  59. Cantón, R. *et al.* Spanish Consensus on the Prevention and Treatment of *Pseudomonas aeruginosa* Bronchial Infections in Cystic Fibrosis Patients. *Arch. Bronconeumol. (English Ed.)* **51**, 140–150 (2015).
  60. Schuster, A., Haliburn, C., Döring, G. & Goldman, M. H. Safety, efficacy and convenience of colistimethate sodium dry powder for inhalation (Colobreathe DPI) in patients with cystic fibrosis: a randomised study. *Thorax* **68**, 344–350 (2013).
  61. Konstan, M. W. *et al.* Safety, efficacy and convenience of tobramycin inhalation powder in cystic fibrosis patients: The EAGER trial. *J. Cyst. Fibros.* **10**, 54–61 (2011).
  62. Retsch-Bogart, G. Z. *et al.* Efficacy and Safety of Inhaled Aztreonam Lysine for Airway *Pseudomonas* in Cystic Fibrosis. *Chest* **135**, 1223–1232 (2009).
  63. Stass, H., Delesen, H., Nagelschmitz, J. & Staab, D. Safety and Pharmacokinetics of Ciprofloxacin Dry Powder for Inhalation in Cystic Fibrosis: A Phase I, Randomized, Single-Dose, Dose-Escalation Study. *J. Aerosol Med. Pulm. Drug Deliv.* **28**, 106–115 (2015).
  64. Stuart Elborn, J. *et al.* A phase 3, open-label, randomized trial to evaluate the safety and efficacy of levofloxacin inhalation solution (APT-1026) versus tobramycin inhalation solution in stable cystic fibrosis patients. *J. Cyst. Fibros.* **14**, 507–514 (2015).
  65. Winnick, S., Lucas, D. O., Hartman, A. L. & Toll, D. How do you improve compliance? *Pediatrics* **115**, (2005).
  66. Tong, S., Pan, J., Lu, S. & Tang, J. Patient compliance with antimicrobial drugs: A Chinese survey. *Am. J. Infect. Control* **46**, e25–e29 (2018).
  67. Yamamoto, Y. *et al.* Compliance with oral antibiotic regimens and associated factors in Japan: Compliance survey of multiple oral antibiotics (COSMOS). *Scand. J. Infect. Dis.* **44**, 93–99 (2012).

68. Mast, M.-P. *et al.* Nanomedicine at the crossroads – A quick guide for IVIVC. *Adv. Drug Deliv. Rev.* 113829 (2021) doi:10.1016/j.addr.2021.113829.
69. Kim, B. Y. S., Rutka, J. T. & Chan, W. C. W. Current concepts: Nanomedicine. *N. Engl. J. Med.* **363**, 2434–2443 (2010).
70. Mirza, A. Z. & Siddiqui, F. A. Nanomedicine and drug delivery: a mini review. *Int. Nano Lett.* **4**, (2014).
71. Loira-Pastoriza, C., Todoroff, J. & Vanbever, R. Delivery strategies for sustained drug release in the lungs. *Adv. Drug Deliv. Rev.* **75**, 81–91 (2014).
72. Nikezić, A. V. V., Bondžić, A. M. & Vasić, V. M. Drug delivery systems based on nanoparticles and related nanostructures. *Eur. J. Pharm. Sci.* **151**, (2020).
73. Yoo, J.-W., Irvine, D. J., Discher, D. E. & Mitragotri, S. Bio-inspired, bioengineered and biomimetic drug delivery carriers. *Nat. Rev. Drug Discov.* **10**, 521–535 (2011).
74. Dehaini, D., Fang, R. H. & Zhang, L. Biomimetic strategies for targeted nanoparticle delivery. *Bioeng. Transl. Med.* **1**, 30–46 (2016).
75. Menina, S. *et al.* Invasin-functionalized liposome nanocarriers improve the intracellular delivery of anti-infective drugs. *RSC Adv.* **6**, 41622–41629 (2016).
76. Haque, S., Whittaker, M. R., McIntosh, M. P., Pouton, C. W. & Kaminskis, L. M. Disposition and safety of inhaled biodegradable nanomedicines: Opportunities and challenges. *Nanomedicine Nanotechnology, Biol. Med.* **12**, 1703–1724 (2016).
77. Luan, X. *et al.* Engineering exosomes as refined biological nanoplatfoms for drug delivery. *Acta Pharmacol. Sin.* **38**, 754–763 (2017).
78. Chow, T. H. *et al.* Improvement of biodistribution and therapeutic index via increase of polyethylene glycol on drug-carrying liposomes in an HT-29/luc xenografted mouse model. *Anticancer Res.* **29**, 2111–2120 (2009).
79. Suk, J. S., Xu, Q., Kim, N., Hanes, J. & Ensign, L. M. PEGylation as a strategy for improving nanoparticle-based drug and gene delivery. *Adv. Drug Deliv. Rev.* **99**, 28–51 (2016).

80. Ishida, T., Maeda, R., Ichihara, M., Irimura, K. & Kiwada, H. Accelerated clearance of PEGylated liposomes in rats after repeated injections. *J. Control. Release* **88**, 35–42 (2003).
81. Ishida, T., Kashima, S. & Kiwada, H. The contribution of phagocytic activity of liver macrophages to the accelerated blood clearance (ABC) phenomenon of PEGylated liposomes in rats. *J. Control. Release* **126**, 162–5 (2008).
82. Liu, D., Yang, F., Xiong, F. & Gu, N. The Smart Drug Delivery System and Its Clinical Potential. *Theranostics* **6**, 1306–1323 (2016).
83. Matsumura, Y. The drug discovery by nanomedicine and its clinical experience. *Jpn. J. Clin. Oncol.* **44**, 515–525 (2014).
84. Farjadian, F. *et al.* *Nanopharmaceuticals and nanomedicines currently on the market: Challenges and opportunities.* *Nanomedicine* vol. 14 (2019).
85. Gill, P. S. *et al.* Randomized phase III trial of liposomal daunorubicin versus doxorubicin, bleomycin, and vincristine in AIDS-related Kaposi's sarcoma. *J. Clin. Oncol.* **14**, 2353–2364 (1996).
86. Andreopoulou, E. *et al.* Pegylated liposomal doxorubicin HCL (PLD; Caelyx/Doxil®): Experience with long-term maintenance in responding patients with recurrent epithelial ovarian cancer. *Ann. Oncol.* **18**, 716–721 (2007).
87. Lasic, D. D. Doxorubicin in sterically stabilized liposomes. *Nature* **380**, 561–562 (1996).
88. Goes, A. & Fuhrmann, G. Biogenic and Biomimetic Carriers as Versatile Transporters to Treat Infections. *ACS Infect. Dis.* **4**, 881–892 (2018).
89. Choi, J. H. *et al.* Lactobacillus paracasei-derived extracellular vesicles attenuate the intestinal inflammatory response by augmenting the endoplasmic reticulum stress pathway. *Exp. Mol. Med.* **52**, 423–437 (2020).
90. Castoldi, A. *et al.* Aspherical and Spherical InvA497-Functionalized Nanocarriers for Intracellular Delivery of Anti-Infective Agents. *Pharm. Res.* **36**, 22 (2019).
91. Yang, X., Shi, G., Guo, J., Wang, C. & He, Y. Exosome-encapsulated antibiotic

- against intracellular infections of methicillin-resistant *Staphylococcus aureus*. *Int. J. Nanomedicine* **13**, 8095–8104 (2018).
92. Menina, S. *et al.* Invasin-functionalized liposome nanocarriers improve the intracellular delivery of anti-infective drugs. *RSC Adv.* **6**, 41622–41629 (2016).
  93. Deatheragea, B. L. & Cooksona, B. T. Membrane vesicle release in bacteria, eukaryotes, and archaea: A conserved yet underappreciated aspect of microbial life. *Infect. Immun.* **80**, 1948–1957 (2012).
  94. Van Niel, G., D'Angelo, G. & Raposo, G. Shedding light on the cell biology of extracellular vesicles. *Nat. Rev. Mol. Cell Biol.* **19**, 213–228 (2018).
  95. Doyle, L. M. & Wang, M. Z. Overview of Extracellular Vesicles, Their Origin, Composition, Purpose, and Methods for Exosome Isolation and Analysis. *Cells* **8**, 727 (2019).
  96. Bang, C. & Thum, T. Exosomes: New players in cell–cell communication. *Int. J. Biochem. Cell Biol.* **44**, 2060–2064 (2012).
  97. Armstrong, J. P. K. & Stevens, M. M. Strategic design of extracellular vesicle drug delivery systems. *Adv. Drug Deliv. Rev.* **130**, 12–16 (2018).
  98. Fuhrmann, G., Neuer, A. L. & Herrmann, I. K. Extracellular vesicles – A promising avenue for the detection and treatment of infectious diseases? *Eur. J. Pharm. Biopharm.* **118**, 56–61 (2017).
  99. Fuhrmann, G. *et al.* Engineering Extracellular Vesicles with the Tools of Enzyme Prodrug Therapy. *Adv. Mater.* (2018) doi:10.1002/adma.201706616.
  100. Welton, J. L. *et al.* Cerebrospinal fluid extracellular vesicle enrichment for protein biomarker discovery in neurological disease; multiple sclerosis. *J. Extracell. Vesicles* **6**, (2017).
  101. Mizutani, K. *et al.* Urinary exosome as a potential biomarker for urinary tract infection. (2019) doi:10.1111/cmi.13020.
  102. Halvaei, S. *et al.* Exosomes in Cancer Liquid Biopsy: A Focus on Breast Cancer. *Mol. Ther. - Nucleic Acids* **10**, 131–141 (2018).
  103. Eppensteiner, J., Davis, R. P., Barbas, A. S., Kwun, J. & Lee, J.

- Immunothrombotic activity of damage-associated molecular patterns and extracellular vesicles in secondary organ failure induced by trauma and sterile insults. *Front. Immunol.* **9**, (2018).
104. Hood, J. L. Post isolation modification of exosomes for nanomedicine applications. *Nanomedicine* **11**, 1745–1756 (2016).
  105. Vader, P., Mol, E. A., Pasterkamp, G. & Schiffelers, R. M. Extracellular vesicles for drug delivery. *Adv. Drug Deliv. Rev.* **106**, 148–156 (2016).
  106. Elsharkasy, O. M. *et al.* Extracellular vesicles as drug delivery systems: Why and how? *Adv. Drug Deliv. Rev.* **159**, 332–343 (2020).
  107. Batrakova, E. V & Kim, M. S. Using exosomes, naturally-equipped nanocarriers, for drug delivery. *J. Control. Release* 396–405 (2016) doi:10.1016/j.jconrel.2015.07.030.Using.
  108. Villa, F., Quarto, R. & Tasso, R. Extracellular vesicles as natural, safe and efficient drug delivery systems. *Pharmaceutics* **11**, 1–16 (2019).
  109. Kuo, W. P., Tigges, J. C., Toxavidis, V. & Ghiran, I. Red Blood Cells: A Source of Extracellular Vesicles. in 15–22 (2017). doi:10.1007/978-1-4939-7253-1\_2.
  110. Woo, H.-K. *et al.* Urine-based liquid biopsy: non-invasive and sensitive AR-V7 detection in urinary EVs from patients with prostate cancer. *Lab Chip* **19**, 87–97 (2019).
  111. Galley, J. D. & Besner, G. E. The Therapeutic Potential of Breast Milk-Derived Extracellular Vesicles. *Nutrients* **12**, 745 (2020).
  112. Perut, F. *et al.* Strawberry-derived exosome-like nanoparticles prevent oxidative stress in human mesenchymal stromal cells. *Biomolecules* **11**, 1–14 (2021).
  113. Schwechheimer, C. & Kuehn, M. J. Outer-membrane vesicles from Gram-negative bacteria: Biogenesis and functions. *Nat. Rev. Microbiol.* **13**, 605–619 (2015).
  114. Knol, J. C. *et al.* Peptide-mediated ‘miniprep’ isolation of extracellular vesicles is suitable for high-throughput proteomics. *EuPA Open Proteomics* **11**, 11–15 (2016).

115. Askeland, A. *et al.* Mass-Spectrometry Based Proteome Comparison of Extracellular Vesicle Isolation Methods: Comparison of ME-kit, Size-Exclusion Chromatography, and High-Speed Centrifugation. *Biomedicines* **8**, 246 (2020).
116. Ortega, A., Martinez-Arroyo, O., Forner, M. J. & Cortes, R. Exosomes as Drug Delivery Systems: Endogenous Nanovehicles for Treatment of Systemic Lupus Erythematosus. *Pharmaceutics* **13**, 3 (2020).
117. Donoso-Quezada, J., Ayala-Mar, S. & González-Valdez, J. State-of-the-art exosome loading and functionalization techniques for enhanced therapeutics: a review. *Crit. Rev. Biotechnol.* **40**, 804–820 (2020).
118. Sun, D. *et al.* A Novel Nanoparticle Drug Delivery System: The Anti-inflammatory Activity of Curcumin Is Enhanced When Encapsulated in Exosomes. *Mol. Ther.* **18**, 1606–1614 (2010).
119. Agrawal, A. K. *et al.* Milk-derived exosomes for oral delivery of paclitaxel. *Nanomedicine Nanotechnology, Biol. Med.* **13**, 1627–1636 (2017).
120. Munagala, R., Aqil, F., Jeyabalan, J. & Gupta, R. C. Bovine milk-derived exosomes for drug delivery. *Cancer Lett.* **371**, 48–61 (2016).
121. Momen-Heravi, F., Bala, S., Bukong, T. & Szabo, G. Exosome-mediated delivery of functionally active miRNA-155 inhibitor to macrophages. *Nanomedicine Nanotechnology, Biol. Med.* **10**, 1517–1527 (2014).
122. Kim, M. S. *et al.* Development of exosome-encapsulated paclitaxel to overcome MDR in cancer cells. *Nanomedicine Nanotechnology, Biol. Med.* **12**, 655–664 (2016).
123. Thaxter, R. On the Myxobacteriaceæ, a New Order of Schizomycetes. *Bot. Gaz.* **17**, 389–406 (1892).
124. Kaiser, D., Robinson, M. & Kroos, L. Myxobacteria, polarity, and multicellular morphogenesis. *Cold Spring Harb. Perspect. Biol.* **2**, 1–27 (2010).
125. Velicer, G. J. & Vos, M. Sociobiology of the Myxobacteria. *Annu. Rev. Microbiol.* **63**, 599–623 (2009).
126. Reichenbach, H. The ecology of the myxobacteria. *Environ. Microbiol.* **1**, 15–21

- (1999).
127. Kaiser, D. Coupling cell movement to multicellular development in myxobacteria. *Nat. Rev. Microbiol.* **1**, 45–54 (2003).
  128. Muñoz-Dorado, J., Marcos-Torres, F. J., García-Bravo, E., Moraleda-Muñoz, A. & Pérez, J. Myxobacteria: Moving, killing, feeding, and surviving together. *Front. Microbiol.* **7**, 1–18 (2016).
  129. Nan, B. *et al.* Myxobacteria gliding motility requires cytoskeleton rotation powered by proton motive force. *Proc. Natl. Acad. Sci. U. S. A.* **108**, 2498–2503 (2011).
  130. Diez, J. *et al.* Myxobacteria: Natural pharmaceutical factories. *Microb. Cell Fact.* **11**, 2–4 (2012).
  131. Xiao, Y., Wei, X., Ebright, R. & Wall, D. Antibiotic production by myxobacteria plays a role in predation. *J. Bacteriol.* **193**, 4626–4633 (2011).
  132. Reichenbach, H. Myxobacteria, producers of novel bioactive substances. *J. Ind. Microbiol. Biotechnol.* **27**, 149–156 (2001).
  133. Reichenbach, H., Gerth, K., Irschik, H., Kunze, B. & Höfle, G. Myxobacteria: a source of new antibiotics. *Trends Biotechnol.* **6**, 115–121 (1988).
  134. Herrmann, J., Fayad, A. A. & Müller, R. Natural products from myxobacteria: novel metabolites and bioactivities. *Nat. Prod. Rep.* **34**, 135–160 (2017).
  135. Korp, J., Vela Gurovic, M. S. & Nett, M. Antibiotics from predatory bacteria. *Beilstein J. Org. Chem.* **12**, 594–607 (2016).
  136. Thiery, S. & Kaimer, C. The Predation Strategy of *Myxococcus xanthus*. *Front. Microbiol.* **11**, (2020).
  137. Berleman, J. E., Scott, J., Chumley, T. & Kirby, J. R. Predataxis behavior in *Myxococcus xanthus*. *Proc. Natl. Acad. Sci.* **105**, 17127–17132 (2008).
  138. Keane, R. & Berleman, J. The predatory life cycle of *Myxococcus xanthus*. *Microbiology* **162**, 1–11 (2016).
  139. Toyofuku, M., Nomura, N. & Eberl, L. Types and origins of bacterial membrane vesicles. *Nat. Rev. Microbiol.* **17**, 13–24 (2019).

140. Evans, A. G. L. *et al.* Predatory activity of *Myxococcus xanthus* outer-membrane vesicles and properties of their hydrolase cargo. *Microbiology* **158**, 2742–2752 (2012).
141. Berleman, J. E. *et al.* The lethal cargo of *Myxococcus xanthus* outer membrane vesicles. *Front. Microbiol.* **5**, 1–11 (2014).
142. Irene, C. *et al.* Bacterial outer membrane vesicles engineered with lipidated antigens as a platform for *Staphylococcus aureus* vaccine. *Proc. Natl. Acad. Sci. U. S. A.* **116**, 21780–21788 (2019).
143. van der Pol, L., Stork, M. & van der Ley, P. Outer membrane vesicles as platform vaccine technology. *Biotechnol. J.* **10**, 1689–1706 (2015).
144. Mancini, F., Rossi, O., Necchi, F. & Micoli, F. OMV vaccines and the role of TLR agonists in immune response. *Int. J. Mol. Sci.* **21**, 1–19 (2020).
145. Schooling, S. R. & Beveridge, T. J. Membrane vesicles: An overlooked component of the matrices of biofilms. *J. Bacteriol.* **188**, 5945–5957 (2006).
146. Kulp, A. & Kuehn, M. J. Biological Functions and Biogenesis of Secreted Bacterial Outer Membrane Vesicles. *Annu. Rev. Microbiol.* **64**, 163–184 (2010).
147. Beveridge, T. J. Structures of gram-negative cell walls and their derived membrane vesicles. *J. Bacteriol.* **181**, 4725–33 (1999).
148. Turnbull, L. *et al.* Explosive cell lysis as a mechanism for the biogenesis of bacterial membrane vesicles and biofilms. *Nat. Commun.* **7**, 11220 (2016).
149. Roier, S. *et al.* A novel mechanism for the biogenesis of outer membrane vesicles in Gram-negative bacteria. *Nat. Commun.* **7**, 257–259 (2016).
150. Koning, R. I. *et al.* Cryo-electron tomography analysis of membrane vesicles from *Acinetobacter baumannii* ATCC19606T. *Res. Microbiol.* **164**, 397–405 (2013).
151. Sjöström, A. E., Sandblad, L., Uhlin, B. E. & Wai, S. N. Membrane vesicle-mediated release of bacterial RNA. *Sci. Rep.* **5**, 1–10 (2015).
152. Bitto, N. J. *et al.* Bacterial membrane vesicles transport their DNA cargo into host cells. *Sci. Rep.* **7**, 1–11 (2017).

153. Remis, J. P. *et al.* Bacterial social networks: Structure and composition of *Myxococcus xanthus* outer membrane vesicle chains. *Environ. Microbiol.* **16**, 598–610 (2014).
154. Palsdottir, H. *et al.* Three-dimensional macromolecular organization of cryofixed *myxococcus xanthus* biofilms as revealed by electron microscopic tomography. *J. Bacteriol.* **191**, 2077–2082 (2009).
155. Cao, P., Wei, X., Awal, R. P., Müller, R. & Wall, D. A highly polymorphic receptor governs many distinct self- recognition types within the myxococcales order. *MBio* **10**, (2019).
156. DSMZ-German Collection of Microorganisms and Cell Cultures GmbH. *Cystobacter velatus* DSM 14718. <https://www.dsmz.de/collection/catalogue/details/culture/DSM-14718>.
157. Baumann, S. *et al.* Cystobactamids: Myxobacterial Topoisomerase Inhibitors Exhibiting Potent Antibacterial Activity. *Angew. Chemie Int. Ed.* **53**, 14605–14609 (2014).
158. Groß, S., Schnell, B., Haack, P. A., Auerbach, D. & Müller, R. In vivo and in vitro reconstitution of unique key steps in cystobactamid antibiotic biosynthesis. *Nat. Commun.* **12**, 1–15 (2021).
159. DSMZ-German Collection of Microorganisms and Cell Cultures GmbH. *Cystobacter ferrugineus* DSM 52764. <https://www.dsmz.de/collection/catalogue/details/culture/DSM-52764>.
160. Raju, R., Mohr, K. I., Bernecker, S., Herrmann, J. & Müller, R. Cystodienoic acid: A new diterpene isolated from the myxobacterium *Cystobacter* sp. *J. Antibiot. (Tokyo)*. **68**, 473–475 (2015).
161. Holdsworth, S. R. & Can, P. Y. Cytokines: Names and numbers you should care about. *Clin. J. Am. Soc. Nephrol.* **10**, 2243–2254 (2015).
162. Planke, T. *et al.* Cystobactamids 920-1 and 920-2: Assignment of the Constitution and Relative Configuration by Total Synthesis. *Org. Lett.* **21**, 1359–1363 (2019).
163. Turnbull, L. *et al.* Explosive cell lysis as a mechanism for the biogenesis of

- bacterial membrane vesicles and biofilms. *Nat. Commun.* **7**, (2016).
164. Löffler, B., Tuchscher, L., Niemann, S. & Peters, G. Staphylococcus aureus persistence in non-professional phagocytes. *Int. J. Med. Microbiol.* **304**, 170–176 (2014).
  165. Ganbat, D. *et al.* Mycobacteria infect different cell types in the human lung and cause species dependent cellular changes in infected cells. *BMC Pulm. Med.* **16**, 19 (2016).
  166. Anversa Dimer, F. *et al.* PLGA nanocapsules improve the delivery of clarithromycin to kill intracellular Staphylococcus aureus and Mycobacterium abscessus. *Nanomedicine Nanotechnology, Biol. Med.* **24**, 102125 (2020).
  167. Loree, J. & Lappin, S. L. *Bacteriostatic Antibiotics. StatPearls* (2021).
  168. Stewart, P. S. & William Costerton, J. Antibiotic resistance of bacteria in biofilms. *Lancet* **358**, 135–138 (2001).
  169. Bryers, J. D. Medical biofilms. *Biotechnol. Bioeng.* **100**, 1–18 (2008).
  170. Beloin, C. *et al.* Global impact of mature biofilm lifestyle on Escherichia coli K-12 gene expression. *Mol. Microbiol.* **51**, 659–674 (2004).
  171. Skolnik, K., Kirkpatrick, G. & Quon, B. S. Nontuberculous Mycobacteria in Cystic Fibrosis. *Curr. Treat. Options Infect. Dis.* **8**, 259–274 (2016).
  172. Novosad, S. A., Beekmann, S. E., Polgreen, P. M., Mackey, K. & Winthrop, K. L. Treatment of mycobacterium abscessus infection. *Emerg. Infect. Dis.* **22**, 511–514 (2016).
  173. Gilljam, M., Scherstén, H., Silverborn, M., Jönsson, B. & Ericsson Hollsing, A. Lung transplantation in patients with cystic fibrosis and Mycobacterium abscessus infection. *J. Cyst. Fibros.* **9**, 272–276 (2010).
  174. Mougari, F. *et al.* Infections caused by *Mycobacterium abscessus*: epidemiology, diagnostic tools and treatment. *Expert Rev. Anti. Infect. Ther.* **14**, 1139–1154 (2016).
  175. Grotz, E. *et al.* Nanotechnology in Tuberculosis: State of the Art and the Challenges Ahead. *Pharm. Res.* **35**, (2018).

176. Zeller, B. *et al.* Biofilm formation on metal alloys, zirconia and polyetherketoneketone as implant materials in vivo. *Clin. Oral Implants Res.* **31**, 1078–1086 (2020).
177. Kniha, K., Heussen, N., Modabber, A., Hölzle, F. & Möhlhenrich, S. C. The effect of zirconia and titanium surfaces on biofilm formation and on host-derived immunological parameters. *Int. J. Oral Maxillofac. Surg.* **50**, 1361–1374 (2021).
178. Taylor, P. K., Yeung, A. T. Y. & Hancock, R. E. W. Antibiotic resistance in *Pseudomonas aeruginosa* biofilms: Towards the development of novel anti-biofilm therapies. *J. Biotechnol.* **191**, 121–130 (2014).
179. Yonezawa, H., Osaki, T. & Kamiya, S. Biofilm Formation by *Helicobacter pylori* and Its Involvement for Antibiotic Resistance. *Biomed Res. Int.* **2015**, 1–9 (2015).
180. Vuotto, C., Donelli, G., Buckley, A. & Chilton, C. *Clostridium difficile* Biofilm. in 97–115 (2018). doi:10.1007/978-3-319-72799-8\_7.
181. Spigaglia, P., Mastrantonio, P. & Barbanti, F. Antibiotic Resistances of *Clostridium difficile*. in 137–159 (2018). doi:10.1007/978-3-319-72799-8\_9.

## 6 SCIENTIFIC OUTPUT

### 6.1 PAPER 1: “Biogenic and biomimetic carriers as versatile transporters to treat infections”

**Adriely Goes** and Gregor Fuhrmann

Helmholtz-Institute for Pharmaceutical Research Saarland (HIPS), Helmholtz-Centre for Infection Research (HZI), Biogenic Nanotherapeutics group (BION), Campus E8.1, 66123 Saarbrücken, Germany

Department of Pharmacy, Saarland University, Campus Building E8.1, 66123 Saarbrücken, Germany

Published: March 19, 2018

ACS Infect. Dis. 2018, 4, 6, 881–892

DOI: [10.1021/acsinfecdis.8b00030](https://doi.org/10.1021/acsinfecdis.8b00030)

# Biogenic and Biomimetic Carriers as Versatile Transporters To Treat Infections

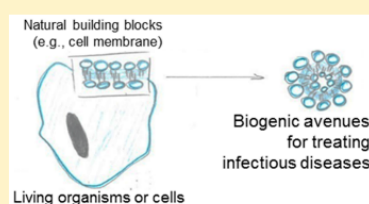
Adriely Goes<sup>1</sup> and Gregor Fuhrmann\*<sup>1,2</sup>

Helmholtz-Institute for Pharmaceutical Research Saarland (HIPS), Helmholtz-Centre for Infection Research (HZI), Biogenic Nanotherapeutics group (BION), Campus E8.1, 66123 Saarbrücken, Germany

Department of Pharmacy, Saarland University, Campus Building E8.1, 66123 Saarbrücken, Germany

**ABSTRACT:** Biogenic and biomimetic therapeutics are a relatively new class of systems that are of physiological origin and/or take advantage of natural pathways or aim at mimicking these to improve selective interaction with target tissue. The number of biogenic and bioengineered avenues for drug therapy and diagnostics has multiplied over the past years for many applications, indicating the high expectations associated with this biological route. Nevertheless, the use of “bio”-related approaches for treating or diagnosing infectious diseases is still rare. Given that infectious diseases, in particular bacterial resistances, are seriously on the rise, there is an urgent need to take advantage of biogenic and bioengineered systems to target these challenges. In this manuscript, we first give a definition of the various “bio” terms, including biogenic, biomimetic, bioinspired, and bioengineered and we highlight them using tangible applications in the field of infectious diseases. Our examples cover cell-derived systems, including bioengineered bacteria, virus-like particles, and different cell-mimetics. Moreover, we discuss natural and bioengineered particles such as extracellular vesicles from mammalian and bacterial sources and liposomes. A concluding section outlines the potential for biomaterial-related avenues to overcome challenges associated with difficult-to-treat infections. We critically discuss benefits and risks for these applications and give an outlook on the future of biogenic engineering.

**KEYWORDS:** nanoantibiotics, biogenic drug delivery, biomimetics, bioinspired delivery systems, extracellular vesicles, outer membrane vesicles, cell-mimetics, virus-like particles



## ■ BIOGENIC, BIOINSPIRED, AND BIOENGINEERED SYSTEMS: A DEFINITION

In recent years, drug therapy and diagnostic avenues that take advantage of biological systems or natural (biogenic) principles have rapidly multiplied. Indeed, nature is the ideal prototype for developing novel approaches for selectively delivering compounds<sup>1</sup> or detecting physiological markers in a highly sensitive way.<sup>2</sup> These new systems take advantage of natural pathways or may mimic these in order to optimize physiological interactions with tissue or target cells and ultimately enhance therapeutic performance in clinical trials.<sup>3</sup> Such natural principles of selective cell recognition have evolved over time to maximize functionality and selectivity, thus offering a stronger specificity than purely synthetic systems. The nomenclature for these nature-related and nature-inspired systems is diverse and ranges from “biogenic” and “biomimetics” to “bioinspired” or “bioengineered” (Figure 1).

In the field of targeted drug delivery, the use of such “bio”-systems may be advantageous compared to chemically inert drug carriers or materials, which merely serve as the matrix in which an active compound is embedded. In contrast, biogenic and bioengineered approaches are postulated to lead to an active interplay of the carrier system with the biology encountered in the human body and will additionally enhance the drug activity or diagnostic readout in a physiological manner. Moreover, compared to their artificial counterparts, such natural approaches may reduce recognition by the immune system, diminish complement activation, and minimize

accumulation in other tissue.<sup>4</sup> In return, reduced side effects, enhanced localized drug concentration at the site of action, and thus an augmented therapeutic outcome may be observed. For these reasons, biogenic and bioengineered avenues are promising future alternatives to purely synthetic systems which often show limited efficacy in (pre)clinical assessments.<sup>3</sup>

In the present Perspective, we first aim to define and differentiate between the various “bio”-terms and discuss advantages of each approach (Box 1). We subsequently give an overview of current biogenic and bioinspired systems for the selective therapy and detection of bacterial infections. Difficult-to-treat infections are an increasing healthcare problem worldwide, and we thus discuss the potential of bioavenues to target these emerging problems.

## ■ BIOGENIC AS A PROMISING OPTION FOR ANTI-INFECTIVE AVENUES

There is an urgent need to develop new treatment options for resistant and multiresistant pathogens, in particular bacteria. The number of deaths induced by these difficult-to-treat infections is currently estimated to be up to 25 000 per year in Europe, with an even larger number of affected patients worldwide.<sup>5</sup> In the UK 2014 Review on Antimicrobial Resistance, it was estimated that by 2050 an incredible number of 10 million

Received: February 2, 2018

Published: March 19, 2018

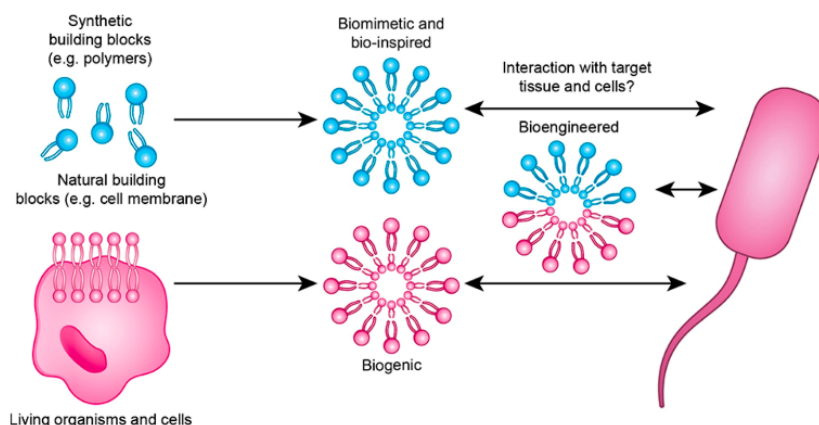


**Figure 1.** Differences in origin of various “bio” systems. Living cells and organisms produce *biogenic* entities, such as cells or cell-derived vesicles which in nature serve a specific function, a process that may be utilized to deliver compounds in a specific manner. In comparison, *biomimetic* and *bioinspired* systems are synthetic and artificial approaches that imitate physiological model systems or biological processes. Successful examples for synthetic biomimetic approaches are liposomal or polymeric carriers. When biogenic and biomimetic systems are combined, *bioengineered* avenues are developed. These systems are based on the application of engineering approaches on biological and medical building blocks, such as semisynthetic polymer–drug conjugates or functionalized natural vesicles. Overall, “bio”-systems are thought to possess better interactions with cells and living tissue rendering them promising avenues for targeted anti-infectives’ delivery or detection of bacterial and viral illnesses.

### Box 1. Definitions of Biogenic, Biomimetic/Bioinspired, and Bioengineered Approaches

Glossary: What are similarities and differences between the “bio” terms?

**Biogenic:** Produced or originating from a living organism.

Any cell, particle, or compound that is derived from cells or living tissues; e.g., erythrocytes, extracellular vesicles, or enzymes.

The complexity of biogenic systems may hinder their (semi)synthetic replication, but they give a competitive edge due to their physiological role in translating biological interactions.

**Biomimetic and Bioinspired:** Imitation of model systems and elements of nature and natural processes.

Mostly synthetic and artificial model systems or approaches that take inspiration from natural principles and mechanisms; e.g., liposomes, artificial viruses, and synthetic peptides.

The level of complexity is often reduced in order to create simple systems that resemble the most important principles of their natural archetype.

**Bioengineered:** Biological and medical application of engineering methods and techniques.

Combinations of natural building blocks with artificial counterparts or the utilization of engineering approaches on physiological systems; e.g., functionalization of cells, cell/bacterio-mimetics, and drug–polymer conjugates.

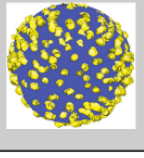
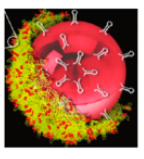
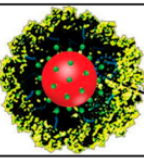
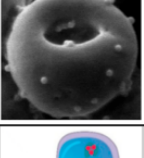
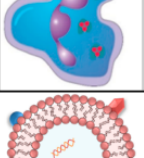
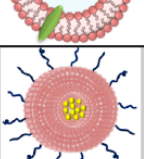
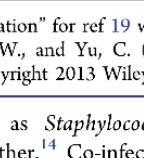
By using known engineering methods, the degree of complexity for manufacturing these systems is substantially diminished but without compromising on their natural and selective interaction with living cells and tissue.

deaths per year worldwide will be caused by those bacteria, exceeding the incidence of cancer-associated deaths ([www.amr-review.org](http://www.amr-review.org)). The World Health Organization (WHO) has recently published a list of highly relevant pathogens for which novel therapeutic approaches need to be developed. Among these are several multidrug resistant bacteria including *Pseudomonas*, *Acinetobacter*, and different types of *Enterobacteriaceae*,

that often cause problems in hospitals and nursing homes and among patients with medical devices ([www.who.int](http://www.who.int)). One way of addressing the challenging question of how to tackle problem bacteria is still the discovery of novel antibiotic compounds.<sup>6</sup> In recent years, a few promising candidates and novel targets have been developed, such as lectin inhibitors<sup>7</sup> and drugs interfering with the bacterial quorum sensing system.<sup>8</sup> Such novel drugs represent powerful new ways to target resistant bacteria, but efficient carriers for their selective delivery are needed in order to increase tissue specific delivery. Encapsulation of antibiotics into nanoparticulate drug delivery systems, such as liposomes, create so-called “nanoantibiotics,” which improve drug transport to the site of infection, enhance antibiotic uptake into bacteria, and increase overall antibiotic efficiency.<sup>9</sup> Nanoparticles are among the most promising avenues to allow existing antibiotics to reach their site of action, thereby enhancing anti-infective strength and overcoming certain types of microbial drug resistance, such as efflux pumps.<sup>10</sup> Nevertheless, the ability of current nanoantibiotics to exclusively target pathogenic bacteria is often insufficient, as their stability under physiological conditions is suboptimal and they may induce side effects due to their synthetic origin. Biogenic approaches offer the potential to counterbalance the drawbacks of artificial carriers, as they may naturally overcome barriers associated with anti-infective therapy. Biogenic avenues provide exciting opportunities to develop novel future concepts for enhanced-sensitivity diagnostics.<sup>11</sup>

Several bacteria that are considered traditionally as extracellular pathogens have now been investigated also as intracellular pathogens not only in professional phagocytes (e.g., macrophages) but also in nonprofessional phagocytes (e.g., epithelial cells). The pathogen becomes intracellular as a strategy to evade the immune system and treatment with antibiotics. An important example of such pathogens is *Staphylococcus aureus*.<sup>12</sup> Besides becoming intracellular, bacteria can also form biofilms. Biofilms are small colonies of bacteria inserted in an extracellular matrix, where they become stable and tolerant to antimicrobial treatment and the immune system.<sup>13</sup> It has been reported that biofilms can incorporate different species of

Table 1. Overview of Recent Biogenic, Bioengineered, and Biomimetic Approaches for Targeting Bacterial Infections<sup>a</sup>

Representation	Type of carrier	Method	Results	Reference	Year
	Magnetotactic bacteria biohybrid microswimmers.	Non-pathogenic magnetotactic bacteria ( <i>Magnetospirillum gryphiswalense</i> , MSR-1) integrated with ciprofloxacin-loaded mesoporous silica microtubes; resulting in controllable “microswimmers” (biohybrids).	Biohybrid system able to be magnetically guided through <i>E. coli</i> biofilms, delivering the ciprofloxacin cargo.	18	2017
	Non-viral nanoparticles mimicking virus surface topography.	Negatively charged silica nanoparticles (NPs) modified with amine groups or polyethylenimine (PEI) to become positively charged; attachment of smaller silica NPs resulting in NPs with a rough surface.	Higher cellular uptake in HeLa cells compared to smooth carriers.	19	2013
	Virus-like particles (VLPs) of bacteriophage MS2 to deliver NPs, drugs, siRNA and proteins.	MS2 VLPs surface modified with a HCC (human hepatocellular carcinoma)-specific peptide (SP94), a fusogenic peptide and PEG-1000; MS2 VLPs further modified with histidine-rich fusogenic peptide (H5WYG).	Targeted VLPs deliver drugs, siRNA, protein toxins, and quantum dots to HCC; SP94-targeted VLPs rapidly internalized by HCC but not by normal hepatocytes; Particles further modified with H5WYG promoted endosomal escape.	20	2011
	Genetically engineered hepatitis B core VLPs loaded with Fe <sub>3</sub> O <sub>4</sub> NPs.	Functional particles encapsulated into VLPs through histidine tags affinity for nickel-nitrilotriacetic acid (NTA) chelate.	Increased uptake in HeLa cells compared to pure Fe <sub>3</sub> O <sub>4</sub> nanoparticles.	21	2015
	Polystyrene NPs attached to the surface of red blood cells (RBC hitchhiking).	Polystyrene NPs incubated at varying particle to RBC ratios.	NP-Attachment to RBCs at low doses did not affect circulation time, avoided mononuclear phagocyte system (MPS) and enabled delivery to difficult-to-reach tissues.	22	2013
	Nanoparticle <i>in situ</i> hitchhiking activated neutrophils.	Intravenous administered albumin NPs specifically internalized by activated neutrophils.	NP-Neutrophils transmigrated across blood vessel wall and in response to inflammation induced by the pathogen invasion.	23	2015
	Extracellular vesicles (EVs) and outer membrane vesicles (OMVs).	EVs and OMVs isolated by filtration, ultracentrifugation, density gradients, immunoaffinity, gel chromatography and commercially available kits.	Potential long distance targeting; intrinsically compatible; high targeting efficacy.	24,25	2015, 2017
	Liposomes functionalized with bacterial invasion protein invasins.	Liposomes prepared by lipid film hydration followed by membrane extrusion and surface functionalization with invasins.	Functionalized liposomes adhered to epithelial cells (HEp-2) with higher efficiency than those functionalized by BSA.	26,27	2015, 2016

<sup>a</sup>The “Representation” for ref 19 was adapted with permission from Niu, Y., Yu, M., Hartono, S. B., Yang, J., Xu, H., Zhang, H., Zhang, J., Zou, J., Dexter, A., Gu, W., and Yu, C. (2013) Nanoparticles Mimicking Viral Surface Topography for Enhanced Cellular Delivery. *Adv. Mater.* 25, 6233–6237. Copyright 2013 Wiley-VCH Verlag GmbH & Co. KGaA.

bacteria, such as *Staphylococcus aureus* and *Pseudomonas aeruginosa* together.<sup>14</sup> Co-infection and biofilm formation are especially important in cases of chronic pulmonary disease (e.g., cystic fibrosis),<sup>15</sup> making the infection hard to be treated and deteriorating the condition of the patient clinically. When using nanodelivery approaches, a major challenge is to overcome or disrupt this rigid biofilm barrier and to reach the underlying pathogens.<sup>16</sup>

Here, we summarize recent efforts using natural systems and, as this is an emerging field of research, we focus specifically on publications and reports from 2013 onward (Table 1). We emphasize *biogenic* and *bioengineered* approaches (i.e., avenues that are fully or partially based on natural components or entities), but we also highlight a few very important examples of bioinspired avenues, as we believe that mimicking physiological elements is crucial for an optimal drug transfer with minimal side

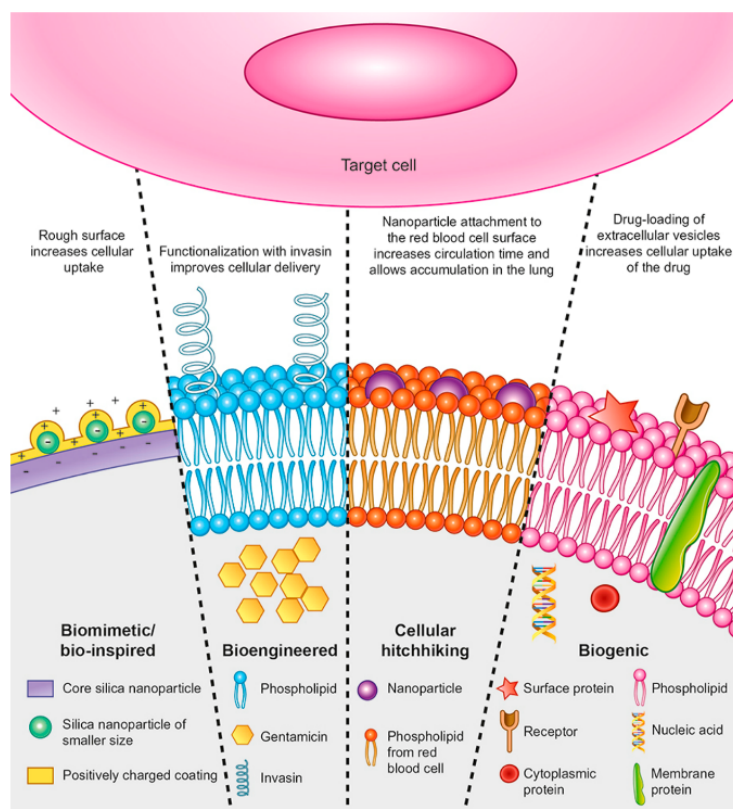


**Figure 2.** Schematic overview of selected biogenic and bioengineered avenues for targeting infections. Approaches for biomimetic, bioengineered, cellular hitchhiking, and biogenic avenues are displayed. Biomimicry may take advantage of reproducing the rough surface of viruses by coating larger core particles with smaller nanoparticles, both made of silica. Such a rough surface may enhance cellular uptake in a comparable manner to viruses. Surface bioengineering of plain liposomes with a bacterial invasion protein (invasin) rendered bacterio-mimetic carriers for enhanced targeting of difficult-to-reach intracellular pathogens. Nanoparticles may also be coupled onto the surface of red blood cells to employ them for cellular hitchhiking. Erythrocytes possessed enhanced systemic circulation time and may shuttle their backpack-cargo to the narrow vasculature in the lungs. Finally, extracellular vesicles are currently under investigation as potentially biocompatible and cell-selective carriers. These biogenic particles are derived from cells and subsequently are of natural composition, making them promising in the field of targeted drug delivery.

effects (Figure 2). Fully synthetic approaches are beyond the scope of this work but are summarized in a comprehensive recent review.<sup>17</sup> Nevertheless, combining biogenic with artificial systems may in the future lead to enhanced semisynthetic avenues where both approaches may benefit from one another. The approaches in this manuscript are organized by cell-derived systems and natural and bioengineered nanocarriers, followed by a concluding section on bioinspired materials and their importance in the future of this field of research.

#### ■ CELL-DERIVED SYSTEMS FOR DELIVERY OF ANTI-INFECTIVE COMPOUNDS

**Bioengineered Bacteria.** The motility of flagellated bacteria can be utilized to deliver molecules to areas of difficult reach. Taherkhani and collaborators developed a magnetotactic bacteria–nanoliposome complex as a drug delivery system.<sup>28</sup> Using *Magnetococcus marinus* MC-1 magnetotactic bacteria (MTB), nanoliposomes (LPs) were covalently bound to their surfaces without impairing the bacteria's motility. Their results show that the MTB–LP complex is rapidly internalized by phagocytic cells (J774), while the opposite is seen for nonphagocytic cells (NIH/3T3 mouse fibroblasts and Colo 205 human metastatic colon cells).<sup>28</sup> Although this concept is

focused on delivery of cytotoxic compounds, it may be translated to infectious diseases by encapsulation of liposomes with antibiotic drugs. Moreover, the potential of this bacterial self-propeller could be further enhanced when drug-loaded nanoliposomes are detached in a specific tissue and/or following a stimulus such as pH decrease during infections.

In an infection setting, Stanton and co-workers recently used the magnetotactic flagellated bacteria *Magnetospirillum gryphiswalense* (MSR-1). MSR-1 was integrated into mesoporous silica microtubes loaded with ciprofloxacin by incubation in a buffer solution, resulting in a magnetically responsive biohybrid system.<sup>18</sup> The biohybrid system was tested against *Escherichia coli* biofilms and was shown to be able to be magnetically guided into them. The acidic biofilm microenvironment was instrumentalized for a selective drug release (Figure 3). This system is interesting for its ability to physically penetrate and attack the biofilms, contributing to their disruption. However, further study is needed on biocompatibility and on elucidating how many biohybrids need to be administered to reach therapeutic levels of antibiotics at the site of infection. In a similar approach, Park and collaborators loaded doxorubicin into polyelectrolyte multilayer (PEM) micro-particles with embedded magnetic nanoparticles and then

D

DOI: 10.1021/acsinfectdis.8b00030  
ACS Infect. Dis. XXXX, XXX, XXX–XXX

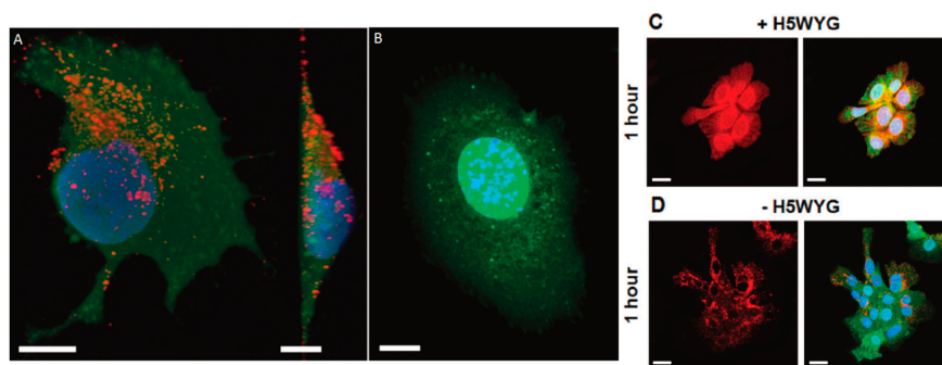


**Figure 3.** (A and B) Confocal fluorescence microscopy images showing that SP94-targeted VLPs (red) are internalized by Hep3B (A) but not by hepatocytes (B). (C and D) VLPs comodified with the SP94 targeting peptide and the H5WYG fusogenic peptide become distributed in the cytosol of Hep3B cells, while VLPs modified with only SP94 remain in the endosomes. Hep3B cells exposed to SP94-targeted VLPs (red) for 1 h. VLPs were comodified with ~60 SP94 peptides/particle and ~75 H5WYG peptides/particle in panel C, while they were modified with only ~60 SP94 peptides/particle in panel D. Scale bars: 10  $\mu\text{m}$ . Reprinted from Ashley, C. E., Carnes, E. C., Phillips, G. K., Durfee, P. N., Buley, M. D., Lino, C. A., Padilla, D. P., Phillips, B., Carter, M. B., Willman, C. L., Brinker, C. J., Caldeira, J. D. C., Chackerian, B., Wharton, W., and Peabody, D. S. (2011) Cell-specific delivery of diverse cargos by bacteriophage MS2 virus-like particles. *ACS Nano* 5, 5729–5745 (ref 20). Copyright 2011 American Chemical Society.

attached them to the *E. coli* surface, successfully guiding them to a specific target.<sup>29</sup> Translating this guided approach to human patients may be challenging. Nevertheless, taking advantage of magnetotactic bacteria and carrier systems, it is an innovative and promising approach to deliver drugs to a specific site and consequently optimize the therapy and avoid adverse effects caused by drugs.

**Viruses and Virus-Like Particles.** Viruses have an excellent ability to avoid the immune system and invade cells to “unload” their genes and replicate.<sup>1</sup> Several research groups have been exploiting this ability of the viruses to develop carriers that mimic their behavior but without the risk of inducing infections. These approaches include developing nanoparticles mimicking the natural virus-surface and virus-like particles that resemble viral structures without being infectious. For example, enveloped viruses have a size of 30–400 nm, which is adequate for uptake by cells, and their surface is rough with glycoprotein spikes.<sup>19</sup> In an attempt to investigate the role of this surface roughness on the cellular delivery efficiency, excluding the receptor-specific interactions influence, Niu and collaborators prepared negatively charged silica nanoparticles which were coated with positively charged amine groups and polyethyleneimine, resulting in a positively charged nanoparticle. In addition, negatively charged small diameter silica particles were prepared separately and bound to the larger nanoparticles prepared previously. The resulting particle had a rough surface, mimicking those of viruses.<sup>19</sup> Particles with a rough surface showed a better binding ability and a 5.6 times higher cellular uptake in HeLa cells compared to smooth nanocarriers. These results indicate that rough particles mimicking natural viruses enhance the interaction at the cellular level, which may be an important consideration during design of anti-infective nanocarriers. It remains to be determined whether enhanced uptake of such rough particles also improves the delivery of loaded anti-infective cargo.

Such specific delivery of drugs loaded into bioengineered virus-like particles (VLPs) was investigated by Ashley and colleagues, who developed an interesting strategy to transfer a variety of molecules to specific targets. Producing VLPs from bacteriophages MS2 and modifying their surfaces with a

peptide (SP94) that binds to human hepatocellular carcinoma (HCC), they showed that the VLPs have a higher avidity to HCC when compared to normal hepatocytes (Figure 3A,B), endothelial cells (HUVECs), and immune cells such as T-lymphocytes.<sup>20</sup> They also demonstrated that, with further modification of the VLPs with histidine-rich fusogenic peptide (H5WYG), it is possible to avoid the endosomal pathway, allowing the VLPs to be dispersed in the cytosol (Figure 3C,D).<sup>20</sup> This approach has potential to be adapted to deliver antimicrobial drugs to specific targets by surface modification.

The concept of VLP carriers may also be combined with an imaging/diagnostic option. In an interesting bioengineering approach,  $\text{Fe}_3\text{O}_4$  nanoparticles were encapsulated into genetically engineered hepatitis B core (HBC) virus-like particles through the specific affinity of histidine tags to the nickel nitrilotriacetic acid (NTA) chelate.<sup>21</sup> The resulting HBC-144-His virus-like particles with loaded  $\text{Fe}_3\text{O}_4$  nanoparticles were highly monodisperse and uniform (Figure 4). The encapsulation efficiency for the iron oxide nanoparticles into the virus-like cores was found to be strongly dependent on the core size. When assessed in an *in vitro* model of HeLa cells, the obtained core-containing VLPs exhibited higher cellular uptake compared to the free iron oxide particles. These iron oxide particles may serve as contrast agents to visualize *in vivo* uptake at sites of infection. It would also be conceivable to encapsulate other metal nanoparticles such as gold into these VLPs to render theranostic carriers, for both therapy and diagnostic use. In any case, extended biocompatibility assessments will be required to evaluate whether this promising approach may be translated to preclinical studies.

In general, VLPs are not only promising for transport of drug compounds but also more interesting in developing safe vaccines that induce strong immune responses. They offer favorable properties regarding chemical and genetic modification, but they are not self-replicative. A comprehensive overview on their bioengineering was recently published.<sup>30</sup>

Another strategy that has been investigated to overcome the bacterial resistance to antibiotics is the use of bacteriophages. Bacteriophages, or simply phages, have been used to treat infections for almost 100 years.<sup>31,32</sup> Phages have several

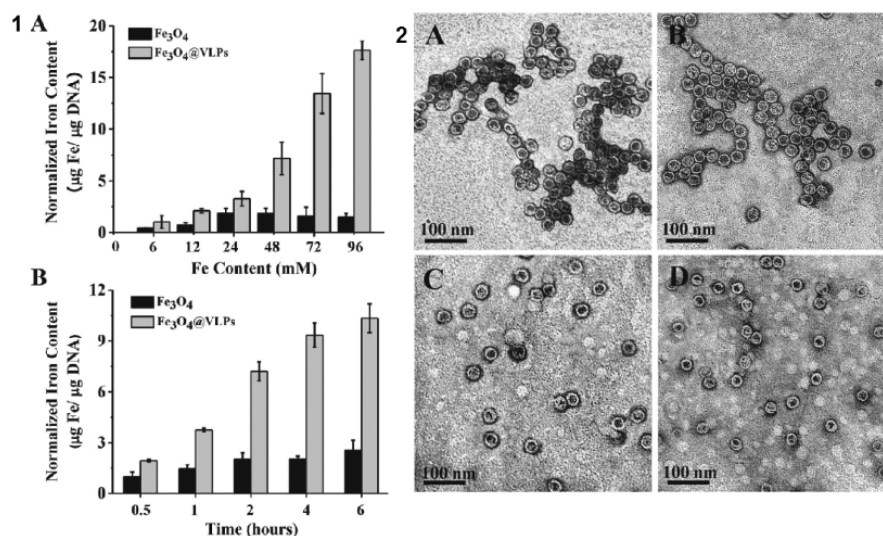


**Figure 4.** Genetically engineered hepatitis B core (HBC) virus-like particles (VLP) with a histidine tag rendered HBC-144-His VLPs loaded with Fe<sub>3</sub>O<sub>4</sub>-NTA-Ni<sup>2+</sup> nanoparticles with various diameters (1A, 1B). Their cellular uptake was assessed in HeLa cells. (2A–D) TEM images of negatively stained samples of engineered hepatitis B core virus-like particles loaded with Fe<sub>3</sub>O<sub>4</sub>. Reprinted with permission from Shen, L., Zhou, J., Wang, Y., Kang, N., Ke, X., Bi, S., and Ren, L. (2015) Efficient encapsulation of Fe<sub>3</sub>O<sub>4</sub> nanoparticles into genetically engineered hepatitis B core virus-like particles through a specific interaction for potential bioapplications. *Small* 11, 1190–1196 (ref 21). Copyright 2014 WILEY-VCH Verlag GmbH & Co. KGaA, Weinheim.

advantages over traditional antibiotic treatment, including self-amplification, low toxicity, and species specificity.<sup>32,33</sup> In a hamster model, Nale et al. showed that the combination of phages on the treatment of *Clostridium difficile* limited its proliferation. *In vitro*, the combination of phages reduced *C. difficile* growth.<sup>34</sup> The use of phages has also been linked to the restoration of antibiotic susceptibility in multidrug-resistant *Pseudomonas aeruginosa*.<sup>35</sup> The use of phage therapy has potential to eradicate infections by its sole use or by combination with traditional antibiotics. A comprehensive review on phage therapy has been recently published discussing the main challenges of this field.<sup>32</sup>

**Cell-Hitchhiking Approaches.** Red blood cells (RBCs) are natural, biocompatible, and biodegradable delivery vehicles which have numerous properties that can inspire the development of biomimetic carriers.<sup>36</sup> Their structure consists of a semipermeable membrane that can release small-molecule drugs in a sustained pattern. They are able to encapsulate and protect cargos by forming compartments and can circulate in the body for a long period of time due to their non-immunogenic and biocompatible characteristics,<sup>36</sup> both proven in clinical trials.<sup>37</sup> The main challenge of using RBCs as a drug delivery system is loading them while maintaining their biological properties.<sup>38</sup> There are now several methods for RBC encapsulation of drugs of choice, including the antibiotics primaquine<sup>39</sup> and amikacin,<sup>40</sup> which are summarized in a recent review.<sup>41</sup>

Another elegant avenue for using erythrocytes would be their surface modification with drugs or nanoparticles in a cellular hitchhiking concept (Figure 2). Anselmo and collaborators have attached polystyrene nanoparticles to the surface of mice RBCs to deliver drugs or particles to specific sites, such as the lung. Both were incubated at varying particle to RBC ratios (Figure 5). The nanoparticles remained attached to the RBCs

under static conditions but detached upon mimicking the shear stress present under physiological conditions (5 Pa for 15 min at 37 °C), such as in the lung microvasculature. When the erythrocytes reach the capillaries in the lung, the nanoparticles detach from the RBCs, stick to the walls of the capillary, and may be taken up by target cells.<sup>22</sup> When loading nanoparticles with antibiotics of choice, this approach has potential to treat lung infection, such as persistent bacterial infections in cystic fibrosis patients.<sup>42</sup> A major advantage of this technology is the simple isolation of RBC carriers from individual patients which may evoke even lower immunogenicity and facilitate a sort of individualized medicine approach to treat difficult lung infections.

Immune cells, such as neutrophils, exhibit a natural affinity for and homing to inflamed and infected tissue, making them promising transfer avenues to carry diagnostic and therapeutic molecules to sites of infections.<sup>43</sup> Drug-loaded, denatured albumin nanoparticles are often taken up by neutrophils that are activated and adherent to the blood vessel wall (Figure 6A).<sup>44</sup> Chu and co-workers demonstrated by intravital microscopy of mouse cremaster venules that these albumin nanoparticles (NPs) were internalized by neutrophils, which subsequently transmigrated through the blood vessel wall and into the muscle to reach inflamed tissues.<sup>23</sup> They showed that neutrophils carrying albumin NPs can cross the vessel barrier in an acute lung inflammation model in mice.<sup>23</sup> To investigate the antimicrobial therapeutic potential of these albumin NPs-carrier neutrophils, the NPs were loaded with a broad spectrum antibiotic, cefoperazone acid, and tested against *Pseudomonas aeruginosa* lung infection in mice (Figure 6B). The antibiotic-loaded NPs did not impair the neutrophil mobility and activation or the lung integrity, but they reduced bacterial burden 3-fold compared to a free solution of cefoperazone acid.<sup>23</sup> Although the biocompatibility and immune-stimulatory potential

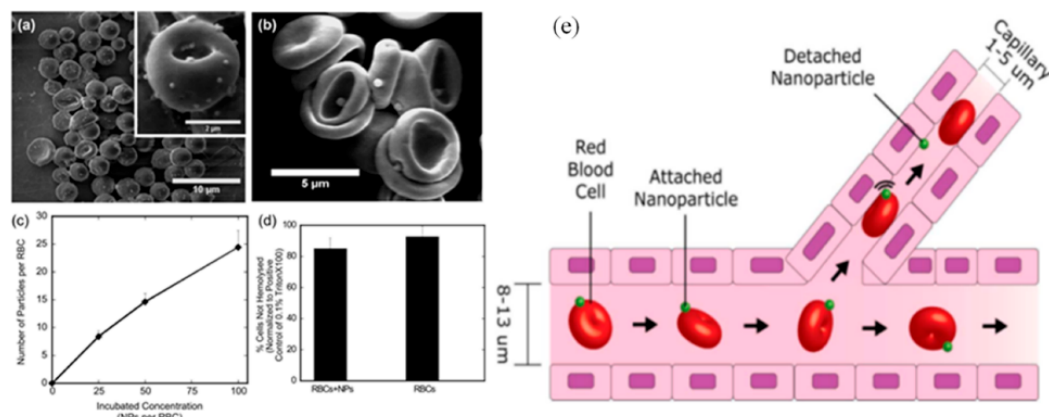


**Figure 5.** (a, b) Representative SEM images of polystyrene NPs attached to the surface of RBCs. (c) Graph showing that the amount of NPs attached on the surface of RBCs is concentration dependent. (d) The attachment of NPs to RBCs did not cause hemolysis. (e) Schematic representation of the detachment of NPs from RBCs in tiny capillaries present in the lung microvasculature. Reprinted from Anselmo, A. C., Gupta, V., Zern, B. J., Pan, D., Zakrewsky, M., Muzykantov, V., and Mitragotri, S. (2013) Delivering nanoparticles to lungs while avoiding liver and spleen through adsorption on red blood cells. *ACS Nano* 7, 11129–11137 (ref 22). Copyright 2013 American Chemical Society.

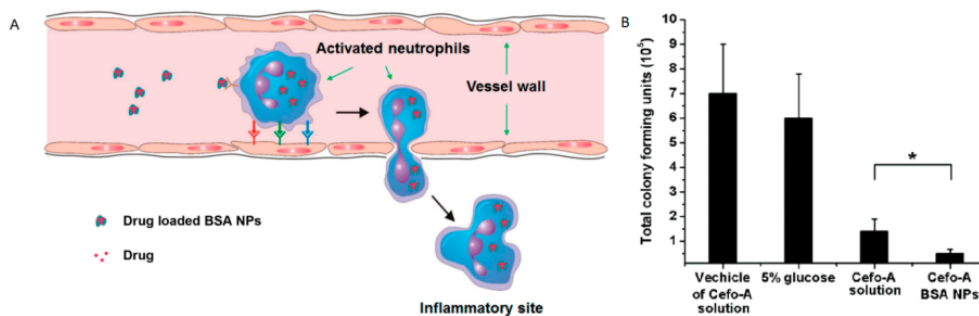


**Figure 6.** (A) Schematic representation of the concept of neutrophil-mediated delivery. Activated neutrophils may actively transmigrate blood vessel walls and accumulate in inflammatory tissue. (B) Albumin nanoparticles loaded with antibiotic cefoperazone acid (Cefo-A) NPs reduced bacterial proliferation of *Pseudomonas aeruginosa* 3-fold when compared to the free drug. Reprinted from Chu, D., Gao, J., and Wang, Z. (2015) Neutrophil-Mediated Delivery of Therapeutic Nanoparticles across Blood Vessel Barrier for Treatment of Inflammation and Infection. *ACS Nano* 9, 11800–11811 (ref 23). Copyright 2015 American Chemical Society.

of these neutrophil carriers needs to be further assessed, this approach successfully exemplifies the potential of immune cells as natural carriers by exploiting their physiological mechanisms to deliver compounds to sites of infection and inflammation.

## ■ NATURAL AND BIOENGINEERED PARTICLES AS BIOGENIC CARRIERS FOR ANTI-INFECTIVES

### Extracellular Vesicles for Targeted Drug Transport.

Extracellular vesicles (EVs) are natural nanoparticles produced by the majority of prokaryotic and eukaryotic cells.<sup>24,45</sup> Initially, they were thought to be inert cellular debris, but they are increasingly recognized as playing important roles in intercellular communication.<sup>46</sup> EVs are classified according to their biogenesis and size, dividing them mostly into two classes: exosomes, with a size range of 50–200 nm, and shedding microvesicles, that may have sizes of 100 nm up to several micrometers.<sup>25,47</sup> Due to their structure, a lipid bilayer membrane containing proteins, they have been referred to as natural liposomes.<sup>25,47</sup> They are postulated to have a natural role in transferring information between cells and tissues; thus, their potential as drug carriers has been investigated for various applications ranging from inflammation,<sup>48</sup> cancer,<sup>49</sup> infections,<sup>25</sup> and cardiovascular diseases.<sup>50</sup> The use of EVs as drug

carriers largely depends on effective methods of incorporating suitable drugs.<sup>51</sup> It has been shown that they may be loaded with various compounds, such as small molecule drugs, enzymes, and nucleic acids (Figure 2).<sup>52–54</sup>

Some EVs were shown to be inherently anti-infective. Using such preformed vesicles would take advantage of their physiological properties without extensive postprocessing. In literature, there are examples for both EV surface proteins and EV-contained compounds that induce such antimicrobial effect. When neutrophils are challenged with *S. aureus*, their microvesicles induce significantly better aggregation of exogenously added bacteria, compared to microvesicles from nonchallenged neutrophils.<sup>55</sup>

This aggregation was mediated by CD11 $\beta$ -binding of bacteria onto the microvesicle surface, an effect that is also applied for infection diagnostics. A few recent examples have indicated that exosomes may also naturally contain anti-infective compounds, such as those isolated from urine of healthy humans containing proteins known to be bacteriostatic (e.g., mucin-1) and bactericidal (e.g., lysozyme C).<sup>56</sup> Immunogold electron microscopy imaging revealed that these proteins are naturally loaded into EVs. After identifying these proteins in urinary exosomes, Hiemstra and collaborators investigated their ability to inhibit

the growth of strains of *E. coli* that are responsible for urinary tract infections. The urinary exosomes were able to inhibit the growth of *E. coli*,<sup>56</sup> suggesting that they play an important role in innate immunity. Indeed, exosomes induced bacterial lysis during 15 min of incubation with *E. coli*, suggesting release of their cargo in close proximity of bacteria, but the detailed mechanism was not studied. Lässer et al. showed that nasal exosomes contain a number of proteins responsible for cell trafficking and present antibacterial properties.<sup>57</sup> Using a Boyden chemotaxis chamber, a standard assay measuring cell migration through a porous membrane, it was revealed that immune cells isolated from blood migrate to the exosome-containing chamber.<sup>57</sup> They also investigated exosomal proteins by exclusion list-based liquid chromatography–MS/MS and discovered that proteins with antifungal and antibacterial activity are decreased in patients that present respiratory diseases, such as asthma, when compared to healthy individuals.<sup>57</sup> These results suggest that individuals who have pulmonary diseases might be more susceptible to infections and that exosomes contribute to an innate infection defense mechanism in healthy individuals. The focus of this study was on identification of exosomal proteins, but it would be highly relevant to know more about the mechanism by which these EV induce antimicrobial activity. Hu et al. also demonstrated the importance of exosomes in infections by assessing the release of biliary and intestinal epithelium EVs upon infection by *Cryptosporidium parvum*, a parasite.<sup>58</sup> Exposure of the parasite to those exosomes decreased its viability and ability of infection *in vitro* in H69 human lung carcinoma cells and in urine cholangiocyte 603B cells and in mice.<sup>58</sup> These examples indicate a potential of physiological EVs to become an important delivery system for transferring natural or antibacterial cargos in a relevant infection setting. The exploration of the origin and therapeutic applicability of these EVs needs further evaluation, for example, concerning the functional diversity of EV subpopulations,<sup>59</sup> and will clarify whether the biogenic EV approach is a viable future strategy in the clinics.<sup>60</sup>

**Outer Membrane Vesicles as Vaccines.** Bacteria are also able to produce EVs and, when they are Gram-negative, these vesicles are called outer membrane vesicles (OMVs), while EVs produced by Gram-positive bacteria are called membrane vesicles (MVs).<sup>61</sup> Mycobacteria and fungi are also known to pinch off small vesicles, but the mechanism for this is still debated.<sup>62</sup> There are different examples of inherently antimicrobial OMVs that may attack other bacteria during the fight for environmental niches, such as from *Pseudomonas aeruginosa*<sup>63</sup> or *Myxococcus xanthus*.<sup>64</sup> The production of OMVs can be induced by the use of low concentrations of antibiotics during bacterial culture, but those OMVs are bigger than OMVs obtained at normal bacterial homeostasis. However, both particle types have the same content, such as the presence of enzymes which may degrade competing microbes.<sup>63</sup> The immunogenicity of OMVs may be reduced by engineering of their lipopolysaccharide composition which is important for using them as biogenic carriers.<sup>65</sup> Still, it is necessary to assess their biocompatibility under *in vivo* conditions to validate whether the use of bacteria-derived vesicles for treatment approaches is feasible. In contrast, OMVs have been studied in more detail for vaccine applications as they represent cell-free carriers displaying many relevant bacterial antigens. Such a nonreplicative approach is highly promising, and there are first formulations now in clinical assessment for meningitides therapy.<sup>66</sup>

**Bioengineered Liposomes as Carriers for Antibiotics.** Some bacteria have invasion factors that facilitate their entrance

into host cells. This is the case for *Yersinia pseudotuberculosis*, which uses a protein called invasin to enhance host cell attachment and uptake into epithelial cells via integrin binding.<sup>67</sup> Inspired by this ability of invading microbes, Labouta and collaborators developed a liposome formulation functionalized with the *Y. pseudotuberculosis* invasion protein (InvA497) (Figure 2). InvA497 was coupled onto the surface of monodisperse phospholipid fluorescent liposomes,<sup>26</sup> and it was shown that the invasin-functionalized carriers had a higher cell adhesion and better cellular uptake compared to nonfunctionalized liposomes. The uptake studies indicated an active mechanism of internalization, mimicking the pathological uptake route of *Y. pseudotuberculosis*.<sup>26</sup> In a follow-up study, Menina and collaborators showed that the invasin-functionalized liposomes loaded with the model antibiotic gentamicin had a greater antimicrobial effect on intracellular *Y. pseudotuberculosis* and *Salmonella enterica* in HEp-2 epithelial cells when compared to nonfunctionalized liposomes, due to their surface modification.<sup>27</sup> This approach indicates that taking advantage of the natural bacterial invasion characteristics may aid in enhancing the antibacterial activity of drugs that have poor permeability, such as gentamicin. Nevertheless, it remains to be determined to which degree the functionalized liposomal carrier interacts with other gastrointestinal cells upon oral administration and whether or not invasin recognition is specific to enterocytes suffering from intracellular pathogens.

In another liposome-based approach, Henry and collaborators engineered vesicles with cholesterol and sphingomyelin that sequester pore-forming toxins produced by Gram-positive bacteria, competing with host cells for toxin binding.<sup>68</sup> Once they are bound to the liposomes, these toxins cannot lyse mammalian cells *in vitro*.<sup>68</sup> Using an *in vivo* model, it was shown that engineered liposomes prevented *S. aureus* and *S. pneumoniae* septicemia within 10 h after infection in mice.<sup>68</sup> Moreover, when used in a combination treatment of engineered liposomes plus administration of antibiotic vancomycin, lethal effects caused by the infection of *S. aureus* and *S. pneumoniae* were successfully prevented *in vivo*.<sup>68</sup> This impressive example shows that, by exploiting naturally derived principles, it is possible to create effective and simple therapy options for such yet challenging to treat septicemia. As several liposomal formulations have already been marketed for other dispositions, the translation of the present approach into clinical assessment may be facilitated.

## ■ BIOENGINEERED BIOMATERIALS FOR OVERCOMING CHALLENGES ASSOCIATED WITH INFECTIONS

Biomimetic approaches may also be combined with engineering techniques to create bioengineered materials to combat bacterial infections.<sup>69</sup> One such approach is conjugation of molecules or proteins to natural or (semi)synthetic polymers, creating bioengineered drug–polymer conjugates. These conjugates have shown to exhibit enhanced stability under pulmonary<sup>70</sup> or oral administration,<sup>71</sup> indicating that this method may be feasible. A comprehensive overview discussing such orally administered bioinspired approaches is summarized in our recent review manuscript.<sup>72</sup>

Hydrogels offer easily accessible chemical modifications and are often studied as bioinspired systems, as they may be tuned to render mechanical stiffness of living tissue or they may release their cargo in a trigger-dependent way.<sup>73</sup> Thus, hydrogels have been shown to modulate cell behavior<sup>74</sup> or to constitute biomechanical functions of native tissue.<sup>75</sup>

Hydrogels also offer the possibility for a localized and thus highly controlled application of biogenic and bioengineered approaches. A recent example of such an avenue is the development of a 3D-imprinted hydrogel to sequester bacterial  $\beta$ -lactamase.<sup>76</sup>  $\beta$ -Lactamase is a bacterial enzyme, and there is a known factor of increasing resistance and lack of efficiency of  $\beta$ -lactam antibiotics.<sup>5</sup> These enzymes may cleave and inactivate different classes of anti-infectives, such as penicillins or cephalosporins. In the present example, a hydrogel made of *N*-isopropylacrylamide was  $\beta$ -lactamase imprinted. The resulting temperature-sensitive scaffold was able to selectively sequester  $\beta$ -lactamase enzymes, resulting in an increased susceptibility of bacteria toward conventional penicillin G treatment. Successful application of the systems was shown both *in vitro* and in an animal model of wound infection. Bacterial growth in simulated wounds was abolished almost completely by using the imprinted gel in combination with antibiotic treatment. A major advantage of such approach is that it aims for an extra-bacterial factor which may overall reduce the evolution pressure on pathogens and thus the rate of occurrence of resistances. In general, extra-bacterial targets are a promising avenue to develop materials that less likely induce resistances in the long run.<sup>77</sup> Different stimuli-responsive systems are currently explored for on-demand release of nano-antibiotics.<sup>78</sup> One such approach are self-assembled vesicles with encapsulated antimicrobial agents.<sup>79</sup> In the presence of specific enzymes produced by resistant bacteria, vesicles would disintegrate and release their cargo in a selective manner. Probiotics and other nonpathogenic bacteria are not thought to be harmed. Although it only represents a bioinspired approach, it is worth mentioning and may in the future help to achieve bacteria-selective killing without typical gastrointestinal side effects often associated with anti-infective therapy. In general, combining such approaches with novel biomimetic and bioinspired materials may open further opportunities in fighting difficult-to-treat infections. Another example of such efforts is the development of a polysaccharide-based, biodegradable hydrogel that mimics glycosaminoglycans in the natural extracellular matrix.<sup>80</sup> These hydrogels, composed of the natural polymers dextran and chitosan and loaded with vancomycin, have shown promising antimicrobial activity *in vitro*, indicating that they may be used as wound dressing. This approach combines the drug activity of antimicrobial agents with the anti-infective effect of natural chitosan which underlines the importance of biomaterials that show additional interactions with the target tissue.

Finally, another important issue in biomaterials research is to prevent infections on prosthetic surfaces during clinical application. These infections constitute important challenges concerning clinical implication of materials. In an effort to overcome such biomaterial-associated infections and biofilm formation, strategies that involve novel biomaterials have been investigated, such as the enzyme-mimicking polymer brush-functionalized surface that mimics DNase, an enzyme that prevents bacterial adhesion and subsequently, biofilm formation.<sup>81</sup> The natural DNase, however, is very vulnerable, which impairs its performance in antibacterial applications, but the use of the DNase-mimicking polymer brushes prolonged its bioactivity.<sup>81</sup> Several other approaches to preventing infections on prosthetic biomaterials are summarized in a comprehensive review, but most of them are of (fully) synthetic origin and are thus beyond the scope of the present work.<sup>82</sup>

## ■ WHAT IS THE FUTURE FOR BIOGENIC APPROACHES TO TACKLE INFECTIOUS DISEASES?

The field of biogenic and bioinspired approaches for treatment and diagnosis of infections is still young and thriving; we see it full of challenges but also promises. Many clinically established antimicrobial compounds are not efficient (anymore), and new drugs have yet to show biocompatibility and efficiency. Moreover, their tissue-selective delivery is very important, especially when antibiotics with strong side effects come into play. In other fields of drug delivery research, such as cancer treatment, it can be seen that synthetic nanoparticles may improve the targeted transport of compounds only to a certain extent.<sup>83</sup> Thus, we believe that using physiological, natural, biogenic systems is safer and possibly more efficient.<sup>84</sup> Nature has developed and optimized these principles over millions of years of evolution, and the examples discussed in this Perspective show us that specific and selective interaction with target pathogens may be within reach. A bottleneck at the moment is the isolation and preparation of these nature-derived approaches in a reproducible and upscalable manner. Nevertheless, chemical synthesis may never replicate the chemical and biological complexity of these mechanisms that appear under physiological conditions, indicating that at the moment we have to rely on the available natural sources (e.g., red blood cells). Advanced biotechnological approaches for large cell culture and established production techniques for biomimetic carriers such as liposomes are of avail when also taking biogenic avenues to the next step.

Another avenue of circumventing current issues with large scale production of biogenic systems would be their semisynthetic bioengineering. We foresee that a combination of nature-derived systems and clinically established approaches is most promising to succeed in targeting future challenges in infection research, such as by creating cell-like hybrids<sup>85</sup> or by developing hierarchically organized nanomaterials.<sup>86</sup> Such “joint partnership” has already been recommended for combining EV avenues with known liposomal principles to render next-generation delivery systems<sup>87</sup> or to even create synthetic exosomes.<sup>88</sup> Semisynthetic EV systems may be obtained in a biotechnologically controllable manner and would enhance their extended use. The combination of novel biogenic and bioengineered principles with responsive and intelligent biomaterials is another prerequisite to transform physiological avenues into real and applicable formulations and systems. Taking advantage of nature’s exceptional ability to design novel responsive biomaterials to specifically target pathogenic bacteria will undoubtedly help to recuperate the anti-infective power of our current antibiotic arsenal for future anti-infective avenues.

## ■ AUTHOR INFORMATION

### Corresponding Author

\*Phone: +49 68198806 1500. E-mail: [gregor.fuhrmann@helmholtz-hzi.de](mailto:gregor.fuhrmann@helmholtz-hzi.de).

### ORCID

Adriely Goes: 0000-0003-2629-6068

Gregor Fuhrmann: 0000-0002-6688-5126

### Notes

The authors declare no competing financial interest.

## ■ ACKNOWLEDGMENTS

This work was supported by the NanoMatFutur Junior Research programme from the Federal Ministry of Education

and Research, Germany (Grant Number 13XP5029A). The authors acknowledge help from Eilien Schulz and Sara Menina during figure design, Basant Eldessouki for her help with literature research, and Bryan Weaver for proofreading.

## ■ ABBREVIATIONS

EVs, extracellular vesicles; H5WYG, histidine-rich fusogenic peptide; Hbc, genetically engineered hepatitis B core; HCC, human hepatocellular carcinoma; LP, nanoliposome; MTB, magnetotactic bacteria; NPs, nanoparticles; NTA, nitrilotriacetic acid; OMVs, outer membrane vesicles; PEI, polyethylenimine; PEM, polyelectrolyte multilayer; RBC, red blood cell; VLPs, virus-like particles

## ■ REFERENCES

- Parodi, A., Molinaro, R., Sushnitha, M., Evangelopoulos, M., Martinez, J. O., Arrighetti, N., Corbo, C., and Tasciotti, E. (2017) Bio-inspired engineering of cell- and virus-like nanoparticles for drug delivery. *Biomaterials* 147, 155–168.
- Yang, K. S., Im, H., Hong, S., Pergolini, I., Fernandez, A., Wang, R., Clardy, S., Huang, C., Pille, C., Ferrone, S., Yang, R., Castro, C. M., Lee, H., Fernandez, C., and Weissleder, R. (2017) Multiparametric plasma EV profiling facilitates diagnosis of pancreatic malignancy. *Sci. Transl. Med.* 9, eaal3226.
- Yoo, J.-W., Irvine, D. J., Discher, D. E., and Mitragotri, S. (2011) Bio-inspired, bioengineered and biomimetic drug delivery carriers. *Nat. Rev. Drug Discovery* 10, 521–535.
- Dehaini, D., Fang, R. H., and Zhang, L. (2016) Biomimetic strategies for targeted nanoparticle delivery. *Bioeng. Transl. Med.* 1, 30–46.
- Blair, J. M. A., Webber, M. A., Baylay, A. J., Ogbolu, D. O., and Piddock, L. J. V. (2015) Molecular mechanisms of antibiotic resistance. *Nat. Rev. Microbiol.* 13, 42–51.
- Perros, M. (2015) A sustainable model for antibiotics. *Science* 347, 1062–1064.
- Wagner, S., Hauck, D., Hoffmann, M., Sommer, R., Joachim, I., Müller, R., Imberty, A., Varrot, A., and Titz, A. (2017) Covalent Lectin Inhibition and Application in Bacterial Biofilm Imaging. *Angew. Chem., Int. Ed.* 56, 16559–16564.
- Thomann, A., de Mello Martins, A. G. G., Brengel, C., Empting, M., and Hartmann, R. W. (2016) Application of Dual Inhibition Concept within Looped Autoregulatory Systems toward Antiviral Agents against *Pseudomonas aeruginosa* Infections. *ACS Chem. Biol.* 11, 1279–1286.
- Zazo, H., Colino, C. I., and Lanao, J. M. (2016) Current applications of nanoparticles in infectious diseases. *J. Controlled Release* 224, 86–102.
- Mofazzal Jahromi, M. A., Sahandi Zangabad, P., Moosavi Basri, S. M., Sahandi Zangabad, K., Ghamarypour, A., Aref, A. R., Karimi, M., and Hamblin, M. R. (2018) Nanomedicine and advanced technologies for burns: Preventing infection and facilitating wound healing. *Adv. Drug Delivery Rev.* 123, 33–64.
- Fuhrmann, G., Herrmann, I. K., and Stevens, M. M. (2015) Cell-derived vesicles for drug therapy and diagnostics: Opportunities and challenges. *Nano Today* 10, 397–409.
- Löffler, B., Tuchscher, L., Niemann, S., and Peters, G. (2014) Staphylococcus aureus persistence in non-professional phagocytes. *Int. J. Med. Microbiol.* 304, 170–176.
- Bjarnsholt, T., Ciofu, O., Molin, S., Givskov, M., and Høiby, N. (2013) Applying insights from biofilm biology to drug development—can a new approach be developed? *Nat. Rev. Drug Discovery* 12, 791–808.
- Thet, N. T., Wallace, L., Wibaux, A., Boote, N., and Jenkins, A. T. A. (2018) Development of a mixed-species biofilm model and its virulence implications in device related infections. *J. Biomed. Mater. Res., Part B*, 1–9.
- Filkins, L. M., and O’Toole, G. A. (2015) Cystic Fibrosis Lung Infections: Polymicrobial, Complex, and Hard to Treat. *PLoS Pathog.* 11, e1005258.
- Foier, K., Raemdonck, K., De Smedt, S. C., Demeester, J., Coenye, T., and Braeckmans, K. (2014) Lipid and polymer nanoparticles for drug delivery to bacterial biofilms. *J. Controlled Release* 190, 607–623.
- Sheikhpour, M., Barani, L., and Kasaean, A. (2017) Biomimetics in drug delivery systems: A critical review. *J. Controlled Release* 253, 97–109.
- Stanton, M. M., Park, B. W., Vilela, D., Bente, K., Faivre, D., Sitti, M., and Sánchez, S. (2017) Magnetotactic Bacteria Powered Biohybrids Target E. coli Biofilms. *ACS Nano* 11, 9968–9978.
- Niu, Y., Yu, M., Hartono, S. B., Yang, J., Xu, H., Zhang, H., Zhang, J., Zou, J., Dexter, A., Gu, W., and Yu, C. (2013) Nanoparticles Mimicking Viral Surface Topography for Enhanced Cellular Delivery. *Adv. Mater.* 25, 6233–6237.
- Ashley, C. E., Carnes, E. C., Phillips, G. K., Durfee, P. N., Buley, M. D., Lino, C. A., Padilla, D. P., Phillips, B., Carter, M. B., Willman, C. L., Brinker, C. J., Caldeira, J. D. C., Chackerian, B., Wharton, W., and Peabody, D. S. (2011) Cell-specific delivery of diverse cargos by bacteriophage MS2 virus-like particles. *ACS Nano* 5, 5729–5745.
- Shen, L., Zhou, J., Wang, Y., Kang, N., Ke, X., Bi, S., and Ren, L. (2015) Efficient encapsulation of Fe<sub>3</sub>O<sub>4</sub> nanoparticles into genetically engineered hepatitis B core virus-like particles through a specific interaction for potential bioapplications. *Small* 11, 1190–1196.
- Anselmo, A. C., Gupta, V., Zern, B. J., Pan, D., Zakrewsky, M., Muzykantov, V., and Mitragotri, S. (2013) Delivering nanoparticles to lungs while avoiding liver and spleen through adsorption on red blood cells. *ACS Nano* 7, 11129–11137.
- Chu, D., Gao, J., and Wang, Z. (2015) Neutrophil-Mediated Delivery of Therapeutic Nanoparticles across Blood Vessel Barrier for Treatment of Inflammation and Infection. *ACS Nano* 9, 11800–11811.
- György, B., Hung, M. E., Breakefield, X. O., and Leonard, J. N. (2015) Therapeutic Applications of Extracellular Vesicles: Clinical Promise and Open Questions. *Annu. Rev. Pharmacol. Toxicol.* 55, 439–464.
- Fuhrmann, G., Neuer, A. L., and Herrmann, I. K. (2017) Extracellular vesicles – A promising avenue for the detection and treatment of infectious diseases? *Eur. J. Pharm. Biopharm.* 118, 56–61.
- Labouta, H. I., Menina, S., Kochut, A., Gordon, S., Geyer, R., Dersch, P., and Lehr, C. M. (2015) Bacteriomimetic invasion-functionalized nanocarriers for intracellular delivery. *J. Controlled Release* 220, 414–424.
- Menina, S., Labouta, H. I., Geyer, R., Krause, T., Gordon, S., Dersch, P., and Lehr, C.-M. (2016) Invasion-functionalized liposome nanocarriers improve the intracellular delivery of anti-infective drugs. *RSC Adv.* 6, 41622–41629.
- Taherkhani, S., Mohammadi, M., Daoud, J., Martel, S., and Tabrizian, M. (2014) Covalent binding of nanoliposomes to the surface of magnetotactic bacteria for the synthesis of self-propelled therapeutic agents. *ACS Nano* 8, 5049–5060.
- Park, B. W., Zhuang, J., Yasa, O., and Sitti, M. (2017) Multifunctional Bacteria-Driven Microswimmers for Targeted Active Drug Delivery. *ACS Nano* 11, 8910–8923.
- Mohsen, M. O., Zha, L., Cabral-Miranda, G., and Bachmann, M. F. (2017) Major findings and recent advances in virus-like particle (VLP)-based vaccines. *Semin. Immunol.* 34, 123–132.
- Chanishvili, N. (2012) Phage Therapy—History from Twort and d’Herelle Through Soviet Experience to Current Approaches, in *Advances in Virus Research*, 1st ed., pp 3–40, Elsevier Inc, New York, DOI: 10.1016/B978-0-12-394438-2.00001-3.
- Lin, D. M., Koskella, B., and Lin, H. C. (2017) Phage therapy: An alternative to antibiotics in the age of multi-drug resistance. *World J. Gastrointest. Pharmacol. Ther.* 8, 162.
- Bourdin, G., Navarro, A., Sarker, S. A., Pittet, A. C., Qadri, F., Sultana, S., Cravioto, A., Talukder, K. A., Reuteler, G., and Brüßow, H. (2014) Coverage of diarrhoea-associated Escherichia coli isolates from

different origins with two types of phage cocktails. *Microb. Biotechnol.* 7, 165–176.

(34) Nale, J. Y., Spencer, J., Hargreaves, K. R., Buckley, A. M., Trzepinski, P., et al. (2016) Bacteriophage Combinations Significantly Reduce *Clostridium difficile* Growth In Vitro and Proliferation In Vivo. *Antimicrob. Agents Chemother.* 60, 968–981.

(35) Chan, B. K., Sstrom, M., Wertz, J. E., Kortright, K. E., Narayan, D., and Turner, P. E. (2016) Phage selection restores antibiotic sensitivity in MDR *Pseudomonas aeruginosa*. *Sci. Rep.* 6, 1–8.

(36) Hu, C. M. J., Fang, R. H., and Zhang, L. (2012) Erythrocyte-inspired delivery systems. *Adv. Healthcare Mater.* 1, 537–547.

(37) Godfrin, Y., Horand, F., Franco, R., Dufour, E., Kosenko, E., Bax, B. E., Banz, A., Skorokhod, O. A., Lanao, J. M., Vitvitsky, V., Sinauridze, E., Bourgeaux, V., and Gunter, K. C. (2012) International seminar on the red blood cells as vehicles for drugs. *Expert Opin. Biol. Ther.* 12, 127–133.

(38) Favretto, M. E., Cluitmans, J. C. A., Bosman, G. J. C. G. M., and Brock, R. (2013) Human erythrocytes as drug carriers: Loading efficiency and side effects of hypotonic dialysis, chlorpromazine treatment and fusion with liposomes. *J. Controlled Release* 170, 343–351.

(39) Alanazi, F. K., Harisa, G. E. D. I., Maqboul, A., Abdel-Hamid, M., Neau, S. H., and Alsarra, I. A. (2011) Biochemically altered human erythrocytes as a carrier for targeted delivery of primaquine: An in vitro study. *Arch. Pharmacol. Res.* 34, 563–571.

(40) Gutiérrez Millán, C., Zarzuelo Castañeda, A., González López, F., Sayalero Marinero, M. L., Lanao, J. M., and Arévalo, M. (2005) Encapsulation and in vitro evaluation of amikacin-loaded erythrocytes. *Drug Delivery* 12, 409–416.

(41) Sun, Y., Su, J., Liu, G., Chen, J., Zhang, X., Zhang, R., Jiang, M., and Qiu, M. (2017) Advances of blood cell-based drug delivery systems. *Eur. J. Pharm. Sci.* 96, 115–128.

(42) Sherrard, L. J., Tunney, M. M., and Elborn, J. S. (2014) Antimicrobial resistance in the respiratory microbiota of people with cystic fibrosis. *Lancet* 384, 703–13.

(43) Timin, A. S., Litvak, M. M., Gorin, D. A., Atochina-Vasserman, E. N., Atochin, D. N., and Sukhorukov, G. B. (2018) Cell-Based Drug Delivery and Use of Nano- and Microcarriers for Cell Functionalization. *Adv. Healthcare Mater.* 7, 1700818.

(44) Wang, Z., Li, J., Cho, J., and Malik, A. B. (2014) Prevention of vascular inflammation by nanoparticle targeting of adherent neutrophils. *Nat. Nanotechnol.* 9, 204–210.

(45) EL Andaloussi, S., Mäger, I., Breakefield, X. O., and Wood, M. J. A. (2013) Extracellular vesicles: biology and emerging therapeutic opportunities. *Nat. Rev. Drug Discovery* 12, 347–357.

(46) Camussi, G., Derigibus, M. C., Bruno, S., Cantaluppi, V., and Biancone, L. (2010) Exosomes/microvesicles as a mechanism of cell-to-cell communication. *Kidney Int.* 78, 838–848.

(47) Armstrong, J. P. K., Holme, M. N., and Stevens, M. M. (2017) Re-Engineering Extracellular Vesicles as Smart Nanoscale Therapeutics. *ACS Nano* 11, 69–83.

(48) Sun, D., Zhuang, X., Xiang, X., Liu, Y., Zhang, S., Liu, C., Barnes, S., Grizzle, W., Miller, D., and Zhang, H. G. (2010) A novel nanoparticle drug delivery system: The anti-inflammatory activity of curcumin is enhanced when encapsulated in exosomes. *Mol. Ther.* 18, 1606–1614.

(49) Samuel, P., Fabbri, M., and Carter, D. R. F. (2017) Mechanisms of Drug Resistance in Cancer: The Role of Extracellular Vesicles. *Proteomics* 17, 1600375.

(50) Bei, Y., Das, S., Rodosthenous, R. S., Holvoet, P., Vanhaverbeke, M., Monteiro, M. C., Monteiro, V. V. S., Radosinska, J., Bartekova, M., Jansen, F., Li, Q., Rajasingh, J., and Xiao, J. (2017) Extracellular vesicles in cardiovascular theranostics. *Theranostics* 7, 4168–4182.

(51) García-Manrique, P., Matos, M., Gutiérrez, G., Pazos, C., and Blanco-López, M. C. (2018) Therapeutic biomaterials based on extracellular vesicles: classification of bio-engineering and mimetic preparation routes. *J. Extracell. Vesicles* 7, 1422676.

(52) Fuhrmann, G., Serio, A., Mazo, M., Nair, R., and Stevens, M. M. (2015) Active loading into extracellular vesicles significantly improves the cellular uptake and photodynamic effect of porphyrins. *J. Controlled Release* 205, 35–44.

(53) Somiya, M., Yoshioka, Y., and Ochiya, T. (2017) Drug delivery application of extracellular vesicles; insight into production, drug loading, targeting, and pharmacokinetics. *AIMS Bioeng.* 4, 73–92.

(54) Haney, M. J., Klyachko, N. L., Zhao, Y., Gupta, R., Plotnikova, E. G., He, Z., Patel, T., Piroyan, A., Sokolsky, M., Kabanov, A. V., and Batrakova, E. V. (2015) Exosomes as drug delivery vehicles for Parkinson's disease therapy. *J. Controlled Release* 207, 18–30.

(55) Herrmann, I. K., Bertazzo, S., O'Callaghan, D. J. P., Schlegel, A. A., Kallepitis, C., Antcliffe, D. B., Gordon, A. C., and Stevens, M. M. (2015) Differentiating sepsis from non-infectious systemic inflammation based on microvesicle-bacteria aggregation. *Nanoscale* 7, 13511–13520.

(56) Hiemstra, T. F., Charles, P. D., Gracia, T., Hester, S. S., Gatto, L., Al-Lamki, R., Floto, R. A., Su, Y., Skepper, J. N., Lilley, K. S., and Karet Frankl, F. E. (2014) Human Urinary Exosomes as Innate Immune Effectors. *J. Am. Soc. Nephrol.* 25, 2017–2027.

(57) Lässer, C., O'Neil, S. E., Shelke, G. V., Sihlbom, C., Hansson, S. F., Gho, Y. S., Lundbäck, B., and Lötvall, J. (2016) Exosomes in the nose induce immune cell trafficking and harbour an altered protein cargo in chronic airway inflammation. *J. Transl. Med.* 14, 181.

(58) Hu, G., Gong, A.-Y., Roth, A. L., Huang, B. Q., Ward, H. D., Zhu, G., LaRusso, N. F., Hanson, N. D., and Chen, X.-M. (2013) Release of Luminal Exosomes Contributes to TLR4-Mediated Epithelial Antimicrobial Defense. *PLoS Pathog.* 9, e1003261.

(59) Tkach, M., Kowal, J., and Théry, C. (2018) Why the need and how to approach the functional diversity of extracellular vesicles. *Philos. Trans. R. Soc., B* 373, 20160479.

(60) Fais, S., O'Driscoll, L., Borrás, F. E., Buzas, E., Camussi, G., Cappello, F., Carvalho, J., Cordeiro da Silva, A., Del Portillo, H., El Andaloussi, S., Ficko Trček, T., Furlan, R., Hendrix, A., Gursel, I., Kralj-Iglic, V., Kaeffer, B., Kosanovic, M., Lekka, M. E., Lipps, G., Logozzi, M., Marcilla, A., Sammar, M., Llorente, A., Nazarenko, I., Oliveira, C., Pocsfalvi, G., Rajendran, L., Raposo, G., Rohde, E., Siljander, P., van Niel, G., Vasconcelos, M. H., Yáñez-Mó, M., Yliperttula, M. L., Zarovni, N., Zavec, A. B., and Giebel, B. (2016) Evidence-Based Clinical Use of Nanoscale Extracellular Vesicles in Nanomedicine. *ACS Nano* 10, 3886–3899.

(61) Manning, A. J., and Kuehn, M. J. (2013) Functional advantages conferred by extracellular prokaryotic membrane vesicles. *J. Mol. Microbiol. Biotechnol.* 23, 131–141.

(62) Brown, L., Wolf, J. M., Prados-Rosales, R., and Casadevall, A. (2015) Through the wall: Extracellular vesicles in Gram-positive bacteria, mycobacteria and fungi. *Nat. Rev. Microbiol.* 13, 620–630.

(63) Kadurugamuwa, J. L., and Beveridge, T. J. (1996) Bacteriolytic effect of membrane vesicles from *Pseudomonas aeruginosa* on other bacteria including pathogens: conceptually new antibiotics. *J. Bacteriol.* 178, 2767–2774.

(64) Evans, A. G. L., Davey, H. M., Cookson, A., Currinn, H., Cooke-Fox, G., Stanczyk, P. J., and Whitworth, D. E. (2012) Predatory activity of *Myxococcus xanthus* outer-membrane vesicles and properties of their hydrolase cargo. *Microbiology* 158, 2742–2752.

(65) Baker, J. L., Chen, L., Rosenthal, J. A., Putnam, D., and DeLisa, M. P. (2014) Microbial biosynthesis of designer outer membrane vesicles. *Curr. Opin. Biotechnol.* 29, 76–84.

(66) Kaparakis-Liaskos, M., and Ferrero, R. L. (2015) Immune modulation by bacterial outer membrane vesicles. *Nat. Rev. Immunol.* 15, 375–387.

(67) Dersch, P., and Isberg, R. R. (2000) An immunoglobulin superfamily-like domain unique to the *Yersinia pseudotuberculosis* invasion protein is required for stimulation of bacterial uptake via integrin receptors. *Infect. Immun.* 68, 2930–2938.

(68) Henry, B. D., Neill, D. R., Becker, K. A., Gore, S., Bricio-Moreno, L., Ziobro, R., Edwards, M. J., Mühlemann, K., Steinmann, J., Kleuser, B., Japtok, L., Luginbühl, M., Wolfmeier, H., Scherag, A., Gulbins, E., Kadioglu, A., Draeger, A., and Babiychuk, E. B. (2015)

Engineered liposomes sequester bacterial exotoxins and protect from severe invasive infections in mice. *Nat. Biotechnol.* 33, 81–88.

(69) Wohl, B. M., Smith, A. A. A., Jensen, B. E. B., and Zelikin, A. N. (2014) Macromolecular (pro)drugs with concurrent direct activity against the hepatitis C virus and inflammation. *J. Controlled Release* 196, 197–207.

(70) Das, D., Chen, J., Srinivasan, S., Kelly, A. M., Lee, B., Son, H.-N., Radella, F., West, T. E., Ratner, D. M., Convertine, A. J., Skerrett, S. J., and Stayton, P. S. (2017) Synthetic Macromolecular Antibiotic Platform for Inhalable Therapy against Aerosolized Intracellular Alveolar Infections. *Mol. Pharmaceutics* 14, 1988–1997.

(71) Matoori, S., Fuhrmann, G., and Leroux, J.-C. (2013) Celiac Disease: A Challenging Disease for Pharmaceutical Scientists. *Pharm. Res.* 30, 619–626.

(72) Fuhrmann, K., and Fuhrmann, G. (2017) Recent advances in oral delivery of macromolecular drugs and benefits of polymer conjugation. *Curr. Opin. Colloid Interface Sci.* 31, 67–74.

(73) Fuhrmann, G., Chandrawati, R., Parmar, P. A., Keane, T. J., Maynard, S. A., Bertazzo, S., and Stevens, M. M. (2018) Engineering Extracellular Vesicles with the Tools of Enzyme Prodrug Therapy. *Adv. Mater.*, 1706616.

(74) Santos, L., Fuhrmann, G., Juenet, M., Amdursky, N., Horejs, C.-M., Campagnolo, P., and Stevens, M. M. (2015) Extracellular Stiffness Modulates the Expression of Functional Proteins and Growth Factors in Endothelial Cells. *Adv. Healthcare Mater.* 4, 2056–2063.

(75) Parmar, P. A., Chow, L. W., St-Pierre, J. P., Horejs, C. M., Peng, Y. Y., Werkmeister, J. A., Ramshaw, J. A. M., and Stevens, M. M. (2015) Collagen-mimetic peptide-modifiable hydrogels for articular cartilage regeneration. *Biomaterials* 54, 213–225.

(76) Li, W., Dong, K., Ren, J., and Qu, X. (2016) A  $\beta$ -Lactamase-Imprinted Responsive Hydrogel for the Treatment of Antibiotic-Resistant Bacteria. *Angew. Chem., Int. Ed.* 55, 8049–8053.

(77) Allen, R. C., Popat, R., Diggle, S. P., and Brown, S. P. (2014) Targeting virulence: can we make evolution-proof drugs? *Nat. Rev. Microbiol.* 12, 300–308.

(78) Crucho, C. I. C. (2018) The Attack of the Smart Particles: Should Bacteria Be Afraid? *ACS Med. Chem. Lett.* 9, 2–3.

(79) Li, Y., Liu, G., Wang, X., Hu, J., and Liu, S. (2016) Enzyme-Responsive Polymeric Vesicles for Bacterial-Strain-Selective Delivery of Antimicrobial Agents. *Angew. Chem., Int. Ed.* 55, 1760–1764.

(80) Zhao, Y., Zhang, X., Wang, Y., Wu, Z., An, J., Lu, Z., Mei, L., and Li, C. (2014) In situ cross-linked polysaccharide hydrogel as extracellular matrix mimics for antibiotics delivery. *Carbohydr. Polym.* 105, 63–69.

(81) Jiang, R., Xin, Z., Xu, S., Shi, H., Yang, H., Song, L., Yan, S., Luan, S., Yin, J., Khan, A. F., and Li, Y. (2017) Enzyme-mimicking polymer brush-functionalized surface for combating biomaterial-associated infections. *Appl. Surf. Sci.* 423, 869–880.

(82) Campoccia, D., Montanaro, L., and Arciola, C. R. (2013) A review of the biomaterials technologies for infection-resistant surfaces. *Biomaterials* 34, 8533–8554.

(83) Wilhelm, S., Tavares, A. J., Dai, Q., Ohta, S., Audet, J., Dvorak, H. F., and Chan, W. C. W. (2016) Analysis of nanoparticle delivery to tumours. *Nat. Rev. Mater.* 1, 16014.

(84) Le, N. T., Kalluri, J. R., Loni, A., Canham, L. T., and Coffey, J. L. (2017) Biogenic Nanostructured Porous Silicon as a Carrier for Stabilization and Delivery of Natural Therapeutic Species. *Mol. Pharmaceutics* 14, 4509–4514.

(85) Xiao, Q., Yadavalli, S. S., Zhang, S., Sherman, S. E., Fiorin, E., da Silva, L., Wilson, D. A., Hammer, D. A., André, S., Gabius, H.-J., Klein, M. L., Goulian, M., and Percec, V. (2016) Bioactive cell-like hybrids coassembled from (glyco)dendrimerosomes with bacterial membranes. *Proc. Natl. Acad. Sci. U. S. A.* 113, E1134–E1141.

(86) Wang, C. X., Braendle, A., Menyó, M. S., Pester, C. W., Perl, E. E., Arias, I., Hawker, C. J., and Klinger, D. (2015) Catechol-based layer-by-layer assembly of composite coatings: a versatile platform to hierarchical nano-materials. *Soft Matter* 11, 6173–6178.

(87) Johnsen, K. B., Gudbergsson, J. M., Duroux, M., Moos, T., Andresen, T. L., and Simonsen, J. B. (2018) On the use of liposome

controls in studies investigating the clinical potential of extracellular vesicle-based drug delivery systems – A commentary. *J. Controlled Release* 269, 10–14.

(88) García-Manrique, P., Gutiérrez, G., and Blanco-López, M. C. (2018) Fully Artificial Exosomes: Towards New Theranostic Biomaterials. *Trends Biotechnol.* 36, 10–14.

## 6.2 PAPER 2: “Biocompatible bacteria-derived vesicles show inherent antimicrobial activity”

Eilien Schulz<sup>a,b</sup>, **Adriely Goes**<sup>a,b</sup>, Ronald Garcia<sup>c,d</sup>, Fabian Panter<sup>c</sup>, Marcus Koch<sup>e</sup>, Rolf Müller<sup>b,c,d</sup>, Kathrin Fuhrmann<sup>a</sup>, Gregor Fuhrmann<sup>a,b</sup>

<sup>a</sup> Helmholtz Centre for Infection Research (HZI), Biogenic Nanotherapeutics Group (BION), Helmholtz Institute for Pharmaceutical Research Saarland (HIPS), Campus E8.1, Saarbrücken 66123, Germany

<sup>b</sup> Department of Pharmacy, Saarland University, Campus E8.1, Saarbrücken 66123, Germany

<sup>c</sup> Helmholtz Centre for Infection Research (HZI), Department of Microbial Natural Products (MINS), Helmholtz Institute for Pharmaceutical Research Saarland (HIPS), Campus E8.1, Saarbrücken 66123, Germany

<sup>d</sup> German Center for Infection Research (DZIF), Braunschweig 38124, Germany

<sup>e</sup> INM – Leibniz Institute for New Materials, Campus D2 2, Saarbrücken 66123, Germany

Accepted: 30 September 2018

J. Control. Release 2018, 290, 46–55

DOI: 10.1016/j.jconrel.2018.09.030



## Biocompatible bacteria-derived vesicles show inherent antimicrobial activity

Eilien Schulz<sup>a,b</sup>, Adriely Goes<sup>a,b</sup>, Ronald Garcia<sup>c,d</sup>, Fabian Panter<sup>c</sup>, Marcus Koch<sup>e</sup>, Rolf Müller<sup>b,c,d</sup>, Kathrin Fuhrmann<sup>a</sup>, Gregor Fuhrmann<sup>a,b,\*</sup>

<sup>a</sup> Helmholtz Centre for Infection Research (HZI), Biogenic Nanotherapeutics Group (BION), Helmholtz Institute for Pharmaceutical Research Saarland (HIPS), Campus E8.1, Saarbrücken 66123, Germany

<sup>b</sup> Department of Pharmacy, Saarland University, Campus E8.1, Saarbrücken 66123, Germany

<sup>c</sup> Helmholtz Centre for Infection Research (HZI), Department of Microbial Natural Products (MINS), Helmholtz Institute for Pharmaceutical Research Saarland (HIPS), Campus E8.1, Saarbrücken 66123, Germany

<sup>d</sup> German Center for Infection Research (DZIF), Braunschweig 38124, Germany

<sup>e</sup> INM – Leibniz Institute for New Materials, Campus D2 2, Saarbrücken 66123, Germany

### ARTICLE INFO

#### Keywords:

Outer membrane vesicles  
Extracellular vesicles  
Biogenic drug carriers  
Nanoantibiotics  
Myxobacteria  
Electron cryomicroscopy

### ABSTRACT

Up to 25,000 people die each year from resistant infections in Europe alone, with increasing incidence. It is estimated that a continued rise in bacterial resistance by 2050 would lead up to 10 million annual deaths worldwide, exceeding the incidence of cancer deaths. Although the design of new antibiotics is still one way to tackle the problem, pharmaceutical companies investigate far less into new drugs than 30 years ago. Incorporation of antibiotics into nanoparticle drug carriers (“nanoantibiotics”) is currently investigated as a promising strategy to make existing antibiotics regain antimicrobial strength and overcome certain types of microbial drug resistance. Many of these synthetic systems enhance the antimicrobial effect of drugs by protecting antibiotics from degradation and reducing their side effects. Nevertheless, they often cannot selectively target pathogenic bacteria and – due to their synthetic origin – may induce side-effects themselves.

In this work, we present the characterisation of naturally derived outer membrane vesicles (OMVs) as biocompatible and inherently antibiotic drug carriers. We isolated OMVs from two representative strains of myxobacteria, *Cystobacter velutus* Cbv34 and Sorangiineae species strain SBSr073, a bacterial order with the ability of lysing other bacterial strains and currently investigated as sources of new secondary metabolites. We investigated the myxobacteria's inherent antibacterial properties after isolation by differential centrifugation and purification by size-exclusion chromatography. OMVs have an average size range of 145–194 nm. We characterised their morphology by electron cryomicroscopy and found that OMVs are biocompatible with epithelial cells and differentiated macrophages. They showed a low endotoxin activity comparable to those of control samples, indicating a low acute inflammatory potential. In addition, OMVs showed inherent stability under different storage conditions, including 4 °C, –20 °C, –80 °C and freeze-drying. OMV uptake in Gram-negative model bacterium *Escherichia coli* (*E. coli*) showed similar to better incorporation than liposome controls, indicating the OMVs may interact with model bacteria via membrane fusion. Bacterial uptake correlated with antimicrobial activity of OMVs as measured by growth inhibition of *E. coli*. OMVs from Cbv34 inhibited growth of *E. coli* to a comparable extent as the clinically established antibiotic gentamicin. Liquid-chromatography coupled mass spectrometry analyses revealed the presence of cystobactamids in OMVs, inhibitors of bacterial topoisomerase currently studied to treat different Gram-negative and Gram-positive pathogens. This work, may serve as an important basis for further evaluation of OMVs derived from myxobacteria as novel therapeutic delivery systems against bacterial infections.

### 1. Introduction

Over the last decades bacterial resistance to antibiotics is rapidly

rising, largely as a result of their wide availability, overuse and misuse [1]. As a result, antibiotic-resistant bacteria that are difficult to treat such as methicillin-resistant *Staphylococcus aureus* (*S. aureus*) [2]

\* Corresponding author.

E-mail address: [gregor.fuhrmann@helmholtz-hzi.de](mailto:gregor.fuhrmann@helmholtz-hzi.de) (G. Fuhrmann).

<https://doi.org/10.1016/j.jconrel.2018.09.030>

Received 3 June 2018; Received in revised form 21 September 2018; Accepted 30 September 2018

Available online 05 October 2018

0168-3659/© 2018 Elsevier B.V. All rights reserved.

become highly common and are causing a serious global health problem [3]. In Europe alone up to 25,000 patients die each year as a result of those infections which is costing the European Union €1.5 billion annually [2]; and these numbers are seriously on the rise. One way of addressing the challenging question of how to deal with drug-resistant bacteria is still the discovery of novel antibiotic compounds [4]. However due to the risk of spontaneous resistance development, pharmaceutical companies investigate far less into the cost-intensive development process for new antibiotics than 30 years ago [1,3]. Another viable strategy to bypass bacterial resistance is to encapsulate known antibiotics into nanoparticulate drug delivery systems (“nanoantibiotics”) [5,6]. Nanoparticles are among the promising avenues to improve drug transport to the site of infection [7,8]. Loading of antibiotics polymyxin B and ampicillin into liposomes was shown to significantly increase the antibiotic activity, even against difficult pathogens such as *P. aeruginosa* and *S. aureus* [9]. Moreover, encapsulation into nanoparticles can reduce adverse side-effects such as acute kidney injury induced by aminoglycosides [10,11]. However, the ability of certain nanoantibiotics to exclusively target pathogenic bacteria leaving commensal bacteria of the natural microflora unaffected is often suboptimal [9] and they may potentially induce immunogenicity due to their synthetic origin [9,10], both problems manifest upon repeated administration which is necessary during long-term antibiotic therapy. Biogenic approaches, such as cell-derived vesicles [12], are found in nature or based on natural processes and they represent a promising alternative to artificial systems as they can potentially bypass immune activation and are inherently biocompatible [13,14]. Such avenues offer a unique opportunity to learn from their physiological role and tissue interaction paving the way to develop new bioinspired drug carriers [15].

Extracellular vesicles (EVs) are small phospholipid based nanoparticles decorated with membrane and surface proteins and they are thought to be involved in cell-to-cell transfer of information [16,17]. EVs are currently explored for potential therapy of different applications ranging from cancer therapy [18], inflammation [19], gene delivery [20] and to fighting infections [21] because of their natural composition and inherent targeting properties [22]. Nevertheless, ongoing limitations of EVs include issues of upscale production in a biotechnologically controllable manner and post-processing regarding loading and modification for targeted tissue interaction [23] which may overall compromise their applicability in clinical trials. In this work, we investigate a non-toxic and biocompatible type of EVs, namely outer membrane vesicles (OMVs) isolated from non-pathogenic soil-bacteria called myxobacteria. Since myxobacteria are inexpensive to ferment, their OMVs may thus be biotechnologically easily accessible and on top of that we show that they are inherently loaded with a recently discovered class of antibiotics effective against Gram-negative bacteria.

Outer membrane vesicles (OMVs) are spherical nanoparticles produced by Gram-negative bacteria [24,25]. They originate from budding of the bacterial outer membrane and have been shown to hold manifold functions, including communication among bacteria themselves [26], involvement in procurement of nutrients, biofilm formation [27], transfer of virulence factors [28] or immunomodulation of the host [29]. OMVs are studied in detail for vaccination applications [30] with candidates now tested in clinical studies. OMVs have also been engineered for cancer therapy applications [31] but not in detail for delivery of antimicrobial compounds. Interestingly, OMVs can naturally carry bacteriolytic secondary metabolites, using them as weapons during the competition for environmental niches [32]. There are examples of inherently bacteriolytic OMVs derived from pathogens such as *Pseudomonas aeruginosa* [33]. It has been shown that some OMVs derived from other strains, e.g. *Enterobacter* or *Citrobacter* are able to kill other bacteria by transporting peptidoglycan hydrolases into their prey [34]. Although an interesting property, it remains doubtful whether such potentially strong immunogenic particles may be used in humans. To bypass these biocompatibility issues, we employed myxobacteria as

producers of OMVs [35]. Myxobacteria are a class of  $\delta$ -proteobacteria, which are predominantly found in soil. They are producers of versatile secondary metabolites, which offer new effective mechanisms of action and, among other effects, have antibacterial activity [36]. Most importantly, myxobacteria are non-pathogenic to humans but they show a predatory lifestyle and prey on other bacterial competitors [37]. Myxobacteria prey on Gram-negative and Gram-positive bacteria as nutrient source [38] and they are not able to synthesise three branched chain amino acids such as leucine, valine and isoleucine [39]. It was previously shown that *Myxococcus xanthus* produces hydrolase containing OMVs to kill competing bacteria [40]. Such unspecific enzyme induced antimicrobial effect may not be selective enough to kill prokaryotic cells while leaving human tissue unaffected.

Here, we thus aimed at identifying new candidates of myxobacterial OMVs that physiologically contain antibiotic compounds for a selective and efficient treatment of bacterial infection. We further investigated the natural properties of myxobacteria OMVs including their inherent antimicrobial potential against Gram-negative model bacteria *E. coli* and their compatibility with human cells. We characterised OMVs from two myxobacterial strains, namely *Cystobacter velatus* strain Cbv34 and the unclassified Sorangiineae species strain SBSr073 and show that they are biocompatible and stable at different storage conditions. OMVs possess an inherent antimicrobial effect against model pathogens which was comparable to the clinically used antibiotic gentamicin. Our results create an important basis for an advanced development of bacterial OMVs as alternative antimicrobial drug carriers.

## 2. Materials and methods

### 2.1. Microbial culture

Strain SBSr073 of the Sorangiineae suborder was cultivated in 2SWT medium (0.3% bacto tryptone, 0.1% soytone, 0.2% glucose, 0.2% soluble starch, 0.1% maltose monohydrate, 0.2% cellobiose, 0.05%  $\text{CaCl}_2 \cdot 2\text{H}_2\text{O}$ , 0.1%  $\text{MgSO}_4 \cdot 7\text{H}_2\text{O}$  and 10mM HEPES, pH 7.0 adjusted with KOH). *Cystobacter velatus* (Cbv34), a member of the Cystobacterineae suborder, was cultivated in M-medium (1.0% soy peptone, 1.0% maltose, 0.1%  $\text{CaCl}_2$ , 0.1%  $\text{MgSO}_4$ , 50 mM HEPES pH 7.2) at 30 °C and maintained at 180 rpm. *Escherichia coli* (*E. coli*) DH5- $\alpha$  bacteria (DSM 6897) were incubated at 37 °C and 180 rpm in lysogeny broth medium. All cultures were split after reaching stationary phase (Fig. S1). SBSr073 forms aggregates and therefore the measured optical density at 600 nm (OD600) was inconclusive. Hence, the culture was split after 8 days of incubation of a 1% (v/v) inoculum. A growth curve of Cbv34 was established by measuring the OD600 twice a day with a cell density meter model 40 (Fischer Scientific, USA) with semi-micro cuvettes using medium as blank. Cbv34 bacterial culture was started at an OD600 of 0.1 and the stationary phase was reached after 4 days at an OD600 of 3.8. A cryogenic culture of all strains was established in 25% (v/v) glycerol.

### 2.2. Isolation and purification of OMVs

For optimal OMV isolation from conditioned media, myxobacteria needed to be cultured for at least four passages when they reached their stationary phase. Conditioned media from all strains were collected in 50 mL falcon tubes and their OMVs isolated using our previously established protocol [41]. In brief, they were centrifuged at 9500 x g for 10 min at 4 °C, 40 mL of the supernatant was then carefully transferred by pipetting into new falcon tubes and centrifuged at 9500 x g for 15 min at 4 °C. Afterwards, 30 mL of this supernatant was filled into ultracentrifugation tubes and pelleted at 100,000 x g and 4 °C for 2 h (rotor SW 32 Ti, Beckman Coulter). The supernatant was removed carefully and the pellet was re-suspended with 400  $\mu\text{L}$  filtered phosphate buffered saline (PBS, Gibco PBS tablets without calcium, magnesium and phenol red). To check if the isolation successfully removed

living bacteria, 100  $\mu$ L of this pellet were spread on agar plates, containing all nutrients from each media plus 1.5% (w/v) agar and incubated at 30 °C for 8 days.

For further purification, the pellet was applied on a size exclusion chromatography (SEC) column filled with sepharose CL-2B (GE Life Science, United Kingdom) to separate vesicles from proteins that may have as well been pelleted during ultracentrifugation. The pellet to gel ratio was approximately 1 in 100 parts. Fractions of 0.5 to 1 mL were collected into polypropylene (PP) tubes (Axygen) (Fig. S2) and stored at 4 °C for up to one week before further characterisation.

### 2.3. Characterisation of OMVs

Size distribution and yield of OMVs were assessed using Nanoparticles Tracking Analysis (NTA LM-10, Malvern, United Kingdom). To ensure equivalent results, samples were diluted up to 1:1000 in order to have a concentration of 20 to 120 particles per frame. 100  $\mu$ L of sample were applied onto the chamber equipped with a green laser. A video was recorded with a camera level varying between 13 and 15 using NanoSight 3.1. Each sample was recorded three times for 30 s and calculated with a detection threshold of approximately 5 to ensure results are comparable among each other.

To determine the protein concentration of the fractions collected from SEC, a bicinchoninic assay kit (Sigma Aldrich) was used, according to manufacturer's specification. All samples were analysed in duplicates against an albumin standard with concentrations of 0.5, 5, 10, 20 and 30  $\mu$ g/mL. Polydispersity index (PDI) and zeta potential of OMVs was measured on a Malvern Zetasizer.

### 2.4. Electron microscopy of OMVs

For electron cryomicroscopy (cryo-EM), OMVs were purified as described above and dispersions with a concentration of  $\sim 10^{11}$  particles/mL were used for analysis. For sample preparation a 3  $\mu$ L droplet was placed onto a holey carbon film (type S147-4, Plano) before plotting for 2 s using a Gatan cryoplunger model CP3 (Pleasanton) and plunging into liquid ethane at  $T = 108$  K. The frozen samples were transferred under liquid nitrogen to a Gatan model 914 cryo-TEM sample holder and investigated by bright-field TEM imaging at  $T = 100$  K and 15 pA/cm<sup>2</sup> (JEM-2100 LaB6, Jeol).

### 2.5. Biocompatibility of OMVs

A ToxinSensor™ Chromogenic LAL Endotoxin assay kit (GenScript), which is an enzyme based chromogenic test, was used to determine the endotoxin concentration of OMVs. It is an alternative to the gel-clot and turbidimetric tests for lipopolysaccharide (LPS) quantification. According to the manufacturer's specification all samples were examined within either 24 h after isolation or stored at  $-20$  °C before analysis. After mixing the sample with a limulus amoebocyte lysate, the proteolytic activity of factor C was activated by endotoxins. The protease then catalysed the cleavage of p-nitroaniline (pNA) of a synthetic peptide (Ac-Ile-Glu-Ala-Arg-pNA). After diazo-coupling of pNA the absorbance was read at 545 nm using a polystyrene 96 well plate. All samples were measured in technical duplicates.

Biocompatibility of OMVs was studied by assessing viability and cytotoxicity in two cell types, namely epithelial lung carcinoma cells (A549) and acute monocytic leukemia monocytes (THP-1) which were activated to macrophages. These cell lines were chosen to simulate interactions of OMVs with epithelial barriers and immune cells present at sites of infections. A549 cells were seeded into 96-well plates at densities of 10,000 to 20,000 cells/well and left to grow for 48 h. THP-1 cells were seeded into 96-well plates at densities of 100,000 cells/well, subsequently differentiated to adherent macrophages (dTHP-1) with 30 ng/mL of phorbol 12-myristate 13-acetate (PMA) and left to grow for 48 h. Then, the old cell culture medium was replaced with fresh

serum free and phenol red free RPMI 1640 medium (Thermo Fisher) and the cells were incubated with 50, 500, 5000 and 50,000 purified OMVs/cell, and PBS as negative control and Triton X 1% (w/v) as positive control for 24 h. 100  $\mu$ L of cell-free supernatant were transferred to a fresh 96-well plate for subsequent lactate dehydrogenase assay (LDH assay, see below). To assess cell viability, cells were washed and mixed with 100  $\mu$ L fresh medium and 100  $\mu$ L 10% PrestoBlue Cell Viability Reagent (Thermo Fisher) in medium. Cells were incubated at 37 °C for 10 min to 2 h, bottom fluorescence was read (excitation 560 nm and emission 590 nm) and viability calculated in comparison to PBS controls. For LDH detection in supernatants, a kit (Cytotoxicity Detection Kit, Merck) was used per supplier's instructions by incubating with the reaction mixture and an absorbance measurement at 490 nm.

### 2.6. Storage stability of OMVs

Each OMV sample was stored in PBS and at 4 °C,  $-20$  °C,  $-80$  °C and freeze dried to evaluate their stability [42]. Aliquots of 100  $\mu$ L of each sample were kept in MaxyClear microtubes (Axygen) to avoid vesicles absorption to the plastic surface of the tubes. After determining particle concentration and size by NTA (correspond to 100%), the samples were stored for 7 to 75 days. For freeze-drying (lyophilisation), samples were snap frozen with liquid nitrogen and then dried overnight for at least 16 h using a Lypocube (Christ) freeze dryer.

### 2.7. Liposome controls

Liposomes were prepared using a mixture of 1,2-dimyristoyl-sn-glycero-3-phosphorylcholine (DMPC) and dipalmitoyl phosphatidylcholine (DPPC) at a ratio of 2:3 (mol%) and a concentration of 5 mM in a final volume of 1 mL. They were prepared using thin-film hydration as described previously [43]. In brief, lipids were suspended in filtered PBS at 42 °C, and extruded 21 times through a 200 nm polycarbonate membrane (all material from Avanti Lipids).

### 2.8. Uptake assessment and antibiotic activity of OMVs

Liposomes and OMVs were labelled and their cellular uptake was assessed in *E. coli* DH5-alpha model bacterium grown to an OD600 of 0.15. Liposomes and OMVs of SBSr073 and Cbv34 were incubated with 1  $\mu$ L DiI (Vybrant DiI Cell-labelling solution) for 30 min. Non-incorporated dye was removed by SEC. The fluorescence intensity of each fraction was measured and the two most concentrated OMV fractions were used for further evaluation. After incubating *E. coli* with OMVs and liposomes for 1 h, 8 h and 24 h the bacteria were labelled with 1.5  $\mu$ L SYTO 9 Green fluorescent nucleic acid stain and incubated at 37 °C for 10 min. After centrifugation at 9500  $\times$ g for 5 min, bacteria were fixed with 4% paraformaldehyde for 10–15 min at 37 °C. Before applying 10  $\mu$ L of sample on a coverslip with a drop of mounting medium all samples were washed with PBS. Images were taken using a Leica TCS SB8 confocal microscope with a 63 $\times$  magnification lens. A laser with an excitation wavelength of 561 nm (digital gain: 82%, pinhole: 111.5  $\mu$ m, filter: 566–673 nm, laser intensity: 2.0%) was set up to visualise DiI labelled vesicles and liposomes. Another laser with a wavelength of 488 nm (digital gain: 11%, pinhole: 111.5  $\mu$ m, filter: 493–554 nm, laser intensity: 2.0%) was used to visualise SYTO 9 stained bacteria. All images were taken with the same set up, averaging and speed to allow sample comparison; and analysed using the Leica Application Suite X software.

The antimicrobial effect of vesicles on *E. coli* DH5-alpha was analysed by incubating 100  $\mu$ L of bacteria suspension (OD600 of 0.1) with 100  $\mu$ L OMVs in a 96 PS well plate. Sterile PBS was used as a negative control and antibiotic gentamicin (16  $\mu$ g/mL) was applied as positive control. To prevent evaporation, the outer wells of the microplate were filled with water. The plate was incubated at 37 °C in a Tecan infinite 200 Pro plate reader, measuring the absorbance at 600 nm every 15 min

for at least 16 h. OMVs were also diluted 1:5, 1:10, 1:50 or 1:100 with sterile PBS in order to calculate a dose response curve. Colony-forming units (CFU) were measured by incubating OMVs with *E. coli*. For this, *E. coli* DH5- $\alpha$  was cultivated in lysogeny broth at 37 °C and 180 rpm until log phase was reached. The bacterial culture was diluted to 10<sup>8</sup> CFU/mL and incubated overnight with different concentrations of purified OMVs (10<sup>10</sup>, 10<sup>11</sup> and 10<sup>12</sup> vesicles/mL). Serial dilutions of the samples were prepared, inoculated on lysogeny broth agar plates and incubated overnight at 37 °C. Afterwards CFUs/mL were counted and quantified.

### 2.9. Liquid-chromatography coupled mass spectrometry

To assess the active principle within myxobacterial OMVs, they were analysed by liquid-chromatography coupled mass spectrometry (LC-MS). First, 1 mL of purified OMV sample was mixed with 1 mL of methanol to achieve complete solubilisation of EVs. After solvent evaporation the residue was taken up in 150  $\mu$ L of methanol and centrifuged at 21500  $\times$  g for 5 min to remove debris and insoluble salts. 1 mL of this sample was subsequently analysed by UHPLS-HRMS on a Dionex Ultimate 3000 RSLC system using a Waters BEH C18 column (50  $\times$  2.1 mm, 1.7  $\mu$ m) connected to a Waters VanGuard BEH C18 1.7  $\mu$ m guard column. Separation of 1  $\mu$ L sample was achieved by a linear gradient from (A) H<sub>2</sub>O + 0.1% FA to (B) ACN + 0.1% FA at a flow rate of 600  $\mu$ L/min and 45 °C column temperature. Gradient conditions were as follows: 0–0.5 min, 5% B; 0.5–18.5 min, 5–95% B; 18.5–20.5 min, 95% B; 20.5–21 min, 95–5% B; 21–22.5 min, 5% B. UV spectra were recorded by a diode-array detector in the range from 200 to 600 nm. The LC flow was split to 75  $\mu$ L/min before entering the Bruker Daltonics maXis 4G hr-qToF mass spectrometer using the Apollo II ESI source. Mass spectra were acquired in centroid mode ranging from 150 to 2500  $m/z$  at a 2 Hz full scan rate and data were annotated using the in house myxobacterial metabolome *MXbase Database*, established at the Helmholtz Institute for Pharmaceutical Research Saarland (HIPS), by automated comparison of retention time, exact mass and isotope pattern accuracy using Bruker Daltonics Target analysis 1.3. A detailed description of spectra annotation can be found in the supplementary information.

### 2.10. Statistical analysis

All data are displayed as mean  $\pm$  standard deviation (SD), indicating the number of  $n$  independent experiment in each figure. All measurements were at least made in independent triplicates. Results were analysed statistically with Sigma Plot using One-way ANOVA followed by Tukey *post-hoc* test to compare the mean values between individual groups. Significant  $p$ -values were illustrated as \* for  $p < 0.05$  and \*\* $p < 0.005$ .

## 3. Results and discussion

### 3.1. OMVs are efficiently isolated from bacterial culture and they show a promising storage stability

In this work, we compared two strains of myxobacteria from representative suborders as source for OMVs, namely SBSr073 (Sorangiineae suborder) and Cbv34 (*Cystobacterineae* suborder). According to our growth curves strain Cbv34 showed a doubling time of  $t_{D_{Cbv34}} = 4.7 \text{ h} \pm 1.0$ , reaching stationary phase after 50 h (Fig. S1a). To obtain the maximum amount of OMVs while avoiding artefacts of dead cells or presence of protein aggregates, we decided to use conditioned medium after 80 h (stationary phase) for their isolation (Fig. S1b). It is important to mention, that both strains require at least four full passages after starting the culture from cryogenic stocks to achieve optimal bacterial growth (Fig. S1c). Strain SBSr073 formed aggregates when in liquid medium, which made OD600 measurements

inconclusive (Fig. S1d). When dispersing clumps with glass beads and under vortexing, aggregates would form again within 2 days of culture. Thus samples of conditioned medium were generally taken after 8 days of growth and with bacterial morphology not altered. Bright field microscopy of both bacterial strains revealed typical rod shape of myxobacteria and similar culture conditions were used throughout the entire study to ensure reproducible OMV properties. For strain Cbv34, we obtained best OMV results when the culture medium reached a viscous constitution. We were able to keep these myxobacteria in constant culture for > 3 months without loss of phenotype or major alterations of morphology as observed by light microscopy.

OMVs were subsequently isolated from conditioned culture medium using differential ultracentrifugation [43]. Bacteria were removed by centrifuging the culture at 9500  $\times$  g for 10 min and 15 min. After the ultracentrifugation at 100,000  $\times$  g, 100  $\mu$ L of in PBS re-suspended pellet were plated on agar plates and incubated for 8 days to verify that all bacteria had been removed during centrifugation and the final pellet contained only OMVs (Fig. S1e). Re-suspended OMV pellets were purified by SEC to separate protein aggregates from vesicles. This technique is effective for separating molecules and particles according to their size. The successful purification of the OMVs from soluble proteins is shown in Fig. S2, suggesting that OMVs mainly eluted at 6–8 mL for SBSr073 and 7–9 mL for Cbv34 with free protein aggregates eluting in fractions 15 and later. We subsequently pooled the highest concentrated fractions to assess the OMVs using cryo-EM (Fig. 1a). This method was mainly applied to study morphology and shape of vesicles derived from both bacterial strains [44]. The lipid-bilayer is clearly visible which indicates that OMVs were not destroyed during isolation and purification. These images also show that the combination of ultracentrifugation with SEC to purify OMVs was reproducible without inducing artefacts from membrane fusion or disruption. In few images we observed multi-lamellar vesicles which may be a type of the recently described outer-inner membrane vesicles [45]. These particles were reported to occur in only up to 1.2% of OMV preparations from selected strains, which is consistent with our observations in cryo-EM images. To verify these findings, the particle concentration and size of all collected fractions was analysed by NTA (Fig. 1b). In all subsequent experiments, OMV quantification was only based on NTA measurements. The most abundant fractions contained concentrations of 10<sup>10</sup>–10<sup>11</sup> particles/mL which is 10–100fold more than vesicle concentrations reported for mammalian cells [43]. Indeed, low EV amount is one of the major challenges when developing these biogenic carriers for drug therapy [23]. However, microbial culture is already an established biotechnological process with the possibility to upscale which is a big asset to produce these nanodelivery systems. The average hydrodynamic radius of OMVs measured by NTA was 145 nm for Cbv34, and 194 nm for SBSr073 OMVs. When further assessing the physio-chemical properties of purified OMVs, we observed a relatively small PDI of 0.14 and 0.22 for SBSr073 and Cbv34 (Table S1), respectively, which may suggest that with these sizes OMVs can be filtered to sterility [46]. Despite OMVs are derived from cells, their size distribution is rather narrow and it suggests that the majority of the particles have a homogenous distribution.

Due to their cellular origin, the zeta potential of OMVs was slightly negative which is often associated with low stability and tendency to aggregate. We thus investigated the stability of these vesicles by storing samples at 4 °C, –20 °C, –80 °C and upon lyophilisation (freeze-drying) (Fig. 2). After 7 and 75 days, size and particle concentration was measured and compared to day zero (set to 100%). A reduction in particle concentration was seen at all conditions after 7 days but was less pronounced for Cbv34 OMVs with a decrease to 70% when freeze-dried and 40% when stored at –80 °C (Fig. 2a). Such loss may be due to unspecific agglomeration or disintegration of vesicles. After 75 days only 14% of OMVs were recovered when stored at –20 °C but 40% remained when samples were lyophilized. SBSr073 OMVs were most stable during lyophilisation, even after 75 days (Fig. 2c). Interestingly, a

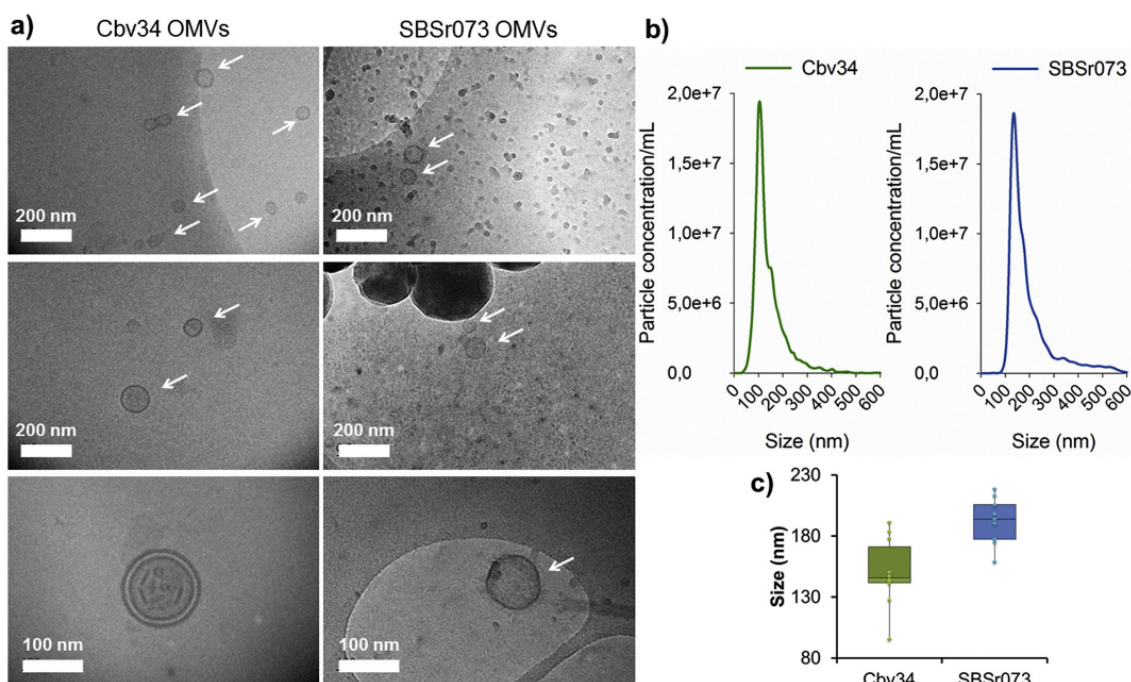


**Fig. 1.** Electron cryomicroscopy characterisation and size distribution of myxobacterial OMVs. a) OMVs were analysed by cryo-EM at different magnifications and are marked with arrows. Bright areas in the images indicate regions of lower transmission, small and big black spots in the SBSr073 samples are ice crystals as identified by their shape. b) Averaged spectra of size distribution of OMVs from Cbv34 and SBSr073 measured by nanoparticle tracking analysis after size exclusion chromatography purification and c) corresponding boxplot of average OMV sizes, Mean  $\pm$  SD, n = 10.

major size drift was observed when storing these OMVs at 4 °C (Fig. 2d). Until now, there are very little reports on a standardized and preferred method for storing OMVs and EVs yet although it is essential for advanced studies [42,47] and storage of vesicles at -80 °C is recommended [48]. Our results indicate that freeze-drying is a valid alternative for storing OMVs as it was also shown in literature [42,49]. Based on our stability data we decided to use OMVs within 3 days after

purification. In all subsequent evaluations, OMVs and liposomes of 148 nm size were used at similar concentrations for appropriate comparison (Fig. S3a).

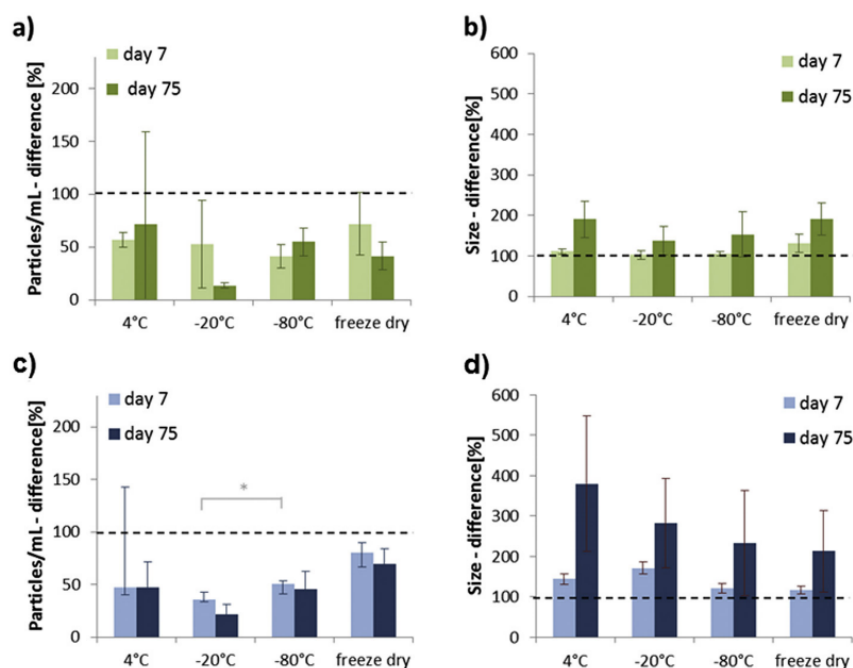


**Fig. 2.** Stability of myxobacterial OMVs upon different storage conditions. OMVs from Cbv34 and SBSr073 were isolated, purified, and stored for 7 and 75 days in PBS and under different conditions (4 °C, -20 °C, -80 °C, and after freeze-drying and at RT). a) Particle concentration of Cbv34 OMVs and b) evolution in size of Cbv34 OMVs, c) Particle concentration of SBSr073 OMVs, d) evolution in size of SBSr073 OMVs. Mean  $\pm$  SD, n = 3, \*p < 0.05 (ANOVA followed by Tukey *post-hoc* test).

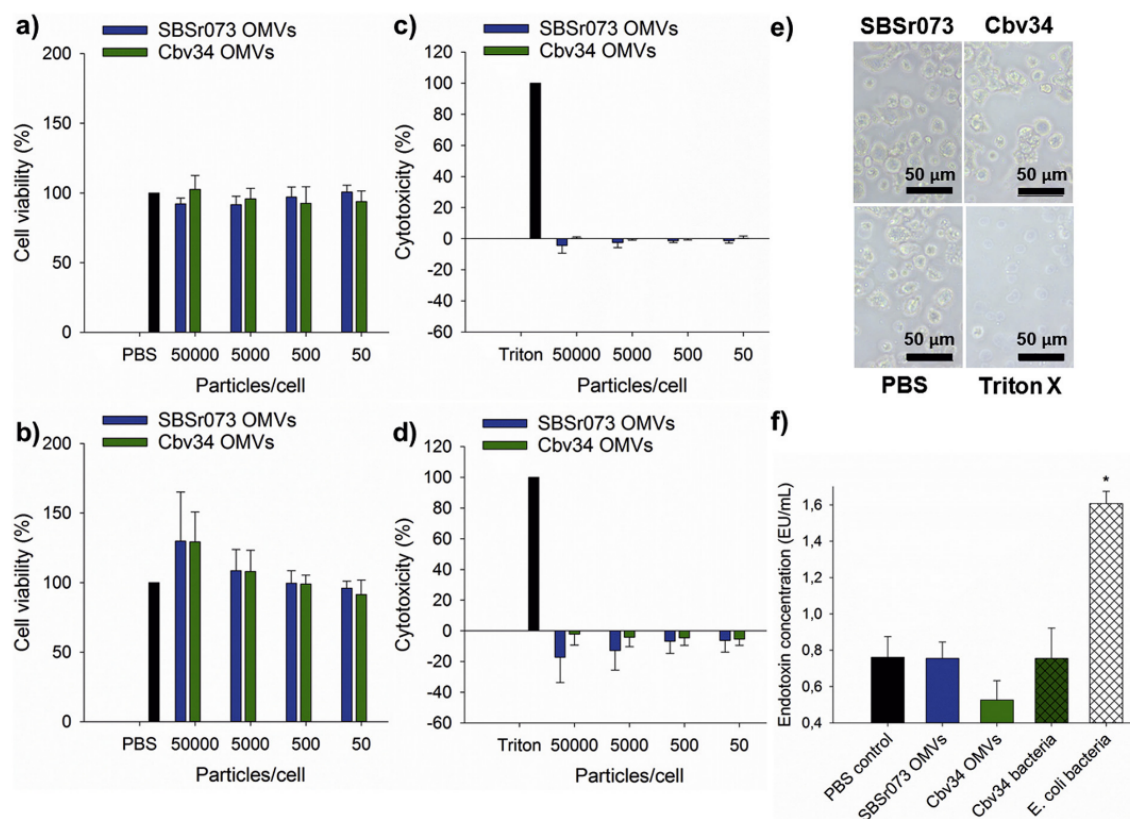


**Fig. 3.** Biocompatibility and endotoxin assessment of myxobacterial OMVs. Cell viability of Cbv34 and SBSr073 OMVs when incubated for 24 h with a) A549 epithelial cells and b) dTHP-1 macrophage cells, and lactate-dehydrogenase cytotoxicity assay of OMVs incubated for 24 h with c) A549 and d) dTHP-1 cells. Mean  $\pm$  SD,  $n = 4-6$ . e) Representative light microscopy images of dTHP-1 cells incubated for 24 h with SBSr073 OMVs, Cbv34 OMVs, PBS (negative control) or Triton X (1%, positive control). f) Endotoxin activity of OMVs compared to control PBS collected from the SEC column under similar conditions. Cbv34 bacteria showed a lower concentration of endotoxins compared to *E. coli* when culturing samples with similar cell densities. Mean  $\pm$  SD,  $n = 3$ , \* $p < 0.05$  (ANOVA followed by Tukey *post-hoc* test).

### 3.2. OMVs show very good biocompatibility and only little endotoxin activity

Biocompatibility of myxobacterial OMVs was evaluated using epithelial A549 cells and differentiated dTHP-1 macrophages to assess cell viability and cytotoxicity (Fig. 3). A549 cells were used as normal epithelial control cells while dTHP-1 cells were stimulated with concentrations of PMA (30 ng/mL) to induce differentiation to macrophages and mimic inflammatory processes that are often associated with bacterial infections [50]. When incubating OMVs with A549 and dTHP-1 cells at different vesicle-to-cell ratios, no impact on general cell viability was observed for any of the cells compared to PBS controls (Fig. 3a and b). We further evaluated whether any underlying cytotoxicity was present by applying a lactate-dehydrogenase test which measures cellular toxicity and cytolysis. Interestingly, even at very high concentrations of 50,000 OMVs/cell no cytotoxic effects were observed which indicated no imminent toxicity in our *in vitro* cell models (Fig. 3c and d). Differentiated dTHP-1 cells are macrophage cells with a high phagocytosis rate and are potentially sensitive towards external stimuli but in our hands we did not see signs of distress or alterations in cell morphology when dTHP-1 cells were incubated at high OMV concentrations (Fig. 3e) and in comparison to positive controls using cytotoxic Triton X. In dTHP-1 cells we see a small increase in cell viability upon addition of very large quantities of OMVs which may be induced by a nutrient bolus of lipids due to the high OMV concentration. No toxic effects were observed for control liposomes used at the same concentrations as OMVs (Fig. S3b and c).

To analyse the potential of OMVs to induce immune reactions during application in a therapeutic setting, a chromogenic limulus amoebocyte lysate endotoxin assay was performed. Such endotoxin assay allows an estimation on the biocompatibility of a material as it gives information if samples contain immunostimulatory lipopolysaccharides. As OMVs could not be prepared under sterile conditions, we used the PBS wash from the SEC column as negative control. We observed that the endotoxin concentration of OMVs was not increased compared to the PBS negative control (Fig. 3f). As another control, the endotoxin activity of strain Cbv34 and *E. coli* bacteria were measured when reaching the same OD600 of 3.5. Interestingly, although the bacterial density was comparable, *E. coli* showed a higher concentration of endotoxins (1.60 EU/mL), while strain Cbv34 exhibited low levels of endotoxins comparable to their OMVs (0.75 EU/mL) and to PBS controls. Our results suggest a lower endotoxin activity of myxobacterial OMVs compared to other Gram-negative microbial materials in general. It has been shown that some myxobacteria have a lack of LPS as a component of their outer membrane [51]. Ruiz et al. found an altered immune response of myxospores in sheep compared to other Gram-negative spores [52], which may be due to a partial modification of polysaccharides [53]. Our results suggest inherent biocompatibility of bacterial OMVs from myxobacteria, which may aid for their applicability in therapeutic settings.

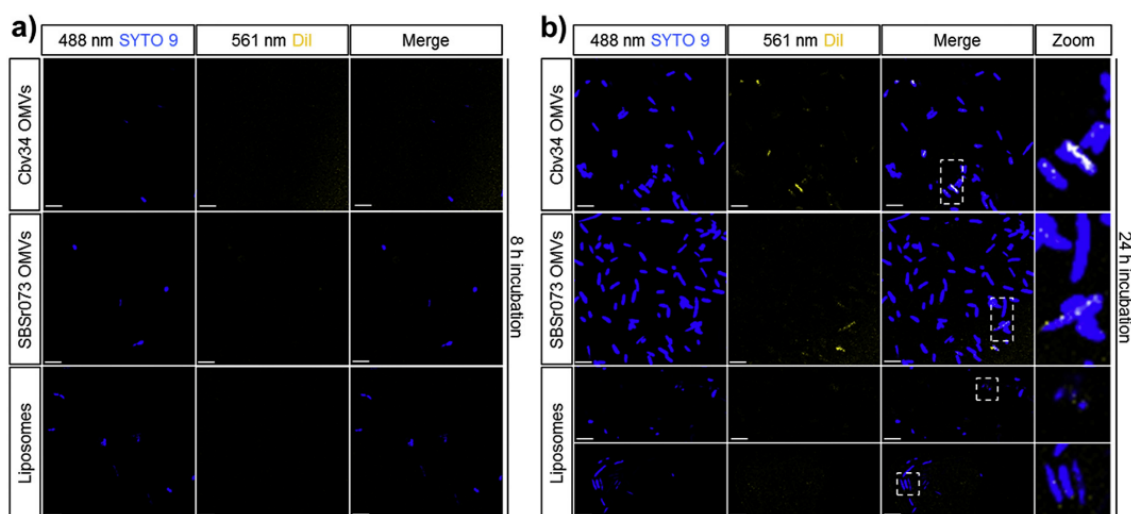


**Fig. 4.** Representative confocal fluorescence images of *E. coli* incubated with OMVs. *E. coli* DH5- $\alpha$  incubated with fluorescently (DiI)-labelled Cbv34 OMVs ( $10^{11}$ /mL), SBSr073 ( $10^{10}$ /mL) OMVs, and Liposomes ( $10^{11}$ /mL) for a) 8 h and b) 24 h. Images were taken using the same laser settings at 561 nm and 488 nm. Scale bars represent 5  $\mu$ m. Zoomed-in images displayed, show co-localisation of fluorescently labelled OMVs with magnified bacteria. Measurement settings and image analysis is similar for all images; false colouring was set to blue and yellow to better visualise co-localisation in the merged images. (For interpretation of the references to colour in this figure legend, the reader is referred to the web version of this article.)

### 3.3. The co-localisation of OMVs with model bacteria is comparable to standard liposomes

*E. coli* DH5- $\alpha$  were incubated with DiI labelled OMVs or liposomes for 1, 8, and 24 h in order to visualise interaction of OMVs with target model bacteria. The dyes were excited with two different lasers, for DiI at 561 nm and for detection of SYTO 9 labelled bacteria at 488 nm. SYTO 9 was used for visualisation of all live and dead bacteria during microscopy. After 1 h (Fig. S4) and 8 h of incubation with *E. coli*, very little to no co-localisation was detected for both types of OMVs and for liposomes. As seen in Fig. 4 after 24 h incubation, we observed co-localisation of SYTO 9 labelled bacteria with DiI labelled OMVs (zoom in Fig. 4b and arrows in Fig. S4). Control samples incubating *E. coli* with DiI dye alone and in the absence of OMVs did not show co-localised fluorescence (Fig. S5b). After 24 h of incubation with DiI labelled liposomes, we qualitatively observed less co-localisation. Liposomes may have accumulated in the extracellular matrix of the bacteria as indicated by a diffuse bright halo around the *E. coli*. For all experiments, comparable labelling efficiency of OMVs versus liposomes was employed (Fig. S5a). We further studied z-stack images of *E. coli* incubated for 20 h with Cbv34 OMVs (final concentration  $10^{12}$  OMVs/mL) which were washed before imaging (Fig. S6). For some bacteria we observed co-localisation (indicated by arrows) but we also saw unspecific accumulation of OMVs in bacterial proximity. Overall, our results suggest that OMVs are co-localising with *E. coli* similarly to synthetic liposomes. There are three possible scenarios for OMVs to interact with cells, whether they belong to their own or competing other species: i) releasing cargo nearby cells, ii) physical fusion with the target outer membrane, or iii) by interaction with mammalian cell membranes via receptors. For OMV uptake into mammalian cells, different mechanisms ranging from direct fusion to endocytic uptake are currently discussed [54]. Evans et al. observed an increased fusion effect of OMVs when Glyceraldehyde 3-phosphate dehydrogenase (GDPH) was added to *E. coli* [40]. The GDPH is an enzyme involved in eukaryotic membrane fusion, which may indicate that OMVs are eventually taken up through direct membrane fusion. We qualitatively observed a comparable co-localisation of natural vs. synthetic lipid carriers (i.e., OMVs vs. liposomes) in *E. coli* which may relate to the fluidity of the nanoparticle membrane in bacterial uptake as shown previously [55]. For other

OMVs fusion with target bacteria was proposed [35], but upcoming assessments will need to indicate whether OMVs from Cbv34 and SBSr073 also follow this mechanism. Our findings nevertheless give a first insight into how interaction of OMVs compares to synthetic carriers which may serve as a point of reference to the creation of semi-synthetic OMV-mimetics with enhanced bacterial interaction.

### 3.4. OMVs are intrinsically loaded with antimicrobial drugs and show a growth inhibition using model bacteria

Following the promising results during uptake experiments in *E. coli* model bacteria, we investigated the antibacterial effect of OMVs. To do so, they were incubated with *E. coli* in a 96 well plate, screening the OD600 every 15 min. This simple real-time detection method showed that OMVs from Cbv34 had a strong inhibitory effect on *E. coli* growth when incubated at concentrations of  $10^{12}$  vesicles/mL (Fig. 5a). As control, concentrations of  $10^{12}$  OMVs/mL did not influence our OD600-based measurements in absence of bacteria. The OMV-induced inhibitory effect was comparable to a standard aminoglycoside antibiotic, gentamicin, at concentrations of 16  $\mu$ g/mL. To elucidate whether this inhibitory effect of OMVs was bacteriostatic or bactericidal we performed counting of CFUs after incubation with *E. coli* (Fig. 5b). It was shown that Cbv34 OMVs completely inhibited bacterial growth when incubated at concentrations of  $10^{12}$  vesicles/mL. Indeed, CFU counting confirmed our previously seen growth inhibition and the OMVs' effect was proven to be bacteriolytic because very small amounts of living colonies were observed upon plating. We calculated that 16  $\mu$ g/mL gentamicin correspond to approximately  $4 \times 10^{15}$  drug molecules to inhibit bacterial growth, while  $2 \times 10^{11}$  OMVs induced a comparable effect. To further investigate this effect, we incubated *E. coli* with varying concentrations of OMVs which revealed a typical sigmoidal dose-response curve (Fig. 5c). In this OD600-based assay, OMV concentrations between  $10^{11}$  and  $10^{12}$  vesicles/mL were necessary to obtain the growth inhibition effect, which also matched our CFU data. Concentrations of  $10^{11}$  to  $10^{12}$  vesicles/mL corresponded in our assay to an antimicrobial activity range of 140–2500 OMVs/CFU. We did not observe any impact on *E. coli* growth when incubating bacteria with comparable concentrations of control liposomes (Fig. S3c). When further studying the OMV producers, we observed that Cbv34 bacteria

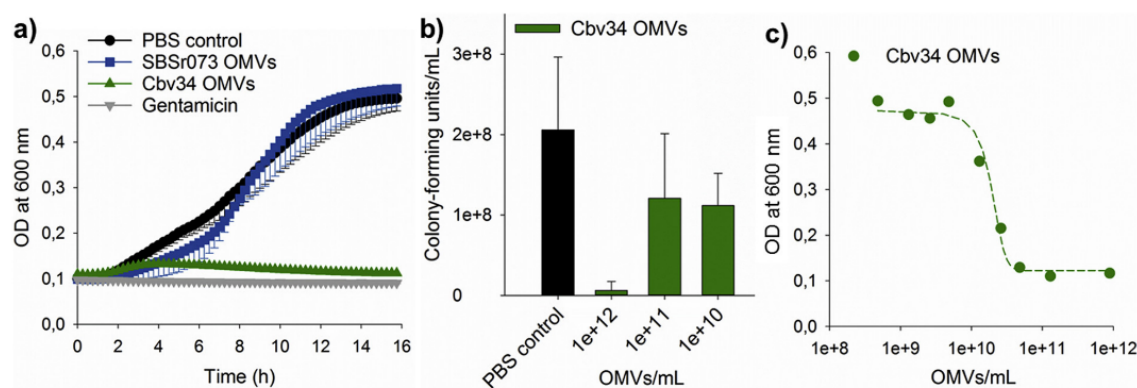


**Fig. 5.** Inherent antibiotic effect of OMVs when incubated with *E. coli*. a) Incubation of Cbv34 OMVs (concentration  $10^{11}$ /mL) and SBSr073 OMVs (concentration  $10^{10}$ /mL) with *E. coli* and in comparison to free gentamicin (16  $\mu$ g/mL). Mean  $\pm$  SD,  $n = 3$ . b) Counting of colony-forming units of *E. coli* DH5-alpha incubated with different concentrations of Cbv34 OMVs. Mean  $\pm$  SD,  $n = 3$ . c) Dose response curve of Cbv34 OMVs by incubating increasing concentrations of OMVs with *E. coli*.

were able to predate and lyse *E. coli* within 48 h of cultivation on agar (Fig. S7), while SBSr073 bacteria were slowly swarming and showed weak predation. In consistency with these results, we only observed a small influence of SBSr073 OMVs on the growth rate of *E. coli* DH5-alpha. As seen in Fig. 5a, SBSr073 OMVs appeared to induce a small bacteriostatic effect until 4–6 h of incubation with model bacteria which was not maintained during the entire incubation period of 16 h. Nevertheless, given their biocompatibility profile, SBSr073 OMVs may in the future be loaded with common antibiotics to assess their delivery potential in an infection setting.

Myxobacteria are promising producers of various antibacterial compounds, as it was shown in literature [36]. We thus investigated the Cbv34 OMVs' active principle. In doing so, OMV samples were extracted using methanol as solvent and analysed by LC-MS. We identified a cystobactamid in the vesicle samples derived from Cbv34, eluting at a retention time of approximately 9 min and with an extracted ion chromatogram at  $920.309 \pm 0.02$  Da (Fig. S8). A scheduled precursor list based targeted MS<sup>2</sup> experiment was applied to this main chromatographic peak in order to rule out mass-spectrometric artefacts and to confirm our finding. When comparing the OMV peak with a cystobactamid 919-1 standard we observed very good agreement in MS<sup>2</sup> spectral fingerprint and displaying the subsequent losses of the derivatised p-aminobenzoic acid moieties from the cystobactamid backbone (Fig. S9) which confirmed presence of the compound within Cbv34 OMVs. Unfortunately, it was not possible to quantify the amount of cystobactamid within acceptable error margins because of the limit of quantification and potential ion suppression effects induced by the OMV background signal. We further aimed at better analysing the antimicrobial effect of OMVs by determining the minimal inhibitory concentration of free cystobactamid 919-1 to be 32  $\mu$ g/mL using *E. coli* DH5-alpha model bacteria while Cbv34 OMVs showed a minimal inhibitory concentration of  $10^{12}$  particles/mL. We also performed CFU counting of various cystobactamid and OMV concentrations (Fig. S10). Mass spectrometry control experiments additionally revealed that cystobactamid is not contained in SBSr073 OMVs, pointing towards a role as active principle of Cbv34 OMVs. Cystobactamids are an important new class of antimicrobials which inhibit the bacterial type IIa topoisomerases and are effective against *E. coli* as well as several problem pathogens [56,57]. Thus intrinsically loaded biocompatible vesicles, as we showed here, alleviates drug carrier development in many ways: method validation for drug encapsulation is not needed, therefore the risk of modulating the vesicle membrane and its properties during post-processing is low. These naturally-equipped OMVs from strain Cbv34 may be an important step towards using EV-based therapies in the near future.

#### 4. Conclusions

In this work, we present a new type of OMVs derived from myxobacteria that shows intrinsic antibiotic activity. These OMVs exhibit promising properties regarding size distribution and stability upon storage. Bacteria as sources for EVs are ideal as their high-yield cultivation on industrial scale is widely practiced which aides in the clinical translation of the current approach. Uptake studies indicated that OMVs are interacting with Gram-negative bacterial strains in a similarly manner than liposomes but further evaluations of these processes are required. Furthermore, advanced biocompatibility studies, such as an incubation of OMVs in complex *in vitro* models, and additional investigations regarding immunogenicity on other human cell lines or in small animal models are necessary. Regarding the OMV activity profile, it would be important to study other model bacteria or bacterial biofilms, which are an important barrier to successful antibiotic therapy at the moment [58]. Likewise, bacterial loading of cystobactamids into OMVs may be controllable through varying culture conditions. Indeed, lower potency of Cbv34 OMVs was observed when bacteria were used at lower passage numbers after inoculation from cryogenic stock indicating that culture periods may have an influence on antimicrobial activity (Fig. S11).

The ability of these OMVs to target infected tissue would need to be studied using suitable *in vivo* models [6]. As their antimicrobial cargo compounds are naturally packed into OMVs, they are potentially protected from destruction by degrading enzymes which may reduce probability of new resistances [5]. OMVs may be bioengineered to possess small moieties enabling optimised targeting to pathogens while concurrently reducing accumulation in healthy mammalian cells as it was shown for other EVs [59]. These OMVs finally present a water-soluble version of poorly water-soluble cystobactamid which is relevant when developing this promising drug for other application routes, such as lung or oral delivery [60]. Ultimately, our findings provide an important step towards further developing OMVs from myxobacteria as promising antimicrobial drug carriers.

#### Author contributions

E.S. conducted all experiments on OMVs isolation and characterization, prepared figures and analysed experiments; A.G. assessed antimicrobial activity of OMVs together with E.S.; R.G. set-up the myxobacterial cultures and assisted in their maintenance; F.P. executed LC-MS analyses; M.K. collected electron cryomicroscopy images; R.M. provided myxobacterial strains and helped with the study design; K.F. executed biocompatibility analyses and supervised the work. G.F. conceived the study, supervised the project and wrote the main

manuscript text together with E.S. All authors analysed data and reviewed the manuscript.

### Additional information

The authors declare no competing financial interests.

### Acknowledgements

This work was supported by the NanoMatFutur Junior Research programme from the Federal Ministry of Education and Research, Germany (grant number 13XP5029A, BEVA). We thank Jennifer Herrmann for providing cystobactamid 919-1 standards.

### Appendix A. Supplementary data

Supplementary data to this article can be found online at <https://doi.org/10.1016/j.jconrel.2018.09.030>.

### References

- H.R. Meredith, J.K. Srimani, A.J. Lee, A.J. Lopatkin, L. You, Collective antibiotic tolerance: mechanisms, dynamics and intervention, *Nat. Chem. Biol.* 11 (2015) 182–188.
- J.M.A. Blair, M.A. Webber, A.J. Baylay, D.O. Ogbolu, L.J.V. Piddock, Molecular mechanisms of antibiotic resistance, *Nat. Rev. Micro.* 13 (2015) 42–51.
- M. Perros, A sustainable model for antibiotics, *Science* 347 (2015) 1062–1064.
- R. Sommer, S. Wagner, K. Rox, A. Varrot, D. Hauck, E.-C. Wamhoff, J. Schreiber, T. Ryckmans, T. Brunner, C. Rademacher, R.W. Hartmann, M. Brönstrup, A. Imberty, A. Titz, Glycomimetic, Orally Bioavailable LecB Inhibitors Block Biofilm Formation of *Pseudomonas aeruginosa*, *J. Am. Chem. Soc.* 140 (2018) 2537–2545.
- H. Zazo, C.I. Colino, J.M. Lanao, Current applications of nanoparticles in infectious diseases, *J. Control. Release* 224 (2016) 86–102.
- R.S. Santos, C. Figueiredo, N.F. Azevedo, K. Braeckmans, S.C. De Smedt, Nanomaterials and molecular transporters to overcome the bacterial envelope barrier: Towards advanced delivery of antibiotics, *Adv. Drug Deliv. Rev.* (2017), <https://doi.org/10.1016/j.addr.2017.12.010>.
- P. Meers, M. Neville, V. Malinin, A.W. Scott, G. Sardaryan, R. Kurumunda, C. Mackinson, G. James, S. Fisher, W.R. Perkins, Biofilm penetration, triggered release and in vivo activity of inhaled liposomal amikacin in chronic *Pseudomonas aeruginosa* lung infections, *J. Antimicrob. Chemother.* 61 (2008) 859–868.
- C.-M. Huang, C.-H. Chen, D. Pompattananangkul, L. Zhang, M. Chan, M.-F. Hsieh, L. Zhang, Eradication of drug resistant *Staphylococcus aureus* by liposomal oleic acids, *Biomaterials* 32 (2011) 214–221.
- A.J. Huh, Y.J. Kwon, “Nanoantibiotics”: a new paradigm for treating infectious diseases using nanomaterials in the antibiotics resistant era, *J. Control. Release* 156 (2011) 128–145.
- R.Y. Pelgrift, A.J. Friedman, Nanotechnology as a therapeutic tool to combat microbial resistance, *Adv. Drug Deliv. Rev.* 65 (2013) 1803–1815.
- R. Schiffflers, G. Storm, I. Bakker-Woudenberg, Liposome-encapsulated aminoglycosides in pre-clinical and clinical studies, *J. Antimicrob. Chemother.* 48 (2001) 333–344.
- P. García-Manrique, M. Matos, G. Gutiérrez, C. Pazos, M.C. Blanco-López, Therapeutic biomaterials based on extracellular vesicles: classification of bio-engineering and mimetic preparation routes, *J. Extracell. Vesicles* 7 (2018) 1422676.
- A. Parodi, R. Molinaro, M. Sushnitha, M. Evangelopoulos, J.O. Martínez, N. Arrighetti, C. Corbo, E. Tasciotti, Bio-inspired engineering of cell- and virus-like nanoparticles for drug delivery, *Biomaterials* 147 (2017) 155–168.
- A. Goes, G. Fuhrmann, Biogenic and biomimetic carriers as versatile transporters to treat infections, *ACS Infect. Dis.* 4 (2018) 881–892.
- J.-W. Yoo, D.J. Irvine, D.E. Discher, S. Mitragotri, Bio-inspired, bioengineered and biomimetic drug delivery carriers, *Nat. Rev. Drug Discov.* 10 (2011) 521–535.
- H. Zhang, D. Freitas, H.S. Kim, K. Fabijanic, Z. Li, H. Chen, M.T. Mark, H. Molina, A.B. Martin, L. Bojmar, J. Fang, S. Rampsaud, A. Hoshino, I. Matei, C.M. Kenific, M. Nakajima, A.P. Mutvei, P. Sansone, W. Buehring, H. Wang, J.P. Jimenez, L. Cohen-Gould, N. Paknejad, M. Brendel, K. Manova-Todorova, A. Magalhães, J.A. Ferreira, H. Osório, A.M. Silva, A. Massey, J.R. Cubillos-Ruiz, G. Galletti, P. Giannakakou, A.M. Cuervo, J. Blenis, R. Schwartz, M.S. Brady, H. Peinado, J. Bromberg, H. Matsui, C.A. Reis, D. Lyden, Identification of distinct nanoparticles and subsets of extracellular vesicles by asymmetric flow field-flow fractionation, *Nat. Cell Biol.* 20 (2018) 332–343.
- J.P.K. Armstrong, M.N. Holme, M.M. Stevens, Re-engineering extracellular vesicles as smart nanoscale therapeutics, *ACS Nano* 11 (2017) 69–83.
- H. Zhang, T. Deng, R. Liu, M. Bai, L. Zhou, X. Wang, S. Li, X. Wang, H. Yang, J. Li, T. Ning, D. Huang, H. Li, L. Zhang, G. Ying, Y. Ba, Exosome-delivered EGFR regulates liver microenvironment to promote gastric cancer liver metastasis, *Nat. Commun.* 8 (2017) 15016.
- D. Yuan, Y. Zhao, W.A. Banks, K.M. Bullock, M. Haney, E. Batrakova, A.V. Kabanov, Macrophage exosomes as natural nanocarriers for protein delivery to inflamed brain, *Biomaterials* 142 (2017) 1–12.
- D.S. Sutarra, J. Jiang, O.A. Elgamil, S.M. Pomeroy, M. Badawi, X. Zhu, R. Pavlovicz, A.C.P. Azevedo-Pouly, J. Chalmers, C. Li, M.A. Phelps, T.D. Schmittgen, Low active loading of cargo into engineered extracellular vesicles results in inefficient miRNA mimic delivery, *J. Extracell. Vesicles* 6 (2017) 1333882.
- G. Fuhrmann, A.L. Neuer, I.K. Herrmann, Extracellular vesicles – a promising avenue for the detection and treatment of infectious diseases? *Eur. J. Pharm. Biopharm.* 118 (2017) 56–61.
- G. Fuhrmann, I. Herrmann, M.M. Stevens, Cell-derived vesicles for drug therapy and diagnostics: opportunities and challenges, *Nano Today* 10 (2015) 397–409.
- M.I. Ramirez, M.G. Amorim, C. Gadelha, I. Milic, J.A. Welsh, V.M. Freitas, M. Nawaz, N. Akbar, Y. Couch, L. Makin, F. Cooke, A.L. Vettore, P.X. Batista, R. Frezorz, J.A. Pezuk, L. Rosa-Fernandes, A.C.O. Carreira, A. Devitt, L. Jacobs, I.T. Silva, G. Coakley, D.N. Nunes, D. Carter, G. Palmisano, E. Dias-Neto, Technical challenges of working with extracellular vesicles, *Nanoscale* 10 (2018) 881–906.
- L. Brown, J.M. Wolf, R. Prados-Rosales, A. Casadevall, Through the wall: extracellular vesicles in Gram-positive bacteria, mycobacteria and fungi, *Nat. Rev. Micro* 13 (10) (2015) 620–630 advance online publication.
- A. Kulp, M.J. Kuehn, Biological functions and biogenesis of secreted bacterial outer membrane vesicles, *Annu. Rev. Microbiol.* 64 (2010) 163–184.
- J. Berleman, M. Auer, The role of bacterial outer membrane vesicles for intra- and interspecies delivery, *Environ. Microbiol.* 15 (2013) 347–354.
- V. Yonezawa, T. Osaki, S. Kurata, M. Fukuda, H. Kawakami, K. Ochiai, T. Hanawa, S. Kamiya, Outer membrane vesicles of *Helicobacter pylori* TK1402 are involved in biofilm formation, *BMC Microbiol.* 9 (2009) 197.
- L.M. Mashburn, M. Whiteley, Membrane vesicles traffic signals and facilitate group activities in a prokaryote, *Nature* 437 (2005) 422–425.
- M. Kaparakis-Liaskos, R.L. Ferrero, Immune modulation by bacterial outer membrane vesicles, *Nat. Rev. Immunol.* 15 (2015) 375–387.
- K. Watanabe, Bacterial membrane vesicles (MVs): novel tools as nature- and nano-carriers for immunogenic antigen, enzyme support, and drug delivery, *Appl. Microbiol. Biotechnol.* 100 (2016) 9837–9843.
- V. Gujrati, S. Kim, S.H. Kim, J.J. Min, H.E. Choy, S.C. Kim, S. Jon, Bioengineered bacterial outer membrane vesicles as cell-specific drug-delivery vehicles for cancer therapy, *ACS Nano* 8 (2014) 1525–1537.
- I. Olsen, A. Amano, Outer membrane vesicles – offensive weapons or good Samaritans? *J. Oral Microbiol.* 7 (2015), <https://doi.org/10.3402/jom.v7.27468>.
- J.L. Kadorugamuwa, T.J. Beveridge, Bacteriolytic effect of membrane vesicles from *Pseudomonas aeruginosa* on other bacteria including pathogens, *J. Bacteriol.* 178 (1996) 2767–2774.
- Z. Li, A.J. Clarke, T.J. Beveridge, Gram-negative bacteria produce membrane vesicles which are capable of killing other bacteria, *J. Bacteriol.* 180 (1998) 5478–5483.
- D.E. Whitworth, Chapter 1 - Myxobacterial vesicles: death at a distance? in: S.S. Allen, I. Laskin, M.G. Geoffrey (Eds.), *Adv. Appl. Microbiol.*, Academic Press, 2011, pp. 1–31.
- T. Hoffmann, D. Krug, N. Bozkurt, S. Duddela, R. Jansen, R. García, K. Gerth, H. Steinmetz, R. Müller, Correlating chemical diversity with taxonomic distance for discovery of natural products in myxobacteria, *Nat. Commun.* 9 (2018) 803.
- J.E. Berleman, J.R. Kirby, Deciphering the hunting strategy of a bacterial wolfpack, *FEMS Microbiol. Rev.* 33 (2009) 942–957.
- B. Norén, K.B. Raper, Antibiotic activity of Myxobacteria in relation to their bacteriolytic capacity, *J. Bacteriol.* 84 (1962) 157–162.
- B.S. Goldman, W.C. Nierman, D. Kaiser, S.C. Slater, A.S. Durkin, J.A. Eisen, C.M. Ronning, W.B. Barbazuk, M. Blanchard, C. Field, C. Halling, G. Hinkle, O. Iartchuk, H.S. Kim, C. Mackenzie, R. Madupu, N. Miller, A. Shvartsbeyn, S.A. Sullivan, M. Vaudin, R. Wiegand, H.B. Kaplan, Evolution of sensory complexity recorded in a myxobacterial genome, *Proc. Natl. Acad. Sci.* 103 (2006) 15200–15205.
- A.G.L. Evans, H.M. Davey, A. Cookson, H. Currinn, G. Cooke-Fox, P.J. Stanczyk, D.E. Whitworth, Predatory activity of *Myxococcus xanthus* outer-membrane vesicles and properties of their hydrolase cargo, *Microbiology* 158 (2012) 2742–2752.
- G. Fuhrmann, R. Chandrawati, P.A. Pamar, T.J. Keane, S.A. Maynard, S. Bertazzo, M.M. Stevens, Engineering extracellular vesicles with the tools of enzyme produg therapy, *Adv. Mater.* 30 (2018) 1706616.
- J. Frank, M. Richter, C. De Rossi, C.-M. Lehr, K. Fuhrmann, G. Fuhrmann, Extracellular vesicles protect glucuronidase model enzymes during freeze-drying, *Sci. Rep.* 8 (2018) 12377.
- G. Fuhrmann, A. Serio, M. Mazo, R. Nair, M.M. Stevens, Active loading into extracellular vesicles significantly improves the cellular uptake and photodynamic effect of porphyrins, *J. Control. Release* 205 (2015) 35–44.
- D. Danino, Cryo-TEM of soft molecular assemblies, *Curr. Opin. Colloid Interface Sci.* 17 (2012) 316–329.
- C. Pérez-Cruz, L. Delgado, C. López-Iglesias, E. Mercade, Outer-inner membrane vesicles naturally secreted by gram-negative pathogenic bacteria, *PLoS One* 10 (2015) e0116896.
- L. Zhang, Z. Cao, Y. Li, J.-R. Ella-Menye, T. Bai, S. Jiang, Softer Zwitterionic Nanogels for longer Circulation and lower Splenic Accumulation, *ACS Nano* 6 (2012) 6681–6686.
- Á.M. Lórinz, C.I. Timár, K.A. Marosvári, D.S. Veres, L. Otkocsi, Á. Kittel, E. Ligeti, Effect of storage on physical and functional properties of extracellular vesicles derived from neutrophilic granulocytes, *J. Extracell. Vesicles* 3 (2014) 25465.
- K.W. Witwer, E.I. Buzás, L.T. Bemis, A. Bora, C. Lässer, J. Lötvall, E.N. Nolte-T Hoen, M.G. Piper, S. Sivaraman, J. Skog, C. Théry, M.H. Wauben, F. Hochberg, Standardization of sample collection, isolation and analysis methods in

- extracellular vesicle research, *J. Extracell. Vesicles* 2 (2013) 20360.
- [49] C. Arigita, W. Jiskoot, J. Westdijk, C. van Ingen, W.E. Hennink, D.J.A. Crommelin, G.F.A. Kersten, Stability of mono- and trivalent meningococcal outer membrane vesicle vaccines, *Vaccine* 22 (2004) 629–642.
- [50] E.K. Park, H.S. Jung, H.I. Yang, M.C. Yoo, C. Kim, K.S. Kim, Optimized THP-1 differentiation is required for the detection of responses to weak stimuli, *Inflamm. Res.* 56 (2007) 45–50.
- [51] M. Keck, N. Gisch, H. Moll, F.-J. Vorhölder, K. Gerth, U. Kahmann, M. Lissel, B. Lindner, K. Niehaus, O. Holst, Unusual outer membrane lipid composition of the gram-negative, Lipopolysaccharide-lacking myxobacterium *Sorangium cellulosum* So ce56, *J. Biol. Chem.* 286 (2011) 12850–12859.
- [52] C. Ruiz, A. Ruiz-Bravo, G.A. De Cienfuegos, A. Ramos-Cormenzana, Immunomodulation by myxospores of *Myxococcus xanthus*, *Microbiology* 131 (1985) 2035–2039.
- [53] C. Ruiz, A. Ruiz-Bravo, A. Ramos-Cormenzana, Endotoxin-like activities in *Myxococcus xanthus*, *Curr. Microbiol.* 15 (1987) 343–345.
- [54] E.J. O'Donoghue, A.M. Krachler, Mechanisms of outer membrane vesicle entry into host cells, *Cell. Microbiol.* 18 (2016) 1508–1517.
- [55] K. Forier, K. Raemdonck, S.C. De Smedt, J. Demeester, T. Coenye, K. Braeckmans, Lipid and polymer nanoparticles for drug delivery to bacterial biofilms, *J. Control. Release* 190 (2014) 607–623.
- [56] S. Baumann, J. Herrmann, R. Raju, H. Steinmetz, K.I. Mohr, S. Hüttel, K. Harmrolfs, M. Stadler, R. Müller, Cystobactamids: Myxobacterial topoisomerase inhibitors exhibiting potent antibacterial activity, *Angew. Chem. Int. Ed.* 53 (2014) 14605–14609.
- [57] S. Hüttel, G. Testolin, J. Herrmann, T. Planke, F. Gille, M. Moreno, M. Stadler, M. Brönstrup, A. Kirschning, R. Müller, Discovery and total synthesis of natural cystobactamid derivatives with superior activity against gram-negative pathogens, *Angew. Chem. Int. Ed.* 56 (2017) 12760–12764.
- [58] T. Bjarnsholt, O. Ciofu, S. Molin, M. Givskov, N. Hoiby, Applying insights from biofilm biology to drug development - can a new approach be developed? *Nat. Rev. Drug Discov.* 12 (2013) 791–808.
- [59] S.A.A. Kooijmans, L.A.L. Fliervoet, R. van der Meel, M.H.A.M. Fens, H.F.G. Heijnen, P.M.P. van Bergen En Henegouwen, P. Vader, R.M. Schiffelers, PEGylated and targeted extracellular vesicles display enhanced cell specificity and circulation time, *J. Control. Release* 224 (2016) 77–85.
- [60] K. Fuhrmann, G. Fuhrmann, Recent advances in oral delivery of macromolecular drugs and benefits of polymer conjugation, *Curr. Opin. Colloid Interface Sci.* 31 (2017) 67–74.



Contents lists available at ScienceDirect

Journal of Controlled Release

journal homepage: [www.elsevier.com/locate/jconrel](http://www.elsevier.com/locate/jconrel)



## Corrigendum

### Corrigendum to biocompatible bacteria-derived vesicles show inherent antimicrobial activity [Journal of controlled release, volume 290, page 46–55 (2018), page 46–55]

Eilien Schulz<sup>a,b</sup>, Adriely Goes<sup>a,b</sup>, Ronald Garcia<sup>c,d</sup>, Fabian Panter<sup>c</sup>, Marcus Koch<sup>c</sup>, Rolf Müller<sup>b,c,d</sup>, Kathrin Fuhrmann<sup>a</sup>, Gregor Fuhrmann<sup>a,b,\*</sup>

<sup>a</sup> Helmholtz Centre for Infection Research (HZI), Biogenic Nanotherapeutics Group (BION), Helmholtz Institute for Pharmaceutical Research Saarland (HIPS), Campus E8.1, Saarbrücken 66123, Germany

<sup>b</sup> Department of Pharmacy, Saarland University, Campus E8.1, Saarbrücken 66123, Germany

<sup>c</sup> Helmholtz Centre for Infection Research (HZI), Department of Microbial Natural Products (MINS), Helmholtz Institute for Pharmaceutical Research Saarland (HIPS), Campus E8.1, Saarbrücken 66123, Germany

<sup>d</sup> German Center for Infection Research (DZIF), Braunschweig 38124, Germany

<sup>e</sup> INM – Leibniz Institute for New Materials, Campus D2 2, Saarbrücken 66123, Germany.

The authors regret that there was a mistake in calculating the number of outer membrane vesicles incubated with each cell. On page 48, paragraph 2.5., line 25, it should read “and the cells were incubated with 10, 100, 1,000 and 10,000 purified OMVs” and page 51, paragraph 3.2., line 13, should read “concentrations of 10,000 OMVs/cell no cytotoxic effects were observed”. According to this, Figs. 3 and S3 were

modified. These errors do not change the conclusions published in this work.

The authors also regret to correct that bacto peptone and not soy peptone was used for the preparation of M-medium (page 47, paragraph 2.1., line 6).

The authors would like to apologise for any inconvenience caused.

DOI of original article: <https://doi.org/10.1016/j.jconrel.2018.09.030>

\* Corresponding author at: Helmholtz Centre for Infection Research (HZI), Biogenic Nanotherapeutics Group (BION), Helmholtz Institute for Pharmaceutical Research Saarland (HIPS), Campus E8.1, Saarbrücken 66123, Germany.

E-mail address: [gregor.fuhrmann@helmholtz-hips.de](mailto:gregor.fuhrmann@helmholtz-hips.de) (G. Fuhrmann).

<https://doi.org/10.1016/j.jconrel.2018.11.027>

Available online 05 December 2018

0168-3659/© 2018 Elsevier B.V. All rights reserved.

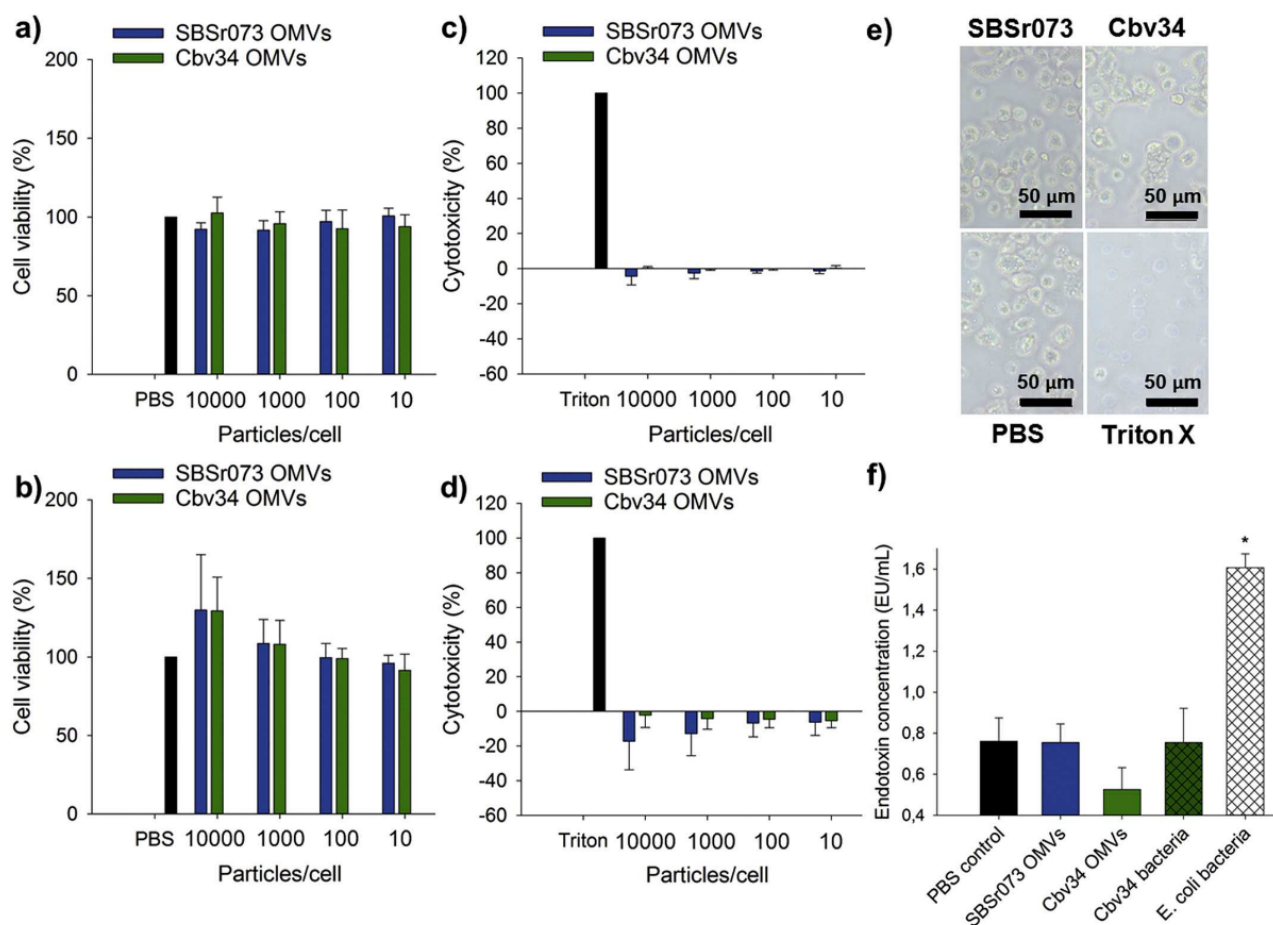


**Fig. 3.** Biocompatibility and endotoxin assessment of myxobacterial OMVs. Cell viability of Cbv34 and SBSr073 OMVs when incubated for 24 h with a) A549 epithelial cells and b) dTHP-1 macrophage cells, and lactate-dehydrogenase cytotoxicity assay of OMVs incubated for 24 h with c) A549 and d) dTHP-1 cells. Mean  $\pm$  SD,  $n = 4-6$ . e) Representative light microscopy images of dTHP-1 cells incubated for 24 h with SBSr073 OMVs, Cbv34 OMVs, PBS (negative control) or Triton X (1%, positive control). f) Endotoxin activity of OMVs compared to control PBS collected from the SEC column under similar conditions. Cbv34 bacteria showed a lower concentration of endotoxins compared to *E. coli* when culturing samples with similar cell densities. Mean  $\pm$  SD,  $n = 3$ , \* $p < .05$  (ANOVA followed by Tukey post-hoc test).

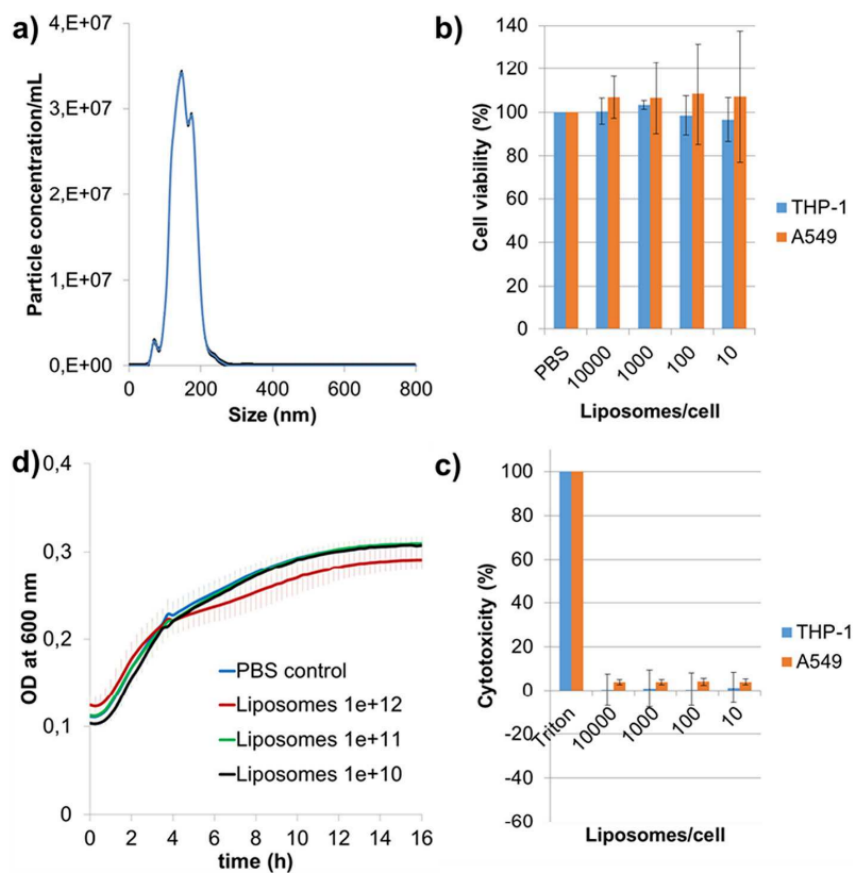


**Fig. S3.** Complementary liposome control experiments. a) Size distribution of liposomes (1,2-dimyristoyl-sn-glycero-3-phosphorylcholine (DMPC) and dipalmitoyl phosphatidylcholine (DPPC) at a ratio of 2:3 mol%) measured by NTA (representative sample). b) Cell viability of liposomes when incubated for 24 h with stimulated dTHP-1 macrophage cells and A549 epithelial cells, and c) lactate-dehydrogenase cytotoxicity assay of liposomes incubated for 24 h with dTHP-1 and A549 cells. Mean  $\pm$  SD,  $n = 3-4$ . d) Growth curve of *E. coli* DH5-alpha incubated with different concentration of liposomes or PBS (control). Mean  $\pm$  SD,  $n = 3$ .

## **Supplementary Information**

### **Biocompatible bacteria-derived vesicles show inherent antimicrobial activity**

Eilien Schulz, Adriely Goes, Ronald Garcia, Fabian Panter, Marcus Koch, Rolf Müller, Kathrin Fuhrmann and Gregor Fuhrmann\*

Figure S1. Growth curve and cell morphology of myxobacteria.

Figure S2. Protein and particle concentration of collected fractions from SEC.

Table S1. Physico-chemical characteristics of myxobacterial OMVs.

Figure S3. Complementary liposome control experiments.

Figure S4. Complementary confocal fluorescence images of OMVs incubated with *E. coli*.

Figure S5. Mean fluorescence of labelled OMVs and liposomes used for *in vitro* imaging and control confocal fluorescence microscopy images.

Figure S6. Complementary z-stack confocal fluorescence images of OMVs incubated with *E. coli*.

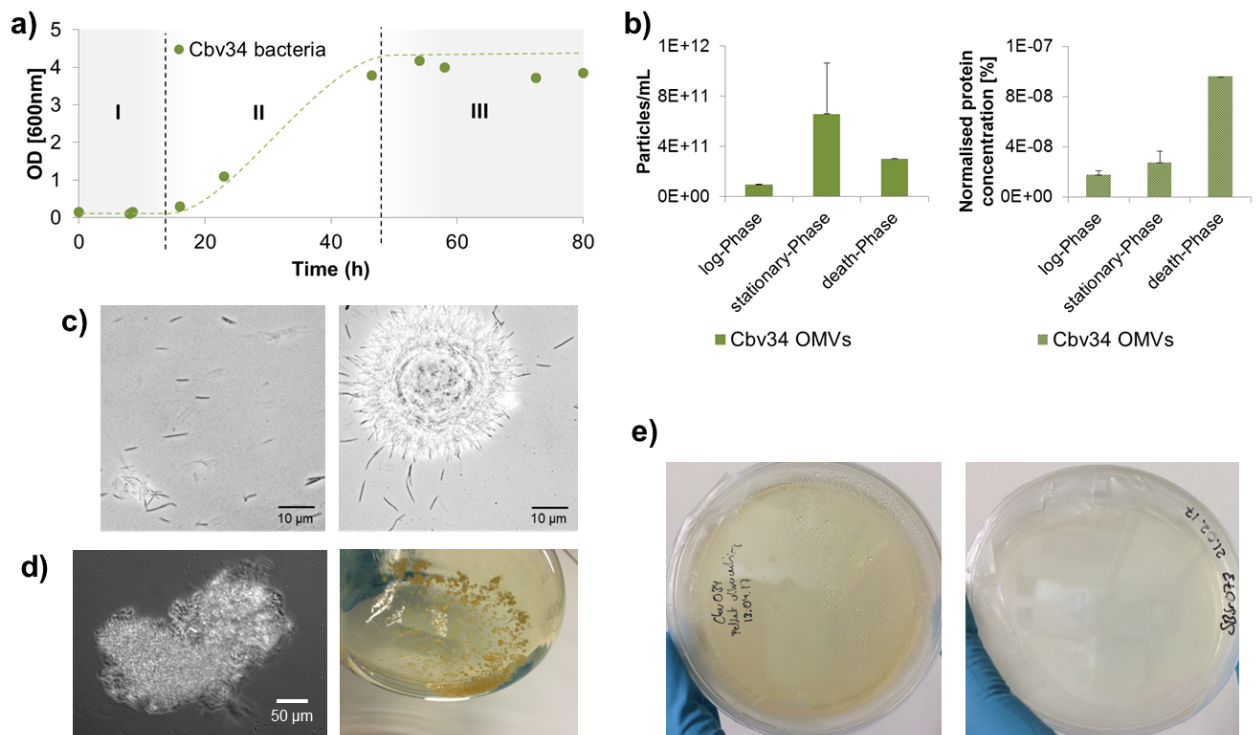
Figure S7. Predatory behaviour of Cbv34 myxobacteria on *E. coli*.

Figure S8. Liquid chromatography-mass spectrometry based identification of Cystobactamid 919-1 in the methanolic crude extract of Cbv34 OMVs.

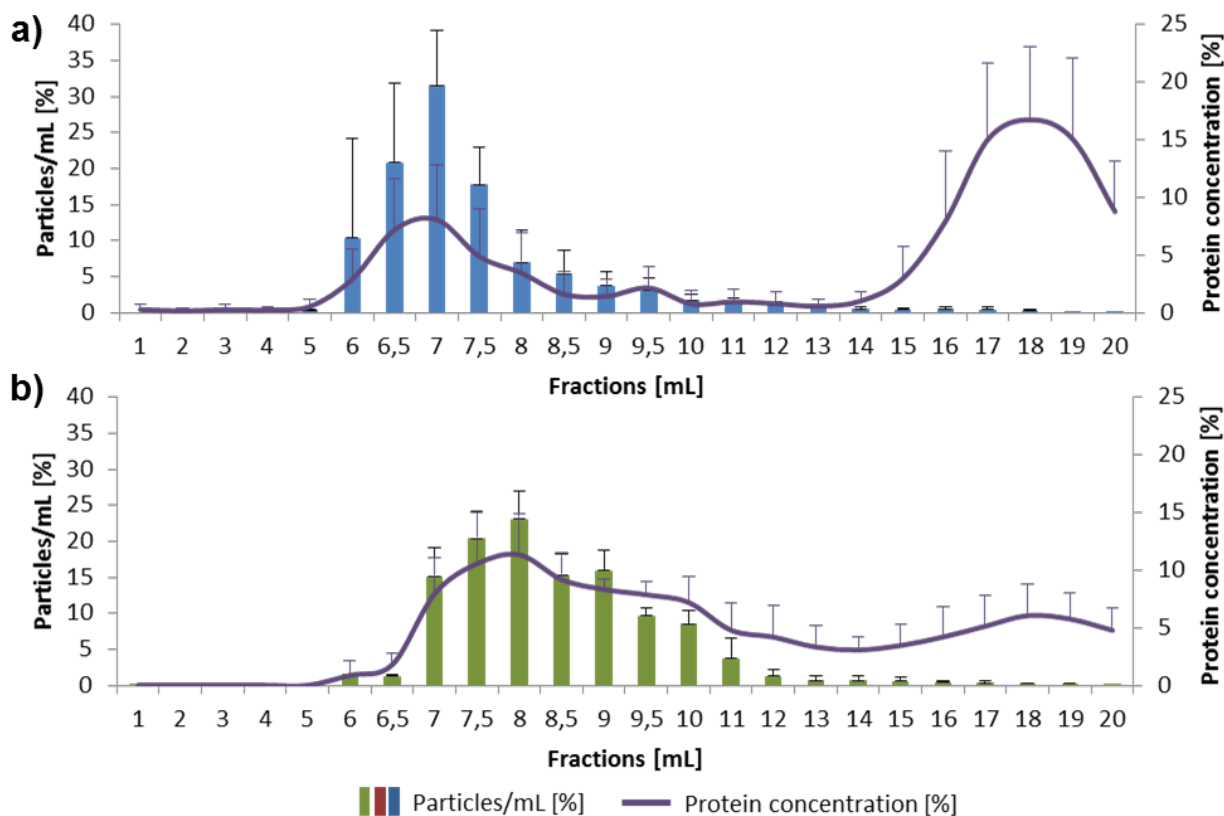
Figure S9. Comparison of the MS<sup>2</sup> spectrum of Cystobactamid 919-1 from Cbv34 OMVs to the MS<sup>2</sup> spectrum of Cystobactamid 919-1 reference standard.

Figure S10. Antimicrobial activity of Cbv34 OMVs compared to free cystobactamid.

Figure S11. Dose response of Cbv34 OMVs obtained from lower passage numbers.



**Figure S1. Growth curve and cell morphology of myxobacteria.** **a)** Growth curve of Cbv34 bacteria during (I) lag-phase, (II) log-phase and (III) stationary-phase. Cbv34 grow in high density and with a doubling time of  $t_{D_{Cbv34}} = 4.7 \text{ h} \pm 1.0$ ; Mean,  $n = 3-4$ . Cbv34 bacteria were grown in M medium (1.0% soy peptone, 1.0% maltose, 0.1%  $\text{CaCl}_2$ , 0.1%  $\text{MgSO}_4$  and 50 mM HEPES pH 7.2) at 30 °C and maintained at 180 rpm. A growth curve of SBSr073 bacteria could not be taken as this culture formed aggregates and the OD could not be measured. SBSr073 bacteria were cultured in 2SWT medium (0.3% bacto tryptone, 0.1% soytone, 0,2% glucose, 0,2% soluble starch, 0,1% maltose monohydrate, 0,2% cellobiose, 0,05%  $\text{CaCl}_2 \cdot 2\text{H}_2\text{O}$ , 0,1%  $\text{MgSO}_4 \cdot 7\text{H}_2\text{O}$  and 10mM HEPES, pH 7.0 adjusted with KOH) **b)** Cbv34 OMV characteristics during different growth phases: particle concentration and protein concentration normalised by particle concentration.  $n = 3$ . **c)** Bright field microscopy images of Cbv34 in culture and after inoculation from a cryo stock. **d)** Bright field microscopy images of myxobacteria SBSr073 and photograph of clumpy bacteria containing flask. **e)** When plating 100 μL of EV-pellet isolated from SBSr073 and Cbv34 for 8 days on 1.5% (w/v) agar no bacterial growth was detected. Agar plates were prepared using the liquid culture media of each bacterium.



**Figure S2. Protein and particle concentration of collected fractions from SEC. a)** SBSr073 OMVs, **b)** Cbv34 OMVs; the sum of all values corresponds to 100%. Each fraction corresponds to the percentage of the total concentration (particles or proteins). Mean  $\pm$  SD,  $n = 3-7$

**Table S1. Physico-chemical characteristics of myxobacterial OMVs.**

OMV source	Particle size $\pm$ SD measured by NTA (n = 16-27)	PDI (n = 3)	Total protein concentration OMVs (n = 4-7)	$\xi$ -potential (n = 3)
SBSr073	194 $\pm$ 18 nm	0.143 $\pm$ 0.01	8.0 $\pm$ 4.0 $\mu$ g/mL	-6.81 $\pm$ 0.61 mV
Cbv34	145 $\pm$ 27 nm	0.222 $\pm$ 0.06	84.8 $\pm$ 71.7 $\mu$ g/mL	-4.76 $\pm$ 0.65 mV

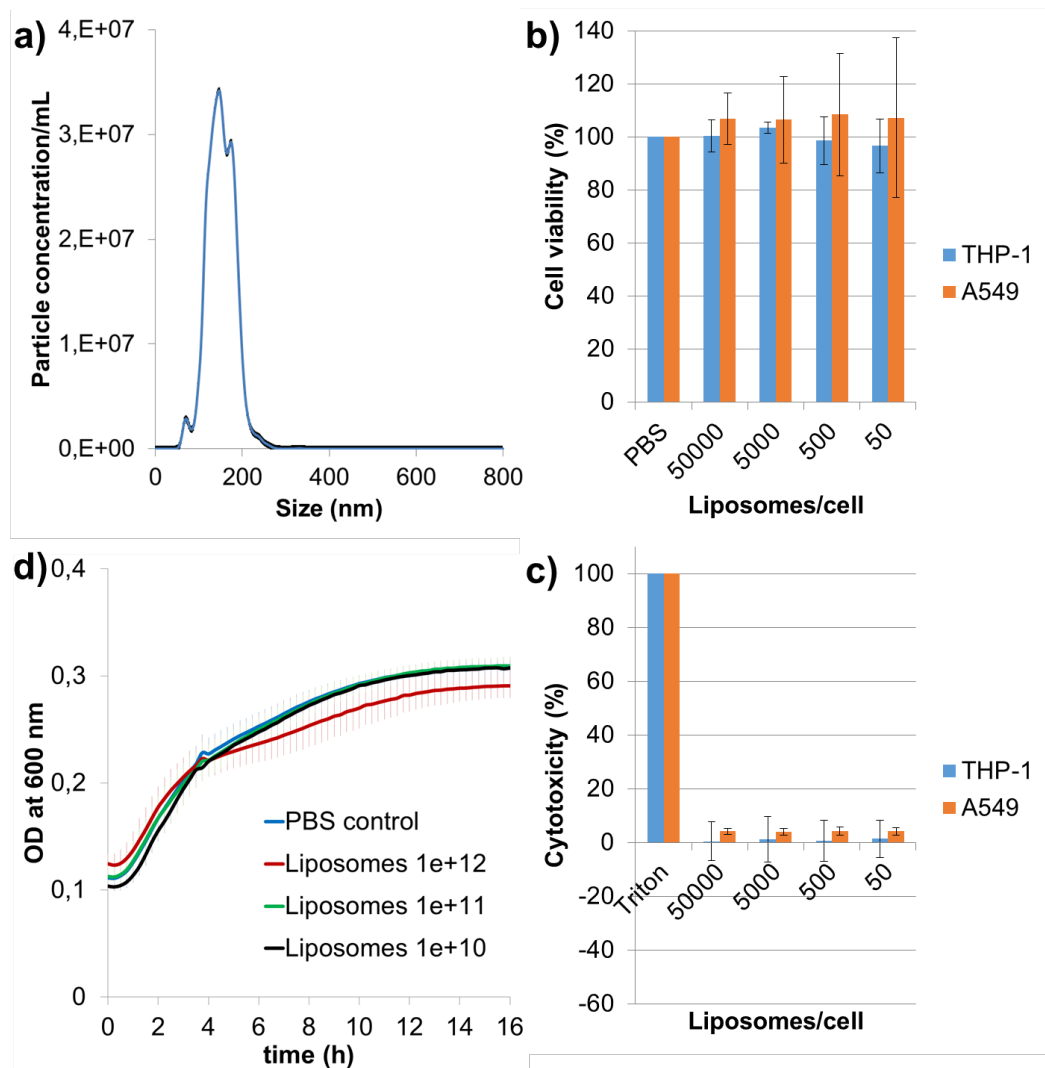


**Figure S3. Complementary liposome control experiments.** **a)** Size distribution of liposomes (1,2-dimyristoyl-sn-glycero-3-phosphorylcholine (DMPC) and dipalmitoyl phosphatidylcholine (DPPC) at a ratio of 2:3 mol%) measured by NTA (representative sample). **b)** Cell viability of liposomes when incubated for 24 h with stimulated dTHP-1-1 macrophage cells and A549 epithelial cells, and **c)** lactate-dehydrogenase cytotoxicity assay of liposomes incubated for 24 h with dTHP-1-1 and A549 cells. Mean  $\pm$  SD,  $n = 3-4$ . **c)** Growth curve of *E. coli* DH5-alpha incubated with different concentration of liposomes or PBS (control). Mean  $\pm$  SD,  $n = 3$

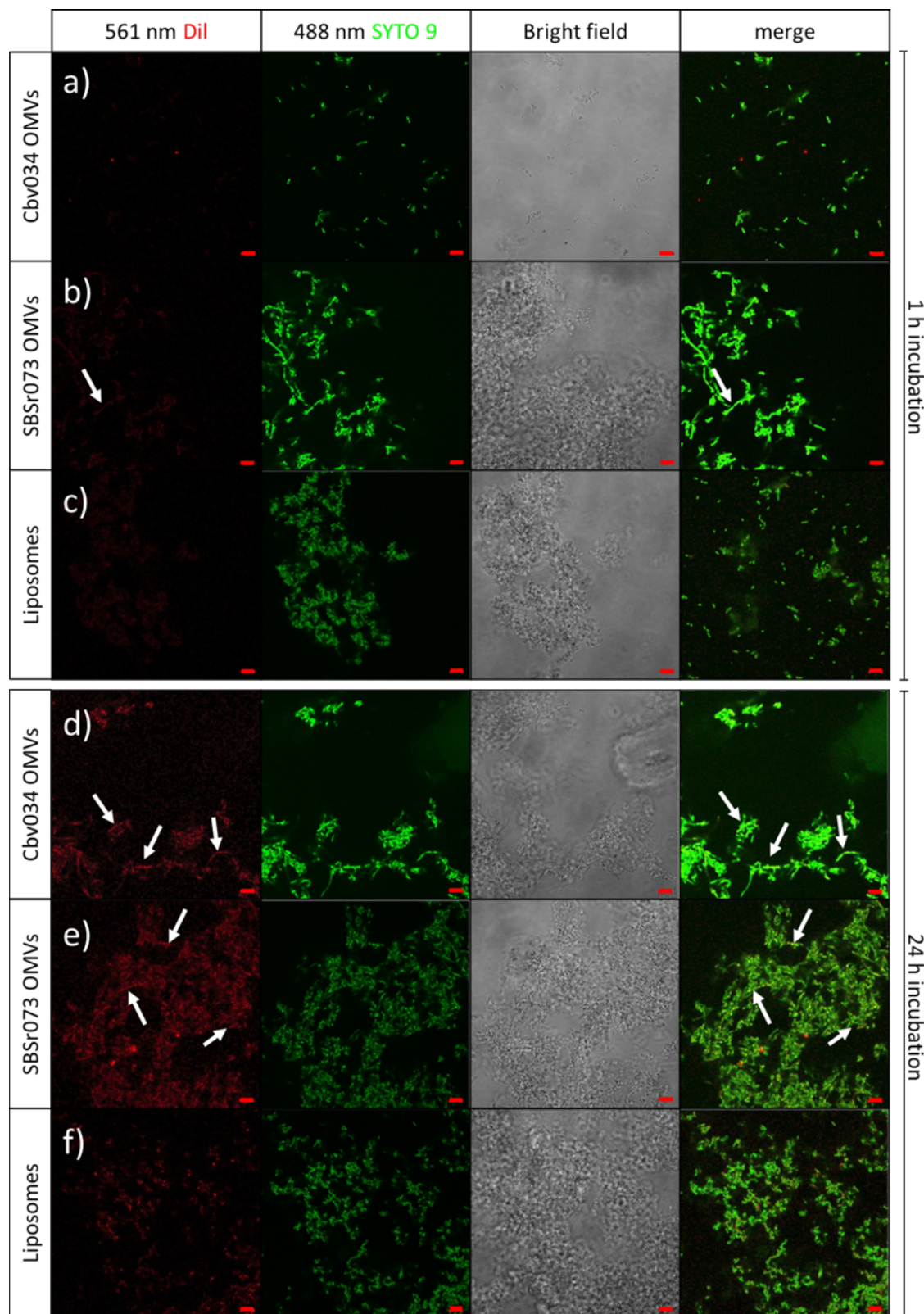


**Figure S4. Complementary confocal fluorescence images of *E. coli* incubated with OMVs.** 1 h incubation of *E. coli* DH5-alpha with a) fluorescently-labelled Cbv34 OMVs, b) SBSr073 OMVs, and c) liposomes. 24 h incubation of *E. coli* DH5-alpha with d) fluorescently-labelled Cbv34 OMVs, e) SBSr073 OMVs, and f) liposomes.

Images were taken using the same settings at 561 nm laser (red colour) and 488 nm laser (green colour). For visualisation, bacteria were stained with SYTO 9. Scale bars are 5  $\mu\text{m}$ . Measurement settings and image analysis is similar for all images.

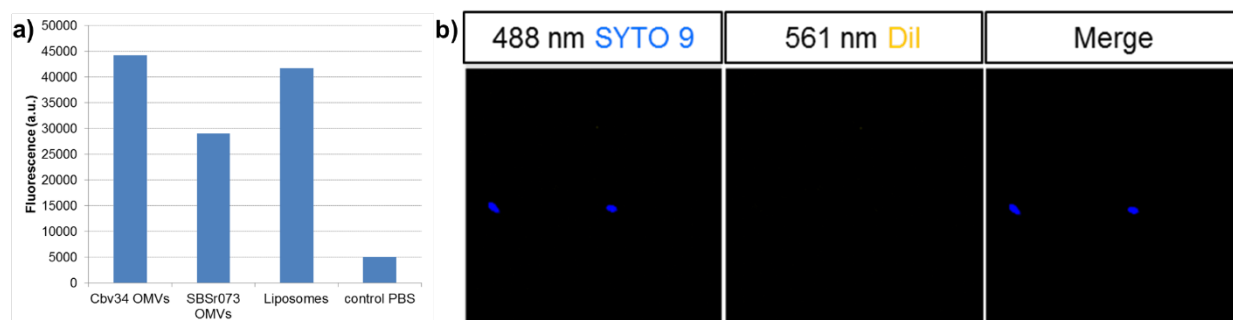


**Figure S5. Mean fluorescence of labelled OMVs and liposomes used for *in vitro* imaging and control confocal fluorescence microscopy images.** a) Detection of fluorescence upon Dil labelling (ex 490nm/em 570 nm) in the most abundant SEC fractions of Cbv34 OMVs ( $10^{11}$  particles/mL), SBSr073 OMVs ( $10^{10}$  particles/mL), and liposomes ( $10^{11}$  particles/mL). Representative measurement using PBS as control. b) Representative confocal fluorescence images of *E. coli* incubated for 24 h with Dil dye alone and in absence of OMVs. All measurement and image analysis settings are similar to those in the main Figure 3.

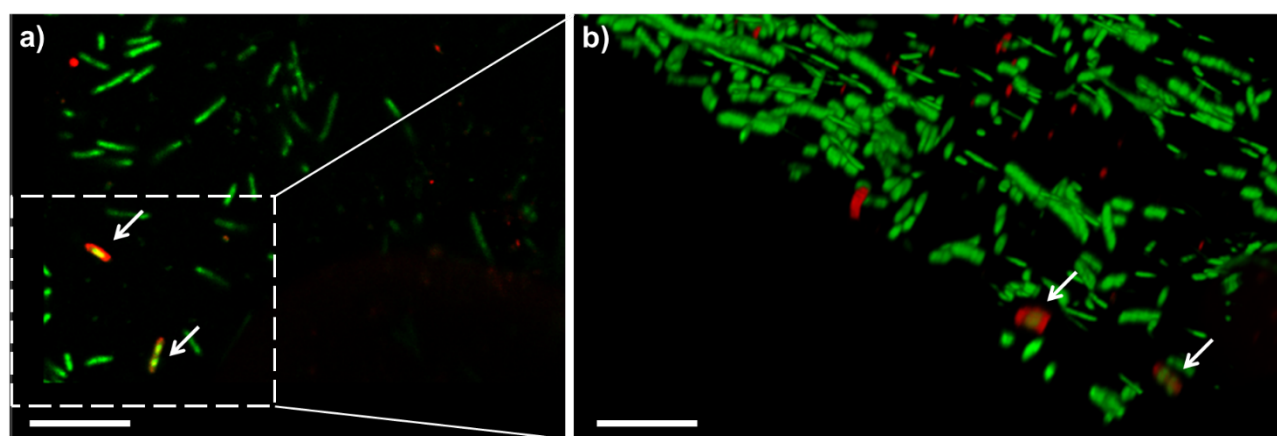


**Figure S6. Complementary z-stack confocal fluorescence images of *E. coli* incubated with OMVs.** 24 h incubation of *E. coli* DH5-alpha with Dil-labelled Cbv34 OMVs (red). **a)** Top view confocal image, **b)** 3D-image of marked rectangle in a) using z-stack mode. Images were taken using the same settings at 561 nm laser (red colour)

and 488 nm laser (green colour). For visualisation, bacteria were stained with SYTO 9 (in green).

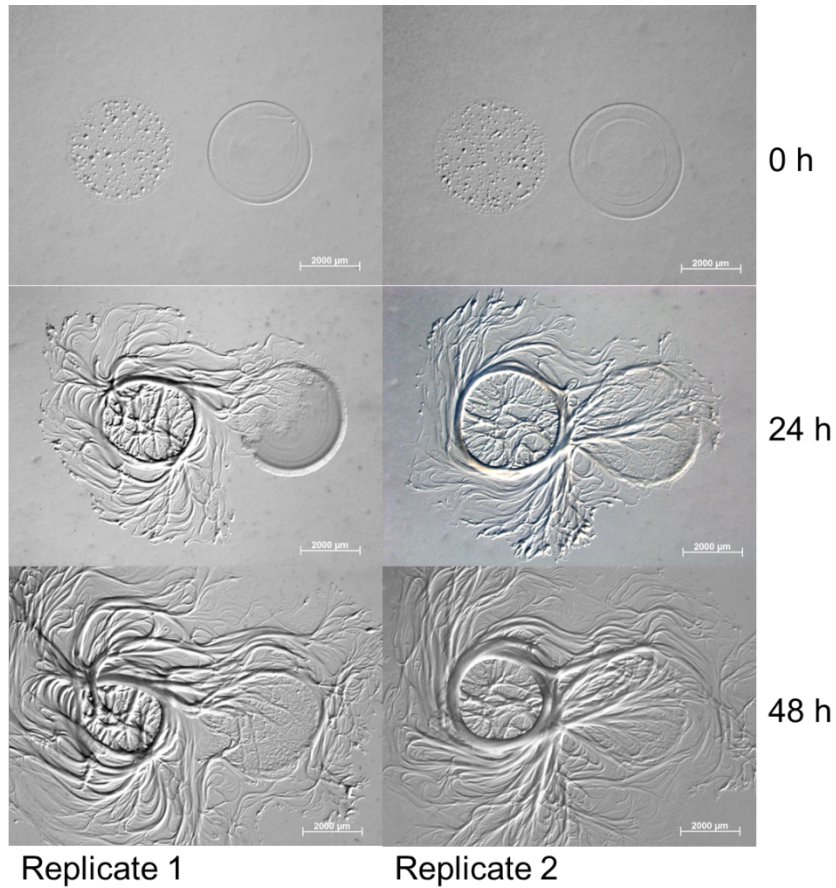


**Figure S7. Predatory behaviour of Cbv34 myxobacteria on *E. coli*.** Myxobacteria (left) and *E. coli* (right, DSM 1116) were seeded on VY/2 agar and both incubated for up to 48 h at 30 °C. VY/2 agar contains baker's yeast 5.00 g, CaCl<sub>2</sub> x 2 H<sub>2</sub>O 1.36 g, Vitamin B12 0.50 mg, Agar 15.00 g and distilled water 1000.0 mL (DSMZ recipe).

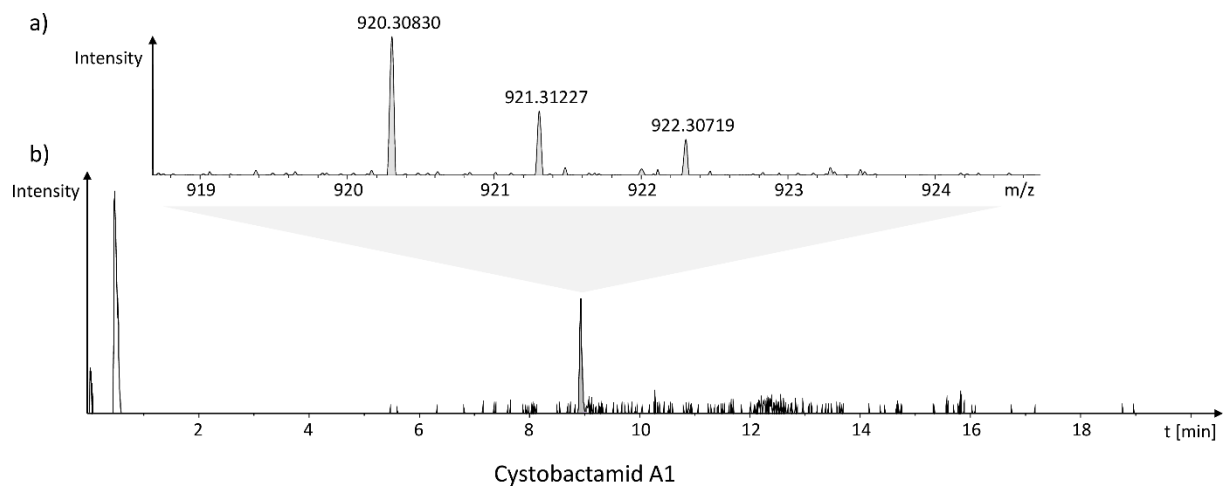


**Figure S8. LC-MS based identification of Cystobactamid 919-1 in the methanolic crude extract of Cbv34 OMVs.** UHPLC-HRMS chromatogram acquired on the Dionex Ultimate 3000 RSLC coupled to a Bruker maXis 4G qTOF mass spectrometer. 1 mL of methanolic OMV extract is separated, **b)** depicts the EIC at  $920.309 \pm 0.02$  Da across the chromatogram visualising the Cystobactamid 919-1 peak, **a)** depicts the magnified mass spectrum at maximum intensity for the Cystobactamid 919-1 peak.

Mass spectra were acquired in centroid mode ranging from 150 – 2500 m/z at a 2 Hz full scan rate. Mass spectrometry source parameters were set to 500V as end plate offset; 4000V as capillary voltage; nebuliser gas pressure 1 bar; dry gas flow of 5 l/min and a dry temperature of 200 °C. Ion transfer and quadrupole settings are set to Funnel RF 350 Vpp; Multipole RF 400 Vpp as transfer settings and Ion energy of 5eV as well as a low mass cut of 300 m/z as Quadrupole settings. Collision cell was set to 5.0 eV and pre pulse storage time is set to 5  $\mu$ s. Spectra acquisition rate was set to 2Hz. Calibration is done automatically before every LC-MS run by injection of sodium formiate and calibration on the sodium formiate clusters forming in the ESI source. All MS analyses were acquired in the presence of the lock masses  $C_{12}H_{19}F_{12}N_3O_6P_3$ ;  $C_{18}H_{19}O_6N_3P_3F_2$  and  $C_{24}H_{19}F_{36}N_3O_6P_3$  which generate the  $[M+H]^+$  ions of 622.028960; 922.009798 and 1221.990638. LCMS data are annotated using the in-house *MXbase* myxobacterial metabolome data at Helmholtz Institute for Pharmaceutical Research Saarland by automated comparison of retention time, exact mass and isotope pattern accuracy using Bruker Daltonics Target analysis 1.3.

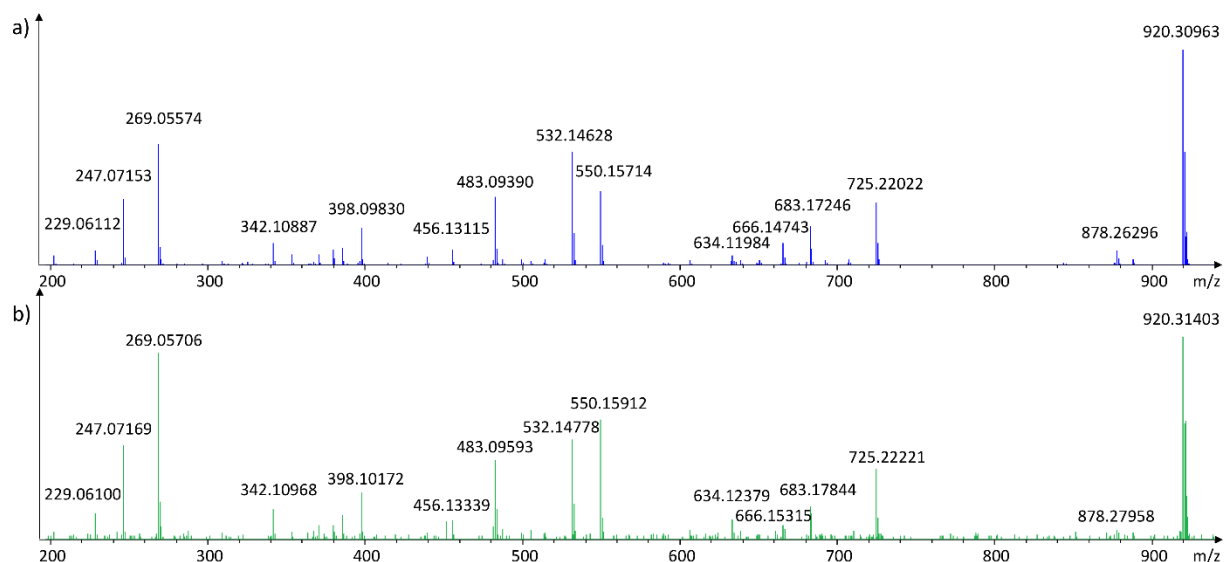


**Figure S9. Comparison of the MS<sup>2</sup> spectrum of Cystobactamid 919-1 from Cbv34 OMVs to the MS<sup>2</sup> spectrum of Cystobactamid 919-1 reference standard.** HRMS<sup>2</sup> spectrum of a) cystobactamid 919-1 standard and b) cystobactamid 919-1 in Cbv34 OMVs on the Bruker maXis 4G qTOF spectrometer to verify the identified peak as cystobactamid 919-1. Identified fragments show excellent agreement to the reference substance. LC and MS conditions for scheduled precursor list (SPL) guided MS<sup>2</sup> data acquisitions were kept constant according to section standardised UHPLC-MS conditions. MS<sup>2</sup> data acquisition parameters were set to exclusively fragment SPL entries. SPL entries were edited manually to selectively target the precursor mass of cystobactamid 919-1. SPL tolerance parameters for precursor ion selection were set to 0.2 minutes and 0.05 m/z in the SPL MS/MS method. CID Energy is ramped from 35 eV for 500 m/z to 45 eV for 1000 m/z and 60 eV for 2000 m/z. MS full scan acquisition rate was set to 2Hz and MS/MS spectra acquisition rates were ramped from 1 to 4 Hz for precursor ion intensities of 10 kcts to 1000 kcts.

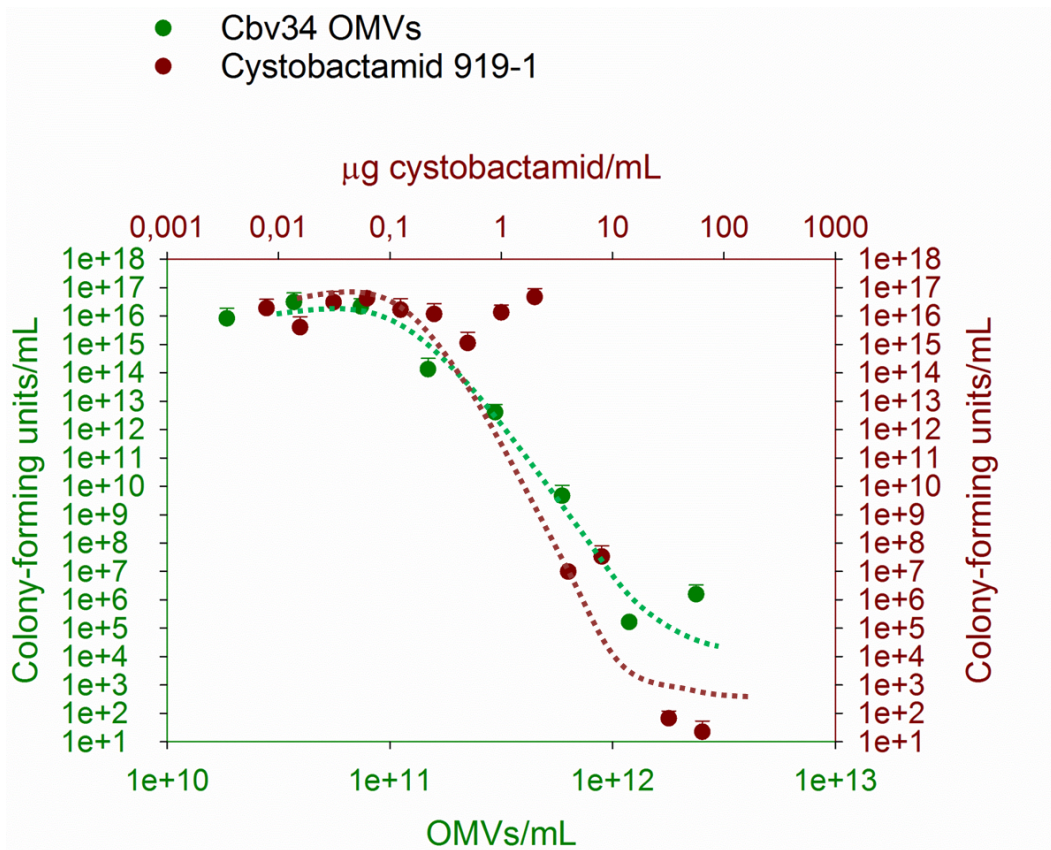


**Figure S10. Antimicrobial activity of Cbv34 OMVs compared to free cystobactamid.** OMVs from Cbv34 and cystobactamid 919-1 were incubated with *E. coli* at different concentrations. Colony-forming units were counted for both samples. Mean  $\pm$  SD,  $n = 3$ .

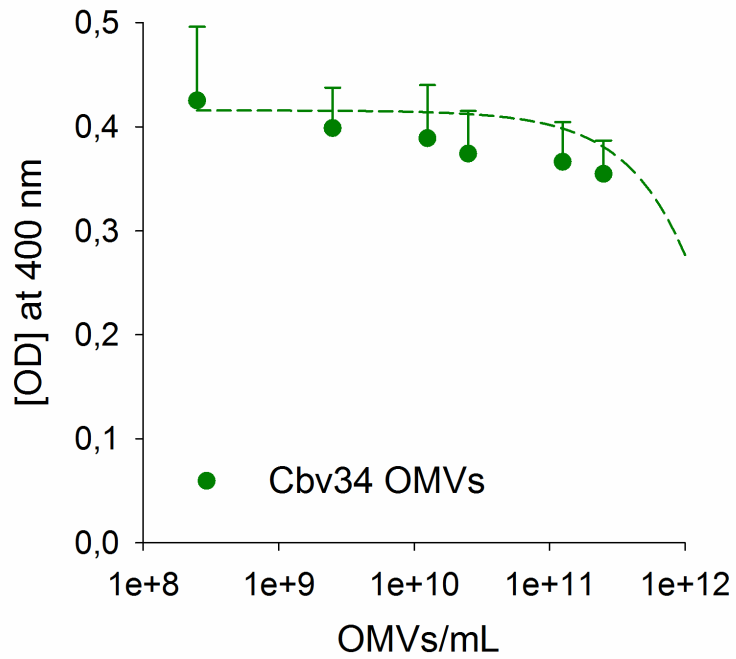


**Figure S11. Dose response of Cbv34 OMVs obtained from lower passage numbers.** Cbv34 myxobacteria were brought into culture from cryo stock and used during passages 1-4. During these lower passage numbers, OMVs isolated from culture supernatant showed a lower antimicrobial activity as seen from the dose response curve. The curve was obtained by incubating increasing concentrations of low passage Cbv34 OMVs with *E. coli*. Mean,  $n = 3$ .

### 6.3 PAPER 3: “Myxobacteria-derived outer membrane vesicles: potential applicability against intracellular infections”

**Adriely Goes**<sup>1,2</sup>, Philipp Lapuhs<sup>1,2</sup>, Thomas Kuhn<sup>1,2</sup>, Eilien Schulz<sup>1,2</sup>, Robert Richter<sup>2,3</sup>, Fabian Panter<sup>4</sup>, Charlotte Dahlem<sup>5</sup>, Marcus Koch<sup>6</sup>, Ronald Garcia<sup>4</sup>, Alexandra K. Kiemer<sup>5</sup>, Rolf Müller<sup>2,4,7</sup> and Gregor Fuhrmann<sup>1,2</sup>

<sup>1</sup> Helmholtz Centre for Infection Research (HZI), Biogenic Nanotherapeutics Group (BION), Helmholtz Institute for Pharmaceutical Research Saarland (HIPS), Campus E8.1, 66123 Saarbrücken, Germany; adriely.goes@helmholtz-hips.de (A.G.); philipp.lapuhs@gmail.com (P.L.); thomas.kuhn@helmholtz-hips.de (T.K.); eilien.schulz@helmholtz-hips.de (E.S.)

<sup>2</sup> Department of Pharmacy, Saarland University, Campus Building E8.1, 66123 Saarbrücken, Germany; Robert.Richter@helmholtz-hips.de (R.R.); rolf.mueller@helmholtz-hips.de (R.M.)

<sup>3</sup> Helmholtz Centre for Infection Research (HZI), Department of Drug Delivery (DDEL), Helmholtz Institute for Pharmaceutical Research Saarland (HIPS), Campus E8.1, 66123 Saarbrücken, Germany

<sup>4</sup> Helmholtz Centre for Infection Research (HZI), Department of Microbial Natural Products (MINS), Helmholtz Institute for Pharmaceutical Research Saarland (HIPS), Campus E8.1, 66123 Saarbrücken, Germany; fabian.panter@helmholtz-hips.de (F.P.); ronald.garcia@helmholtz-hips.de (R.G.)

<sup>5</sup> Department of Pharmacy, Pharmaceutical Biology, Saarland University, 66123 Saarbrücken, Germany; charlotte.dahlem@uni-saarland.de (C.D.); pharm.bio.kiemer@mx.uni-saarland.de (A.K.K.)

<sup>6</sup> INM-Leibniz Institute for New Materials, Campus D2 2, 66123 Saarbrücken, Germany; marcus.koch@leibniz-inm.de

<sup>7</sup> German Center for Infection Research (DZIF), 38124 Braunschweig, Germany

Accepted: 8 January 2020

Cells 2020, 9, 194

DOI: 10.3390/cells9010194

Article

# Myxobacteria-Derived Outer Membrane Vesicles: Potential Applicability Against Intracellular Infections

Adriely Goes <sup>1,2</sup>, Philipp Lapuhs <sup>1,2</sup>, Thomas Kuhn <sup>1,2</sup>, Eilien Schulz <sup>1,2</sup>, Robert Richter <sup>2,3</sup>, Fabian Panter <sup>4</sup>, Charlotte Dahlem <sup>5</sup>, Marcus Koch <sup>6</sup>, Ronald Garcia <sup>4</sup>, Alexandra K. Kiemer <sup>5</sup>, Rolf Müller <sup>2,4,7</sup> and Gregor Fuhrmann <sup>1,2,\*</sup>

<sup>1</sup> Helmholtz Centre for Infection Research (HZI), Biogenic Nanotherapeutics Group (BION), Helmholtz Institute for Pharmaceutical Research Saarland (HIPS), Campus E8.1, 66123 Saarbrücken, Germany; adriely.goes@helmholtz-hips.de (A.G.); philipp.lapuhs@gmail.com (P.L.); thomas.kuhn@helmholtz-hips.de (T.K.); eilien.schulz@helmholtz-hips.de (E.S.)

<sup>2</sup> Department of Pharmacy, Saarland University, Campus Building E8.1, 66123 Saarbrücken, Germany; Robert.Richter@helmholtz-hips.de (R.R.); rolf.mueller@helmholtz-hips.de (R.M.)

<sup>3</sup> Helmholtz Centre for Infection Research (HZI), Department of Drug Delivery (DDEL), Helmholtz Institute for Pharmaceutical Research Saarland (HIPS), Campus E8.1, 66123 Saarbrücken, Germany

<sup>4</sup> Helmholtz Centre for Infection Research (HZI), Department of Microbial Natural Products (MINS), Helmholtz Institute for Pharmaceutical Research Saarland (HIPS), Campus E8.1, 66123 Saarbrücken, Germany; fabian.panter@helmholtz-hips.de (F.P.); ronald.garcia@helmholtz-hips.de (R.G.)

<sup>5</sup> Department of Pharmacy, Pharmaceutical Biology, Saarland University, 66123 Saarbrücken, Germany; charlotte.dahlem@uni-saarland.de (C.D.); pharm.bio.kiemer@mx.uni-saarland.de (A.K.K.)

<sup>6</sup> INM-Leibniz Institute for New Materials, Campus D2 2, 66123 Saarbrücken, Germany; marcus.koch@leibniz-inm.de

<sup>7</sup> German Center for Infection Research (DZIF), 38124 Braunschweig, Germany

\* Correspondence: gregor.fuhrmann@helmholtz-hips.de; Tel.: +49-68-198-806 (ext. 1500)

Received: 6 December 2019; Accepted: 8 January 2020; Published: 12 January 2020



**Abstract:** In 2019, it was estimated that 2.5 million people die from lower tract respiratory infections annually. One of the main causes of these infections is *Staphylococcus aureus*, a bacterium that can invade and survive within mammalian cells. *S. aureus* intracellular infections are difficult to treat because several classes of antibiotics are unable to permeate through the cell wall and reach the pathogen. This condition increases the need for new therapeutic avenues, able to deliver antibiotics efficiently. In this work, we obtained outer membrane vesicles (OMVs) derived from the myxobacteria *Cystobacter velatus* strain Cbv34 and *Cystobacter ferrugineus* strain Cbfe23, that are naturally antimicrobial, to target intracellular infections, and investigated how they can affect the viability of epithelial and macrophage cell lines. We evaluated by cytometric bead array whether they induce the expression of proinflammatory cytokines in blood immune cells. Using confocal laser scanning microscopy and flow cytometry, we also investigated their interaction and uptake into mammalian cells. Finally, we studied the effect of OMVs on planktonic and intracellular *S. aureus*. We found that while Cbv34 OMVs were not cytotoxic to cells at any concentration tested, Cbfe23 OMVs affected the viability of macrophages, leading to a 50% decrease at a concentration of 125,000 OMVs/cell. We observed only little to moderate stimulation of release of TNF-alpha, IL-8, IL-6 and IL-1beta by both OMVs. Cbfe23 OMVs have better interaction with the cells than Cbv34 OMVs, being taken up faster by them, but both seem to remain mostly on the cell surface after 24 h of incubation. This, however, did not impair their bacteriostatic activity against intracellular *S. aureus*. In this study, we provide an important basis for implementing OMVs in the treatment of intracellular infections.

**Keywords:** extracellular vesicles; antimicrobial resistance; *Staphylococcus aureus*; intracellular infection; outer membrane vesicles; biogenic drug carriers

## 1. Introduction

Pulmonary infections represent a serious health risk for today's society. The Global Burden of Disease Study 2016 has estimated that lower respiratory infections are one of the leading causes of death worldwide, especially in children aged five years and younger [1,2]. Lung infection is also a frequent complication for patients with cystic fibrosis (CF), an inherited, systemic disorder caused by a mutation in the cystic fibrosis trans-membrane regulator channel [3,4]. CF lung disease is characterized by the accumulation of a thick mucus in the airway, which favors lung inflammation and persistent, chronic bacterial infection. One of the main pathogens causing lung infections in CF patients is *Staphylococcus aureus* (*S. aureus*) [5,6]. Besides being able to form biofilms, it is known that *S. aureus* can also invade professional and non-professional phagocytes and is able to survive intracellularly by escaping the endosomal pathway into the cytoplasm [7–10].

The antibiotics currently available on the market are not optimal for treating intracellular infections, as most of them need higher concentrations and a longer therapy time to induce a positive effect [11]. Generally, free antibiotics (e.g., aminoglycosides) are unable to eradicate intracellular infections due to their hydrophilic characteristics and high polarity, which prevent their permeation into mammalian cells [12–17]. To address this problem, increased efforts have been made towards improved drug delivery using nanotechnology, surface modification, biomimetic and biogenic carriers to overcome this barrier [18–21]. Carriers such as liposomes have been successful at delivering antibiotics to biofilms and eradicating them [22].

Myxobacteria are a group of Gram-negative bacteria that are abundant in soil. Many of these bacteria show predatory behavior [23], and interact, move and prey by forming coordinated swarms [24]. They belong to the class Delta Proteobacteria, phylum Proteobacteria. Myxobacteria are potent producers of antimicrobial compounds [25–28] and they are non-pathogenic to humans. Outer membrane vesicles (OMVs) are nanoparticles shed from the outer membrane of Gram-negative bacteria [29–31]. OMVs derived from myxobacteria have been shown to be involved in intercolony communication but also as predatory weapons against other bacteria [32]. We recently reported on myxobacterial OMVs with inherent antimicrobial properties due to their cystobactamid cargo [33]. Cystobactamids are topoisomerase inhibitors that have potent antibacterial activity [34]. However, the antimicrobial activity of myxobacterial OMVs has only been shown against the planktonic model bacterium (*Escherichia coli* strain DH5-alpha), which is not clinically relevant. Here, we expand the evaluation of these OMVs to clinically important *S. aureus* pathogens. For potential OMV translation, it is necessary to biotechnologically obtain them at large amounts. Myxobacterial cultures are suitable for this purpose, because they can be increased to several liters, which facilitates the large-scale isolation of their OMVs [34].

In this study, we explore the myxobacterial strains *Cystobacter velatus* Cbv34 and *Cystobacter ferrugineus* Cbfe23 for the production of natural antibacterial OMVs and analyze their potential for uptake by mammalian cells and the eradication of intracellular *S. aureus*. Our results show that both Cbv34 and Cbfe23 OMVs are efficiently taken up into macrophages and epithelial cells without affecting their viability. Importantly, they presented an antibacterial effect against intracellular *S. aureus*.

## 2. Materials and Methods

### 2.1. Myxobacterial Culture

The myxobacterial strains Cbv34 (*Cystobacter velatus*) and Cbfe23 (*Cystobacter ferrugineus*) were cultured in 100 mL M-Medium (*w/v*, 1.0% phytone, 1.0% maltose, 0.1% CaCl<sub>2</sub>, 0.1% MgSO<sub>4</sub>, 50 mM HEPES, pH adjusted to 7.2 with KOH) at 30 °C and 180 rpm. Upon reaching the stationary phase at 6–7 days, 50 mL of the culture was removed for OMV isolation. The remaining volume was used as

an inoculum for the next passage of the myxobacterial culture. Growth curves of the cultures were established as described in a previous study [33].

## 2.2. Isolation and Purification of Outer Membrane Vesicles

In order to obtain potent OMVs with a high yield, the myxobacteria were cultured for at least three passages prior to performing the isolation. Fifty milliliters of the cultures were used and centrifuged at  $9500 \times g$  for 10 min at 4 °C. The supernatant was transferred to a new falcon tube and centrifuged once again at  $9500 \times g$ , for 15 min at 4 °C. Thirty milliliters of the resulting supernatant was added into an ultracentrifugation tube and pelleted at  $100,000 \times g$  for 2 h at 4 °C using a rotor type SW 32 Ti (Beckman Coulter). The supernatant was removed, and the pellet was dispersed in 300  $\mu$ L phosphate buffered saline (PBS, Gibco PBS tablets without calcium, magnesium and phenol red) (Sigma-Aldrich; Co., St. Louis, MO, USA) filtered with 0.2  $\mu$ m mixed cellulose ester filters (Whatman, GE Healthcare UK Limited, Little Chalfont, UK). In order to remove the free protein present in the pellet, a size exclusion chromatography (SEC) was performed. The pellet was added to a 60 mL column filled with 35–40 mL of Sepharose CL-2B (GE Healthcare Bio-Sciences AB, Uppsala, Sweden) in PBS. One milliliter fractions of OMVs in PBS were collected into polypropylene (PP) tubes (Axygen, Corning Incorporated, Reynosa, Mexico) next to a Bunsen burner, to obtain aseptic conditions. The fractions were kept at 4 °C for up to one month. Prior to infection, experiments and measurements of particle parameters, the fractions were filtered with Puredisc 25 AS (GE Healthcare UK Limited, Little Chalfont, UK) to assure sterility.

## 2.3. Liquid-Chromatography Coupled Mass Spectrometry

### 2.3.1. OMV Preparation

OMV pellets were resuspended in 500  $\mu$ L of particle-free PBS and lyophilized for 16 h. The dried pellet was mixed with 300  $\mu$ L of MeOH and vortexed for 1–2 min. The OMV extract was centrifuged to remove debris. Then, the supernatant was transferred to a vial for LC-MS analysis.

### 2.3.2. UHPLC MS Conditions

UPLC-hrMS analysis was performed on a Dionex (Germering, Germany) Ultimate 3000 RSLC system using a Waters (Eschborn, Germany) BEH C18 column (50  $\times$  2.1 mm, 1.7  $\mu$ m) equipped with a Waters VanGuard BEH C18 1.7  $\mu$ m guard column. Separation of 1  $\mu$ L sample was achieved by a linear gradient from (A) H<sub>2</sub>O + 0.1% FA to (B) ACN + 0.1% FA at a flow rate of 600  $\mu$ L/min and a column temperature of 45 °C. Gradient conditions were as follows: 0–0.5 min, 5% B; 0.5–18.5 min, 5%–95% B; 18.5–20.5 min, 95% B; 20.5–21 min, 95%–5% B; 21–22.5 min, 5% B. UV spectra were recorded by a DAD in the range 200–600 nm. The LC flow was split to 75  $\mu$ L/min before entering the Bruker Daltonics maXis 4G hrToF mass spectrometer (Bremen, Germany) using the Apollo II ESI source. Mass spectra were acquired in centroid mode ranging from 150–2500  $m/z$  (mass/charge) at a 2 Hz full scan rate. Mass spectrometry source parameters are set to 500 V as end plate offset; 4000 V as capillary voltage; nebulizer gas pressure 1 bar; dry gas flow of 5 L/min and a dry temperature of 200 °C. Ion transfer and quadrupole settings are set to Funnel RF 350 Vpp; Multipole RF 400 Vpp as transfer settings and Ion energy of 5 eV as well as a low mass cut of 300  $m/z$  as Quadrupole settings. Collision cell is set to 5.0 eV and pre pulse storage time is set to 5  $\mu$ s. Spectra acquisition rate is set to 2 Hz. Calibration is done automatically before every LC-MS run by the injection of sodium formate and calibration on the sodium formate clusters forming in the ESI source. All MS analyses are acquired in the presence of the lock masses C<sub>12</sub>H<sub>19</sub>F<sub>12</sub>N<sub>3</sub>O<sub>6</sub>P<sub>3</sub>; C<sub>18</sub>H<sub>19</sub>O<sub>6</sub>N<sub>3</sub>P<sub>3</sub>F<sub>2</sub> and C<sub>24</sub>H<sub>19</sub>F<sub>36</sub>N<sub>3</sub>O<sub>6</sub>P<sub>3</sub>, which generate the [M + H]<sup>+</sup> ions of 622.03; 922.01 and 1221.10.

### 2.3.3. LC-MS Data Bucketing and Annotation Using Metaboscape Software

Acquired LC-MS data are bucketed by Bruker Metaboscape 4.0 SR1 using the qTOF data optimized TReX 3D algorithm. Bucketed analyses are checked for library hits against our in-house database of myxobacterial natural products called myxobase. Library hits are retained if they show a retention time deviation under the described parameters of less than 0.2 min,  $m/z$  value deviation of less than 5 ppm and isotope pattern ratio congruence lower than 30 milliSigma.

### 2.3.4. Conditions for MS<sup>2</sup> Analysis

LC and MS conditions for automatic precursor selection MS<sup>2</sup> data acquisitions remain as described in section-standardized UHPLC-MS conditions. CID Energy is ramped from 35 eV for 500  $m/z$  to 45 eV for 1000  $m/z$  and 60 eV for 2000  $m/z$ . MS full scan acquisition rate was set to 2 Hz and MS/MS spectra acquisition rates were ramped from 1 to 4 Hz for precursor ion intensities of 10 to 1000 kcts.

### 2.3.5. GNPS Clustering Parameters

MS<sup>2</sup> data of the vesicle extracts were uploaded to the Global Natural Product Social Molecular Networking (GNPS) server at University of California San Diego [35]. A molecular network was created, using a parent mass tolerance of 0.05 Da and a fragment ion tolerance of 0.1 Da. Cosine score of edges considered to network was set to extend 0.7 and the minimum matched fragment peaks were set to 5. The clustered dataset was visualized using Cytoscape 3.7.2 (Cytoscape Consortium, UCSD San Diego, USA).

## 2.4. Cryogenic Electron Microscopy

Cryogenic transmission electron microscopy (cryo-TEM) was performed on OMVs pellets after ultracentrifugation and purified fractions as previously described [33]. Three to four microliters of the sample were dropped onto a holey carbon grid (type S147-4, Plano, Wetzlar, Germany) and plotted for 2 s before plunging into liquid ethane at  $T = -165$  °C using a Gatan (Pleasanton, CA, USA) CP3 cryo plunger. The sample was transferred under liquid nitrogen to a Gatan model 914 cryo-TEM sample holder and analyzed at  $T = -173$  °C by low-dose TEM bright-field imaging using a JEOL (Tokyo, Japan) JEM-2100 LaB6 at 200 kV accelerating voltage. Images with  $1024 \times 1024$  pixels were acquired using a Gatan Orius SC1000 CCD camera at 2 s binning and 4 s imaging time.

## 2.5. Cell Culture

The murine macrophage cell line RAW 264.7 was obtained from the European Collection of Authenticated Cell Cultures (ECACC) and cultured in Dulbecco's Modified Eagle Medium (DMEM) (1X) (Life Technologies Limited, Paisley, UK) supplemented with 10% ( $v/v$ ) fetal bovine serum (FBS) (Life Technologies Limited, Paisley, UK). The adenocarcinomic human alveolar basal epithelial cell line (A549) and the human acute leukemia monocyte cell line (THP-1) were both purchased from the German Collection of Microorganisms and Cell Cultures (DSMZ) and cultured in RPMI 1640 (Life Technologies Limited, Paisley, UK) supplemented with 10% ( $v/v$ ) FBS. RAW264.7 and A549 cells were split once a week, starting with  $0.2 \times 10^6$  cells/13 mL for RAW and A549. THP-1 cells were split twice a week to a seeding density of  $2-3 \times 10^6$  cells/13 mL. Mycoplasma tests were conducted regularly.

## 2.6. Cell Viability and Cytotoxicity

To assess the viability and cytotoxicity of cells upon treatment, the cells were seeded into 96-well plates at a density of 20,000 cells/well (RAW 264.7 and A549) and 100,000 cells/well (THP-1). To stimulate the THP-1 cells into macrophages, they were incubated with 30 ng/mL of phorbol 12-myristate 13-acetate (PMA). All cells were grown for 48 h. Within every set of experiments, a live-control, using cells treated with PBS (100  $\mu$ L cell medium plus 100  $\mu$ L PBS), which did not show any change in cell viability or morphology, and a dead-control, using cells treated with 1% ( $v/v$ ) Triton-X 100 (Sigma-Aldrich; Co.,

St. Louis, MO, USA) were included. During the assays, cells were cultured in FCS-free medium to prevent falsified results caused by traces of lactate dehydrogenase (LDH) contained in the medium. Cells were incubated with 100  $\mu$ L of OMV suspension in PBS at different concentrations ( $1 \times 10^{12}$ ,  $1 \times 10^{11}$  and  $1 \times 10^{10}$  OMVs/mL) and 100  $\mu$ L of cell medium for 24 h. For cytotoxicity evaluation, after an incubation time of 24 h, 100  $\mu$ L of medium were removed to be analyzed by LDH-assay, which detects the amount of LDH released into the medium upon cell death after plasma membrane damage, and mixed with 100  $\mu$ L of LDH-reagent (Roche Diagnostics GmbH, Mannheim, Germany), prepared according to the supplier's protocol. After an incubation time of 5 min at room temperature (RT), the absorbance of the solution was measured at 492 nm. For viability, PrestoBlue (Thermo Fisher Scientific, Waltham, MA, USA) reagent, which detects metabolically active cells, was diluted by 1 in 10 with the respective medium of the cells. The remaining medium in the wells was removed and 100  $\mu$ L of the diluted PrestoBlue reagent was added. After 20 min of incubation at 37 °C, fluorescence of the emerging dye was measured at an excitation of 560 nm and emission of 590 nm with a Tecan Infinity Pro 200 (Tecan, Männedorf, Switzerland). plate reader.

### 2.7. Cytokine Detection of OMV-Treated PBMCs

Peripheral blood mononuclear cells (PBMCs) were isolated by centrifugation from buffy coats, derived from three different donors obtained from the Blood Donation Center, Saarbrücken, Germany, authorized by the local ethics committee (State Medical Board of Registration, Saarland, Germany; permission no. 173/18). The cells were cultured in a 96-well plate with 100,000 cells per well in RPMI 1640 (Sigma Aldrich, St. Louis, MO, USA). Pellets of OMVs were isolated by ultracentrifugation as described above. One-hundred microliters of sterile PBS was used to resuspend the pellets. The particle concentration was determined via nanoparticle tracking analysis and the samples were diluted with PBMC medium to a final concentration of  $5 \times 10^6$  and  $5 \times 10^5$  particles per cell. After 4 h of incubation at 37 °C, cell supernatants were collected and stored at  $-80$  °C for further analysis. A BD cytometric bead array human inflammatory cytokines kit was used according to manufacturer's specification to quantify the concentrations of IL-8, IL-10, IL-6, IL-1 beta, TNF alpha and IL-12p70.

### 2.8. Antimicrobial Effect upon Storage

The stability of the OMVs' antimicrobial effect was tested by maintaining the purified fractions at 4 °C for up to four weeks before testing them against *E. coli* DH5-alpha. After treating *E. coli* with different dilutions of OMVs for 18 h at 37 °C, the optical density was measured at 600 nm with a plate reader.

### 2.9. Bacteriomimetic Liposome Preparation

Bacteriomimetic liposomes were prepared by thin film hydration, as previously reported, with minor modifications [36]. A 6% (*w/v*) phospholipid solution was prepared by dissolving 1-hexadecanoyl-2-(9Z-octadecenoyl)-sn-glycero-3-phosphoethanolamine (POPE), 1-hexadecanoyl-2-(9Z-octadecenoyl)-sn-glycero-3-phospho-(1'-rac-glycerol) (sodium salt) (POPG) and 1,1',2,2'-tetra-(9Z-octadecenoyl) cardiolipin (sodium salt) (CL) (Avanti Polar Lipids Inc., Alabaster, AL, USA) (weight ratio 70:20:10) in 5 mL of a chloroform-methanol blend (2:1) in a 250 mL round bottom flask. A Rotavapor R-205 (BÜCHI Labortechnik GmbH, Essen, Germany) was employed to remove the solvent under low pressure (60 min, 200 mbar, 135 rpm, 80 °C; 30 min, 40 mbar, 135 rpm, 80 °C). The remaining lipid film was rehydrated by adding 5 mL PBS (pH 7.4) containing 10% (*v/v*) ethanol and rotating for 60 min (70 °C, 135 rpm, atmospheric pressure). The obtained liposomes were sonicated for 60 min followed by 10 extrusion cycles at 70 °C, employing a Liposofast L-50 extruder (Avestin Europe GmbH, Mannheim, Germany).

### 2.10. Flow Cytometry and Confocal Laser Scanning Microscopy to Assess OMV Uptake into Mammalian Cells

Purified fractions of OMVs and a suspension of the bacteriomimetic liposome control were incubated with 2  $\mu$ L of 1,1'-dioctadecyl-3,3',3'-tetramethylindocarbocyanine perchlorate (DiI) (Molecular Probes Inc., Eugene, OR, USA) for 30 min at 37 °C. Afterwards, the suspensions were purified with a 10 mL column filled with Sepharose CL-2B (GE Life Science, UK) in PBS to remove any unbound dye. The fluorescence of the fractions was measured with a plate reader and the fractions with the highest concentrations were used. The DiI-stained particles were diluted 1:5 in cell culture medium with 1% penicillin and streptomycin (*v/v*) (Life Technologies Corporation, Grand Island, NY, USA) and incubated with cells at different time points.

For flow cytometry experiments, A549 and RAW 264.7 cells were seeded in 24-well plates with a density of  $2 \times 10^5$  cells per well and incubated for 48 h at 37 °C and 5% CO<sub>2</sub>.

Prior to flow cytometry (LSRFortessa, BD Bioscience, San Jose, CA, USA) analysis, the cells were washed with PBS and detached by using trypsin/EDTA (Life Technologies Limited, Paisley, UK) (A549) or a cell scraper (RAW 264.7). The cells were diluted with 2% (*v/v*) FCS in PBS and then added into FACS tubes for uptake analysis. Cells treated with PBS diluted in mammalian cell culture medium (1:5 dilution) were used as a negative control to set up the Phycoerythrin (PE) channel gate. A 10,000 live cells threshold was set to be analyzed from forward versus side scatter (FSC vs. SSC) gating. Single cells were determined by forward height versus forward area scatter (FCS-H vs. FCS-A) gating. The percentage of positive cells and the mean fluorescence intensity (MFI), which can be used to evaluate the amount of fluorescent particles taken up by the cells, were determined by analysis with the FlowJo 10.6.1 software (FlowJo LLC, Ashland, OR, USA) using the Phycoerythrin area channel (PE-A).

For confocal laser scanning microscopy (CLSM), the cells were seeded in 8-well chambers (SPL Life Sciences, Pocheon-si, Gyeonggi-do, Korea) with  $4 \times 10^4$  cells per well. After the incubation time points, the cells seeded in the 8-well chambers were washed with PBS and fixed with 3.7% (*v/v*) paraformaldehyde in PBS. The cells were stained with Alexa Fluor 488 Phalloidin (Life Technologies Corporation, Eugene, OR, USA) for 1 h and DAPI (4',6-Diamidino-2-phenylindole dihydrochloride) (Sigma-Aldrich Co., St. Louis, USA) for 30 min, washing the cells with PBS between the staining steps. The chambers were disassembled and mounted on a coverslip prior to CLSM analysis (Leica TCS SP8, Leica Microsystems, Wetzlar, Germany). The captured images were processed with the LAS X software (LAS X 1.8.013370, Leica Microsystems, Wetzlar, Germany).

### 2.11. Bacterial Culture

*Staphylococcus aureus* strain Newman and *Escherichia coli* strain DH5-alpha were obtained from the DSMZ (German Collection of Microorganisms and Cell Culture). Overnight cultures were prepared using 20 mL of brain heart infusion (BHI) broth (Becton; Dickinson and Company, Sparks, MD, USA) for *S. aureus* and Luria broth (LB) (Sigma-Aldrich; Co., St. Louis, MO, USA) for *E. coli* inoculated with a single colony. Cultures were incubated at 37 °C and 180 rpm.

### 2.12. Intracellular Infection

A549 cells were seeded ( $2 \times 10^4$  cells/well) into 96-well plates and incubated for 48 h. Ten milliliters of the bacterial overnight culture was pelleted at  $2000 \times g$ , 4 °C, for 5 min and resuspended in PBS. The bacterial suspension in PBS was then diluted to approximately  $2 \times 10^6$  colony forming units per mL (CFU/mL) in mammalian cell medium. The cells were infected for 2 h (approximately multiplicity of infection (MOI) = 100), following washing with PBS and treatment with 50  $\mu$ g/mL gentamicin for 30 min. After an additional washing step, cells were treated for 24 h with different concentrations of OMVs and controls, each diluted in cell culture medium. After 24 h incubation, the cells were lysed with HBSS (Hanks Buffered Saline Solution) (Life Technologies Limited, Paisley, UK) supplemented with 0.1% bovine serum albumin (Sigma-Aldrich Co., St. Louis, MO, USA) (*w/v*) and 0.1% Triton-X 100 (Sigma-Aldrich; Co., St. Louis, MO, USA) (*v/v*). Serial dilutions were prepared in a PBS solution

containing 0.05% Tween-20 (Sigma-Aldrich, Co., St. Louis, MO, USA) (*v/v*) and inoculated on BHI agar plates (Becton; Dickinson and Company, Sparks, MD, USA), which were then incubated at 37 °C overnight. Afterwards, the single colonies were counted and the CFU/mL values calculated.

### 2.13. Statistical Analysis

The data is displayed as mean  $\pm$  standard error of the mean (SEM). The number of independent experiments (*n*) is shown in each figure. The experiments and measurements were conducted at least in triplicates. The results were analyzed by GraphPad Prism 8.3 (GraphPad Software, San Diego, CA, USA), using Kruskal-Wallis test by ranks, followed by Dunn's multiple comparisons test. Significant *P*-values were illustrated as \* *p* < 0.05, \*\* *p* < 0.005, \*\*\* *p* < 0.0005 and \*\*\*\* *p* < 0.0001.

## 3. Results

### 3.1. OMVs are Successfully Isolated by Ultracentrifugation and SEC

The OMVs were isolated from the myxobacterial cultures (Figure S1) and successfully separated from free proteins remaining in the pellet by SEC (Figure S2), using our standardized protocol [33]. The Cbfe23 OMVs were round-shaped and electron-dense, with a well delimited membrane, shown in the cryo-TEM micrographs (Figure 1). The main fractions of OMVs were about 120–150 nm in size (Figure S3). Cbfe23 OMVs had a zeta potential of  $-5.3 \pm 0.7$  mV while Cbv34 OMVs showed a zeta potential of  $-4.7 \pm 0.6$  mV, as recently reported by our group [33]. The liposomes used as a control for the uptake studies had a zeta potential of  $-24.5 \pm 1.2$  mV.

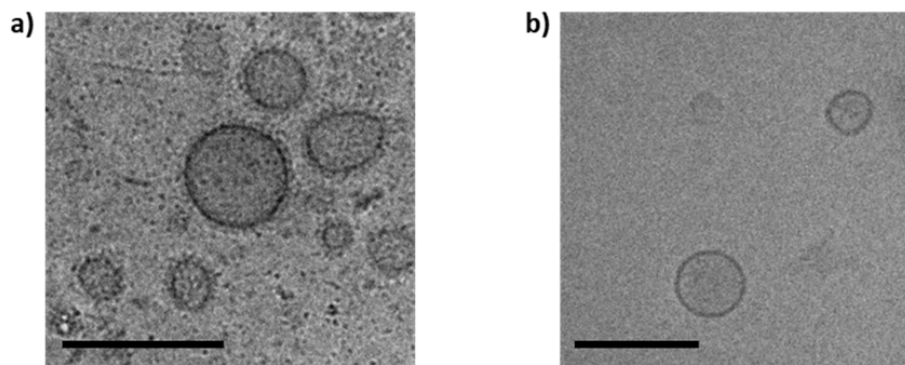


**Figure 1.** Cryo-TEM micrographs of (a) Cbfe23 outer membrane vesicles (OMVs) and (b) Cbv34 OMVs. Both OMVs are spherical and about 150 nm in size. Scale bars = 200 nm.

### 3.2. Myxobacterial OMVs Neither Affect Viability of Mammalian Cells nor Induce Cytotoxicity

The viability of alveolar epithelial cells A549, the macrophage cell line RAW 264.7 and differentiated THP-1 were investigated upon 24 h of incubation with different OMV concentrations (Figure 2). Cbv34 OMVs did not impact the viability of the cells at any concentration tested. The Cbfe23 OMVs were well tolerated until concentrations of 125,000 OMVs/cell. Very high amounts of OMVs (i.e., 125,000 OMVs/cell) decreased the macrophage cell line viability by 50% (Figure 2c,e), and by around 60% when incubated with A549 cells (Figure 2a). A comparable effect was observed for serial dilutions of cystobactamid, the natural compound previously identified in Cbv34 OMVs (Figure 2g) [33]. Cbv34 OMVs increased viability above 100% when incubated with dTHP-1 cells. We had previously observed this effect, which may be due to the nutrient bolus of lipids provided by high amounts of OMVs [33]. To further evaluate this effect, the cytotoxicity was assessed by LDH assay. As seen in Figure 2b,d,f, we did not detect any underlying cytotoxicity in all concentrations of OMVs tested and a similar result was obtained from different concentrations of cystobactamid (Figure 2h).

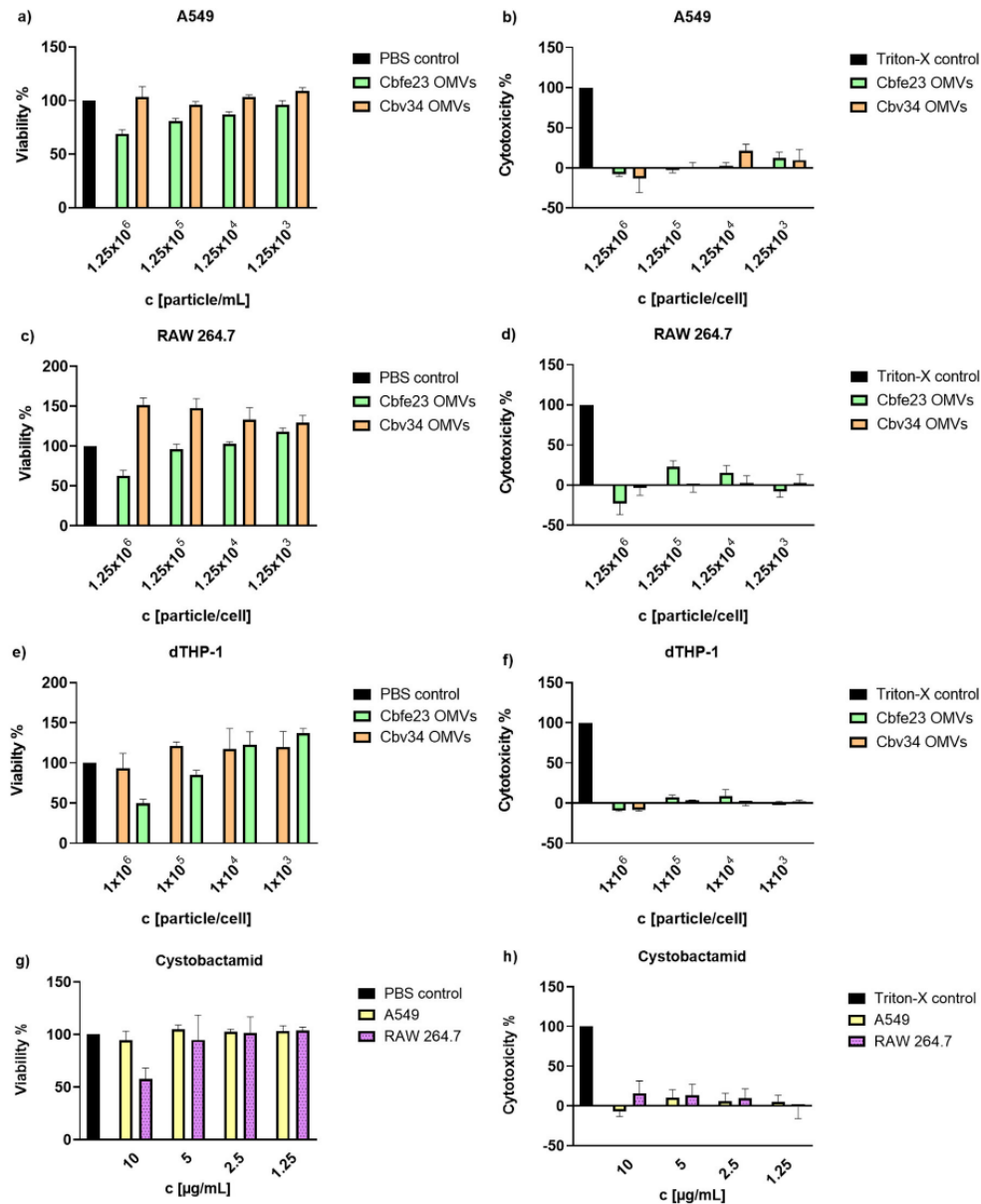


**Figure 2.** Cell viability and cytotoxicity of Cbv34 OMVs and Cbfe23 OMVs upon 24 h of treatment. Viability of (a) A549, (c) RAW 264.7 and (e) differentiated THP-1 cells, and lactate-dehydrogenase cytotoxicity of OMVs incubated with (b) A549, (d) RAW 264.7 and (f) differentiated THP-1 cells. Effect of cystobactamid on the (g) viability and (h) cytotoxicity of A549 and RAW 264.7 cells. Mean ± SEM, n = 3. No statistically significant differences were observed for any sample.

### 3.3. Proinflammatory Cytokine Detection by Flow Cytometry

To better understand the effect that OMVs may have on primary immune cells, we isolated peripheral blood mononuclear cells and incubated them with different concentrations of myxobacterial OMVs. As seen in Figure 3, in comparison to the positive control lipopolysaccharide, we only observed a tendency for the stimulation of release of TNF-alpha, IL-8, IL-6 and IL-1beta. Only at concentrations of  $1 \times 10^{13}$  particles/mL of Cbv34 OMVs, an increase in production of IL-1beta was found. The treatment with high concentrations of OMVs ( $1 \times 10^{13}$  particles/mL) seemed to affect the viability of PBMCs, as seen by light microscopy (Figure S5).

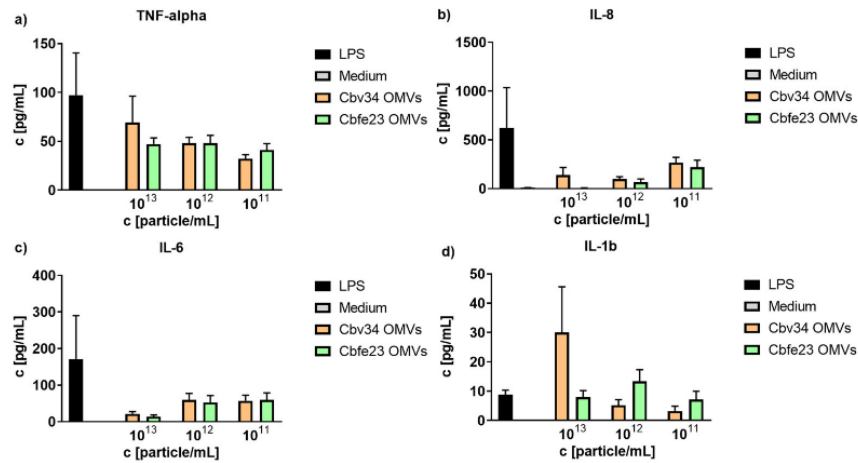


**Figure 3.** Cytokine detection of OMV-treated peripheral blood mononuclear cells (PBMCs). OMV-induced release of (a) TNF-alpha, (b) IL-8), (c) IL-6 and (d) IL 1-b at different concentrations. Mean ± SEM, n = 3.

### 3.4. Myxobacterial OMVs Are Able to Kill Planktonic *S. aureus*

OMVs had a killing effect at concentrations of approximately  $1 \times 10^{12}$  particles/mL. This correlates to a ratio of  $3 \times 10^3$  particles per CFU of *S. aureus* (Figure 4). We credit this effect to the cystobactamid compounds found in the OMV pellets (Figure S6). We were further interested to see if the antibacterial effect of myxobacterial OMVs is preserved during storage. For this, we tested whether Cbv34 OMVs are active against *E. coli* DH5-alpha after storage at 4 °C for up to 28 days based on our recent protocol [33]. Under these conditions, the antimicrobial activity of the OMVs remained potent and dose-dependent over time (Figure 5).

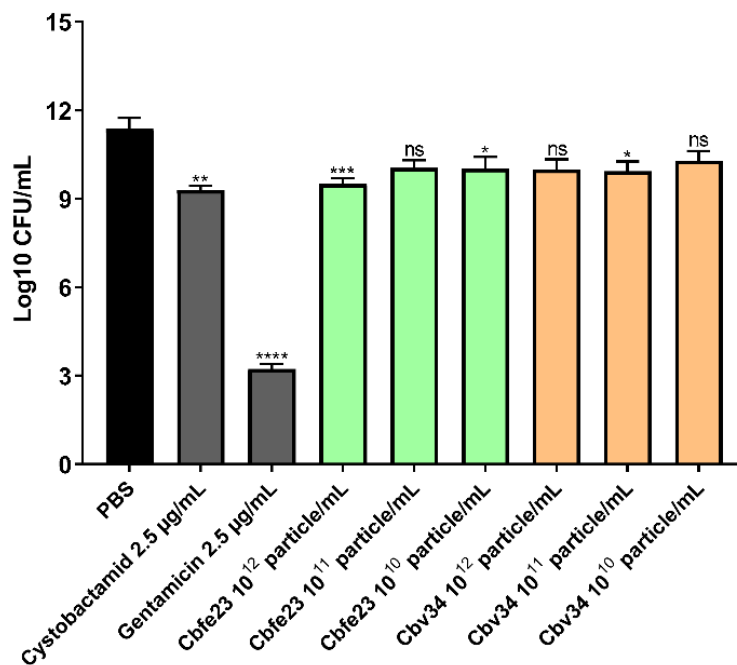


**Figure 4.** Antibacterial activity of Cbfe23 and Cbv34 OMVs against *S. aureus* strain Newman after 4 h of incubation at 37 °C. Mean ± SEM, n = 3. Significance was defined in comparison to the PBS control (black column) as \* p-value < 0.05, \*\*\* p < 0.0005, \*\*\*\* p-value < 0.0001 and ns = not significant.

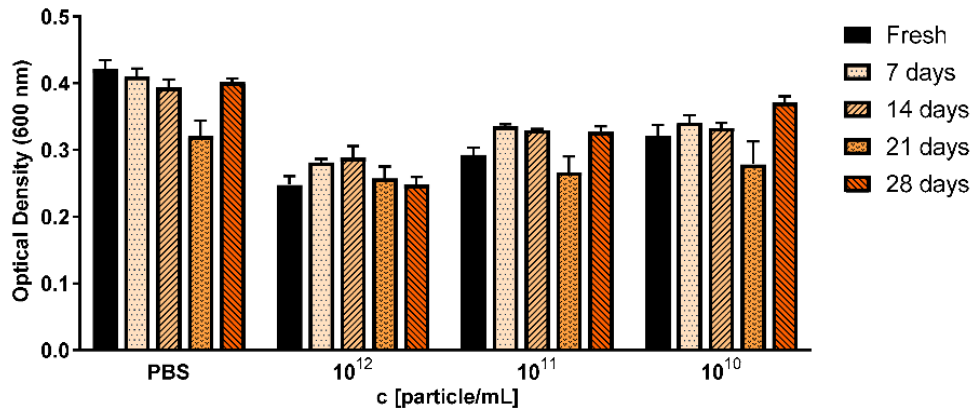


**Figure 5.** Antibacterial activity of Cbv34 OMVs against *E. coli* DH5-alpha right after isolation (fresh), and upon storage at 4 °C for 7, 14, 21 and 28 days. The treatment was done for 18 h at 37 °C. Mean  $\pm$  SEM,  $n = 3$ .

### 3.5. OMVs Are Taken Up by Mammalian Cells

The interaction with and uptake of the OMVs in A549 epithelial cells and RAW 264.7 immune cells were assessed by flow cytometry (Figures 6 and 7) and CLSM (Figure 8). In comparison to liposomes prepared from bacterial phospholipids, we observed a significantly slower uptake of OMVs in A549 cells at 4 and 24 h of incubation (Figure 6a,d). The MFI of the liposomes was significantly higher when compared to the OMVs at the 4 h time point with A549 cells (Figure 6b). The MFI difference remained high between Cbv34 OMVs and liposomes at 24 h, but it was not significant when Cbfe23 OMVs and liposomes were compared (Figure 6e). As for the uptake into RAW 264.7 cells, Cbfe23 OMVs and bacterial liposomes did not show any significant difference in terms of percentage of positive cells and MFI (Figure 7), both having a percentage of positive cells of nearly 90% at 4 h incubation time (Figure 7a). However, Cbv34 OMVs had a significantly lower percentage of positive cells when compared to the bacterial liposomes at 4 h (Figure 7a) and lower MFI at 24 h (Figure 7e). At the 24 h time point, all particles led to 100% of fluorescent cells with RAW 264.7 cells (Figure 7d). MFI remained comparable between all the samples at the 4 h time point (Figure 7b). The representative histograms of the uptake of DiI-stained particles in A549 cells (Figure 6c,f) and RAW 264.7 cells (Figure 7c,f) show the shift in the histograms of the samples compared to the untreated control (red).

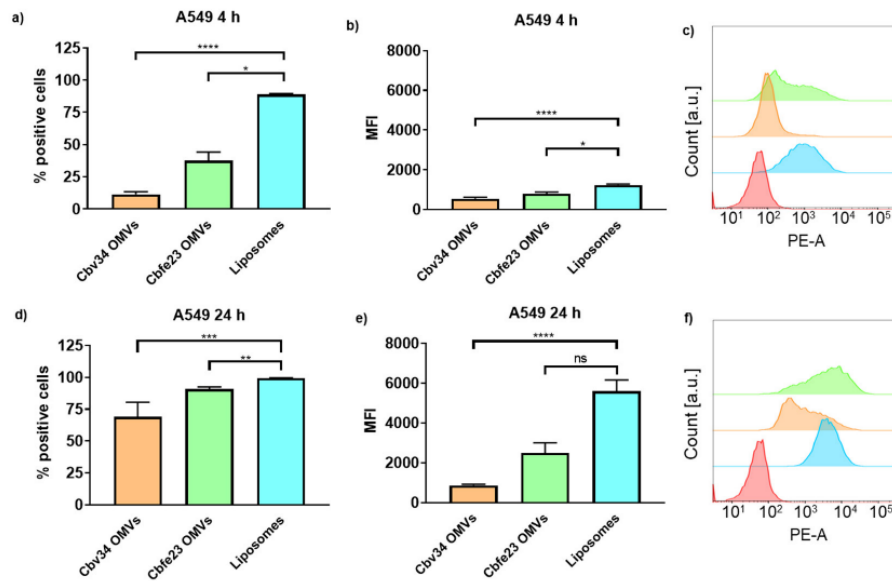


**Figure 6.** Interaction and uptake of OMVs and liposomes after incubation with A549 cells. The percentage of positive cells (which interacted with DiI-labelled OMVs) after (a) 4 h and (d) 24 h of incubation. The MFI after (b) 4 h and (e) 24 h of incubation. Representative histograms of Cbfe23 OMVs (green), Cbv34 OMVs (orange), liposomes (blue) and untreated control (red) after (c) 4 h and (f) 24 h of incubation. Mean  $\pm$  SEM,  $n = 3$ . \*  $p < 0.05$ , \*\*  $p < 0.005$ , \*\*\*  $p < 0.0005$  and \*\*\*\*  $p < 0.0001$ .

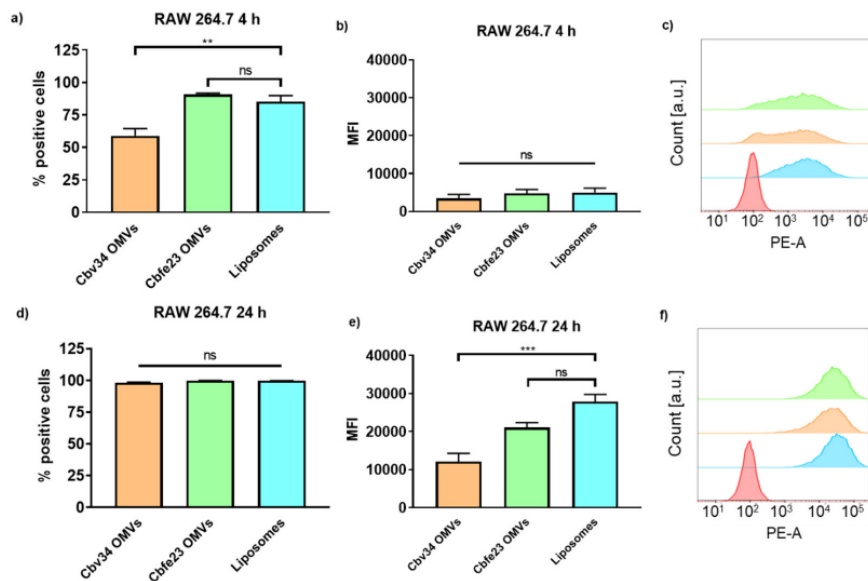


**Figure 7.** Interaction and uptake of OMVs and liposomes after incubation with RAW 264.7 cells. The percentage of positive cells (which interacted with DiI-labelled OMVs) after (a) 4 h and (d) 24 h of incubation. The MFI after (b) 4 h and (e) 24 h of incubation. Representative histograms of Cbfe23 OMVs (green), Cbv34 OMVs (orange), liposomes (blue) and untreated control (red) after (c) 4 h and (f) 24 h of incubation. Mean  $\pm$  SEM,  $n = 3$ . \*\*  $p < 0.005$ , \*\*\*  $p < 0.0005$  and ns = not significant.

As for the localization of the particles within the cells, we observed little fluorescence signal coming from the particles after 4 h of incubation with A549 (Figure S7), and a higher fluorescence of Cbfe23 OMVs when incubated with RAW 264.7 cells for 4 h (Figure S8), when compared to the Cbv34 OMVs. Even though we saw DiI-stained Cbv34 and Cbfe23 OMVs within the cells, we did not observe colocalization with the cytoskeleton at any investigated time point (Figure 8). We noticed

a removal of OMVs by PBS washing during the staining process, which may indicate that they are mostly bound onto the cell surface. When the cells were washed once with PBS and fixed, we observed a high number of fluorescent particles in A549 cells (Figures S9 and S10).

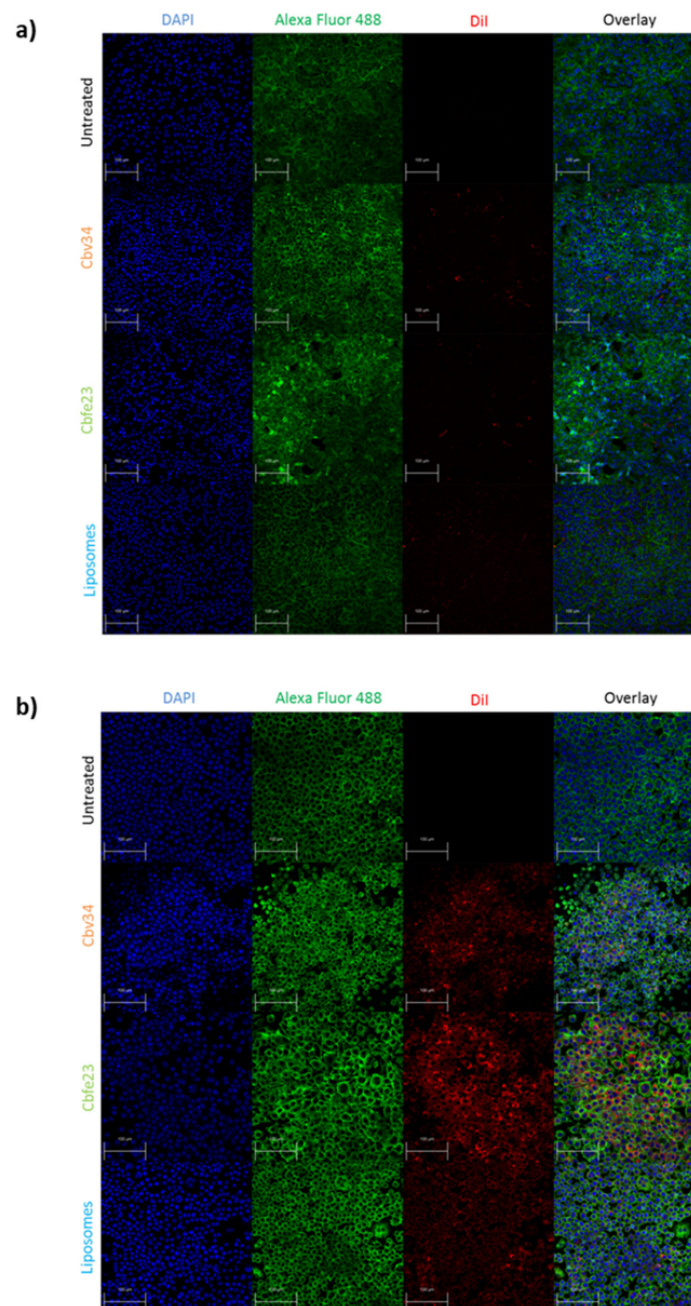


**Figure 8.** Uptake of fluorescent particles investigated by confocal laser scanning microscopy (CLSM) after 24 h of incubation with (a) A549 and (b) RAW 264.7 cells. The cells nuclei are stained with DAPI (blue), while the F-actin is labelled with Alexa Fluor 488 Phalloidin (green). OMVs and bacterial liposomes are stained with DiI (red). Scale bar = 100 µm.

### 3.6. OMVs Are Able to Kill Intracellular Pathogens

We investigated the ability of myxobacterial OMVs to treat intracellular infections caused by *S. aureus* in A549 cells. The most active concentrations were  $10^8$  OMVs/mL and  $10^{11}$  OMVs/mL

for Cbfe23 and Cbv34 OMVs, respectively (Figure 9). The highest concentrations of Cbfe23 OMVs were not tested, because they negatively influenced the viability of the cells, as shown in Figure 2a. Gentamicin is soluble in water, while cystobactamid is dissolved in DMSO (dimethyl sulfoxide), so we included DMSO as a solvent control. The DMSO might contribute to the antibacterial effect of the free cystobactamid, as we observed a tendency of lower CFU amounts in the DMSO sample alone. Both free gentamicin and cystobactamid, together with the solvent control DMSO, were not significantly different when compared among themselves. Our OMVs, which are in aqueous suspension, showed a more pronounced reduction in bacterial growth compared to free antibiotics. By comparing this with the number of bacteria present in the cells after 2 h of uptake (time zero), we see that the effect of the OMVs against *S. aureus* is bacteriostatic. This effect was also confirmed by the statistical analysis, which did not show a significant difference in bacterial growth between the most effective OMV concentrations and the time zero control (blue dashed line in Figure 9).

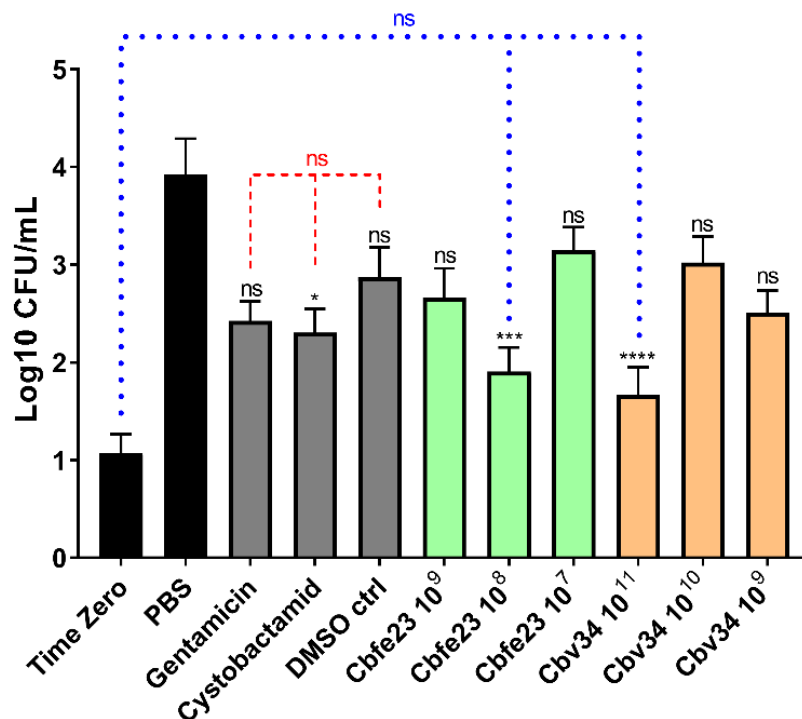


**Figure 9.** Antibacterial effect of OMVs against intracellular *S. aureus* after 24 h of treatment. Mean  $\pm$  SEM,  $n = 3\text{--}4$  independent experiments. Significance was defined in relation to the PBS control as ns = not significant, \*  $p$ -value  $< 0.05$ , \*\*\*  $p$ -value  $< 0.0005$  and \*\*\*\*  $p$ -value  $< 0.0001$ . Red dashed lines represent the comparison between gentamicin 10  $\mu\text{g}/\text{mL}$ , cystobactamid 10  $\mu\text{g}/\text{mL}$  and the DMSO control = not significant. Blue dotted lines represent the comparison between the time zero (2 h bacterial uptake), Cbfe23 10<sup>8</sup> particles/mL and Cbv34 10<sup>11</sup> particles/mL.

#### 4. Discussion

Cbv34 and Cbfe23 OMVs were successfully isolated by differential centrifugation and SEC, presenting a size of approximately 120–150 nm, which is an advantageous size for interaction with target cells and accumulation in inflamed infectious tissue [37]. The Cryo-TEM images showed spherical forms for Cbv34 OMVs, but for Cbfe23 OMVs, rod-shaped particles were also seen (Figure S4). We suspect that these particles might be fragments of outer membrane tubes (OMTs), which are known to be produced by some myxobacterial strains [38].

As for the viability and cytotoxicity, we showed low to absent toxicity for Cbv34 OMVs, as also reported in literature [33]. Cbfe23 OMVs, which were studied here for the first time, reduced the

viability of the cells only at a concentration of 125,000 OMVs/cell. This might be caused by a higher load of antibiotic in comparison to Cbv34 OMVs, since we could see that a concentration of 10 µg/mL cystobactamid also had a similar negative effect on cell viability. No dramatic cytotoxicity was detected at any concentrations tested for either OMV. We have tested whether our OMVs induce the production of proinflammatory cytokines to better understand the potential immunogenicity of our carriers. IL-6, which is a multifunctional cytokine, and TNF, are released in response to inflammation and mediate reactions to its effects, such as fever [39,40]. IL-8 and IL-1b induce chemotaxis and play a key role in inflammation, recruiting neutrophils to the site of infection [41–43]. Our OMVs promoted a mild release of proinflammatory cytokines compared to the LPS control. As an exception, the concentration of  $10^{13}$  Cbfe23 OMVs/mL stimulated a high production of IL-1beta, but possibly induced cell death, as observed by light microscopy (Figure S5). IL-1beta is known to be negatively influenced in production by the use of molecules that induce autophagy [44], which contributes to cell survival. This result might also lead to a clue about the mechanisms of how Cbfe23 OMVs induce cell death at high concentrations.

Even though high concentrations of OMVs were needed to inhibit the growth of planktonic bacteria, concentrations of  $10^{12}$  OMVs/mL and higher did not seem to be required for an antibacterial effect against intracellular pathogens. When intracellular CFUs were assessed to investigate the OMVs' activity against *S. aureus*, a bacterial growth inhibition was identified, especially from Cbfe23 OMVs. In literature, the Cbfe23 strain has not been reported to produce cystobactamids [45]. Here, we modified the composition of the bacterial culture medium by using phytone as a carbon source, instead of the previously reported skimmed milk and soy flour [45]. Due to this modification, we were able to identify cystobactamids 919-1 and 920-1 [46–48] as the active compounds in the OMV extract (Figure S6). For the potential application of OMVs as an antibacterial therapy in the clinic, their formulations must be stable for a certain period, preferably without any special storage conditions, such as deep freezing at  $-80$  °C and the use of cryoprotectants. Since we have already showed an antibacterial effect of Cbv34 OMVs against *E. coli* [26] and the easy handling of this bacterium, we investigated OMV storage stability at 4 °C with this model pathogen. We found that the dose-dependent antibacterial activity of Cbv34 OMVs was conserved during 28 days of storage. This result matches recent findings that show extracellular vesicles' inherent stability under different storage conditions [49,50].

Compared to bacteriomimetic liposomes, OMVs showed different uptake kinetics with immune and epithelial cells. While liposomes are rapidly taken up in all cell types at high amounts, OMVs seemed to have a preferentially better uptake in immune cells than in epithelial cells. Surface charge may play a role in this mechanism, but surface proteins of OMVs are also important for this effect, as was shown for mammalian vesicles [51]. As we show, OMVs have an antibacterial effect against internalized *S. aureus* in A549 cells. Both Cbfe23 and Cbv34 OMVs showed a higher antibacterial effect, when compared to the untreated control, than the free gentamicin and cystobactamid. Free antibiotics generally have a low permeation through mammalian cell membranes and thus favor intracellular infections, which may become persistent and difficult to treat. The use of myxobacterial OMVs as nanocarriers could possibly overcome the cellular barrier and successfully deliver the antibacterial compound to the lungs, potentially being administered locally as an aerosol.

The next steps to further evaluate myxobacterial OMVs as drug carriers are to rule out their immunogenicity in complex in vitro models of inflammation [52], and the evaluation of their antibacterial activity in an infected animal model.

## 5. Conclusions

OMVs from Cbv34 and Cbfe23 are not only low in toxicity in different cell lines, but also in primary immune cells. They are able to mediate killing of one of the most important Gram-positive problem pathogens, *S. aureus*. These OMVs are able to be taken up into infected cells and showed efficient bacteriostatic effect against intracellular *S. aureus* infections.

**Supplementary Materials:** The following are available online at <http://www.mdpi.com/2073-4409/9/1/194/s1>, Figure S1: Morphology of Cbfe23 (passage 3, 5 days in culture) and Cbv34 (passage 9, 7 days in culture),

Figure S2: Particle size measured by dynamic light scattering and protein concentration of Cbfe23 size exclusion chromatography fractions (1 mL each) were measured by BCA (bicinchoninic acid) assay (Sigma-Aldrich Co., St. Louis, MO, USA), Figure S3: Representative graphs of size distributions measured by nanoparticle tracking analysis of a) Cbv34 and b) Cbfe23 OMVs, Figure S4: Cryo-TEM micrographs of Cbfe23 pellets after ultracentrifugation, Figure S5: Light microscopy images showing the morphology of peripheral blood mononuclear cells (PBMCs) after 4 h treatment with OMVs and controls, Figure S6: a) LC-MS Base peak chromatogram of the OMV extract (black) highlighting the two major cystobactamids: cystobactamid 919-1 (A, red,  $m/z$  920.31  $\pm$  0.05 Da) and cystobactamid 920-1 (B, blue,  $m/z$  921.30  $\pm$  0.05 Da) as extracted ion chromatograms, Figure S7: Uptake/interaction of OMVs and liposomes with A549 cells after 4 h incubation measured by confocal laser scanning microscopy, Figure S8: Uptake/interaction of OMVs and liposomes with RAW 264.7 cells after 4 h of incubation measured by confocal laser scanning microscopy, Figure S9: Uptake/interaction imaging of OMVs and liposomes after 4 h incubation with A549, following one single wash with PBS and fixation by confocal laser scanning microscopy, Figure S10: Uptake/interaction imaging of OMVs and liposomes after 24 h incubation with A549, following one single wash with PBS and fixation by confocal laser scanning microscopy.

**Author Contributions:** A.G. performed all bacterial and mammalian cell culture, OMVs isolation, particle measurements, antibacterial assays, infection assays, confocal laser scanning microscopy, flow cytometry, data analysis and wrote the main manuscript draft. P.L. performed particle characterization and staining together with A.G. T.K. performed viability and cytotoxicity assays. E.S. and C.D. isolated PBMCs. E.S. performed cytokine detection. R.R. prepared and characterized the bacteriomimetic liposomal formulation. F.P. performed mass spectrometry measurements. M.K. obtained cryo-TEM images. A.K.K. supervised and revised cytokine detection experiments. R.G. and R.M. kindly provided myxobacterial strains and advised on their culture conditions. G.F. conceived the project, supervised the work and wrote the manuscript together with A.G. All authors contributed to the writing of the manuscript. All authors have read and agreed to the published version of the manuscript.

**Funding:** This work was supported by a Junior Research grant from the Federal Ministry of Research and Education (NanoMatFutur programme, grant number 13XP5029A). This work was supported, in part, by the Deutsche Forschungsgemeinschaft (DFG, to A.K.K., KI702).

**Acknowledgments:** We would like to thank Jana Westhues and Petra König for their help with the mammalian cell culture.

**Conflicts of Interest:** The authors declare no conflict of interest.

## References

1. Troeger, C.; Blacker, B.; Khalil, I.A.; Rao, P.C.; Cao, J.; Zimsen, S.R.M.; Albertson, S.B.; Deshpande, A.; Farag, T.; Abebe, Z.; et al. Estimates of the global, regional, and national morbidity, mortality, and aetiologies of lower respiratory infections in 195 countries, 1990–2016: A systematic analysis for the Global Burden of Disease Study 2016. *Lancet Infect. Dis.* **2018**, *18*, 1191–1210. [[CrossRef](#)]
2. Naghavi, M.; Abajobir, A.A.; Abbafati, C.; Abbas, K.M.; Abd-Allah, F.; Abera, S.F.; Aboyans, V.; Adetokunboh, O.; Ärnlöv, J.; Afshin, A.; et al. Global, regional, and national age-sex specific mortality for 264 causes of death, 1980–2016: A systematic analysis for the Global Burden of Disease Study 2016. *Lancet* **2017**, *390*, 1151–1210. [[CrossRef](#)]
3. Sherrard, L.J.; Tunney, M.M.; Elborn, J.S. Infections in chronic lung diseases 2 Antimicrobial resistance in the respiratory microbiota of people with cystic fibrosis. *Lancet* **2014**, *384*, 703–713. [[CrossRef](#)]
4. Lommatzsch, S.T.; Aris, R. Genetics of cystic fibrosis. *Semin. Respir. Crit. Care Med.* **2009**, *30*, 531–538. [[CrossRef](#)] [[PubMed](#)]
5. Ahmed, M.I.; Mukherjee, S. Treatment for chronic methicillin-sensitive *Staphylococcus aureus* pulmonary infection in people with cystic fibrosis. *Cochrane Database Syst. Rev.* **2018**, *3*, CD011581. [[CrossRef](#)]
6. Ulrich, M.; Herbert, S.; Berger, J.; Bellon, G.; Louis, D.; Münker, G.; Döring, G. Localization of *Staphylococcus aureus* in Infected Airways of Patients with Cystic Fibrosis and in a Cell Culture Model of *S. aureus* Adherence. *Am. J. Respir. Cell Mol. Biol.* **1998**, *19*, 83–91. [[CrossRef](#)]
7. Tranchemontagne, Z.R.; Camire, R.B.; O'Donnell, V.J.; Baugh, J.; Burkholder, K.M. *Staphylococcus aureus* Strain USA300 Perturbs Acquisition of Lysosomal Enzymes and Requires Phagosomal Acidification for Survival inside Macrophages. *Infect. Immun.* **2016**, *84*, 241–253. [[CrossRef](#)]
8. Flannagan, R.S.; Heit, B.; Heinrichs, D.E. Intracellular replication of *Staphylococcus aureus* in mature phagolysosomes in macrophages precedes host cell death, and bacterial escape and dissemination. *Cell. Microbiol.* **2016**, *18*, 514–535. [[CrossRef](#)]
9. Fraunholz, M.; Sinha, B. Intracellular *Staphylococcus aureus*: Live-in and let die. *Front. Cell. Infect. Microbiol.* **2012**, *2*, 1–10. [[CrossRef](#)]

10. Löffler, B.; Tuchscher, L.; Niemann, S.; Peters, G. Staphylococcus aureus persistence in non-professional phagocytes. *Int. J. Med. Microbiol.* **2014**, *304*, 170–176. [[CrossRef](#)]
11. Barcia-Macay, M.; Seral, C.; Mingeot-Leclercq, M.-P.; Tulkens, P.M.; Van Bambeke, F. Pharmacodynamic evaluation of the intracellular activities of antibiotics against Staphylococcus aureus in a model of THP-1 macrophages. *Antimicrob. Agents Chemother.* **2006**, *50*, 841–851. [[CrossRef](#)] [[PubMed](#)]
12. Vaudaux, P.; Waldvogel, F.A. Gentamicin antibacterial activity in the presence of human polymorphonuclear leukocytes. *Antimicrob. Agents Chemother.* **1979**, *16*, 743–749. [[CrossRef](#)] [[PubMed](#)]
13. Carlier, M.-B.; Zenebergh, A.; Tulkens, P.M. Cellular uptake and subcellular distribution of roxithromycin and erythromycin in phagocytic cells. *J. Antimicrob. Chemother.* **1987**, *20*, 47–56. [[CrossRef](#)] [[PubMed](#)]
14. Jacobs, R.F.; Wilson, C.B. Activity of Antibiotics in Chronic Granulomatous Disease Leukocytes. *Pediatr. Res.* **1983**, *17*, 916–919. [[CrossRef](#)] [[PubMed](#)]
15. Jacobs, R.F.; Wilson, C.B. Intracellular penetration and antimicrobial activity of antibiotics. *J. Antimicrob. Chemother.* **1983**, *12*, 13–20. [[CrossRef](#)]
16. Bongers, S.; Hellebrekers, P.; Leenen, L.P.H.; Koenderman, L.; Hietbrink, F. Intracellular Penetration and Effects of Antibiotics on Staphylococcus aureus Inside Human Neutrophils: A Comprehensive Review. *Antibiotics* **2019**, *8*, 54. [[CrossRef](#)]
17. Anversa Dimer, F.; de Souza Carvalho-Wodarz, C.; Goes, A.; Cirnski, K.; Herrmann, J.; Schmitt, V.; Pätzold, L.; Abed, N.; De Rossi, C.; Bischoff, M.; et al. PLGA nanocapsules improve the delivery of clarithromycin to kill intracellular Staphylococcus aureus and Mycobacterium abscessus. *Nanomed. Nanotechnol. Biol. Med.* **2020**, *24*, 102125. [[CrossRef](#)]
18. Menina, S.; Eisenbeis, J.; Kamal, M.A.M.; Koch, M.; Bischoff, M.; Gordon, S.; Loretz, B.; Lehr, C. Bioinspired Liposomes for Oral Delivery of Colistin to Combat Intracellular Infections by Salmonella enterica. *Adv. Healthc. Mater.* **2019**, 1900564. [[CrossRef](#)]
19. Castoldi, A.; Empting, M.; De Rossi, C.; Mayr, K.; Dersch, P.; Hartmann, R.; Müller, R.; Gordon, S.; Lehr, C.M. Aspherical and Spherical InvA497-Functionalized Nanocarriers for Intracellular Delivery of Anti-Infective Agents. *Pharm. Res.* **2019**, *36*, 1–13. [[CrossRef](#)]
20. Yang, X.; Shi, G.; Guo, J.; Wang, C.; He, Y. Exosome-encapsulated antibiotic against intracellular infections of methicillin-resistant Staphylococcus aureus. *Int. J. Nanomed.* **2018**, *13*, 8095–8104. [[CrossRef](#)]
21. Goes, A.; Fuhrmann, G. Biogenic and Biomimetic Carriers as Versatile Transporters to Treat Infections. *ACS Infect. Dis.* **2018**, *4*, 881–892. [[CrossRef](#)] [[PubMed](#)]
22. Forier, K.; Raemdonck, K.; De Smedt, S.C.; Demeester, J.; Coenye, T.; Braeckmans, K. Lipid and polymer nanoparticles for drug delivery to bacterial biofilms. *J. Control. Release* **2014**, *190*, 607–623. [[CrossRef](#)]
23. Reichenbach, H. The ecology of the myxobacteria. *Environ. Microbiol.* **1999**, *1*, 15–21. [[CrossRef](#)] [[PubMed](#)]
24. Wu, Y.; Jiang, Y.; Kaiser, D.; Alber, M. Social interactions in myxobacterial swarming. *PLoS Comput. Biol.* **2007**, *3*, 2546–2558. [[CrossRef](#)] [[PubMed](#)]
25. Reichenbach, H.; Gerth, K.; Irschik, H.; Kunze, B.; Höfle, G. Myxobacteria: A source of new antibiotics. *Trends Biotechnol.* **1988**, *6*, 115–121. [[CrossRef](#)]
26. Weissman, K.J.; Müller, R. Myxobacterial secondary metabolites: Bioactivities and modes-of-action. *Nat. Prod. Rep.* **2010**, *27*, 1276. [[CrossRef](#)]
27. Reichenbach, H. Myxobacteria, producers of novel bioactive substances. *J. Ind. Microbiol. Biotechnol.* **2001**, *27*, 149–156. [[CrossRef](#)]
28. Hoffmann, T.; Krug, D.; Bozkurt, N.; Duddela, S.; Jansen, R.; Garcia, R.; Gerth, K.; Steinmetz, H.; Müller, R. Correlating chemical diversity with taxonomic distance for discovery of natural products in myxobacteria. *Nat. Commun.* **2018**, *9*, 1–10. [[CrossRef](#)]
29. Schwechheimer, C.; Kuehn, M.J. Outer-membrane vesicles from Gram-negative bacteria: Biogenesis and functions. *Nat. Rev. Microbiol.* **2015**, *13*, 605–619. [[CrossRef](#)]
30. Kulp, A.; Kuehn, M.J. Biological Functions and Biogenesis of Secreted Bacterial Outer Membrane Vesicles. *Annu. Rev. Microbiol.* **2010**, *64*, 163–184. [[CrossRef](#)]
31. Woith, E.; Fuhrmann, G.; Melzig, M.F. Extracellular Vesicles—Connecting Kingdoms. *Int. J. Mol. Sci.* **2019**, *20*, 5695. [[CrossRef](#)]
32. Evans, A.G.L.; Davey, H.M.; Cookson, A.; Currinn, H.; Cooke-Fox, G.; Stanczyk, P.J.; Whitworth, D.E. Predatory activity of Myxococcus xanthus outer-membrane vesicles and properties of their hydrolase cargo. *Microbiology* **2012**, *158*, 2742–2752. [[CrossRef](#)] [[PubMed](#)]

## Supplementary Material

Myxobacteria-derived outer membrane vesicles: potential applicability against intracellular infections

Adriely Goes, Philipp Lapuhs, Thomas Kuhn, Eilien Schulz, Robert Richter, Fabian Panter, Charlotte Dahlem, Marcus Koch, Ronald Garcia, Alexandra K. Kiemer, Rolf Müller and Gregor Fuhrmann

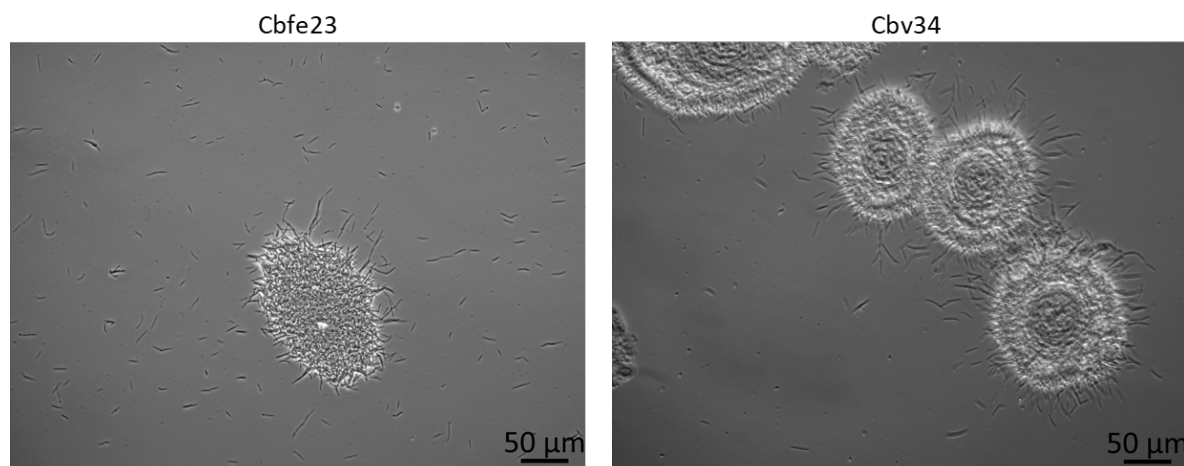


**Figure S1:** Morphology of Cbfe23 (passage 3, 5 days in culture) and Cbv34 (passage 9, 7 days in culture). Myxobacteria form cell aggregates in liquid culture. Images were taken with a light microscope (Zeiss, Germany). Scale bars = 50 μm.

### Protein concentration and particle size of Cbfe23 OMVs

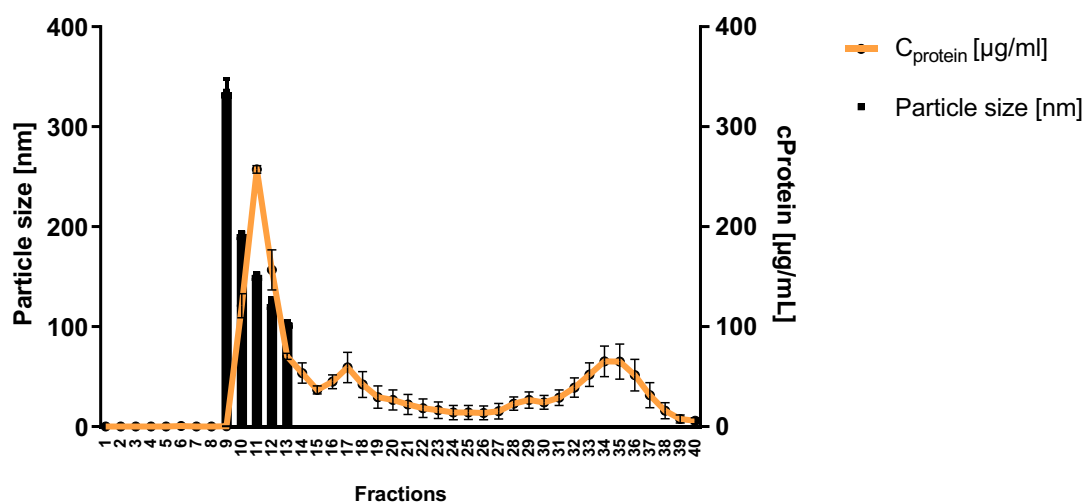


**Figure S2:** Particle size measured by dynamic light scattering and protein concentration of Cbfe23 size exclusion chromatography fractions (1 mL each) were measured by BCA (bicinchoninic acid) assay (Sigma-Aldrich Co., St. Louis, MO, USA). Mean ± SEM,  $n = 3$ .

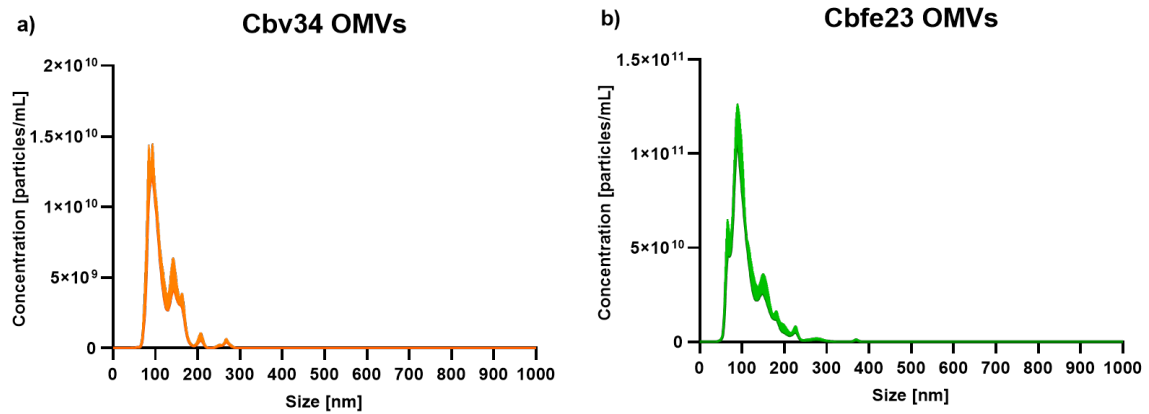


**Figure S3:** Representative graphs of size distributions measured by nanoparticle tracking analysis of a) Cbv34 and b) Cbfe23 OMVs. Mean + SEM.

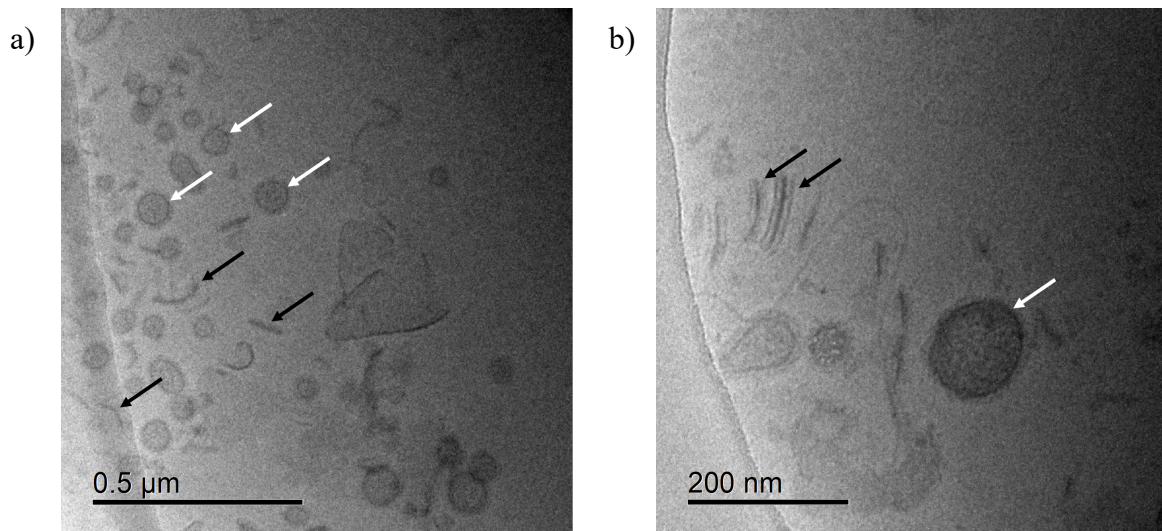


**Figure S4:** Cryo-TEM micrographs of Cbfe23 pellets after ultracentrifugation. The white arrows indicate OMVs with spherical shape and electron dense cores. The black arrows indicate rod-shaped electron dense particles of similar size as the OMVs.

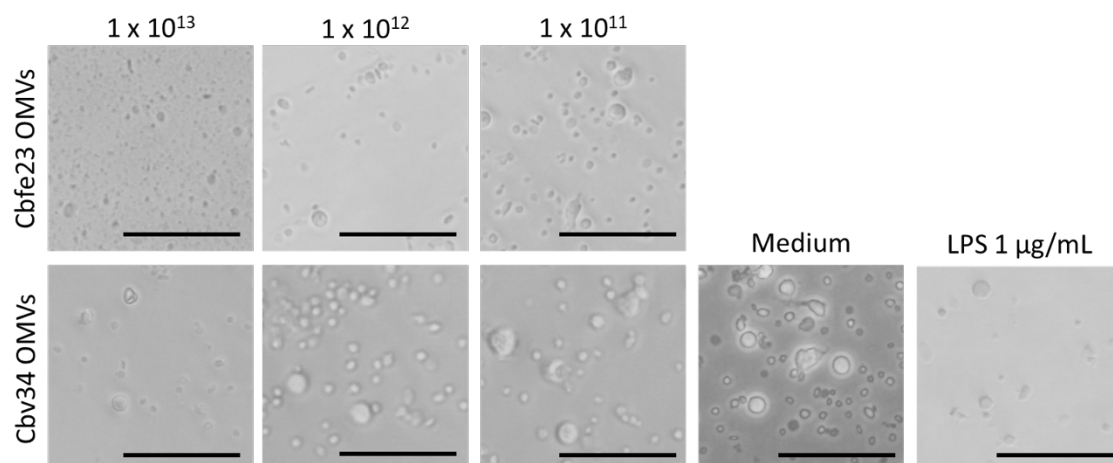


**Figure S5:** Light microscopy images showing the morphology of peripheral blood mononuclear cells (PBMCs) after 4 h treatment with OMVs and controls. The viability of the cells appeared to be compromised upon treatment with high concentrations of OMVs ( $1 \times 10^{13}$  OMVs/mL). Scale bars = 50  $\mu\text{m}$ .

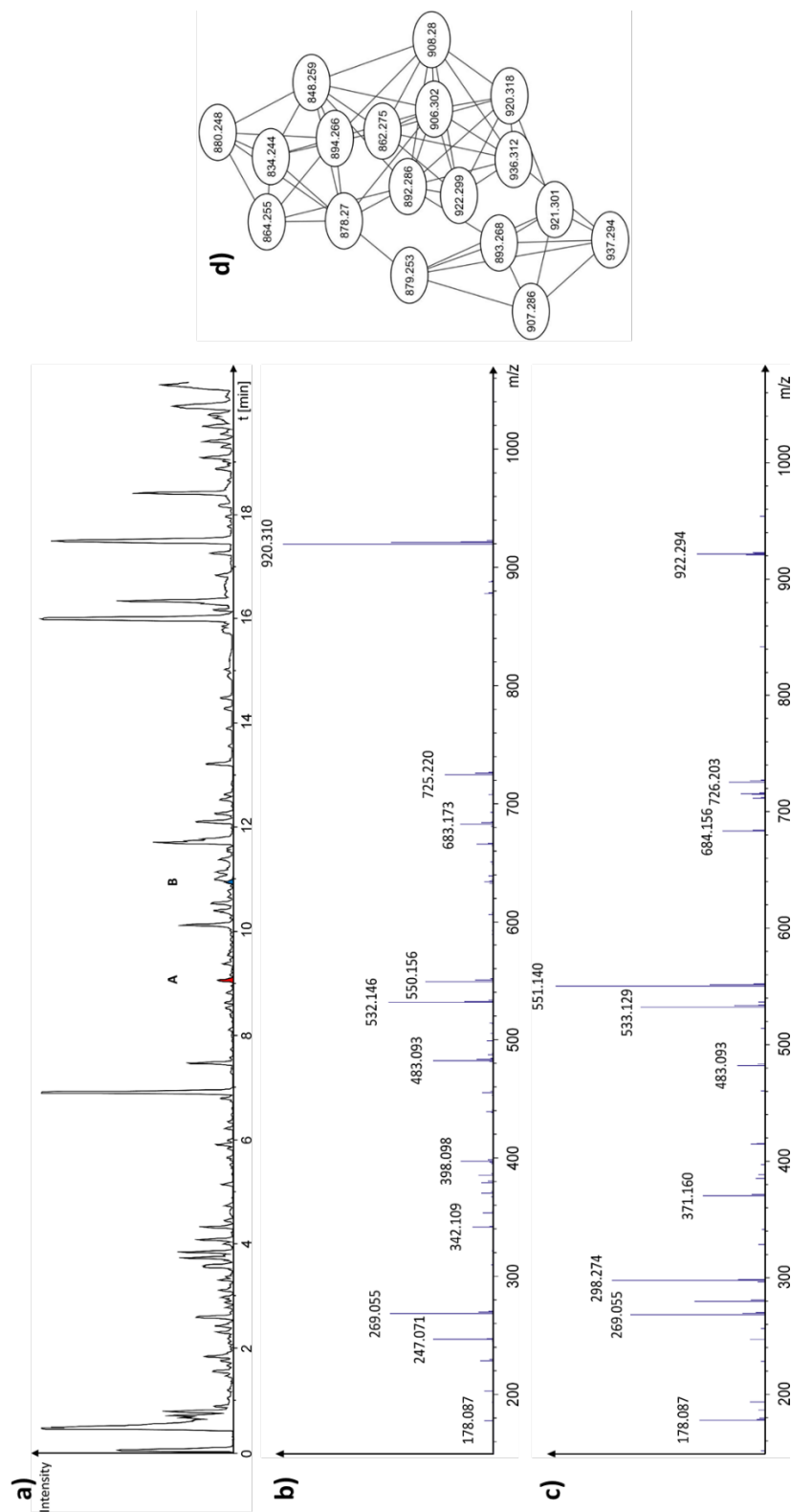


**Figure S6:** a) LC-MS Base peak chromatogram of the OMV extract (black) highlighting the two major cystobactamids: cystobactamid 919-1 (A, red,  $m/z$   $920.31 \pm 0.05$  Da) and cystobactamid 920-1 (B, blue,  $m/z$   $921.30 \pm 0.05$  Da) as extracted ion chromatograms. b) ESI-CID-MS<sup>2</sup> spectrum of cystobactamid 919-1 from the OMV

samples measured on a maXis 4G qTOF spectrometer c) ESI-CID-MS<sup>2</sup> spectrum of cystobactamid 920-1 from the OMV samples measured on a maXis 4G qTOF spectrometer d) Spectral network created by GNPS using the MS<sup>2</sup> data from the OMV extract samples depicting the precursor masses of all cystobactamid derivatives contained in the samples.

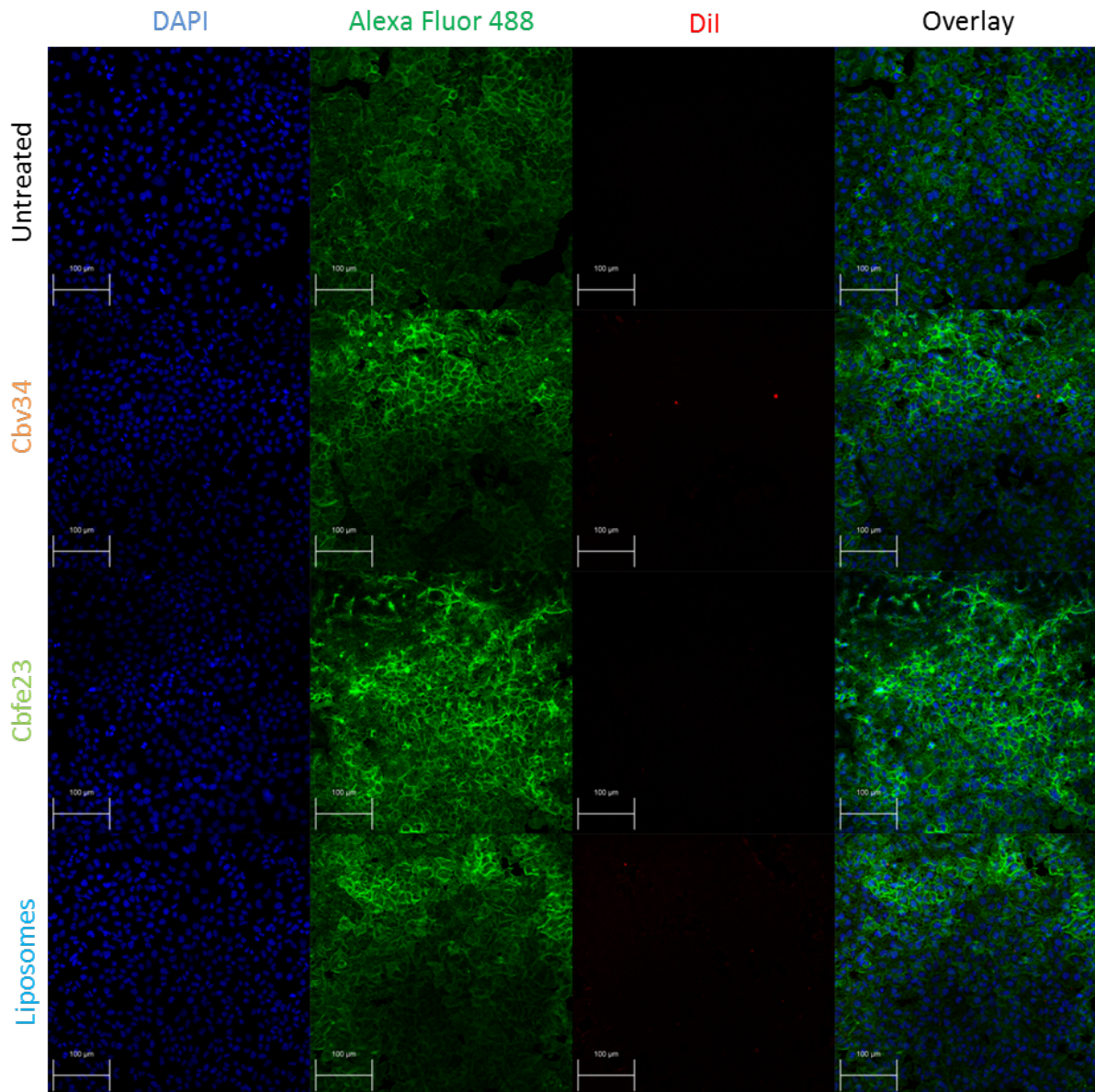


**Figure S7:** Uptake/interaction of OMVs and liposomes with A549 cells after 4 h incubation measured by confocal laser scanning microscopy. The cells nuclei are stained by DAPI (blue), while the F-actin is labelled by Alexa Fluor® 488 Phalloidin (green). Scale bars = 100 μm.

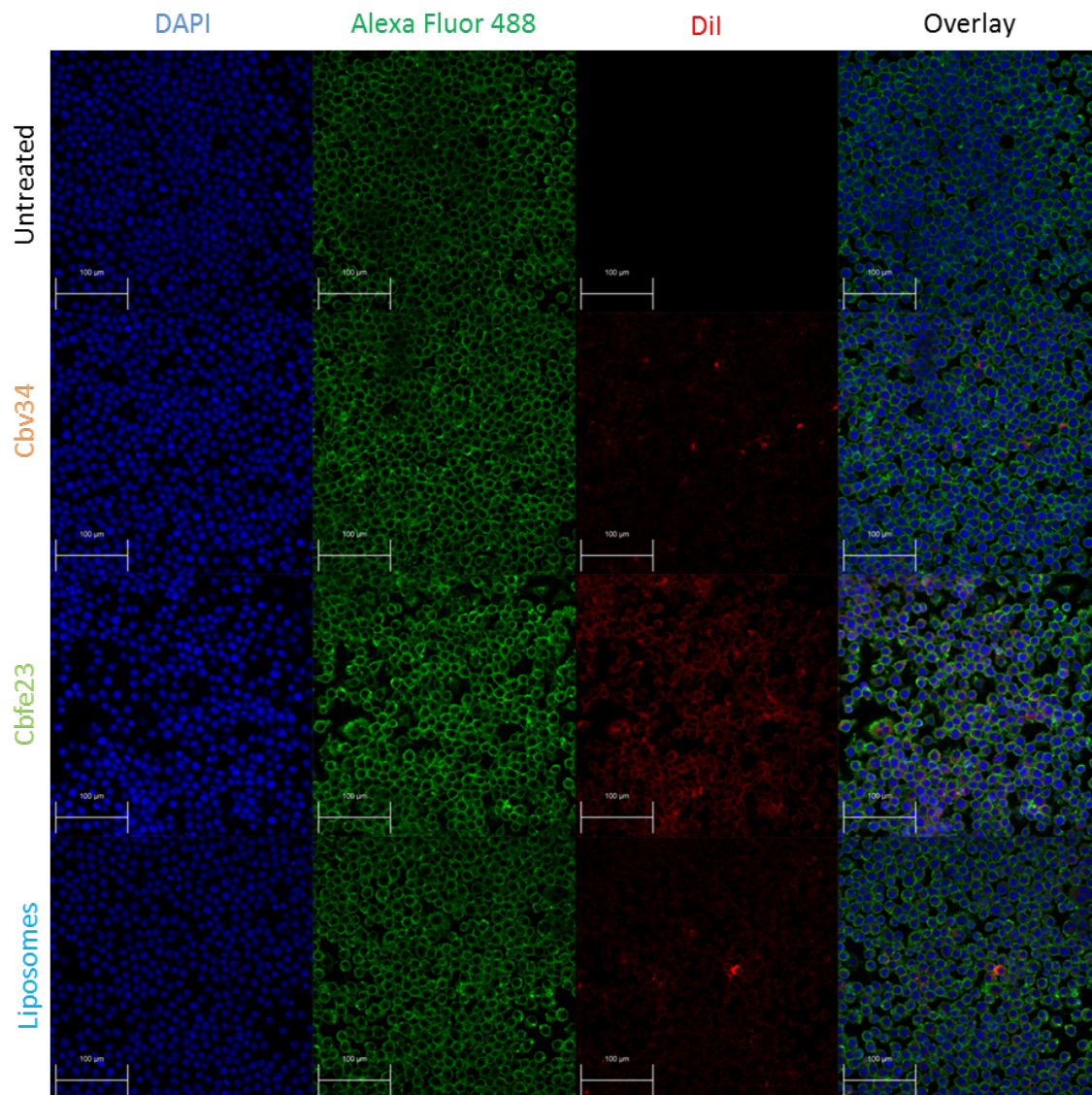


**Figure S8:** Uptake/interaction of OMVs and liposomes with RAW 264.7 cells after 4 h of incubation measured by confocal laser scanning microscopy. The cells nuclei are stained by DAPI (blue), while the F-actin is labelled by Alexa Fluor® 488 Phalloidin (green). Scale bars = 100 µm.

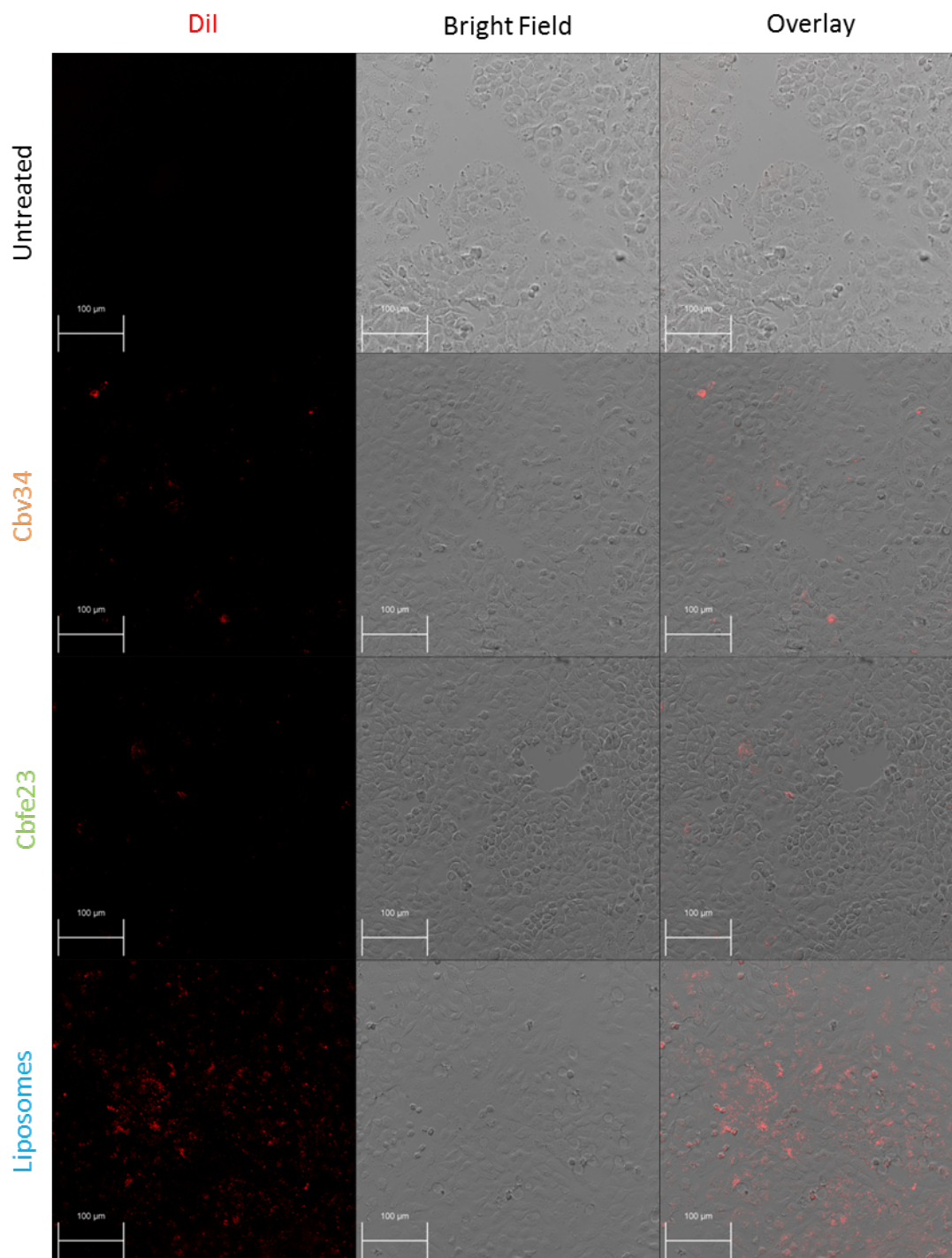


**Figure S9:** Uptake/interaction imaging of OMVs and liposomes after 4 h incubation with A549, following one single wash with PBS and fixation by confocal laser scanning microscopy. Cells were imaged with bright field and OMVs and liposomes were stained with Dil (red). Scale bars = 100  $\mu$ m.

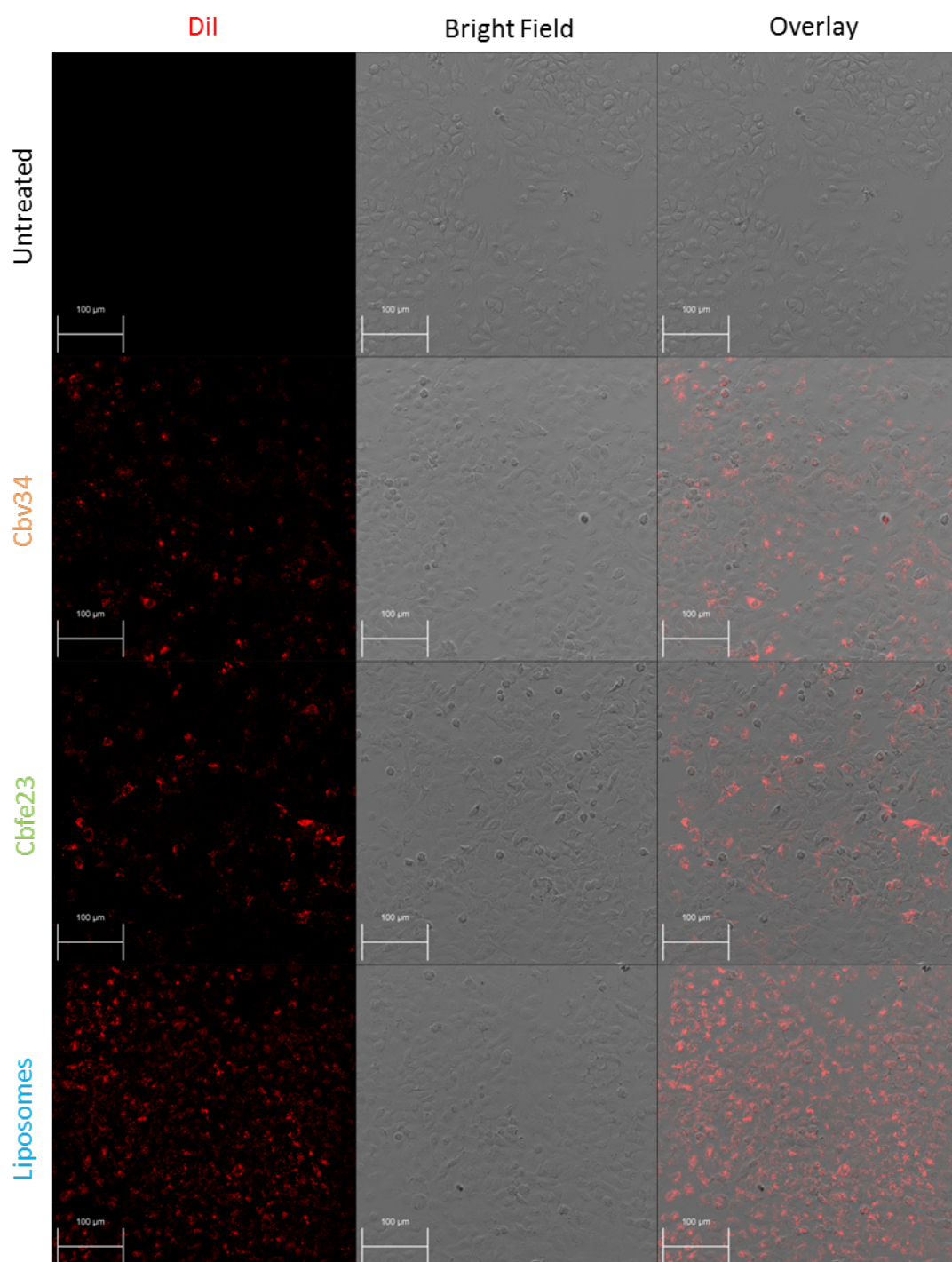


**Figure S10:** Uptake/interaction imaging of OMVs and liposomes after 24 h incubation with A549, following one single wash with PBS and fixation by confocal laser scanning microscopy. Cells were imaged with bright field and OMVs and liposomes were stained with Dil (red). Scale bars = 100  $\mu$ m.

#### 6.4 PAPER 4: “Interaction of myxobacteria-derived outer membrane vesicles with biofilms: antiadhesive and antibacterial effects”

Adriely Goes,<sup>a,b</sup> Lucia Vidakovic,<sup>c</sup> Knut Drescher<sup>c,d,e</sup> and Gregor Fuhrmann<sup>a,b</sup>

<sup>a</sup> Helmholtz Centre for Infection Research (HZI), Biogenic Nanotherapeutics Group (BION), Helmholtz Institute for Pharmaceutical Research Saarland (HIPS), Campus E8.1, 66123 Saarbrücken, Germany. E-mail: gregor.fuhrmann@helmholtz-hips.de

<sup>b</sup> Department of Pharmacy, Saarland University, Campus Building E8.1, 66123 Saarbrücken, Germany

<sup>c</sup> Max Planck Institute for Terrestrial Microbiology, Marburg, Germany

<sup>d</sup> Department of Physics, Philipps-Universität Marburg, Marburg, Germany

<sup>e</sup> Biozentrum, University of Basel, Basel, Switzerland

Accepted: 27 July 2021

Nanoscale 2021

DOI: 10.1039/D1NR02583J



Cite this: DOI: 10.1039/d1nr02583j

Received 23rd April 2021

Accepted 27th July 2021

DOI: 10.1039/d1nr02583j

[rsc.li/nanoscale](https://rsc.li/nanoscale)

## Interaction of myxobacteria-derived outer membrane vesicles with biofilms: antiadhesive and antibacterial effects†

Adriely Goes,<sup>a,b</sup> Lucia Vidakovic,<sup>c</sup> Knut Drescher<sup>c,d,e</sup> and Gregor Fuhrmann<sup>a,b</sup>

**Bacterial biofilms are widespread in nature and in medical settings and display a high tolerance to antibiotics and disinfectants. Extracellular vesicles have been increasingly studied to characterise their origins and assess their potential for use as a versatile drug delivery system; however, it remains unclear whether they also have antibiofilm effects. Outer membrane vesicles are lipid vesicles shed by Gram-negative bacteria and, in the case of myxobacteria, carry natural antimicrobial compounds produced by these microorganisms. In this study, we demonstrate that vesicles derived from the myxobacteria *Cystobacter velatus* Cbv34 and *Cystobacter ferrugineus* Cbfe23 are highly effective at inhibiting the formation and disrupting biofilms by different bacterial species.**

### Introduction

Microorganisms can employ a variety of strategies to survive in the natural environment, including the formation of biofilms. Recent global surveys of microbial abundances in the environment have shown that biofilms are the main form of growth for bacteria and other microorganisms.<sup>1–3</sup> Biofilms can develop when microorganisms attach to a surface, grow or aggregate together, and produce an extracellular matrix composed of polymeric substances.<sup>4–8</sup> They are responsible for 65% to 75% of all human infections,<sup>9,10</sup> such as lung infections in patients with cystic fibrosis, infectious kidney stones, urinary tract infections, and bacterial endocarditis.<sup>11,12</sup>

Biofilm formation is known to result in a high tolerance to antibiotics and disinfectants of the bacteria inside the biofilms.<sup>13–15</sup> The protective barrier provided by biofilms causes major health care issues, such as chronic infections resulting from biofilms that form on biomedical devices. Indeed, recent estimates have indicated that these infections account for 25.6% of all infections acquired in health care settings in the United States of America.<sup>16</sup> These observations highlight the need for the development of new strategies for the treatment of biofilm-derived infections.

Myxobacteria are Gram-negative microorganisms abundantly present in the soil. They have been extensively studied for their ability to produce natural antimicrobial compounds while being non-pathogenic to humans.<sup>17,18</sup>

Myxobacteria can release outer membrane vesicles (OMVs), a type of extracellular vesicle specifically released by Gram-negative bacteria.<sup>19,20</sup>

The OMVs released by myxobacteria can transport antibiotic compounds produced by them, which are known to be able to kill planktonic and intracellular pathogens.<sup>21,22</sup> Many different nanocarrier-based approaches, such as surface modification of liposomes,<sup>23</sup> the use of “biogenic” silver nanoparticles,<sup>24</sup> and quorum-sensing modulation by autoinducer-loaded nanoparticles, have recently been explored as means of eradicating microbial biofilms.<sup>25</sup> However, most of these systems have limitations, such as not being suitable for *in vivo* use, being toxic to mammalian cells, or not being able to fully eradicate biofilms. Here, we propose the use of OMVs derived from two myxobacterial strains, *Cystobacter velatus* Cbv34<sup>26</sup> and *Cystobacter ferrugineus* Cbfe23,<sup>27</sup> natural producers of the antibiotic cystobactamid,<sup>21,22</sup> as a novel approach for preventing the formation and adhesion of bacterial biofilms.

### Results and discussion

*C. velatus* Cbv34 and *C. ferrugineus* Cbfe23 were cultured at least until the fourth passage and their OMVs were isolated

<sup>a</sup>Helmholtz Centre for Infection Research (HZI), Biogenic Nanotherapeutics Group (BION), Helmholtz Institute for Pharmaceutical Research Saarland (HIPS), Campus E8.1, 66123 Saarbrücken, Germany.

E-mail: [gregor.fuhrmann@helmholtz-hips.de](mailto:gregor.fuhrmann@helmholtz-hips.de)

<sup>b</sup>Department of Pharmacy, Saarland University, Campus Building E8.1, 66123 Saarbrücken, Germany

<sup>c</sup>Max Planck Institute for Terrestrial Microbiology, Marburg, Germany

<sup>d</sup>Department of Physics, Philipps-Universität Marburg, Marburg, Germany

<sup>e</sup>Biozentrum, University of Basel, Basel, Switzerland

† Electronic supplementary information (ESI) available. See DOI: 10.1039/d1nr02583j

## Communication

from 7-day-old cultures by differential centrifugation. The pellets were resuspended in 300  $\mu\text{L}$  of particle-free phosphate-buffered saline (PBS) and subjected to nanoparticle tracking

analysis (NTA). Cbv34 presented OMVs with a size of  $121.1 \pm 9.6$  nm and an average concentration of  $1.68 \times 10^{13}$  particles per mL (Fig. S1A†), while those of Cbfe23 had a size of  $101.6 \pm$

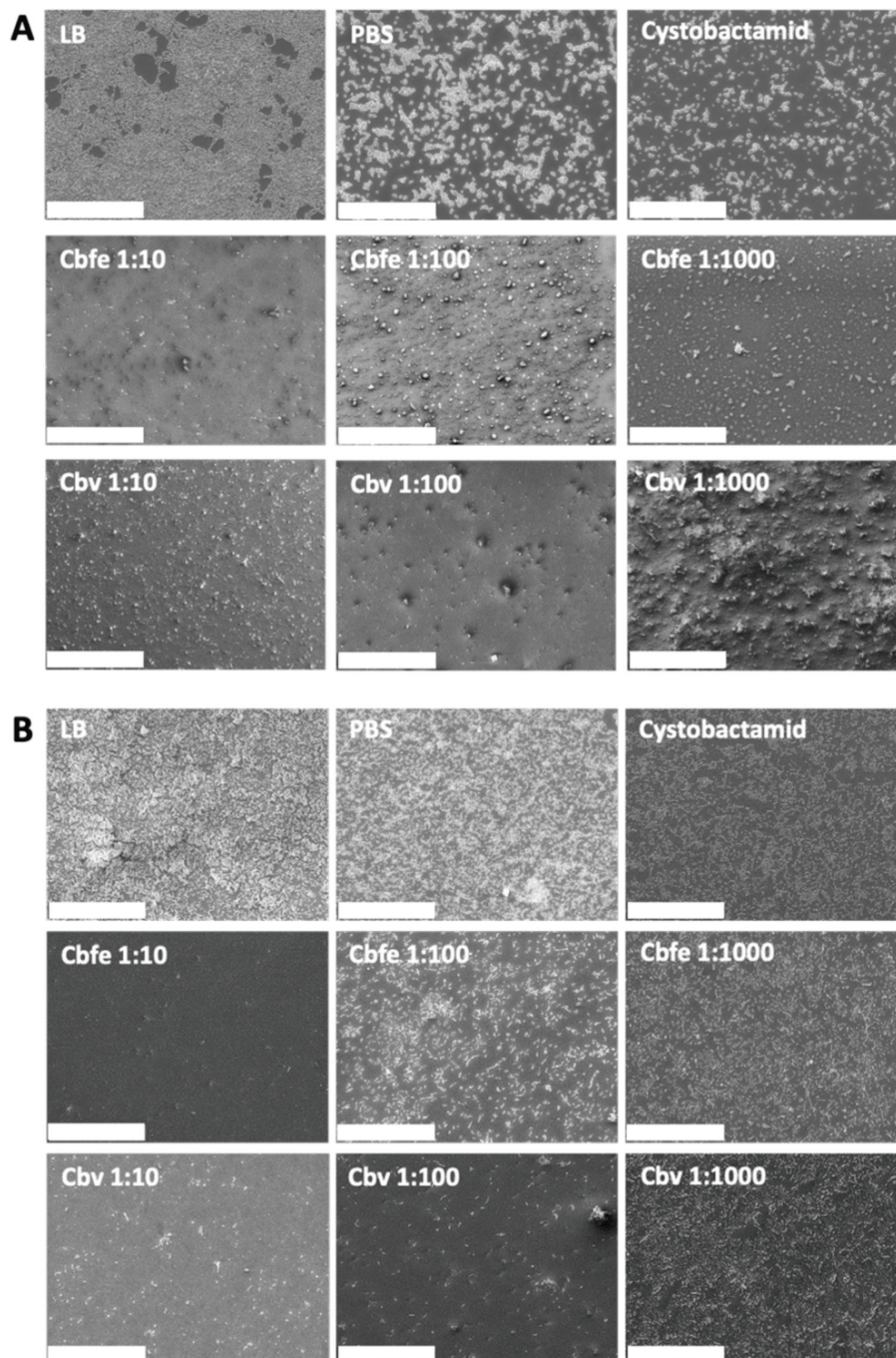


**Fig. 1** Scanning electron micrographs of *E. coli* biofilms grown on glass coverslips. The concentrations of the OMV suspensions are as follows: 1:10 =  $1 \times 10^{12}$  particles per mL for Cbv and  $1 \times 10^{13}$  particles per mL for Cbfe. (A) Biofilm inhibition assay. Biofilms were grown on glass coverslips for 48 h with different concentrations of Cbfe and Cbv OMVs or controls (LB medium, PBS, and cystobactamid). (B) Preformed biofilm assay. Biofilms were grown on glass coverslips for 72 h and then treated with different concentrations of Cbfe and Cbv OMVs for another 24 h. Under both settings, fewer bacteria remained attached to the coverslips when OMV treatment was applied, especially for the preformed biofilms treated with the higher OMV concentration. Micrographs are representative of three independent experiments. Scale bar = 50  $\mu\text{m}$ .

## Nanoscale

2.5 nm and an average concentration of  $1.04 \times 10^{14}$  particles per mL (Fig. S1B†).

To test the effect of these OMVs on *Escherichia coli* biofilms, we designed two different assays, for which we grew *E. coli* TG1 biofilms in 24-well plates with a glass coverslip inserted at the bottom of the wells. In the first assay, we aimed to assess the ability of the OMVs to inhibit biofilm formation (the biofilm inhibition assay). For this, we incubated a bacterial suspension with OMVs or control treatments for 48 h and then proceeded with the analysis. The aim of the second assay—the preformed biofilm assay—was to assess the ability of the OMVs to disrupt a mature biofilm. For this, we first grew biofilms by incubating the bacterial suspension for 72 h. Subsequently, we removed non-adherent bacteria from the well and then applied the OMV treatment for a further 24 h before proceeding with the analysis. Using scanning electron microscopy (SEM) for the biofilm inhibition assay, we observed that fewer bacteria were attached to the surface of the coverslip in the OMV-treated

group when compared with the controls (Fig. 1A), indicating that OMV treatment prevented bacterial attachment to the surface of the coverslip and that this effect was dose-dependent. A similar effect was seen in the preformed biofilm assay, especially when the adherent biofilms were treated with Cbfe-derived OMVs (Fig. 1B). This suggested that OMV treatment could promote bacterial detachment from the surface of the glass coverslip and the disruption of the mature biofilm. Suspensions of Cbv34 and Cbfe23 did not elicit similar effects, even at an optical density that was five-fold higher than that of the OMVs used (Fig. S2†).

The ability to attach to surfaces is a defining feature of biofilms. This ability relies on the same self-produced extracellular matrix that also protects the biofilm-dwelling cells from stresses.<sup>28</sup> The ability to overcome this structural defence mechanism may allow the use of other antibacterial compounds to achieve complete biofilm eradication.<sup>29–31</sup> Both Cbfe- and Cbv-derived OMVs have been shown to exert strong

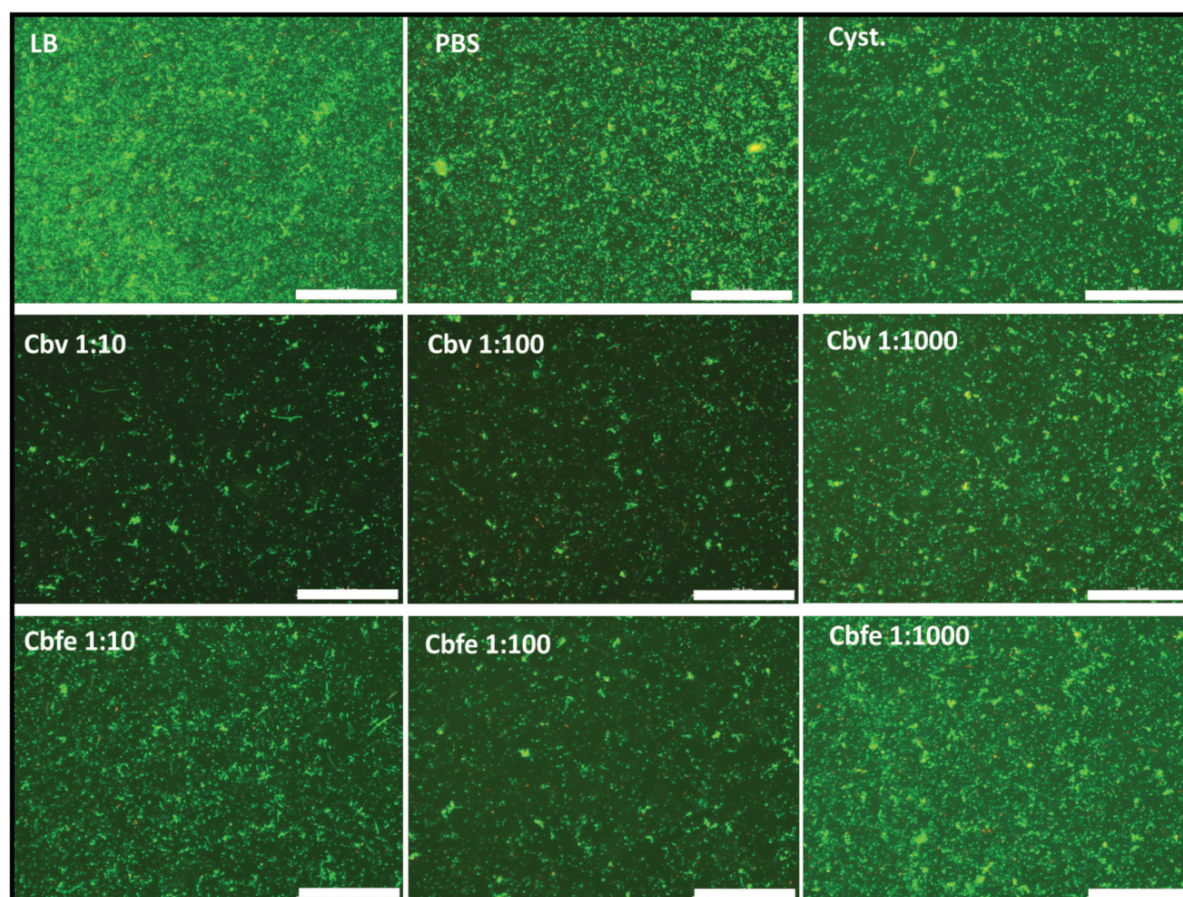


**Fig. 2** Biofilm inhibition assay. Fluorescence microscopy of *E. coli* biofilms grown on glass coverslips for 48 h with various dilutions of Cbfe and Cbv OMV suspensions or control treatments (LB medium, PBS, and cystobactamid [Cyst.]). Syto9 fluorescence (green) labels all cells, propidium iodide fluorescence (red) labels cells with a compromised membrane. The concentrations of the OMV suspensions are 1 : 10 =  $1 \times 10^{12}$  particles per mL for Cbv and  $1 \times 10^{13}$  particles per mL for Cbfe. The 1 : 10 and 1 : 100 treatments result in less green fluorescence (live bacteria) compared with that of the controls or other treatments. The images are maximum intensity z-projections of z-stack images. Scale bar = 100  $\mu$ m. Micrographs are representative of three independent experiments.

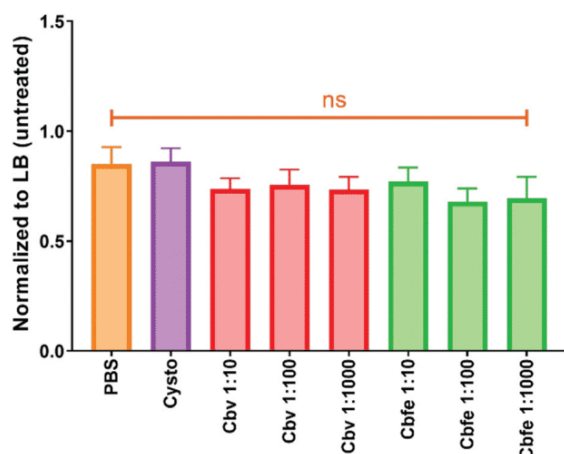


Fig. 3 Biofilm inhibition assay: mean fluorescence intensity of Syto9 (live bacteria) detected by microplate reader. Biofilms were grown for 48 h with dilutions of Cbfe or Cbv OMV suspensions (1 : 10 =  $1 \times 10^{12}$  particles per mL for Cbv and  $1 \times 10^{13}$  particles per mL for Cbfe) and controls (LB medium, PBS, and cystobactamid).  $n = 9$  from three biological replicates. Mean  $\pm$  SEM. ns = not significant.

antibacterial effects against planktonic bacteria;<sup>21,22</sup> however, Cbfe-derived OMVs showed a toxic effect against immune cells when applied at high concentrations.<sup>22</sup> Although the treatment with OMVs may affect biofilm adhesion, our experimental setting does not allow us to clarify whether OMV treatment has antibacterial effects against the biofilm. To address this possibility, we assessed bacterial viability in the biofilm after both biofilm assays using a fluorescence assay.

The biofilms were inoculated in black, clear-bottom 96-well plates followed by staining using the LIVE/DEAD BacLight Bacterial Cell Viability Kit. This kit contains the dyes Syto9 (green), which stains all bacterial cells, and propidium iodide (red), which enters cells with disrupted membranes, staining their nucleic acid, which allows differentiation between intact (green) and non-intact (red) cells. The plates were then imaged using an automated fluorescence microscope (LionheartFX). The fluorescence intensity was assessed using a microplate reader. In the biofilm inhibition assay, the control treatments (Lysogeny broth [LB], PBS, and cystobactamid) promoted the formation of a homogenous biofilm layer (Fig. 2), indicating that the mature biofilms contained viable bacteria, as

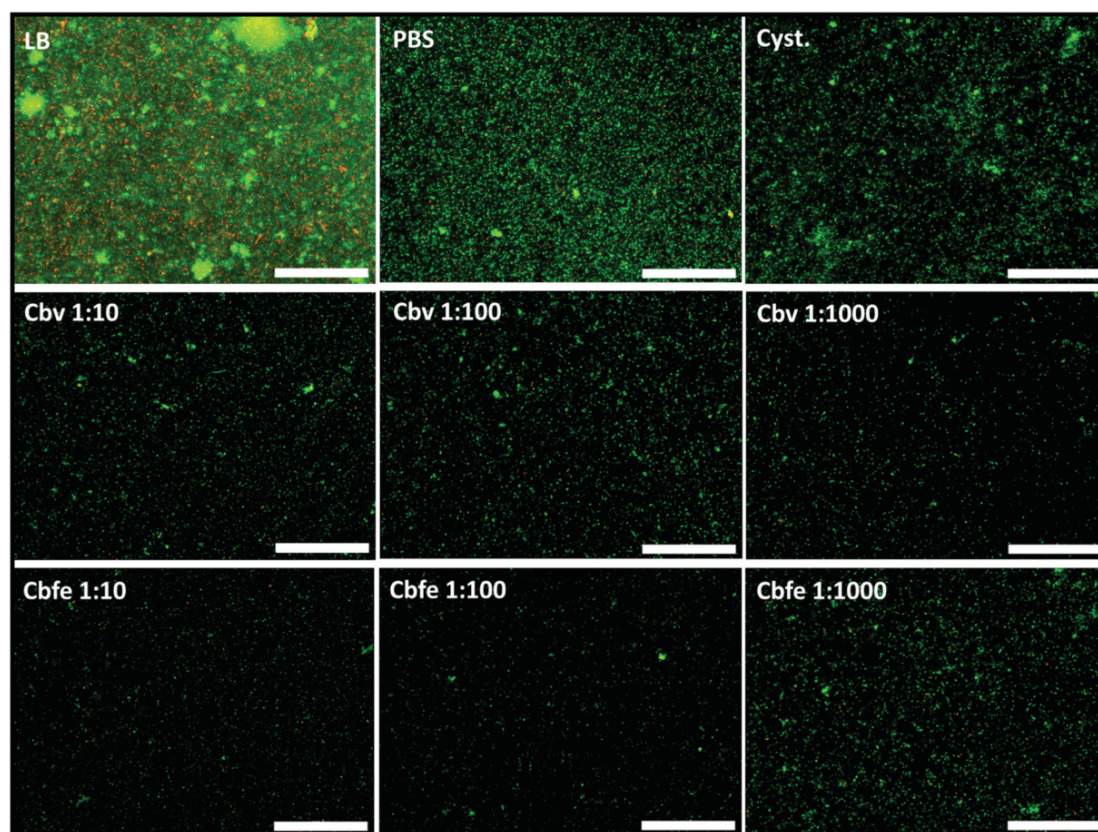


Fig. 4 Preformed biofilm assay. Fluorescence microscopy of *E. coli* biofilms grown for 72 h with various dilutions of Cbfe and Cbv OMV suspensions or control treatments (LB medium, PBS, and cystobactamid [Cyst.]). Syto9 fluorescence (green) labels all cells, propidium iodide fluorescence (red) labels cells with a damaged membrane. The concentrations of the OMV suspensions are 1 : 10 =  $1 \times 10^{12}$  particles per mL for Cbv and  $1 \times 10^{13}$  particles per mL for Cbfe. Treatments with any of the Cbv OMV dilutions resulted in less green fluorescence compared with that for the control treatments. The images are maximum intensity z-projections of z-stack images. Scale bar = 100  $\mu$ m. Micrographs are representative of three independent experiments.

expected. However, when the biofilm was treated with cystobactamid and the OMV suspensions, the fluorescence intensity did not significantly decrease when compared with that for the PBS control treatment (Fig. 3). This result indicated that the treatments could not inhibit the presence of viable bacterial cells.

In the preformed biofilm assay, we observed the formation of large biofilm clumps, a typical characteristic of a mature biofilm,<sup>32</sup> when the *E. coli* were incubated with LB medium (Fig. 4). With the other control treatments (PBS and cystobactamid), live surface-attached bacterial cells also could be observed, but not as abundantly as with the LB medium treatment. This effect may have been due to the lack of nutrients in these solutions. Furthermore, in the preformed biofilm assay, treatment with any of the OMV dilutions resulted in a low Syto9 fluorescence signal for bacterial cells (Fig. 5), while no biofilm formation was observed (Fig. 4). This result could be explained by the presence of a cystobactamid cargo in the OMVs,<sup>21,22</sup> which, in combination with other OMV components, may have elicited an antibiofilm effect rather than a bacteriolytic effect in this assay. The microplate reader analysis showed that the Syto9 fluorescence intensity associated with all the OMV dilutions was significantly lower than that obtained with the PBS control treatment but tended to be comparable among each other (Fig. 5). Nonetheless, no biofilm formation was recorded (Fig. 4). Our results indicated that OMV treatment might not have a direct bacteriolytic effect on the bacteria in the biofilm, but may instead exert anti-aggregation and antibiofilm activity, potentially by acting against biofilm-specific components such as the extracellular matrix.

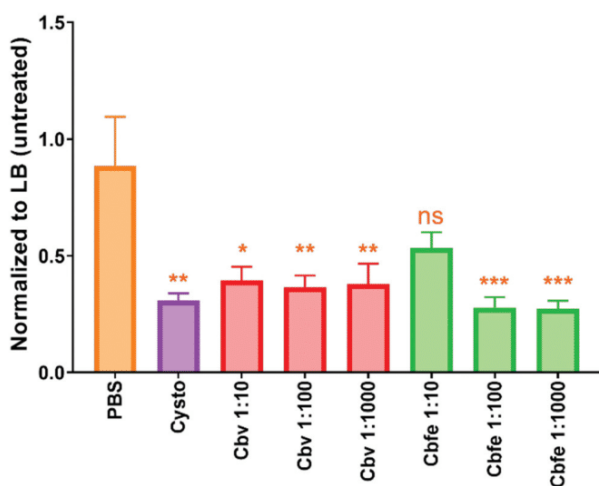


Fig. 5 Preformed biofilm assay: mean fluorescence intensity of Syto9 (live bacteria) detected by microplate reader. Biofilms were grown for 72 h and then treated with the indicated dilutions of Cbfe and Cbv OMV suspensions (1:10 =  $1 \times 10^{12}$  particles per mL for Cbv and  $1 \times 10^{13}$  particles per mL for Cbfe) and controls (LB medium, PBS, and cystobactamid), for 24 h.  $n = 9$  from three biological replicates. Mean  $\pm$  SEM. Orange stars (\*) represent statistical comparisons with PBS treatment. \*  $p = 0.0130$ , \*\*  $p < 0.01$ , \*\*\*  $p < 0.001$ ; ns = not significant.

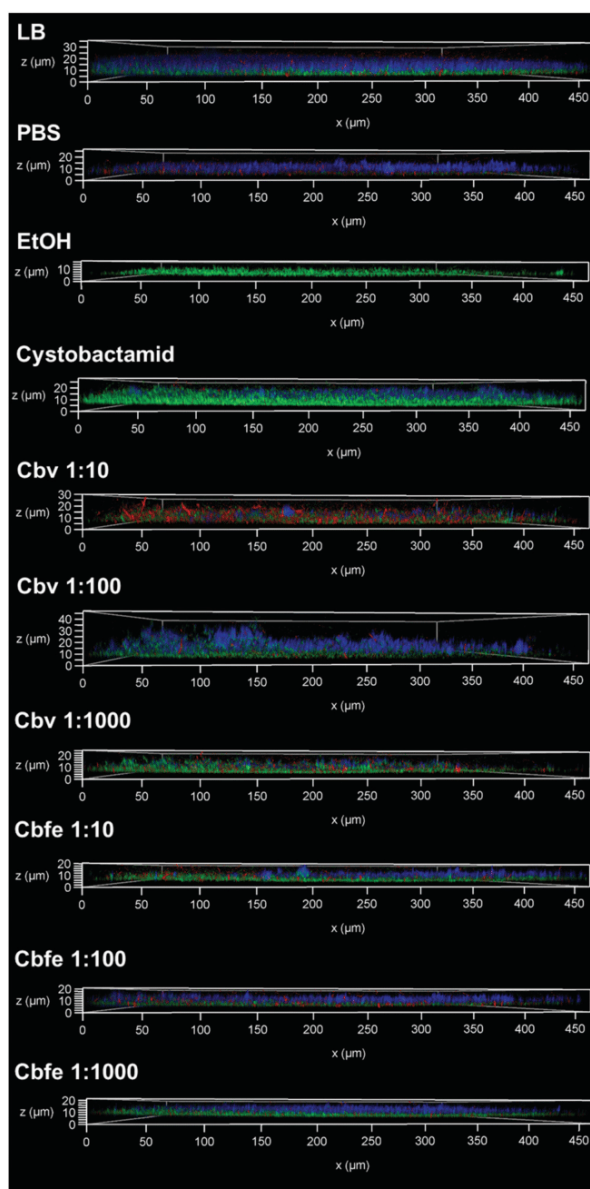


Fig. 6 Confocal laser scanning microscopy of the preformed biofilm assay after 24 h of treatment. The concentrations of the OMV suspensions were 1:10 =  $1 \times 10^{12}$  particles per mL for Cbv and  $1 \times 10^{13}$  particles per mL for Cbfe. Syto9 fluorescence (green) labels all cells, propidium iodide fluorescence (red) labels cells with a damaged membrane, and Hoechst 33342 (blue) labels extracellular DNA. The intact biofilm (treated with LB medium) was homogenous and flat and displayed a stronger Hoechst dye signal when compared with the other treatments. Following treatment with PBS, cystobactamid, or ethanol (EtOH), the thickness of the biofilm was reduced compared with the LB-treated sample. Treatment with the highest concentration of Cbv OMVs (1:10 dilution) resulted in a greater number of bacteria with a damaged membrane (red fluorescence); however, the thickness of the biofilm was similar to that of the LB-treated sample. The biofilm treated with the second highest concentration of Cbv OMVs (1:100 dilution) presented an irregular structure, whereas treatment with the lowest concentration (1:1000 dilution) decreased the thickness of the biofilm. Cbfe OMV treatment at all concentrations reduced biofilm thickness compared with the LB medium control treatment.

## Communication

Interestingly, the effect of the OMV treatment seemed to be more pronounced in the preformed biofilm assay. The extracellular matrix is an important biofilm component and is formed by extracellular polymeric substances (EPSs), the composition of which varies between species; however, EPSs often include proteins, polysaccharides, amphiphilic molecules, and DNA, substances that are essential for maintaining the biofilm architecture and, consequently, its survival. EPSs mediate cell attachment to surfaces, cell-cell adhesion, and hydration through water accumulation, while also being a source of nutrients and providing protection.<sup>33–35</sup> To investigate the overall effect of the OMVs on the biofilm extracellular matrix, the biofilms generated in the preformed biofilm assay were further stained with 100  $\mu\text{L}$  of a 20  $\mu\text{g mL}^{-1}$  Hoechst 33342 solution, a dye that binds to DNA, a common extracellular component of biofilms. Ethanol was used as the negative control. The LB medium and PBS control treatments resulted in a uniform, flat biofilm containing membrane-damaged bacteria (red) and extracellular DNA (blue), with the LB-treated sample presenting a thick biofilm (Fig. 6). With the ethanol control treatment, only a thin layer of bacteria developed, while the cystobactamid-treated sample presented a homogenous layer of bacteria and the presence of a small amount of extracellular DNA. The suspension with the highest concentration of Cbv OMVs (1 : 10) showed the presence of bacteria with compromised membrane integrity and little extracellular DNA (blue fluorescence signal). However, Rosenberg and colleagues have shown that the PI fluorescence in biofilms underestimates the viability of adherent bacterial biofilm cells, where 82% of *E. coli* cells still grown upon cultivation, highlighting the importance of further assays to confirm their viability.<sup>36</sup> The samples treated with the Cbfe OMV suspensions presented extracellular DNA, but the formed biofilms were thinner when compared with those of the controls and other samples. These data indicated that the OMV treatment affected the structure of the preformed biofilm matrix, which may facilitate further treatment with antibiotics.

To further investigate the effects of the treatments on the bacterial cells, we inoculated serial dilutions of samples from the preformed biofilm assays in LB agar plates to quantify the numbers of colony-forming units (viable bacteria). No differences in viability were observed between the treatment and control groups (data not shown), indicating that OMV treatment did not directly kill the biofilm bacteria. We also performed a bacterial vitality assay using the RedoxSensor Green (RSG) bacterial vitality kit and flow cytometry. RSG, a metabolic activity biosensor, is reduced by intracellular reductases involved in aerobic metabolism, resulting in the release of stable green fluorescence representative of bacterial cell metabolism.<sup>37,38</sup> The results showed that bacterial cell vitality was significantly decreased following treatment with the highest concentrations of Cbv and Cbfe OMV suspensions (Fig. 7), indicating that the treatments reduced metabolic activity in bacterial cells, and could potentially be used in conjunction with classic antibiotics to treat biofilm infections.

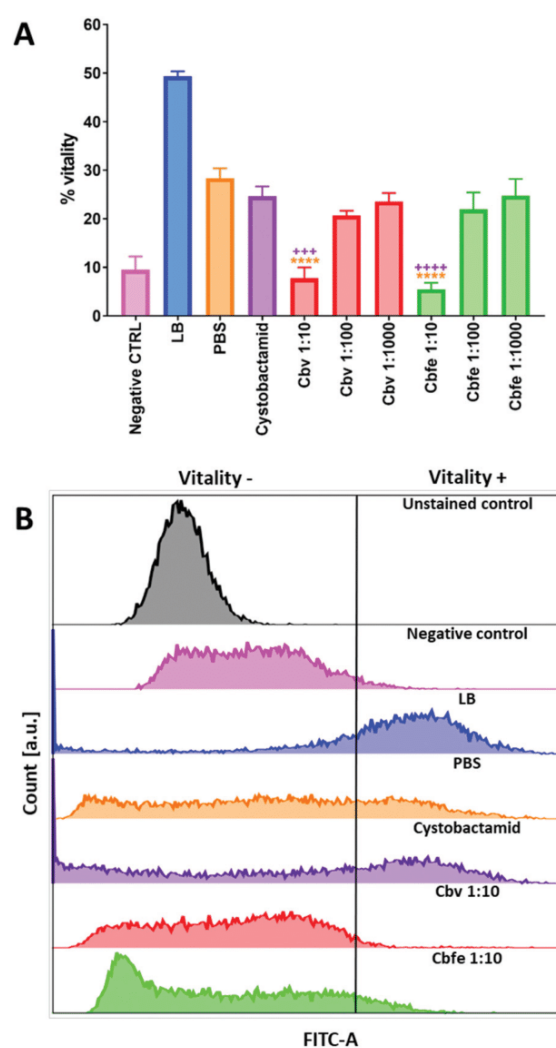
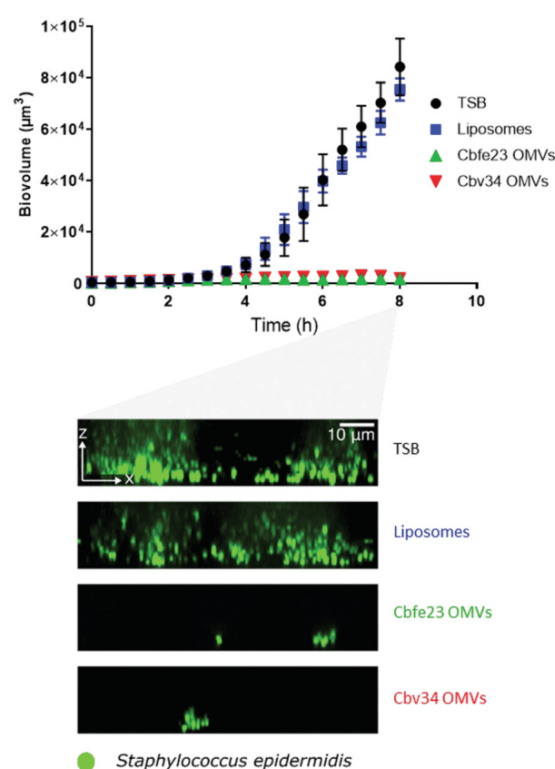


Fig. 7 Flow cytometric analysis of the preformed biofilm assay after 24 h of treatment and staining with RedoxSensor Green (RSG) reagent. The concentrations of the 1 : 10 OMV suspensions were  $1 \times 10^{12}$  particles per mL for Cbv and  $1 \times 10^{13}$  particles per mL for Cbfe. (A) Percentage of *E. coli* TG1 bacteria positive for fluorescein isothiocyanate (FITC), indicative of bacterial vitality. The highest concentrations of the Cbv and the Cbfe suspensions significantly reduced the vitality of the biofilm bacterial cells when compared with that of the LB, PBS, and cystobactamid controls. (B) Representative histogram of the samples.  $n = 6$  of three biological replicates. Mean  $\pm$  SEM. Purple crosses (+) = compared with cystobactamid; orange stars = compared with PBS. \*\*\*\*  $p < 0.0001$ , +++  $p = 0.001$ , ++++  $p < 0.001$ .

To mimic infections such as myocarditis and catheter-associated urinary tract infection, where a biofilm must withstand fluid flow, and to investigate the effect of OMV treatment on a pathogenic bacterium, *Staphylococcus epidermidis* was grown under constant flow in microfluidic chambers. When the bacteria were exposed to Bacto tryptic soy broth (TSB) medium (control) for 8 h, the biovolume increased over time. Bacterial growth further led to the formation of three-dimen-



**Fig. 8** Cbfe23 and Cbv34 OMVs inhibit *S. epidermidis* biofilm formation under flow conditions. Continuous exposure to TSB medium (control) or liposomes (concentration:  $1 \times 10^{12} \text{ mL}^{-1}$ ) for 8 h resulted in bacterial growth, represented by an increase in biovolume over time. Furthermore, the bacteria formed three-dimensional biofilm structures as evidenced by confocal microscopy images in the *xz*-direction. However, in the presence of Cbfe23- or Cbv34-derived OMVs (concentration:  $1 \times 10^{12} \text{ mL}^{-1}$ ), the biovolume did not increase over the 8 h. Additionally, biofilm formation was strongly inhibited, thus showing the antimicrobial effect of the OMVs. Three-four biological replicates were used. Mean  $\pm$  SEM.

sional biofilm structures (Fig. 8). In contrast, continuous OMV treatment exerted a suppressive effect on *S. epidermidis* biofilm formation. Interestingly, treatment with OMVs derived from either strain under these flow conditions markedly inhibited bacterial attachment to the glass surface and biofilm growth. These data demonstrated the unique ability of myxobacterial OMVs to act on biofilm components and inhibit biofilm formation even under physiologically relevant flow conditions. These effects may have been due to their cystobactamid cargo, the presence of a topoisomerase inhibitor,<sup>26</sup> membrane proteins, and/or other OMV-derived cargos. Nevertheless, further investigation is required to elucidate the mechanisms underlying the antibiofilm effects seen in our experiments. To test if this effect was caused by OMV-specific antibacterial and anti-adhesive effects and not unspecific nanoparticle-related effects, *S. epidermidis* was also grown in the presence of bacteriomimetic liposomes made with *E. coli* lipids to mimic the bacterial membrane. The treatment of *S. epidermidis* with these

liposomes did not lead to any antibacterial effects. Within 8 h, the *S. epidermidis* biovolume increased to levels similar to those obtained with the TSB medium-treated controls and the bacteria formed glass surface-attached biofilms, strongly indicating that the OMV treatment alone prevented biofilm formation. These results highlighted the ability of OMVs to act as natural nanocarriers to combat biofilm infections.<sup>39</sup>

## Conclusions

Many microorganisms use biofilm formation as a mechanism to survive in the environment. This allows them to develop tolerance to antibiotics, leading to infections that are difficult to treat. In this study, we evaluated the effects of naturally antibiotic-loaded OMVs derived from *C. velatus* Cbv34 and *C. ferrugineus* Cbfe23 against biofilms and biofilm formation. We found that the OMVs decreased the vitality of the biofilms, being able to detach them from surfaces where they were grown under static incubation, as well as prevent biofilm growth under flow conditions, thus showing their potential applicability in the treatment of these infections.

## Experimental

### Materials

LB broth and hexamethyldisilazane (HMDS) were purchased from Sigma-Aldrich (St Louis, MO, USA). Ethanol (HPLC grade) was purchased from Fisher Scientific (Schwerte, Germany). Bacto tryptic soy broth (TSB) was purchased from BD Biosciences (San Jose, CA, USA). PBS tablets were purchased from Gibco, Life Technologies Corporation (Carlsbad, CA, USA). The LIVE/DEAD BacLight Bacterial Viability Kit and the BacLight RedoxSensor Green Vitality Kit were purchased from Invitrogen Life Technologies Corporation (Carlsbad, CA, USA).

### Myxobacterial culture and OMV isolation

Both *C. velatus* Cbv34 and *C. ferrugineus* Cbfe23 (provided by the Microbial Natural Product Department at the Helmholtz Institute for Pharmaceutical Research Saarland) were cultivated in M-medium (1% papaic digest of soybean meal, 1% maltose, 0.1%  $\text{CaCl}_2$ , 0.1%  $\text{MgSO}_4$ , 50 mM HEPES, pH 7.2) at 30 °C with shaking (180 rpm) until stationary phase as previously described.<sup>21,22</sup> For static biofilm growth assays, a myxobacterial suspension was added to 50 mL falcon tubes and centrifuged for 10 min at 9500g (Beckman Coulter, Brea, CA, USA). The supernatant was then added to a new Falcon tube and centrifuged again for 15 min at 9500g. The resulting supernatant (30 mL) was transferred to polycarbonate ultracentrifuge tubes (ref. number 355631, Beckman Coulter) and the OMVs were pelleted (rotor SW32Ti) for 2 h at 100 000g. All centrifugations were performed at 4 °C. The pellet was resuspended in 300  $\mu\text{L}$  of particle-free PBS. For microfluidic biofilm growth assays, 60 mL of supernatant was added to polycarbo-

## Communication

nate ultracentrifuge tubes (ref. number 355655, Beckman Coulter) and the OMVs were pelleted using a Type 45 Ti fixed-angle titanium rotor at 100 000g for 2 h at 4 °C. The pellets were resuspended in 1 mL of particle-free PBS. Larger particles were pelleted by centrifugation at 300g for 3 min at 4 °C and discarded. The particle size distribution was assessed by NTA (LM-10, Malvern, UK).

#### *E. coli* TG1 and *S. epidermidis* cultivation

*E. coli* strain TG1 (DSM 6056, German Collection of Microorganisms and Cell Cultures) was cultivated overnight on LB agar plates. A single colony was inoculated in 20 mL of liquid LB medium in a sterile conical flask and incubated overnight at 37 °C with shaking at 180 rpm. *S. epidermidis* strain DSM 20044 was grown in LB medium at 37 °C overnight with shaking (250 rpm).

#### Biofilm preparation on glass coverslips for SEM imaging

The *E. coli* TG1 biofilms were cultivated as previously described.<sup>23</sup> Sterilised 12 mm glass coverslips were placed inside the wells of a 24-well plate (Greiner Bio-One, Kremsmünster, Austria). For the preformed biofilm assays, 300 µL of bacterial culture ( $OD_{600} = 0.1$ ; approximately  $1.2 \times 10^8$  CFUs mL<sup>-1</sup>) was added to the wells and incubated statically at 37 °C for 72 h with 5% CO<sub>2</sub>. Non-adherent bacteria were removed and the wells were washed with PBS, resulting in the presence of approximately  $1 \times 10^9$  CFUs mL<sup>-1</sup> in each well. Then, 250 µL of 1:10, 1:100, or 1:1000 dilutions of OMV suspensions or LB medium, PBS, or a 20 µg mL<sup>-1</sup> solution of cystobactamid were added to the wells, followed by incubation for 24 h at 37 °C with 5% CO<sub>2</sub>. The coverslips were subsequently dehydrated *via* serial ethanol dilutions (30, 50, 70, 80, 90, and 100%) for 10 min each. For the biofilm formation inhibition assays, 250 µL of 1:10, 1:100, and 1:1000 dilutions of the OMV suspensions and LB medium, PBS, and a 20 µg mL<sup>-1</sup> solution of cystobactamid were separately added to the wells together with 15 µL of an *E. coli* TG1 overnight culture ( $OD_{600} = 3$ ; approximately  $2 \times 10^9$  CFUs mL<sup>-1</sup>), resulting in the presence of approximately  $2 \times 10^8$  CFUs mL<sup>-1</sup> in each well, and incubated for 48 h at 37 °C with 5% CO<sub>2</sub>. The coverslips were then carefully dehydrated *via* a graded ethanol series as described above and incubated for 20 min with 300 µL of HMDS at room temperature. The HMDS was removed and the coverslips were left to dry overnight under a fume hood. The coverslips were mounted in SEM sample holders, gold-sputtered, and imaged by SEM.

#### Biofilm preparation for fluorescence microscopy imaging and fluorescence intensity quantification

To assess biofilm growth inhibition (the biofilm inhibition assay), 100 µL of an *E. coli* TG1 bacterial suspension ( $OD_{600} = 0.5$ ; approximately  $6 \times 10^8$  CFUs mL<sup>-1</sup>) plus 100 µL of the OMV dilution or control solutions (LB medium, PBS, and 20 µg µL<sup>-1</sup> cystobactamid) were separately added to a 96-well plate (ref. number 655090, Greiner Bio-One) and cultured for 48 h at 37 °C with 5% CO<sub>2</sub>. To assess the effect of the OMVs on pre-

formed biofilms (the preformed biofilm assay), 200 µL of an *E. coli* TG1 bacterial suspension ( $OD_{600} = 0.5$ ; approximately  $6 \times 10^8$  CFUs mL<sup>-1</sup>) was added to a 96-well plate and cultured for 72 h at 37 °C with 5% CO<sub>2</sub>. The number of bacteria used in the fluorescence assays was higher than that used for the SEM assays because, at an  $OD_{600} = 0.1$ , the TG1 bacteria could not form a thick and stable biofilm on the plastic bottom of a 96-well plate. The supernatant was carefully removed, and the wells were washed with 200 µL of PBS. Then, 200 µL of each OMV dilution or each control solution (LB medium, PBS, and 20 µg µL<sup>-1</sup> cystobactamid) was separately added to the wells and incubated for 24 h at 37 °C with 5% CO<sub>2</sub>. After the incubation period, the biofilms from both assays were stained using the LIVE/DEAD BacLight Bacterial Viability Kit (Invitrogen, Thermo Fisher Scientific Corp., Waltham, MA, USA) for 15 min at 37 °C and fixed in 3.7% paraformaldehyde for 30 min at 37 °C. Fluorescence images were obtained with a LionheartFX device (BioTek Instruments, Winooski, VT, USA). The fluorescence intensity of cells (Syto9) in both biofilm assays was quantified with a microplate reader (Infinite M200 Pro, Tecan Group Ltd, Männedorf, Switzerland) using multiple reads per well in a circle (4 × 4), an excitation wavelength of 485 nm, an emission wavelength of 530 nm, a manual gain of 100, and 25 flashes. For confocal laser scanning microscopy, the preformed biofilms were additionally stained with 100 µL of a 20 µg mL<sup>-1</sup> Hoechst 33342 solution for 15 min at 37 °C and imaged with a confocal microscope (Leica TCS SP8, Leica Microsystems, Wetzlar, Germany). The obtained images were processed using LAS X software (LAS X 1.8.013370, Leica Microsystems).

#### Preparation of the biofilm for flow cytometric analysis

To assess the impact of the OMV treatment on the vitality of preformed biofilms (the preformed biofilm assay), 200 µL of an *E. coli* TG1 bacterial suspension ( $OD_{600} = 0.5$ ; approximately  $6 \times 10^8$  CFUs mL<sup>-1</sup>) was added to a black, clear-bottom 96-well plate (ref. number 655090, Greiner Bio-One) and cultured for 72 h at 37 °C with 5% CO<sub>2</sub>. The supernatant was carefully removed, and the wells were washed with 200 µL of PBS. Then, 200 µL of each OMV dilution or each control solution (LB medium, PBS, and 20 µg µL<sup>-1</sup> cystobactamid) was separately added to the wells and incubated for 24 h at 37 °C with 5% CO<sub>2</sub>. After the incubation period, the biofilms were vigorously dispersed using a micropipette and the content of each well was added to flow cytometry tubes. The samples were diluted in 900 µL of PBS and then stained with RSG for 15 min at 37 °C. The negative control was prepared by adding 50 µL of the sodium azide solution included in the kit to a tube containing an untreated control (LB) for 5 min at room temperature. For flow cytometric analysis (LSRFortessa, BD Biosciences), an untreated sample was used to set a 10 000-live-cell threshold to be analysed from the log of a forward *versus* side scatter (FSC *vs.* SSC) gating. A sample treated with sodium azide solution (negative control) was used to set up the fluorescein isothiocyanate (FITC) gate. The numbers of positive cells were determined using FlowJo 10.7 software

(FlowJo LLC, Ashland, OR, USA) in the FITC area channel (FITC-A).

### Bacteriomimetic liposome preparation

Liposomes were prepared following a previously described protocol.<sup>22</sup> A solution of 6% (w/v) phospholipid was obtained by dissolving 1-hexadecanoyl-2-(9Z-octadecenoyl)-sn-glycerol-3-phosphoethanolamine (POPE), 1-hexadecanoyl-2-(9Z-octadecenoyl)-sn-glycerol-3-phospho-(1'-rac-glycerol) (sodium salt) (POPG), and 1,1',2,2'-tetra-(9Z-octadecenoyl) cardiolipin (sodium salt) (CL) (Avanti Polar Lipids Inc., Alabaster, AL, USA) (weight ratio 70:20:10) in 5 mL of a chloroform-methanol mixture (2:1) in a round-bottom flask (250 mL). A Rotavapor R-205 (BÜCHI Labor Technik GmbH, Essen, Germany) was used to remove the solvent under low pressure (60 min, 200 mbar, 135 rpm, 80 °C; 30 min, 40 mbar, 135 rpm, 80 °C). The formed lipid biofilms were rehydrated by adding 5 mL of PBS (pH 7.4) containing 10% (v/v) ethanol and rotating for 60 min (70 °C, 135 rpm, atmospheric pressure). The acquired liposomes were sonicated for 60 min followed by extrusion (10 times) at 70 °C using a Liposfast L-50 extruder (Avestin Europe GmbH, Mannheim, Germany).

### OMV-bacteria interaction during *S. epidermidis* biofilm formation

Overnight cultures of *S. epidermidis* constitutively expressing sfGFP were diluted to an OD<sub>600</sub> of 0.1 in TSB medium and inoculated into microfluidic flow chambers made of polydimethylsiloxane bonded to a glass coverslip (flow chamber dimensions: 500 µm width, 100 µm height, 7 mm length). Following bacterial colonization of the glass surface for 1 h without flow, syringes containing OMVs (diluted in TSB medium) or control treatments were connected to the flow chambers with polyethylene tubing. To remove non-adherent cells, the flow rate was set to 5 µL min<sup>-1</sup> for 1 min using a syringe pump (Harvard Apparatus). After this brief period of high flow, the flow rate was decreased to 0.1 µL min<sup>-1</sup> and kept constant until the end of the experiments.

To monitor *S. epidermidis* biofilm growth in the presence or absence of OMVs, bacteria were imaged with a confocal scanner unit (CSU; Yokogawa) mounted on a Nikon Ti-E inverted microscope using a 100× oil objective with 1.45 NA (Nikon, Tokyo, Japan). sfGFP excitation was performed with a 488 nm laser and images were acquired every 30 min with an Andor iXon EMCCD camera. The hardware was controlled by NIS Elements (Nikon). The microscope was equipped with an incubation chamber to enable *S. epidermidis* biofilm growth at 37 °C. The images were analysed using BiofilmQ software.<sup>40</sup>

### Data analysis

The data are displayed as means ± standard error of the mean (SEM). The number of independent experiments (*n*) is shown in each figure. The experiments and measurements were conducted at least in biological triplicates. The results were analysed in GraphPad Prism 9.1.2 (GraphPad Software, San Diego, CA, USA) using one-way ANOVA with Tukey's multiple comparisons test.

## Author contributions

A.G. performed all the experiments, analysed the data, wrote the manuscript, and prepared the figures. L.V. performed the biofilm experiments with *S. epidermidis*. K.D. supervised the biofilm experiments with *S. epidermidis*. G.F. conceived the project, supervised the work, and wrote the manuscript together with A.G. All the authors revised the text of the manuscript.

## Conflicts of interest

There are no conflicts to declare.

## Acknowledgements

This work was supported by a research grant from the Federal Ministry of Research and Education (NanoMatFutur programme, grant number 13XP5029A) and the European Research Council (StG-716734). The authors would like to thank Dr Ronald Garcia for providing myxobacterial strains and Dr Robert Richter for providing the bacteriomimetic liposomes.

## Notes and references

- 1 L. Hall-Stoodley, J. W. Costerton and P. Stoodley, Bacterial biofilms: from the natural environment to infectious diseases, *Nat. Rev. Microbiol.*, 2004, **2**, 95–108.
- 2 V. M. Siqueira and N. Lima, Biofilm Formation by Filamentous Fungi Recovered from a Water System, *J. Mycol.*, 2013, **2013**, 1–9.
- 3 H.-C. Flemming and S. Wuerz, Bacteria and archaea on Earth and their abundance in biofilms, *Nat. Rev. Microbiol.*, 2019, **17**, 247–260.
- 4 D. de Beer, P. Stoodley, F. Roe and Z. Lewandowski, Effects of biofilm structures on oxygen distribution and mass transport, *Biotechnol. Bioeng.*, 1994, **43**, 1131–1138.
- 5 J. R. Lawrence, D. R. Korber, B. D. Hoyle, J. W. Costerton and D. E. Caldwell, Optical sectioning of microbial biofilms, *J. Bacteriol.*, 1991, **173**, 6558–6567.
- 6 S. Halvaei, *et al.*, Exosomes in Cancer Liquid Biopsy: A Focus on Breast Cancer, *Mol. Ther. Nucleic Acids*, 2018, **10**, 131–141.
- 7 V. Van Giau, S. S. A. An and J. Hulme, Recent advances in the treatment of pathogenic infections using antibiotics and nano-drug delivery vehicles, *Drug Des. Devel. Ther.*, 2019, **13**, 327–343.
- 8 T. Bjarnsholt, O. Ciofu, S. Molin, M. Givskov and N. Høiby, Applying insights from biofilm biology to drug development—can a new approach be developed?, *Nat. Rev. Drug Discovery*, 2013, **12**, 791–808.
- 9 J. D. Bryers, Medical biofilms, *Biotechnol. Bioeng.*, 2008, **100**, 1–18.

## Communication

- 10 D. Davies, Understanding biofilm resistance to antibacterial agents, *Nat. Rev. Drug Discovery*, 2003, **2**, 114–122.
- 11 M. R. Parsek and P. K. Singh, Bacterial Biofilms: An Emerging Link to Disease Pathogenesis, *Annu. Rev. Microbiol.*, 2003, **57**, 677–701.
- 12 A. L. Flores-Mireles, J. N. Walker, M. Caparon and S. J. Hultgren, Urinary tract infections: epidemiology, mechanisms of infection and treatment options, *Nat. Rev. Microbiol.*, 2015, **13**, 269–284.
- 13 N. Høiby, T. Bjarnsholt, M. Givskov, S. Molin and O. Ciofu, Antibiotic resistance of bacterial biofilms, *Int. J. Antimicrob. Agents*, 2010, **35**, 322–332.
- 14 A. Bridier, R. Briandet, V. Thomas and F. Dubois-Brissonnet, Resistance of bacterial biofilms to disinfectants: a review, *Biofouling*, 2011, **27**, 1017–1032.
- 15 U. Römling and C. Balsalobre, Biofilm infections, their resilience to therapy and innovative treatment strategies, *J. Intern. Med.*, 2012, **272**, 541–561.
- 16 C. R. Arciola, D. Campoccia and L. Montanaro, Implant infections: adhesion, biofilm formation and immune evasion, *Nat. Rev. Microbiol.*, 2018, **16**, 397–409.
- 17 J. Herrmann, A. A. Fayad and R. Müller, Natural products from myxobacteria: novel metabolites and bioactivities, *Nat. Prod. Rep.*, 2017, **34**, 135–160.
- 18 H. Reichenbach, K. Gerth, H. Irschik, B. Kunze and G. Höfle, Myxobacteria: a source of new antibiotics, *Trends Biotechnol.*, 1988, **6**, 115–121.
- 19 A. T. Jan, Outer Membrane Vesicles (OMVs) of Gram-negative bacteria: A perspective update, *Front. Microbiol.*, 2017, **8**, 1–11.
- 20 L. P. Jahromi and G. Fuhrmann, Bacterial extracellular vesicles: Understanding biology promotes applications as nanopharmaceuticals, *Adv. Drug Delivery Rev.*, 2021, **173**, 125–140.
- 21 E. Schulz, *et al.*, Biocompatible bacteria-derived vesicles show inherent antimicrobial activity, *J. Controlled Release*, 2018, **290**, 46–55.
- 22 A. Goes, *et al.*, Myxobacteria-Derived Outer Membrane Vesicles: Potential Applicability Against Intracellular Infections, *Cells*, 2020, **9**, 194.
- 23 C. V. Montefusco-Pereira, *et al.*, Coupling quaternary ammonium surfactants to the surface of liposomes improves both antibacterial efficacy and host cell biocompatibility, *Eur. J. Pharm. Biopharm.*, 2020, **149**, 12–20.
- 24 M. B. Estevez, S. Raffaelli, S. G. Mitchell, R. Faccio and S. Alborés, Biofilm Eradication Using Biogenic Silver Nanoparticles, *Molecules*, 2020, **25**, 2023.
- 25 H. D. Lu, *et al.*, Modulating *Vibrio cholerae* Quorum-Sensing-Controlled Communication Using Autoinducer-Loaded Nanoparticles, *Nano Lett.*, 2015, **15**, 2235–2241.
- 26 S. Baumann, *et al.*, Cystobactamids: Myxobacterial Topoisomerase Inhibitors Exhibiting Potent Antibacterial Activity, *Angew. Chem., Int. Ed.*, 2014, **53**, 14605–14609.
- 27 R. Raju, K. I. Mohr, S. Bernecker, J. Herrmann and R. Müller, Cystodienoic acid: A new diterpene isolated from the myxobacterium *Cystobacter* sp, *J. Antibiot.*, 2015, **68**, 473–475.
- 28 D. H. Limoli, C. J. Jones and D. J. Wozniak, Bacterial Extracellular Polysaccharides in Biofilm Formation and Function, *Microbiol. Spectr.*, 2015, **3**, 1–19.
- 29 É. Hell, C. G. Giske, A. Nelson, U. Römling and G. Marchini, Human cathelicidin peptide LL37 inhibits both attachment capability and biofilm formation of *Staphylococcus epidermidis*, *Letts. Appl. Microbiol.*, 2010, **50**, 211–215.
- 30 C. P. Timmerman, *et al.*, Characterisation and functional aspects of monoclonal antibodies specific for surface proteins of coagulase-negative staphylococci, *J. Med. Microbiol.*, 1991, **35**, 65–71.
- 31 M. A. Banner, *et al.*, Localized tufts of fibrils on *Staphylococcus epidermidis* NCTC 11047 are comprised of the accumulation-associated protein, *J. Bacteriol.*, 2007, **189**, 2793–2804.
- 32 P. P. Mahamuni-Badiger, *et al.*, Biofilm formation to inhibition: Role of zinc oxide-based nanoparticles, *Mater. Sci. Eng., C*, 2020, **108**, 110319.
- 33 H. Flemming and J. Wingender, The biofilm matrix, *Nat. Rev. Microbiol.*, 2010, **8**, 623–633.
- 34 S. Schlafer and R. L. Meyer, Confocal microscopy imaging of the biofilm matrix, *J. Microbiol. Methods*, 2017, **138**, 50–59.
- 35 F. Díaz-Pascual, *et al.*, Breakdown of *Vibrio cholerae* biofilm architecture induced by antibiotics disrupts community barrier function, *Nat. Microbiol.*, 2019, **4**, 2136–2145.
- 36 M. Rosenberg, N. F. Azevedo and A. Ivask, Propidium iodide staining underestimates viability of adherent bacterial cells, *Sci. Rep.*, 2019, **9**, 1–12.
- 37 J. Baert, *et al.*, Microbial population heterogeneity versus bioreactor heterogeneity: Evaluation of Redox Sensor Green as an exogenous metabolic biosensor, *Eng. Life Sci.*, 2016, **16**, 643–651.
- 38 M. C. Konopka, *et al.*, Respiration Response Imaging for Real-Time Detection of Microbial Function at the Single-Cell Level, *Appl. Environ. Microbiol.*, 2011, **77**, 67–72.
- 39 A. Goes and G. Fuhrmann, Biogenic and Biomimetic Carriers as Versatile Transporters to Treat Infections, *ACS Infect. Dis.*, 2018, **4**, 881–892.
- 40 R. Hartmann, *et al.*, Quantitative image analysis of microbial communities with BiofilmQ, *Nat. Microbiol.*, 2021, **6**, 151–156.

## Supplementary Information

### Interaction of myxobacteria-derived outer membrane vesicles with biofilms: antiadhesive and antibacterial effects

Adriely Goes, Lucia Vidakovic, Knut Drescher, and Gregor Fuhrmann

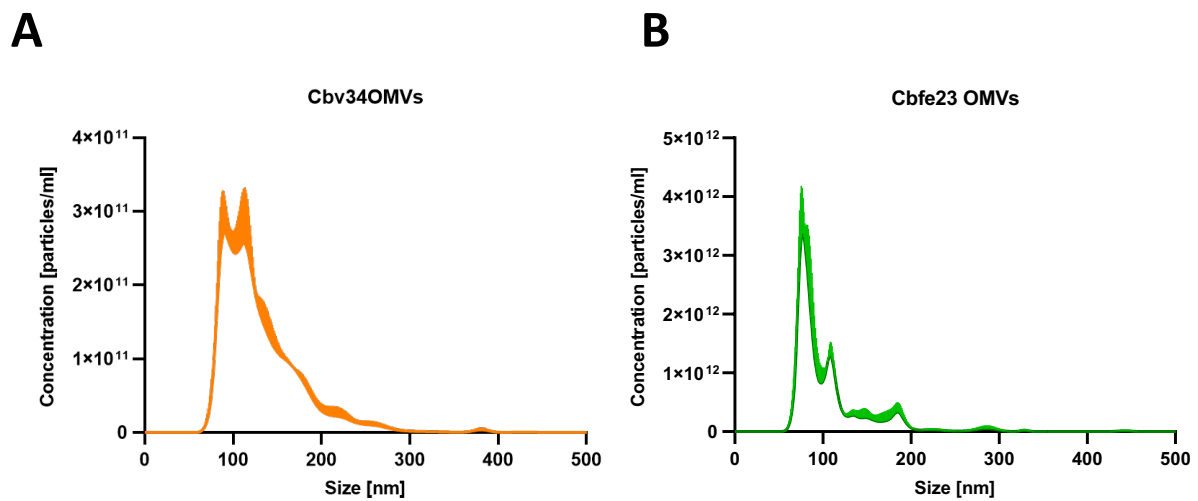


**Figure S1:** Representative graph of size distribution of (A) Cbv34 OMV pellet and (B) Cbfe23 OMV pellet measured by nanoparticle tracking analysis (NTA). Values are the mean + SEM.

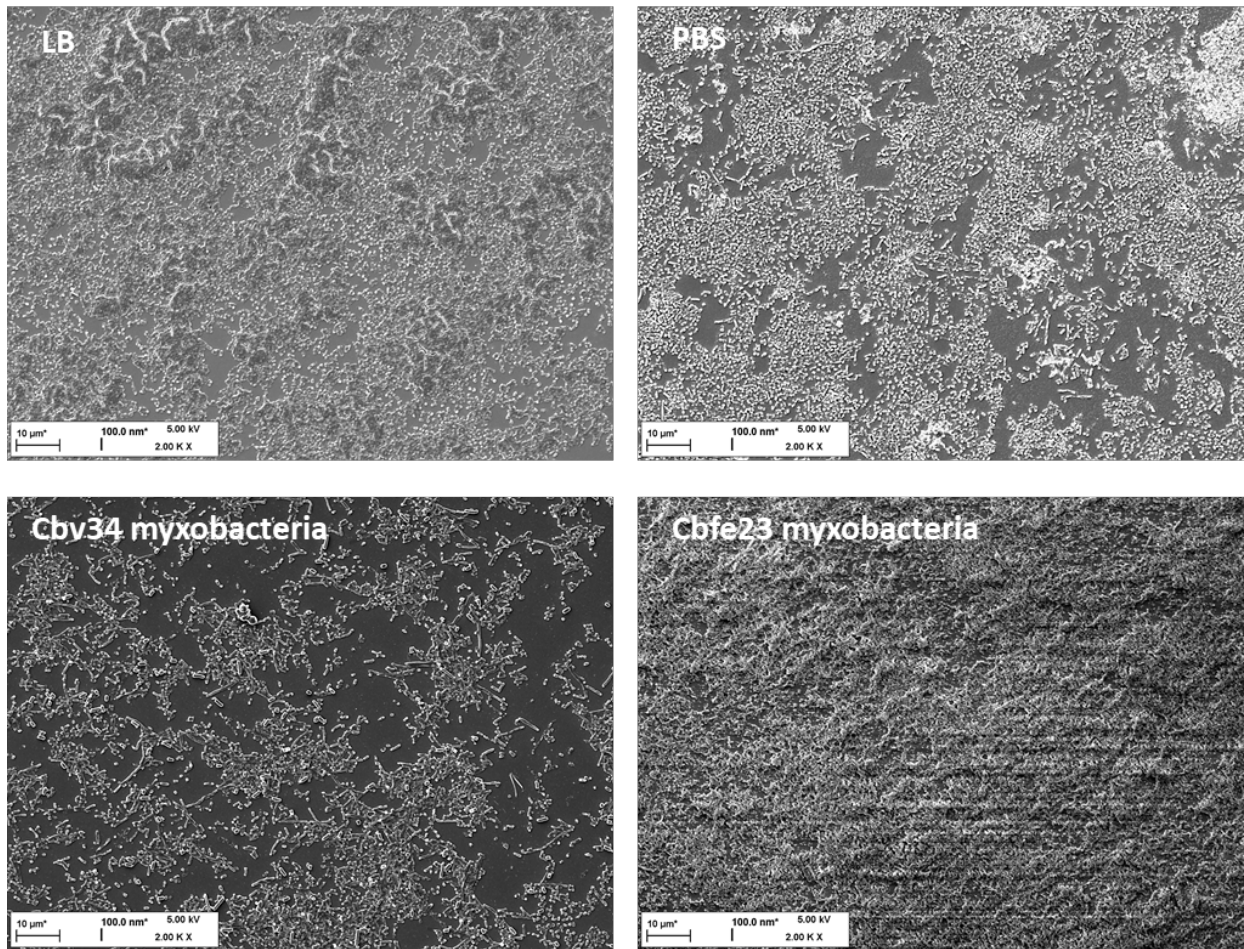


**Figure S2:** Representative scanning electron microscopy (SEM) of the preformed biofilm assay. The biofilm was treated with myxobacterial suspensions of Cbv34 and Cbfe23 diluted to OD<sub>600</sub> 0.5 and incubated for 24 h at 37 °C.

## 7 LIST OF SCIENTIFIC PUBLICATIONS

- (1) **Goes, A.**, & Fuhrmann, G. (2018). Biogenic and Biomimetic Carriers as Versatile Transporters to Treat Infections. *ACS Infectious Diseases*, 4(6), 881–892. <https://doi.org/10.1021/acsinfecdis.8b00030>
- (2) Schulz, E., **Goes, A.**, Garcia, R., Panter, F., Koch, M., Müller, R., Fuhrmann, K., & Fuhrmann, G. (2018). Biocompatible bacteria-derived vesicles show inherent antimicrobial activity. *Journal of Controlled Release*, 290(September), 46–55. <https://doi.org/10.1016/j.jconrel.2018.09.030>
- (3) **Goes, A.**, Lapuhs, P., Kuhn, T., Schulz, E., Richter, R., Panter, F., Dahlem, C., Koch, M., Garcia, R., Kiemer, A. K., Müller, R., & Fuhrmann, G. (2020). Myxobacteria-Derived Outer Membrane Vesicles: Potential Applicability Against Intracellular Infections. *Cells*, 9(1), 194. <https://doi.org/10.3390/cells9010194>
- (4) Anversa Dimer, F., de Souza Carvalho-Wodarz, C., **Goes, A.**, Cirnski, K., Herrmann, J., Schmitt, V., Pätzold, L., Abed, N., De Rossi, C., Bischoff, M., Couvreur, P., Müller, R., & Lehr, C.-M. (2020). PLGA nanocapsules improve the delivery of clarithromycin to kill intracellular *Staphylococcus aureus* and *Mycobacterium abscessus*. *Nanomedicine: Nanotechnology, Biology and Medicine*, 24, 102125. <https://doi.org/10.1016/j.nano.2019.102125>
- (5) Montefusco-Pereira, C. V., Formicola, B., **Goes, A.**, Re, F., Marrano, C. A., Mantegazza, F., Carvalho-Wodarz, C., Fuhrmann, G., Caneva, E., Nicotra, F., Lehr, C., & Russo, L. (2020). Coupling quaternary ammonium surfactants to the surface of liposomes improves both antibacterial efficacy and host cell biocompatibility. *European Journal of Pharmaceutics and Biopharmaceutics*, 149(July 2019), 12–20. <https://doi.org/10.1016/j.ejpb.2020.01.013>
- (6) **Goes, A.**, Vidakovic, L., Drescher, K., & Fuhrmann, G. (2021). Interaction of myxobacteria-derived outer membrane vesicles with biofilms: antiadhesive and antibacterial effects. *Nanoscale*. <https://doi.org/10.1039/D1NR02583J>
- (7) Richter, R., Kamal, M. A. M., Koch, M., Niebuur, B., Huber, A., **Goes, A.**, Volz, C., Vergalli, J., Kraus, T., Müller, R., Schneider-Daum, N., Fuhrmann, G., Pagès, J., & Lehr, C. (2021). An Outer Membrane Vesicle-Based Permeation Assay (OMPA) for Assessing Bacterial Bioavailability. *Advanced Healthcare Materials*, 2101180, 2101180. <https://doi.org/10.1002/adhm.202101180>

## 8 ACKNOWLEDGMENTS

Prof. Dr. Gregor Fuhrmann—for the trust and unshakable optimism while we worked together in this project. Thank you for your guidance, patience and all the opportunities you have given me to learn and grow as a scientist.

Prof. Dr. Claus-Michael Lehr and Dr. Cristiane de Souza Carvalho Wodarz—for giving me a chance to join HIPS for my Diploma thesis in 2016 and for teaching me so much. The knowledge I gained with you was essential in conducting this PhD project.

Prof. Dr. Alexandra Kiemer—for the good advice and for the scientific collaboration.

Sandra Lustig and Alexander Radziewski—for helping me in making my dreams come true! Thank you so much for the trust and support!

My PhD time at HIPS would not be as awesome as it was without the friendship of Dr. Maximilian Richter, Dr. Eilien Heinrich, Thomas Kuhn, Mina Mehanny and Dr. Cristina Zivko (even from far away). We are friends for life!

I am thankful to the whole BION group, especially Phillip Lapuhs, who I had the pleasure to supervise—for the support with OMV characterization and staining for the *Cells* paper.

All my friends at DDEL, especially Dr. Sara Menina, Dr. Hanzey Yasar, Justus Horstmann, Patrick Carius, Olga Hartwig, Sara Nasr, Mohammed Kamal, Sarah Frisch, Lena Kliesch—for the nice times and scientific help.

Jana Westhues, Petra König, Dr. Chiara de Rossi, Pascal Paul, Dr. Annette Boese, Stefanie Neuber—for your valuable technical support.

Karin Gross, Sarah Müller and Annette Herkströter—for your assistance with everything bureaucratic.

Dr. Ronald Garcia—for the great scientific collaboration and for teaching me how to handle our dear myxobacteria.

Remi Hendrix-Jastrzebski—for being an amazing friend! I know I can count on you always and, of course, you can count on me!

Florian Richter—for always having an open ear for me and for supporting and encouraging me.

Dr. Carlos Montefusco—for the friendship, scientific collaboration and all the times you paid for my Camembert-Preiselbeeren burger.

Alana Miranda—who dreamed of this moment with me a very long time ago and supported me all the way.

Bryan Weaver, always my NaviGator—for your friendship and the English revisions throughout my PhD time.

Elder Patten-Ferreira, André Cunha, Derick Rosa, Hyago Oliveira, Renato Oliveira and Fernanda Karen—for all the years of support and friendship.

Dipl.-Psych. Henning Löbbcke—for helping me in this very funny task of understanding my beautiful and “crazy” brain.

Monique Valente—for all the nice meditation and for helping me to connect to myself.

The Goes family—for supporting my education since the beginning. Thank you so much for everything, especially my mother and my grandmother.

I am very thankful to the Richter and the Neumann families for being my family in Germany and for spoiling me so much!

Dr. Robert Richter, who for me is just Roberto—for helping, sharing, supporting and taking care of me in many, many circumstances since we met.

Finally, I would like to thank myself for the persistence and for the will to get an education against all odds. I am proud of myself for this one!